Faculty of Electrical Engineering

Department of Telecommunication Engineering

Radio Resource Management for Relaying in Future Mobile Networks

Habilitation thesis

Pavel Mach

Prague, January 2024

Copyright

Acknowledgement

First of all, I would like to thank all my colleagues at the departments, especially to Zdenek Becvar, with whom I had many fruitful discussions throughout the years, and to department's head Jiri Vodrazka, who managed to create more than friendly environment for my work.

Further, I would like to express eternal gratitude to my close family and friends that helped me to overcome all the obstacles on my journey. Last, but not the least, I would like to give a very special thanks to Ifca and Irca with whom I sweat literally for thousands of hours in the gym and who taught me to never give up.

Abstract

The main scope of this habilitation thesis is radio resource management for mobile networks adopting relaying paradigm. The relaying is able to significantly enhance the performance of mobile networks in terms of sum capacity and/or energy consumption. The main focus of the thesis is on very challenging relaying scenarios with relaying users (based on device-to-device communication) and relaying unmanned aerial vehicles. First, the thesis deal with efficient allocation of resources to enable spectrum efficient relaying via user equipments. Then, the problem on how to motivate users to relay data for other is also discussed. Next, the objective is to optimize the relaying through unmanned aerial vehicles while considering their specifics. Last, the thesis focuses on relevant use-cases where relaying can be of much benefit, if properly optimized. The thesis is in a form of papers' compilation.

CONTENTS

I. Introduction

The idea of relaying in the mobile networks has been conceived already during the development of Worldwide Interoperability for Microwave Access (WiMAX), pushed by IEEE, and Long Term Evolution-Advanced (LTE-A), promoted by 3rd Generation Partnership Project (3GPP) towards 4G mobile networks [1]. The main perceived benefit of the relaying is a potential to increase the network's coverage and capacity, since the users with a low channel quality to a base station (BS), or even out of its coverage, can attach to a close-by relay station (RS) that offers significantly higher channel quality to the BS. The RSs are not connected to the operator's core network by expensive wired connections (as it is done in case of the BSs), but are wirelessly attached to the BS.

In order to enable the operation of the RSs in WiMAX-based networks, 802.16j-2009 standard was approved in 2009 [2]. The 802.16j-2009 standard distinguishes two types of RSs: *transparent* and *non-transparent*. The transparent RSs are very simple relays transmitting neither control nor management signaling. The non-transparent RSs, in contrast, are BS-like nodes handling functionalities similar to the conventional BSs, including own control and management signaling.

The 3GPP followed the IEEE 802.16j-2009 and incorporated the RSs into Release 10 in 2011. Analogously to 802.16j-2009 standard, both non-transparent (also known as Type I) and transparent (Type II) RSs have been initially considered. Nevertheless, only the non-transparent RSs are now fully standardized while the transparent RSs are still being problematic, because these transmit no control information, such as synchronization or reference signals [3]. Consequently, there is no easy way to manage efficiently users' association or handover [4][5].

Depending on mobility, the RSs can be further classified as *fixed*, *nomadic*, or *mobile*. The Fixed RSs are supposed to be located at the strategic locations, where the coverage of conventional BSs is not sufficient and a deployment of entirely new BSs is uneconomical. Even if the non-transparent RSs have BS-like functionalities, their deployment is still much cheaper than the conventional BSs, as the non-transparent RSs do not require a wired connection either to the operator's core network or to other parts of the network infrastructure whatsoever. The second type of RSs, the nomadic ones, are also fixed during their operation, but are deployed only temporarily to boost the performance of the network during peak/busy hours (such as during concerts, football matches, etc.). While Fixed and Nomadic RSs are immobile during their operation, the last type of RSs (i.e., Mobile RSs) are assumed to move during their operation. The Mobile RSs can be mounted on vehicles, such as buses or trams, thus improving quality of service (QoS) of the users on board or in their close proximity. Besides, 3GPP has been studying the possibility to deploy fully Mobile RSs at high speed trains [6][7].

Moreover, the mobile networks can also leverage on device-to-device (D2D) functionality of a user equipment (UE), incorporated into 3GPP for the first time in scope of Release 12 in 2015, allowing even the UEs to relay data for other UEs. This concept is often referred to as a *D2D relaying* [1]. The D2D relaying can be exploited for the cases, where the Relay UE acts as a go-between the cell-edge UE and the BSs in a form of a *UE-to-Network* relaying. Moreover, in case the Relay UEs re-transmit data between two UEs (usually labeled as Source UE and Destination UE, respectively), we speak about a relay-assisted D2D communication or about a *UE-to-UE* relaying.

Besides, with the recent technological evolution of unmanned aerial vehicles (UAVs), an interesting option to deal with a dynamicity of the mobile users is to exploit the UAVs acting as the Flying RSs. Such Flying RSs are able to relay data between the mobile users and the fixed BSs [67]. When compared to the Mobile RSs, the Flying RSs' locations are fully adaptable in 3D space in order to manage fluidity of users' needs and their requirements, as considered in many recent papers [10].

The most interesting relaying options, albeit also the most challenging ones, are relaying via Relay UEs and/or Flying RSs. In particular, the D2D relaying has two *key advantages*: *i)* the

TABLE I: The relative qualitative comparison of individual relaying concepts adopted by the mobile networks [1].

Aspect/relay type	**Fixed/Nomadic RSs**	**Mobile RSs**	**Relay UEs (D2D relaying)**	**Flying RSs**
Deployment cost for operators	**Very high**	**Medium**	**No or minimal cost**	**High (due to potential high OPEX wrt Mobile RSs)**
Number of potential relays	**Several RSs per cell** at most	Usually more than the number of fixed RSs, but still limited	**Many as each UE in the cell is a potential relay**	**Several Flying RSs per cell** at most
Ownership	Mobile operators	Mobile operators	Mobile users	Mobile operators
Location	Fixed or nomadic	Predetermined according to vehicle/train scheduled trajectory	Changing with current user's location disregarding needs of other users	**Highly adaptable** depending on users' needs and requirements
Requirements imposed on users exploiting relays	No requirements	No requirements	Support D2D functionality by the UE is required	No requirements
Security	**High**	**High**	**Low** (depending on the trustworthiness of relaying users)	**High**
Necessity to provide incentive to relay	**No** (RSs are owned by the operator)	**No** (RSs are owned by the operator)	**Yes** (to motivate often selfish users)	**No** (RSs are owned by the operator)

D2D relaying introduces no (or very limited) deployment cost at the mobile operators' side, since the operators do not need to deploy *any additional nodes* (see Table I); and *ii)* there are *many UEs* in the network making, theoretically, *plenty of opportunities and options* for selection of a suitable Relay UE(s). Similarly, the most notable merit of the Flying RSs is that their are highly adaptable and, thus, can cope with very diverse users requirements and their moving patterns.

The comparison given Table I, we observe that both the D2D relaying and relaying via Flying RSs are very intriguing from the operators' point of view to enhance the performance of the mobile networks for wide range of scenarios. To fully unlock all the benefits of the D2D relaying, following crucial aspects should be handled: *(i)* radio resource management (RRM), including relay selection and radio resources/power allocation, *(ii)* interference management between relaying D2D links and conventional cellular links, *(iii)* reduction of power/energy consumption of the Relay UEs, *(iv)* mobility management, as the inherent characteristic of the Relay UE is their mobility that is often very hard to predict, *(v)* security and trust issues, or *(vi)* the motivation of usually selfish users to relay data for others. Of course, also a deployment of the Flying RSs brings many challenges. Similar as in case of D2D relaying, challenges *i) - iii)* needs to be addressed when deploying Flying RSs. Besides, the introduction of the Flying RSs introduces additional challenges including, trajectory planning/positioning of the Flying RSs (usually in 3D space) and users' association. Further, it has been demonstrated that the relaying can improve various interesting mechanisms introduced into mobile networks, such as caching, offloading to mobile/multi-access edge servers, and/or load balancing.

This habilitation thesis focuses on and addresses some of the key challenges in relaying scenarios incorporating either Relay UEs or Flying RSs. In particular, the main scope of this habilitation thesis can be divided into fourth main research areas:

i) Efficient resource allocation for D2D communication: Since D2D relaying, in principle, is facilitated via D2D communication links, we first focus on the efficient resource allocation for D2D communication that can be, then, exploited for allocation of resources for D2D

relaying links.

ii) Radio resource management for D2D relaying: We aim to address critical issue of D2D relaying related to the incentivization of UEs to be willing acting as the Relay UEs in order to fully benefit from D2D relaying paradigm. Further, the benefits of D2D relaying are extended also to users currently unable to initiate D2D relaying and, thus, to address so called spacial unfairness.

iii) Backhaul-aware radio resource allocation for Flying RSs: The main objective of this part is to optimize UEs' association to the Flying RSs, power allocation, positioning of Flying RSs, or efficient reuse, while considering realistic wireless backhaul.

iv) Multi-hop relaying for various use-cases: This part focuses on the optimization of multi-hop relaying, including bandwidth allocation, power allocation, or allocation of time slots duration at individual transmission hops. Further, the use of multi-hop relaying in case-enabled mobile networks is also considered.

In the next sections, the general state-of-the-art in the individual above-listed research areas are discussed and contributions of this habilitation thesis are explained in more detail. Notice that habilitation thesis follows a format with high-level description of the contributions first while the scientific papers are attached in the individual Appendixes at the end.

II. Efficient resource allocation for D2D communication

The efficient resource allocation of D2D communication plays a key role in the incorporation of D2D relaying concept into mobile networks. The reason is that any D2D relaying link, that is the link between the UE and Relay UE, is in fact facilitated via a D2D link. In general, D2D links can use the radio resources in two allocation modes: *i)* a shared mode and *ii)* a dedicated mode (see more detail, e.g., in [11]). We discuss both in the following subsections.

A. Shared mode

In the shared mode, the D2D links are reusing the radio resources initially allocated to the cellular UEs (see Fig. 1). Thus, the main challenge is to efficiently reuse limited radio resources (e.g., in terms of radio channels or radio resource blocks), already exploited by conventional cellular UEs communicating with the BS, by the D2D UEs that exchange data directly among themselves within D2D pair, constituted from D2D transmitter and D2D receiver.

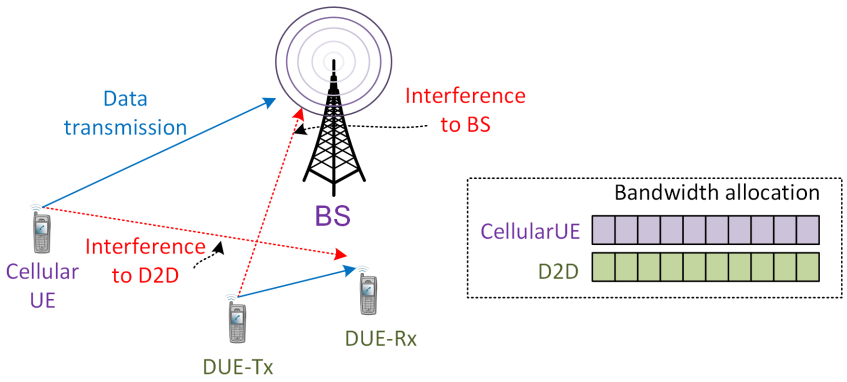

Fig. 1: Illustrative example of shared mode with one cellular UE and one D2D pair constituted from DUE-transmitter (DUE-Tx) and DUE-receiver (Rx). The D2D pair is reusing the uplink resources of the cellular UE resulting in interference from cellular UE to DUE-Rx and from DUE-Tx to the BS.

The reuse of a single channel by more than one D2D pair exploiting share mode is considered, e.g., in [12]-[17]. The main objective of these papers is to maximize the capacity of the D2D pairs while guaranteeing quality of service (QoS) to the cellular UEs. All these papers, however, assume that each D2D pair can access at most one channel at a time. Although this assumption notably simplifies the channel allocation problem, a capacity gain introduced by the channel reuse is fairly limited. The use of more channels by single D2D pair is assumed in [18][19]. Still, in these papers, sharing of one channel by multiple D2D pairs is not possible due to complexity of the resulting solution. The reusing each channel by multiple D2D pairs while multiple channels can be exploited by each D2D pair is assumed in [20]. The authors propose a non-cooperative selfish game for the D2D pairs reuse. However, the game does not converge in realistic scenarios with present mutual interference among D2D pairs. Hence, the solution is applicable only to scenarios with a very low number of the D2D pairs separated by large distances from each other.

In order to ensure high spectral efficient resource allocation, the D2D pairs should be allowed to reuse channels for multiple cellular UEs and, at the same time, each channel should be allowed to be accessed by multiple D2D pairs. Of course, this efficient resource allocation is quite challenging in terms of interference management as UEs using the same channels are interfering to each other, which can degrade their performance significantly. To this end, a novel two-phase channel allocation scheme has been devised. In the first phase, the initial phase, each channel is allocated to one particular D2D pair by means of Hungarian algorithm. In the second phase, the reuse phase, a low-complexity algorithm is proposed. In the reuse phase, the allocation of multiple D2D pairs per each channel is managed according to both the channel quality of each D2D link and interference among individual D2D pairs.

The proposed scheme and results are published in: **P. Mach**, Z. Becvar, and M. Najla, "Resource allocation for D2D communication with multiple D2D pairs reusing multiple channels," *IEEE Wireless Communication Letters*, vol. 8, no. 4, pp. 1008-1011, Aug. 2019. IF (JCR 2022) = **6.3**. The full paper is attached in Appendix A.

B. Dedicated mode

While the previous section focuses on the problem of resource allocation in shared mode, this one is addressing the resource allocation problem in a dedicated mode. In this mode, D2D pairs are assumed to exploit resources not already assigned to the cellular UEs (see Fig. 2). Although, the shared mode offers a higher spectral efficiency than the dedicated one, the higher efficiency is usually at the cost of highly complex solutions for the resource allocation and management. Moreover, the shared mode leads to a mutual interference among the cellular UEs and the D2D users, as already explained in the previous chapter. This interference can be too high and can vary frequently and significantly, especially in the case with huge density of the UEs. Consequently, the reliability of the communication cannot be always guaranteed and overall quality of services (QoS) can be impaired due to the interference in the shared mode [21].

Thus, the D2D UEs with strict requirements on QoS should prefer the dedicated mode, which is suitable for the services that require highly reliable communication with a minimum risk of an unexpected interference from the cellular UEs. Concrete and up-and-coming examples of the use cases for the dedicated mode are the direct communication of vehicles or public safety communication. Then, an ultra-reliable communication with a guaranteed minimum communication capacity should be ensured. In the shared mode, however, interference might lead to the situations when such guarantee is simply not possible and the unreliability in the communication can have grievous consequences. Hence, the dedicated resources are commonly considered for the vehicular or public safety communications.

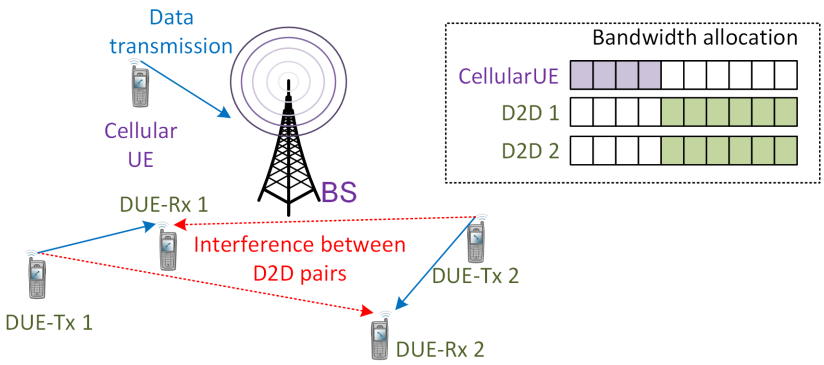

Fig. 2: Illustrative example of dedicated mode with one cellular UE and two D2D pairs. The D2D pairs are reusing the same uplink resources resulting in interference between them.

Similarly as in the previous section, the main objective to maximize the sum system capacity. We assume that multiple D2D pairs can share the same resources to maximize the spectral efficiency (as illustrated in Fig. 2), where both D2D pairs reuse the same channels). This is accomplished by a game theoretic approach where individual D2D pairs are allowed to form the coalitions, within which the radio resources are shared among all D2D pairs.

The initial results are published in conference paper: M. Najla, Z. Becvar and **P. Mach**, "Sequential Bargaining Game for Reuse of Radio Resources in D2D Communication in Dedicated Modes," *IEEE Vehicular Technology Conference (IEEE VTC-Spring 2020)*, 2020. The paper proposes a novel solution that enables the reuse of multiple D2D channels by multiple D2D pairs in the dedicated mode to maximize the sum capacity of the D2D pairs. The proposed solution exploits sequential bargaining games to define coalitions of the D2D pairs mutually reusing multiple channels. Full conference paper is attached in Appendix B.

The extension work is further published in the following journal paper: M. Najla, Z. Becvar, and **P. Mach**, "Reuse of Multiple Channels by Multiple D2D Pairs in Dedicated Mode: Game Theoretic Approach," *IEEE Transactions on Wireless Communications*, vol. 20, no. 7, pp. 4313-4327, July 2021. IF (JCR 2022) = **10.4**. The extension lies in the further optimization of transmission power and bandwidth allocation. The full journal paper is attached in Appendix C.

III. Radio Resource Management for D2D Relaying

While the previous part of the thesis addressed the problem of radio resource management for general D2D links, this section is oriented on D2D relaying facilitated by above-mentioned D2D links. In this regard, this section first focuses on incentive-based resource allocation for D2D relaying, which is essential to motivate the users acting as Relay UEs in the first place. In the sequel, we deal with a spatial unfairness and overloading problem by leveraging on D2D relaying concept.

A. Incentives-based resource allocation for D2D relaying

The D2D relaying is considered to be beneficial in Urban scenario with many potential obstacles in the communication path between the UEs and the BS. For example, the CUE1 and CUE2 in Fig. 3 are exploiting the relay UE (RUE) to overcome the signal attenuation due to the building. The current state-of-the-art proved that D2D relaying is able to significantly enhance the performance of mobile networks. For example, the objective in [22]-[25] is to enhance the capacity of the cell-edge UEs (CUEs) while the authors in [26] minimize the

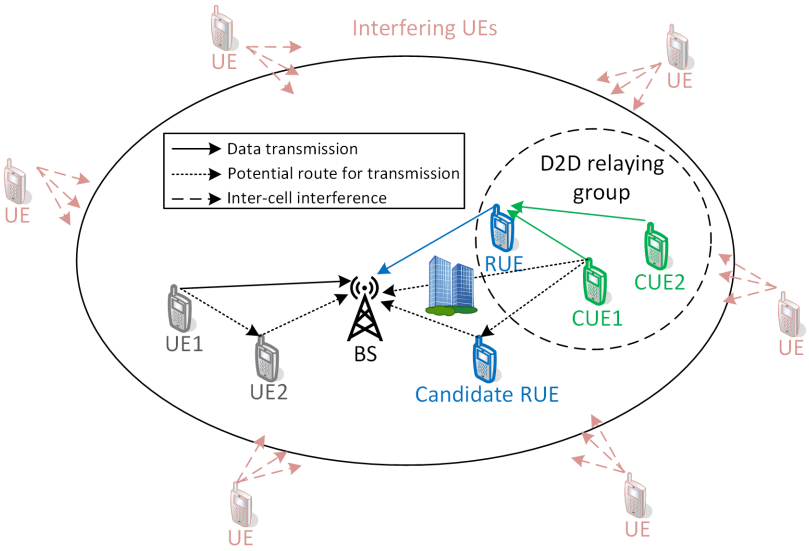

Fig. 3: Illustrative example of Urban scenario where D2D relaying is of benefit. While the UE1 transmits data directly as a matching of UE1 with UE2 is not beneficial for both UEs the CUE1 and CUE2 selects to relay data via the RUE, thus creating D2D relaying group.

energy consumption of the CUEs. All these schemes, however, consider inactive Relay UEs, whose energy consumption is always increased in the process. Thus, *the Relay UE has no tangible motivation to act as the relay* due to the selfish nature of most of the users. This observation gets even more aggravated if the energy spent for a reception of data by the Relay UE from the CUEs, neglected in the above works, is also considered. The use of the active Relay UEs instead of the inactive ones is assumed in [27], where the authors aim to minimize the transmission energy of the Relay UEs and the CUEs via the Hungarian algorithm. However, similar to [26], the reception energy for relaying is not considered, hence, even this solution may increase the overall energy consumption of the RUEs.

Although [22]-[27] show a very promising gains introduced by the D2D relaying, none of them targets a problem of motivating the UEs to act as relays and spend their own energy for the relaying of data form other UEs. One way to motivate the UEs to perform the relaying is considered in [28][29], where a *token-based incentive* mechanism is proposed. In this concept, the UE that receives a help from any idle Relay UE pays with a token. The token can be used by the Relay UE in the future when the RUE asks for the help itself. A similar approach to the one with tokens is considered also in [30]-[32], where the authors suggest a *virtual currency-based incentive* mechanism. The Relay UEs are rewarded with a virtual currency (or a credit) whenever they act as the relays. The received currency is then used by the UEs to pay to other UEs for the relaying services in the future. Other works motivate the users to act as the relays by means of *social-aware incentives*. In [33], the authors explore a social relationship among the users and assume that close friends are more likely to relay the data for each other. Along similar lines, in [34], the authors propose *contract theory-based incentives*, where the users prefer to help their friends rather than strangers. An incentive mechanism for the relaying considering also an energy efficiency is proposed in [35], where the relays are rewarded with a longer transmission time, thus, reducing their energy consumption.

Although all incentive-based works significantly contributes to the problem of the UEs' motivation acting as the relay, they still have following drawbacks. The token- and currency-based approaches [28]-[32] are plagued by two key shortcomings: *i)* it is hard to estimate if the potential future gain (from earning a token or some currency) outweighs the immediate energy

cost of the relaying; *ii)* unless radio channel characteristics and traffic demands are uniformly distributed among all UEs over time, the token-based mechanisms can lead to deadlocks. The main drawback of the social-aware incentive approaches [33][34] is: *i)* there may not be any available friends in vicinity or *ii)* the exploitation of only the friends for relaying is usually far from the optimal in terms of the communication capacity. Moreover, none of the above-mentioned incentive-based approaches addresses the problem of an increased energy consumption of the Relay UEs. Although [35] tackles the energy consumption, it neglects the additional energy required for the data reception at the relay. However, the reception energy eventually increases the overall energy consumption. Besides, the works trying to incentivize the Relay UEs *restricts the number of CUEs exploiting each Relay UE to one*, thus, fairly limits a potential of the whole D2D relaying concept. On top of that, these works either do not address a critical problem of the relay selection ([30][32]) or *no performance guarantees are given* for the proposed relay selection schemes ([28][29][31][33]-[35]).

Motivated by the drawbacks of the above-mentioned papers, a flexible incentive-based relaying framework that guarantees *immediate* rewards for the Relay UE as well as for *all* CUEs exploiting the Relay UE has been proposed. The reward is translated to capacity increase, energy decrease, or combination of both. While the CUEs benefit due to a superior relaying channel quality, the Relay UE profits, as it can exploit a part of the CUE(s) resources for its own transmission.

The initial work and results are published in conference paper: **P. Mach**, Z. Becvar and T. Spyropoulos, "Incentive Mechanism and Relay Selection for D2D Relaying in Cellular Networks, *IEEE Global Communications Conference (IEEE Globecom 2019)*, 2019. The paper provides initial theoretical analysis showing when and if the matching of one or more CUEs with the Relay UE is beneficial in terms of the capacity, energy, or both. Besides, key contribution is a low-complexity greedy algorithm that is able to select among the various ("win-win") relaying options, towards maximizing network-wide performance. Last, a prove that this algorithm has a constant approximation ratio to the optimal performance, in theory, and almost always close-to-optimal performance in practice, is provided. The paper is attached in Appendix D.

The work is further extended in journal paper: **P. Mach**, T. Spyropoulos and Z. Becvar, "Incentive-based D2D Relaying in Cellular Networks, *IEEE Transactions on Communications*, vol. 69, no. 3, 2021. IF (JCR 2022) = **8.3**. The extensions include: *i)* the possibility to use one Relay UE by multiple CUEs and *ii)* derivation of closed-form expressions for the allocation of resources among the UEs in the relaying group to ensure a fairness among the CUEs and the Relay UE in terms of absolute or relative gains. The paper is attached in Appendix E.

B. Coping with Spatial Unfairness/Overloading Problem via D2D Relaying

In the previous section, we have introduced incentive-based resource allocation framework that provides the benefits, in terms of capacity increase and/or energy consumption decrease, solely to the users *directly* involved in relaying, i.e., to the users assisted by the relaying users and to the relaying users themselves. Still, there are users with a low channel quality to the BS that, unfortunately, cannot enjoy the benefits of relaying simply because no suitable relay is in their vicinity. Consequently, Quality of Service (QoS) requirements of these "unlucky" users with low-quality channels to the BS cannot be met due to this spatial unfairness. Besides, the existing incentive solutions are not able to alleviate an overloading problem, when the BS is not able to admit any new users without violating QoS of the already admitted users.

In this section, the aim is to increase the number of users benefiting from D2D relaying, primarily those users who are not satisfied with their QoS or cannot be admitted by the BS due to its overloading. In this regard, the resource allocation framework, which builds upon the existing incentive mechanisms but it enables to extend the benefits of D2D relaying also to the

users not directly involved in relaying itself, is proposed. In particular, the following mechanisms are incorporated in the proposed framework:

- *reuse* resources allocated to D2D links (i.e., links between the users) by the cellular links
- *tax* resources earned or saved by the users benefiting directly from relaying
- *sell* the earned (or saved) resource to other users to convert the relaying gain into monetary gain, increased reputation, or to help others with strong mutual social relationship

The proposed framework is published in: **P. Mach**, Z. Becvar and T. Spyropoulos, " Coping with Spatial Unfairness and Overloading Problem in Mobile Networks via D2D Relaying, to appear in *IEEE Wireless Communications*, vol. 31, no. 1, Feb. 2024. IF (JCR 2022) = **12.9**. The paper is attached in Appendix F.

IV. Backhaul-aware radio resource management for Flying RSs

As already discussed earlier, the mobile networks can also adopt Flying RSs providing a feasible way to cope with the high density of users and dynamicity of the network [36]. The Flying RS acts as a relay between a conventional terrestrial static BS and the UEs. In such a scenario, the UEs receive/transmit data from/to the Flying RS over an access link and the Flying RS, then, relays the UEs' data to/from the SBS via a backhaul link, as illustrated in Fig. 4.

The maximization of the communication capacity by means of the Flying RS's positioning while considering the backhaul with a limited capacity is addressed in [37] and [38]. Nevertheless, both [37] and [38] assume the backhaul with a predefined fixed capacity, which is independent of the Flying RS's position. Unfortunately, such an assumption is not realistic as the capacity of the backhaul directly depends on an allocated bandwidth and the backhaul's channel quality. Hence, the backhaul capacity should naturally be a function of the Flying RS's position.

The backhaul using out-band frequencies is considered in [39]-[42]. In general, the out-band frequencies for the backhaul of the Flying RSs lead to less efficient exploitation of the spectrum (lower spectrum reuse factor). Moreover, the out-band frequencies might not be under the direct control of the mobile operators and it can be hard to guarantee a sufficient backhaul capacity. Besides, both mmWaves and optical waves are highly susceptible to abrupt channel fluctuations.

The backhaul links facilitated by the in-band frequencies are assumed in [43]-[52]. For example, the authors in [43] optimize the 3D trajectory and antenna pattern of a single Flying RS moving between two points. Although the paper assumes the backhaul between the Flying RS and the BS is limited, it does not optimize the backhaul capacity in any way. In [44], bandwidth allocation, power allocation, and trajectory of the single Flying RS are optimized in order to maximize the minimum capacity among all users to guarantee fairness. Similarly as in [43], the

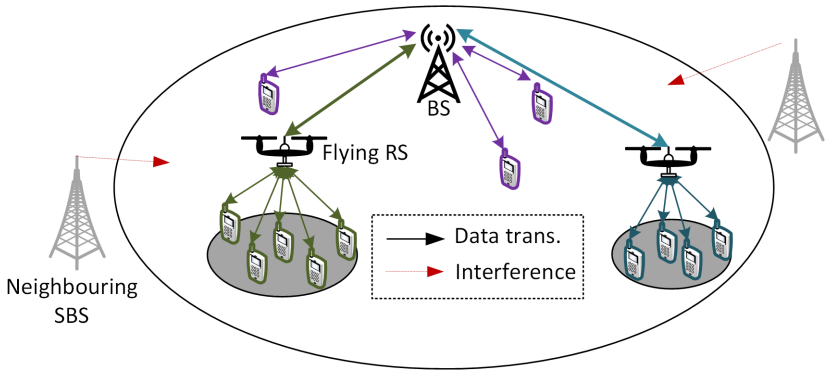

Fig. 4: Illustrative example of mobile networks augmented by the Flying RSs.

backhaul limitation is considered only as a constraint while no optimization with respect to the access links is pursued in [44].

In [45], the authors focus on joint optimization of the Flying RS's position and the bandwidth allocation to the UEs. The authors assume the backhaul is implemented over the radio resources not consumed by the UEs. Thus, the BS may have no resources available for the Flying RSs if the network load is high and all resources are consumed by the UEs associated directly to the BS. The paper [46] studies jointly the placement of Flying RSs, the users' association, and the bandwidth allocation. Although the backhaul link is considered to be limited, the backhaul capacity is only a constraint and the authors do not optimize the access and backhaul links together. The paper [47] proposes the positioning of a single Flying RS, the bandwidth allocation, and the transmission power allocation for full duplex Flying RS exploiting non-orthogonal multiple access (NOMA). Similarly as in [46], the main objective is to minimize the transmission power of the Flying RS while guaranteeing the minimum capacity of the users.

In order to efficiently reuse radio resources at the backhaul and the access links of the Flying RSs, an integrated access and backhaul (IAB) concept, proposed by 3GPP [48], is considered in [49]-[52]. In [49], the main objective is to minimize the transmission power of the single Flying RS while meeting the rate requirements of the UEs. The objective is achieved by a placement of the Flying RS and an allocation of the transmission power at the backhaul and access links. The Flying RSs placement, the UEs association, and the bandwidth allocation are proposed in [50]. The paper, however, disregards the transmission power allocation, which is crucial in IAB, where the access and backhaul links reuse the same resources. The main objective of [51][52] is to manage the interference among the access and backhaul links by the association of the UEs, the power control at the backhaul and access links, and the positioning of the Flying RSs. Nevertheless, if the backhaul quality is below a threshold (defined by signal to noise plus interference ratio, SINR), no transmission at the access link is allowed and the Flying RS is not exploited at all.

None of the papers assuming the limited/constrained backhaul [37]-[52], however, guarantees that the access and backhaul links are of an equal capacity. Thus, the resources either at the access or backhaul links are not utilized efficiently. The goal to ensure the same capacity at the access and backhaul links is considered in [53], where the authors maximize the capacity of indoor users with poor channel conditions to the BSs. The UEs' uplink transmission power is optimally split between the transmissions to the BS and to the Flying RS in a way that one part is used for the users' transmission to the BS and the second part is used for the users' transmission to the Flying RS.

To fill the gaps in the current state-of-the art, we have proposed a *backhaul-aware* framework for the association of the UEs, the power allocation at the Flying RSs, the positioning of the Flying RSs, and the reuse of the access links by multiple UEs with an overall objective to maximize the sum capacity of the UEs.

The initial results are published in: **P. Mach**, Z. Becvar, and M. Najla, "Joint Association, Transmission Power Allocation and Positioning of Flying Base Stations Considering Limited Backhaul", *IEEE Vehicular Technology Conference (IEEE VTC-Fall 2020)*. In the conference paper, a joint power-efficient association of the UEs and allocation of the transmission power to these UEs at the Flying RS is proposed. Further, a closed-form expression for the optimal transmission power allocation at the Flying RSs ensuring the same capacity at the backhaul and access links is derived. Last, a low complexity re-positioning of the Flying RSs, which have some remaining transmission power budget after the association to further boost the sum capacity provided by these Flying RSs, is proposed. The paper is attached in Appendix G.

The initial work is extended in journal publication: **P. Mach**, Z. Becvar, and M. Najla, "Power Allocation, Channel Reuse, and Positioning of Flying Base Stations with Realistic Backhaul,"

IEEE Internet of Things Journal, vol. 9, no. 3, 2022. IF (JCR 2022) = **10.6**. The main extension is a scheme reusing the access links among the UEs by means of a coalition structure generation to decrease the allocated transmission power at the Flying RSs. The reduced transmission power facilitates either a further increase in the sum capacity of the UEs (via an additional re-positioning of the Flying RSs) or a decrease in interference generated to the various underlying devices not exploiting the Flying RSs. The problem of the coalition structure generation is solved optimally by the dynamic programming and, subsequently, by a low complexity algorithm suitable for practical applications. The journal paper can be found in Appendix H.

V. Multi-hop relaying for various use-cases

This section first focuses on offloading of highly computationally demanding tasks to the mobile/multi-access edge computing (MEC). In the sequel, the focus is reoriented to the caching of popular contents.

A. Multi-hop Relaying with Mixed Half and Full Duplex Relays for Offloading to MEC

This section is oriented on very relevant research area dealing with the offloading of computationally demanding tasks to the edge servers, i.e., the paradigm known as mobile/multi-access edge computing (MEC) [56]. This way, the energy consumption of the devices and computation latency can be significantly minimized. To fully grab the potential of the relays, multi-hop relaying for the offloading purposes should be utilized, as indicated in Fig. 5 where two relays are exploited. Notice that, in general, we focus on a case where relay can be any energy-constrained device, including D2D relay, UAV, etc.

The multi-hop relaying is addressed from a perspective of balancing the load among MEC servers [69], minimizing the processing delay of the tasks offloaded from the vehicles to the MEC servers [70]-[72] or to other computing vehicles [73][74], or to offload the tasks from one UE to other neighboring computing UEs [75]. The primary objective of all existing studies on the offloading with multi-hop relaying is to find a proper route between the offloading UE and the MEC server or other computing UE. All works but [75] assume only less efficient half-duplex (HD) mode adopted at each relay with the task subsequently offloaded over each hop in individual time intervals, thus, increasing communication delay. The paper [75] considers full-duplex (FD) mode, however, the paper fully disregards the problem of self-interference (SI) with which the FD is inevitably plagued [66]. Moreover, none of the existing works optimize multi-hop relaying in terms of radio resource management including *i*) allocation of time slots at each hop, *ii*) allocation of transmission power of the offloading UE as well as relays, and *iii*) allocation of bandwidth at each hop.

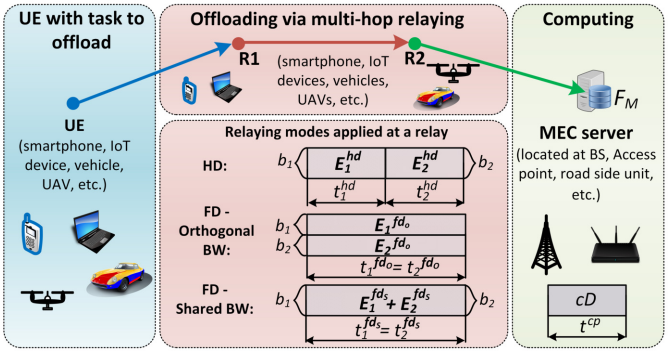

Fig. 5: Illustrative example multi-hop relaying system exploited for offloading of computing tasks to MEC.

Motivated by the above-mentioned gaps, our objective is to optimize radio resource management aspects of multi-hop relaying for the task offloading. Since the offloading UE and relays are usually energy-constrained, such as smartphones, UAVs, or internet of things (IoT) devices, we formulate the problem as the minimization of the sum energy consumed by the energy-constrained UEs involved in the multi-hop relaying under the constraint on the maximum processing time of the computing tasks. First, we propose several unique relaying cases combining HD and FD at each relay involved in multi-hop relaying. Note that existing works always assume the same relaying mode at all relays. Second, we adapt the general problem for each multi-hop relaying case and we prove its convexity so that we can solve it in an optimal way. Finally, we demonstrate that the proposal increases the probability of the tasks being processed within required time by up to 38% and, at the same time, decreases energy consumption by up to 28% with respect to state-of-the-art works.

The work has been presented at the following conference: **P. Mach**, Z. Becvar, and M. Nikooroo, "Multi-hop Relaying with Mixed Half and Full Duplex Relays for Offloading to MEC," in Proc. *IEEE Global Communications Conference (Globecom)*, Kuala Lumpur, Malaysia, Dec. 2023. Available online: https://arxiv.org/abs/2401.06908. The conference paper can be found in Appendix CH.

B. Cache-enabled networks enhanced by multi-hop relaying

The emerging 6G-based mobile networks will have to cope with unprecedented data transmissions originated form plethora of communicating devices, such as smartphones, sensors, vehicles, or any internet of things (IoT) devices. This will inevitably pose high requirements on provided data rates over backhaul and experienced latencies. To alleviate backhaul load and to enable low latencies, caching of popular content seems to be a very promising approach [76]. Obviously, the popular content should be cached in proximity of a user equipment (UE), such as at a ground BS.

To improve systems-wide performance, the UAVs can be exploited as caching servers as well [77]. Such cache-enabled UAVs can store popular contents, thus reducing content delivery duration and backhaul traffic load [78]. The UAV caching can be particularly beneficial during peak hours to offload traffic of the GBSs or to mitigate severe shadowing in urban or mountainous scenarios by leveraging their ability to establish line-of-sight (LoS) connections with ground nodes. The mobile networks can also benefit from the device-to-device (D2D) functionality of UE; to transmit data to other relaying UEs (RUEs) [79]. In such cached-enable, UAV-assisted, and D2D-enabled networks, the main challenges are the selection of proper route over which the content should be traversed in order to reach the UEs, power allocation, content placement, or UAVs' deployment.

The problem of route selection and power allocation in cache-enabled UAV-assisted D2D-enabled cellular network is considered in many works targeting various objectives, including optimization of minimum secrecy rate among requesting UEs [80], sum throughput [81], and energy efficiency [82]. Whereas the afore-mentioned studies [80], [81] confine their scope to direct communication, [82] enables two-hop communication using UAV-relaying. Still, as the distance between the source and target nodes increases or the communication environment deteriorates, direct communication or even two-hop communication with single UAV relay is generally insufficient to reduce the content delivery duration [83]. For instance, in a densely populated urban environment, wireless communication links are susceptible to blockage by tall buildings. Consequently, the mitigation of such link blockage problems typically necessitates the employment of multi-hop communication incorporating both UAV relays and the RUEs in order to provide sufficient degrees of freedom.

In addition, some studies propose different methods to minimize content delivery duration. For example, in [84], a deep deterministic policy gradient-based caching placement strategy is proposed. In [85], the UAV deployment and content placement are jointly studied. However, in both [84] and [85], transmission nodes send contents sequentially rather than simultaneously. Nevertheless, this approach does not minimize transmission duration, as the duration is not linearly proportional to the allocated transmission power.

In our work, we aim to cover the gaps of the existing related works. To this end, we formulate the problem as joint route selection and power allocation problem minimizing sum content delivery duration. Unlike [80], [81], [82], where up to 2-hop communication is enabled, we target multi-hop scenario (i.e., more than 2 hops). To the best of our knowledge, no multi-hop transmission route selection for delivery of cached content has not been considered so far. First, we propose the transmission power allocation managing the splitting of transmission power budget by each transmitting node (i.e., the GBS, the UAV, or RUE) to each content currently being sent. We guarantee the continuous utilization of the entire transmission power by the transmitting nodes, resulting in a reduction in the overall transmission duration. Second, we propose a low-complexity greedy algorithm that jointly considers the route selection while exploiting proposed power allocation.

The work is going to be presented at: E. Gures and **P. Mach**, "Joint Route Selection and Power Allocation in Multi-hop Cache-enabled Networks," in Proc. *IEEE Wireless Communications and Networking Conference (WCNC)*, Dubai, United Arab Emirates, April. 2024. Available online: https://arxiv.org/abs/2401.09060. The conference paper can be found in Appendix I.

VI. Conclusions and future research

This Habilitation thesis has been focused on the area of radio resource management for relaying in future mobile networks, thus contributing in small part to the tremendous effort of the researches around the globe to make 5G, and newly emerging 6G, mobile networks an integral part of everyone's life. Of course, the evolution of mobile networks is a never-ending story as these have to cope still with unprecedented requirements on ultra-high data rates, ultra-low latency, high energy and spectral efficiency, or very high mobility, etc. Just for an example, 6G mobile networks, on which the current research is focused on the most, are expected to:

- incorporate an advanced interference and radio resource management techniques to handle further networks densification [54],
- use significantly broader bands by taping from terahertz and VLC frequencies that cope with a very high path loss and subsequent very short communication distances [54],
- exploit AI- and ML-based techniques to manage and optimize highly complex 6G networks [55].

In the light of foreseen requirements imposed on emerging 6G mobile networks, I would like to contribute in the following areas:

i) Enhancements to D2D relaying: In order to ensure high spectral efficiency, as expected in 6G networks, it is worth to further dig deeper into the utilization of the shared mode utilized by D2D relaying links, where the D2D relaying reuses resources already allocated to the Cellular UEs. Besides, to bring the spectral efficiency to yet another level, it is necessary to further explore the scenarios, where individual D2D relaying links reuse resources of multiple cellular UEs, while multiple D2D relaying links can reuse the radio resources of the same Cellular UE (e.g., the same channel, same set of resource blocks, etc.).

ii) Enhancements to incentive mechanisms: The alpha and omega of the whole D2D relaying concept is to provide proper incentives to the relaying users. One of the critical point not addressed properly thus far by the research works on incentives is the impact of users'

mobility on the given incentive(s). Especially, in case of high mobility scenarios foreseen in the future 6G networks, the incentivization of the relaying users may be often problematic if the relaying itself is of benefit for only a limited amount of time. Then, the challenge is to determine a cost paid by the users to the relaying user if the improvement in the capacity is only temporary and not easily predictable.

iii) Joint optimization of D2D relaying and UAV relaying: There is a actually lot of effort dedicated to an optimization of the UAV communication/relaying, where the Flying RSs assist the cellular UEs to relay data from/to the BS. Nevertheless, there is so far no synergy effect gained from the joint optimization of D2D relaying and the UAV relaying. In particular, one of the crucial problem related to the UAV communication is the positioning of Flying RSs with respect to users' locations. Then, the D2D relay selection can be optimized jointly with the Flying RSs positioning, where the UEs with unfavorable channel conditions are helped by intermediate Relay UEs forwarding data to/from the Flying RS. As a result, the Flying RSs positions do not have to be optimized with respect to weak users and, thus, an overall performance can be improved.

iv) Multi-hop relaying for various use-cases: The optimization of relaying for the offloading or caching can be done as long as devices in communication path are static and channel quality during such offloading/caching can be assumed to be constant as well. Due to inherent mobility of devices, however, optimal solutions are very hard to obtained. In this regard, my intention is to address the offloading/caching via relaying in highly dynamic scenario and find the solutions that are able to still yield close-to-optimal performance while, at the same time, be of reasonable complexity.

REFERENCES

[1] P. Mach and Z. Becvar, "Device-to-Device Relaying: Optimization, Performance Perspectives, and Open Challenges towards 6G Networks," *IEEE Communications Surveys & Tutorials*, vol. 24, no. 3, 3rd Quarter, pp. 1336-1393, 2022.

[2] IEEE 802.16j: Amendment to IEEE standard for local and metropolitan area networks, Air interface for fixed and mobile broadband wireless access systems multihop relay specification, 2009.

[3] R. N. Braithwaite, "Improving data throughput for cell-edge users in a LTE network using up-link HARQ relays," in *Proc. IEEE Veh. Technol. Conf. (VTC Fall)*, San Francisco, CA, USA, Sep. 2011, pp. 1–5.

[4] *Type 2 Relay Summary*, document RAN1 #60, R1-100951, ALU, ALU Shanghai Bell, CHTTL, San Francisco, CA, USA, Feb. 2010.

[5] Najla, M. and Becvar, Z. and Mach, P. and Gesbert, D., "Positioning and Association Rules for Transparent Flying Relay Stations," *IEEE Wireless Commun. Lett.*, vol. 10, no. 6, pp. 1276-1280, June 2021.

[6] 3GPP TR 36.836, 3rd Generation Partnership Project; Technical Specification Group Radio Access Network; Evolved Universal Terrestrial Radio Access (E-UTRA); Study on mobile relay, (Release 12), June 2014.

[7] M.-S. Pan, T.-M. Lin, and W.-T. Chen, "An Enhanced Handover Scheme for Mobile Relays in LTE-A High-Speed Rail Networks," *IEEE Trans. Veh. Technol.*, vol. 64, no. 2, pp. 743-756, Feb. 2015.

[8] H. Nishiyama, M. Ito, and N. Kato, "Relay-by-Smartphone: Realizing Multihop Device-to-Device Communications," *IEEE Commun. Mag.*, vol. 52, no. 4, pp. 56-65, Apr. 2014.

[9] P. Mach, Z. Becvar, M. Najla, "Power Allocation, Channel Reuse, and Positioning of Flying Base Stations with Realistic Backhaul," *IEEE Internet Things J.*, vol. 9, no. 3, pp. 1790-1805, Feb. 2022.

[10] M. Mozaffari, W. Saad, M. Bennis, Y.-H. Nam, and M. Debbah, "A Tutorial on UAVs for Wireless Networks: Applications, Challenges, and Open Problems," *IEEE Communications Surveys and Tutorials*, vol. 21, no. 3, pp. 2334-2360, 2019.

[11] P. Mach, Z. Becvar, and T. Vanek, "In-Band Device-to-Device Communication in OFDMA Cellular Networks: A Survey and Challenges," *IEEE Communications Surveys & Tutorials*, vol. 17, no. 4, 2015.

[12] W. Zhao and S. Wang, "Resource Sharing Scheme for Device-to-Device Communication Underlaying Cellular Networks," *IEEE Trans. Commun.*, 63(12), 4838-4848, Dec. 2015.

[13] D. Ma, N. Wang, and X. Mu, "Resource Allocation for Hybrid Mode Device-to-Device Communication Networks," *WCSP*, 2016.

[14] Y. Li, M. C. Gursoy, and S. Velipasalar, "Joint Mode Selection and Resource Allocation for D2D Communications under Queueing Constraints," *IEEE INFOCOM WKSHPS*, 20(3), 490-495, 2016.

[15] R. Wang, et al., "QoS-Aware Joint Mode Selection and Channel Assignment for D2D Communications," *IEEE ICC*, 2016.

[16] M.C. Lucas-Estan and J. Gozalvez, "Distributed radio resource allocation for device-to-device communications underlaying cellular networks," *Journal of Network and Computer Applications*, 120-130, 2017.

[17] S. M. A. Kazmi, et al., "Mode Selection and Resource Allocation in Device-to-Device Communications: A Matching Game Approach," *IEEE Trans. Mobile Comput.*, 16(11), 3126-3141, Nov 2017.

[18] Y. Qian, T. Zhang, and D. He, "Resource allocation for multichannel device-to-device communications underlaying QoS-protected cellular networks," *IET Communications*, 11(4), 558-565, 2017.

[19] R. AliHemmati, et .al., "Multi-Channel Resource Allocation Toward Ergodic Rate Maximization for Underlay Device-to-Device Communications," *IEEE Trans. Wireless Commun*, 17(2), 1011-1025, 2018.

[20] R. Yin, et al., "Joint Spectrum and Power Allocation for D2D Communications Underlaying Cellular Networks," *IEEE Trans. Veh. Technol*, 65(4), 2182-2195, 2016.

[21] J. Dai, et al., "Analytical Modeling of Resource Allocation in D2D Overlaying Multihop Multichannel Uplink Cellular Networks," *IEEE Transactions on Vehicular Technology*, 66(8), pp. 6633–6644, 2017.

[22] J. Deng, Alexis A. Dowhuszko, R. Freij, O. Tirkkonen, "Relay Selection and Resource Allocation for D2D-Relaying under Uplink Cellular Power Control," in *Proc. IEEE Globecom worskshops*, San Diego, CA, USA, December 2015, pp. 1-6.

[23] J. Zhao, et al, "Two-Level Game for Relay-Based Throughput Enhancement via D2D Communications in LTE Networks," in *Proc. IEEE Int. Conf. on Commun.*, Kuala Lumpur, Malaysia, May 2016, pp. 1-6.

[24] J. Gui and J. Deng, "Multi-Hop Relay-Aided Underlay D2D Communications for Improving Cellular Coverage Quality," *IEEE Access*, vol. 6, pp. 14318-14338, 2018.

[25] X. Xu, J. Wang, and X. Tao, "Analytical Modeling for Caching Enabled UE-to-Network Relay in Cellular Networks," *IEEE Access*, vol. 6, pp. 51061-51068, 2018.

[26] J. Wang, et al, "Analytical Modeling of Mode Selection for UE-to-Network Relay Enabled Cellular Networks with Power Control," in *Proc. IEEE Int. Conf. on Commun. Workshops*, Kansas City, MO, USA, May 2018, pp. 1-6.

[27] S. Zhang, et al, "Energy Efficient Uplink Transmission for UE-to-Network Relay in Heterogeneous Networks," in *Proc. IEEE PIMRC*, Montreal, QC, Canada, October 2017, pp. 1-7.

[28] N. Mastronarde, et al, "Learning Relaying Strategies in Cellular D2D Networks with Token-Based Incentives," in *Proc. IEEE Globecom Wkshps*, Atlanta, GA, USA, December 2013, pp. 1-7.

[29] N. Mastronarde, V. Patel, and L. Liu, "Device-to-device relay assisted cellular networks with token-based incentives," in *Proc. IEEE Int. Conf. on Commun. Workshop*, London, UK, June 2015, pp. 698–704.

[30] Z. Zhu, S. Jin, Y. Yang, H. Hu, and X. Luo, "Time Reusing in D2D-Enabled Cooperative Networks," *IEEE Trans. Wireless Commun.* , vol. 17, no. 5, pp. 3185-3200, May 2018.

[31] Q. Xu, Z. Su, and S. Guo, "A game theoretical incentive scheme for relay selection services in mobile social networks," *IEEE Trans. Veh. Technol.*, vol. 65, no. 8, pp. 6692-6702, August 2016.

[32] Q. Shen, W. Shao, and X. Fu, "D2D Relay Incenting and Charging Modes That Are Commercially Compatible With B2D Services," *IEEE Access*, vol. 7, pp. 36446-36458, 2019.

[33] Y. Li, Z. Zhang, H. Wang, and Q. Yang, "SERS: Social-Aware Energy-Efficient Relay Selection in D2D Communications," *IEEE Trans. Veh. Technol.*, vol. 67, no. 6, pp. 5331-5345, June 2018.

[34] P. Yang, Z. Zhang, J. Yang, and X. Wang, "Incorporating User Willingness in Contract-Based Incentive Mechanism for D2D Cooperative Data Forwarding," *IEEE Access*, vol. 6, pp. 54927-54937, 2018.

[35] Q. Sun, L. Tian, Y. Zhou, J. Shi, and X. Wang, "Energy Efficient Incentive Resource Allocation in D2D Cooperative Communications," in *Proc. IEEE Int. Conf. on Commun.*, London, UK, June 2015, pp. 1-6.

[36] Y. Zeng, et al., "Wireless communications with unmanned aerial vehicles: Opportunities and challenges," *IEEE Communications Magazine*, 54(5), pp. 36–42, 2016.

[37] E. Kalantari, M. Z. Shakir, H. Yanikomeroglu, and A. Yongacoglu, "Backhaul-aware Robust 3D Drone Placement in 5G+ Wireless Networks," *IEEE ICC WKSHP*, 2017.

[38] E. Kalantari, I. Bor-Yaliniz, A. Yongacoglu, and H. Yanikomeroglu, "User association and bandwidth allocation for terrestrial and aerial base stations with backhaul considerations," *IEEE PIMRC*, 2017.

[39] M. Gapeyenko, et al., "Flexible and Reliable UAV-Assisted Backhaul Operation in 5G mmWave Cellular Networks," *IEEE Journal on Selected Areas in Communications*, 31(11), 2018.

[40] Y. Hu, M. Chen, and W. Saad, "Joint Access and Backhaul Resource Management in Satellite-Drone Networks: A Competitive Market Approach," arXiv:1908.11038v1, 2019.

[41] G. Castellanos, M. Deruyck, L. Martens, and W Joseph, "Performance Evaluation of Direct-Link Backhaul for UAV-Aided Emergency Networks," *Sensors*, 19, 2019.

[42] N. Ansari, D. Wu, and X. Sun, "FSO as backhaul and energizer for drone-assisted mobile access networks," *ICT Express*, 6, 2020.

[43] M. M. U. Chowdhury, et al., "3-D Trajectory Optimization in UAV-Assisted Cellular Networks Considering Antenna Radiation Pattern and Backhaul Constraint," *IEEE Transactions on Aerospace and Electronic Systems*, vol. 56, no. 5, pp. 3735 – 3750, 2020.

[44] D. Huang, M. Cui, G. Zhang, X. Chu, and F. Lin, "Trajectory optimization and resource allocation for UAV base stations under in-band backhaul constraint," *EURASIP Journal on Wireless Communications and Networking*, 2020.

[45] C. T. Cicek, H. Gultekin, B. Tavli, and H. Yanikomeroglu, "Backhaul-Aware Optimization of UAV Base Station Location and Bandwidth Allocation for Profit Maximization," arXiv:1810.12395v2, 2020.

[46] E. Kalantari, H. Yanikomeroglu, and A. Yongacoglu, "Wireless Networks With Cache-Enabled and Backhaul-Limited Aerial Base Stations," *IEEE Trans. Wireless Commun.*, vol. 19, no. 11, pp. 7363-7376, 2020.

[47] M.-J. Youssef , J. Farah, C. A. Nour, and C. Douillard, "Full-Duplex and Backhaul-Constrained UAV-Enabled Networks Using NOMA," *IEEE Trans. Veh. Technol*, vol. 69, no. 9, pp. 9667-9681, 2020.

[48] Technical Specification Group Radio Access Network, Study on Integrated Access and Backhaul, document 3GPP TR38.874 v16.0.0, Dec. 2018.

[49] M.-J. Youssef, C. A. Nour, J. Farah, and C. Douillard, "Backhaul-Constrained Resource Allocation and 3D Placement for UAV-Enabled Networks," *IEEE VTC-fall*, 2019.

[50] C. Pan, et al., "Joint 3D UAV Placement and Resource Allocation in Software-Defined Cellular Networks With Wireless Backhaul," *IEEE Access*, 7, 2019.

[51] A. Fouda, A. S. Ibrahim, I. Guvenc, and M. Ghosh, "UAV-Based in-band Integrated Access and Backhaul for 5G Communications," *IEEE VTC-fall*, 2018.

[52] A. Fouda, A. S. Ibrahim, I. Guvenc, and M. Ghosh, "Interference Management in UAV-Assisted Integrated Access and Backhaul Cellular Networks," *IEEE Access*, Vol. 7, 2019.

[53] Y. Li, G. Feng, M. Ghasemiahmadi, and L. Cai, "Power Allocation and 3-D Placement for Floating Relay Supporting Indoor Communications," *IEEE Trans. Mobile Comput.*, vol. 18, no. 3, pp. 618-631, 2018.

[54] K. David, J. Elmirghani, H. Haas, and X.-H. You, "Defining 6G: Challenges and Opportunities [from the guest editors]," *IEEE Veh. Tech. Mag.*, vol. 14, no. 3, pp. 14–16, Sept. 2019.

[55] K. B. Letaief, W. Chen, Y. Shi, J. Zhang, and Y.-J. Angela Zhang, "The Roadmap to 6G: AI Empowered Wireless Networks," *IEEE Commun. Mag.*, vol. 57, no. 8, pp. 84–90, Aug. 2019.

[56] P. Mach and Z. Becvar, "Mobile Edge Computing: A Survey on Architecture and Computation Offloading," *IEEE Commun. Surveys Tuts.*, vol. 19, no. 3., 3rd Quarter, pp. 1628-1656, 2017.

[57] Y. Liu, at al., "Joint Communication and Computation Resource Scheduling of a UAV-Assisted Mobile Edge Computing System for Platooning Vehicles," *IEEE Trans. Intell. Transp. Syst.*, vol. 23, no. 7, 2022.

[58] T. Ren, at al. "Enabling Efficient Scheduling in Large-Scale UAV-Assisted Mobile-Edge Computing via Hierarchical Reinforcement Learning," *IEEE Internet Things J.*, vol. 9, no. 10, pp. 7095-7109, 2022.

[59] M. Li, *et al.*, "Multi-Relay Assisted Computation Offloading for Multi-Access Edge Computing Systems With Energy Harvesting," *IEEE Trans. Veh. Technol.*, vol. 70, no. 10, 2021.

[60] J. Hajipour, "Fairness and Efficiency in Stochastic Buffer-Aided Relay-Assisted MEC,", *IEEE Wireless Commun. Letters*, vol. 11, no. 7, 2022.

[61] T. Zhang, *at al.* "Joint Computation and Communication Design for UAV-Assisted Mobile Edge Computing in IoT," *IEEE Transactions on Industrial Informatics*, vol. 16, no. 8, 2020

[62] S. Zheng, Z. Ren, X. Hou, and H. Zhang, "Optimal Communication-Computing-Caching for Maximizing Revenue in UAV-Aided Mobile Edge Computing," In Proc. *GLOBECOM*, Taipei, Taiwan, 2020.

[63] L. Zhao, at al. "A Novel Cost Optimization Strategy for SDN-Enabled UAV-Assisted Vehicular Computation Offloading," *IEEE Trans. Intell. Transp. Syst.*, vol. 22, no. 6, 2021.

[64] X. Diao, *et al.*, "UAV-Relaying-Assisted Multi-Access Edge Computing With Multi-Antenna Base Station: Offloading and Scheduling Optimization," *IEEE Trans. Veh. Technol.*, vol. 70, no. 9, pp. 9495-9509, 2021.

[65] L. Wang, at al. “Computation Efficiency Maximization for UAV-Assisted Relaying and MEC Networks in Urban Environment,” *IEEE Trans. Green Commun. Netw.*, vol. 7, no 2, 2023.
[66] H. Wang, *et al.*, “Spectrum sharing planning for full-duplex UAV relaying systems with underlaid D2D communications,” *IEEE J. Sel. Areas Commun.*, vol. 36, no. 9, pp. 1986–1999, Sep. 2018.
[67] P. Mach, Z. Becvar, and M. Najla, “Power Allocation, Channel Reuse, and Positioning of Flying Base Stations with Realistic Backhaul,” *IEEE Internet Things J.*, vol. 9, no. 3, pp. 1790-1805, 2022.
[68] J. Gong, X. Chen, and M. Xia, “Transmission Optimization for Hybrid Half/Full-Duplex Relay With Energy Harvesting,” *IEEE Trans. Wireless Commun.*, vol. 17, no. 5, 2018.
[69] Y. Deng, Z. Chen, X. Chen, and Y. Fang, “Task Offloading in Multi-Hop Relay-Aided Multi-Access Edge Computing,” *IEEE Trans. Veh. Technol.*, vol. 72, no. 1, pp. 1372-1376, Jan. 2023.
[70] C.-M. Huanga, S.-Y. Linb, and Z.-Y. Wua, “The k-hop-limited V2V2I VANET data offloading using the Mobile Edge Computing (MEC) mechanism,” *Vehicular Communications*, vol. 26, 2020.
[71] Z. Deng, Z. Cai, and M. Liang, “A Multi-Hop VANETs-Assisted Offloading Strategy in Vehicular Mobile Edge Computing,” *IEEE Access*, vol. 8, pp. 53062-53071, 2020.
[72] Y. Deng, *et al.*, “Spectrum-aware Multi-hop Task Routing in Vehicle-assisted Collaborative Edge Computing,” arxiv, Apr. 2023.
[73] C. Chen, Y. Zeng, H. Li, Y. Liu, and S. Wan, “A Multihop Task Offloading Decision Model in MEC-Enabled Internet of Vehicles,” *IEEE Internet Things J.*, vol. 10, no. 4, Feb. 2023.
[74] L. Liu, *at al.*, “Mobility-Aware Multi-Hop Task Offloading for Autonomous Driving in Vehicular Edge Computing and Networks,” *IEEE Trans. Intell. Transport. Syst.*, vol. 24, no. 2, Feb. 2023.
[75] J. Xie, Y. Jia, W. Wen, Z. Chen, and L. Liang, “Dynamic D2D Multihop Offloading in Multi-Access Edge Computing From the Perspective of Learning Theory in Games,” *IEEE Trans. Netw. Service Manag.*, vol. 20, no. 1, pp. 305-318, March 2023.
[76] I. Zyrianoff, A. Trotta, L. Sciullo, F. Montori, and M. Di Felice, “IoT edge caching: taxonomy, use cases and perspectives,” *IEEE Internet of Things Magazine*, vol. 5, no. 3, pp. 12-18, 2022.
[77] T. Q. Duong, K. J. Kim, Z. Kaleem, M.-P. Bui, and N.-S. Vo, ”UAV caching in 6G networks: A survey on models, techniques, and applications,” *Physical Communication*, vol. 51, p. 101532, 2022.
[78] N. Zhao *et al.*, ”Caching unmanned aerial vehicle-enabled small-cell networks: Employing energy-efficient methods that store and retrieve popular content,” *IEEE Veh. Technol. Mag.*, vol. 14, no. 1, 71-79, 2019.
[79] P. Mach, and Z. Becvar, ”Device-to-device relaying: Optimization, performance perspectives, and open challenges towards 6G networks,” *IEEE Commun. Surv. Tutor.*, vol. 24, no. 3, pp. 1336-1393, 2022.
[80] J. Ji *et al.*, ”Joint trajectory design and resource allocation for secure transmission in cache-enabled UAV-relaying networks with D2D communications,” *IEEE Internet Things J.*, vol. 8, no. 3, pp. 1557-1571, 2020.
[81] M. S. Al-Abiad *et al.*, ”Throughput Maximization of Network-Coded and Multi-Level Cache-Enabled Heterogeneous Network,” *IEEE Trans. Veh. Technol.*, vol. 70, no. 10, pp. 11039-11043, 2021.
[82] X. Qi, M. Yuan, Q. Zhang, and Z. Yang, ”Joint power-trajectory-scheduling optimization in a mobile UAV-enabled network via alternating iteration,” *China Communications*, vol. 19, no. 1, pp. 136-152, 2022.
[83] G. Zhang, H. Yan, Y. Zeng, M. Cui, and Y. Lui, ”Trajectory optimization and power allocation for multi-hop UAV relaying communications,” *IEEE Access*, vol. 6, pp. 48566-48576, 2018.
[84] D. Wang *et al.*, ”Deep Reinforcement Learning for Caching in D2D-Enabled UAV-Relaying Networks,” *IEEE ICCC*, 2021, pp. 635-640.
[85] L. Luo, R. Sun, R. Chai, and Q. Chen, ”Cost-Efficient UAV Deployment and Content Placement for Cellular Systems With D2D Communications,” *IEEE Systems Journal*, 2023.

VII. List of publications

This section summarizes the list of publications that are core part of Habilitation thesis. Further, also other selected publications (published since 2015) that are not the main part of Habilitation thesis are summarized.

A. Summary of publications directly related to Habilitation thesis (in order of appearance)

[1] **P. Mach**, Z. Becvar, and M. Najla, "Resource allocation for D2D communication with multiple D2D pairs reusing multiple channels," *IEEE Wireless Communication Letters*, vol. 8, no. 4, pp. 1008-1011, Aug. 2019. IF (JCR 2022) : **6.3**.

[2] M. Najla, Z. Becvar and **P. Mach**, "Sequential Bargaining Game for Reuse of Radio Resources in D2D Communication in Dedicated Modes," *IEEE Vehicular Technology Conference (IEEE VTC-Spring 2020)*, 2020.

[3] M. Najla, Z. Becvar, and **P. Mach**, "Reuse of Multiple Channels by Multiple D2D Pairs in Dedicated Mode: Game Theoretic Approach," *IEEE Transactions on Wireless Communications*, vol. 20, no. 7, pp. 4313-4327, July 2021. IF (JCR 2022) : **10.4**.

[4] **P. Mach**, Z. Becvar and T. Spyropoulos, "Incentive Mechanism and Relay Selection for D2D Relaying in Cellular Networks, *IEEE Global Communications Conference (IEEE Globecom 2019)*, 2019.

[5] **P. Mach**, T. Spyropoulos and Z. Becvar, "Incentive-based D2D Relaying in Cellular Networks, *IEEE Transactions on Communications*, vol. 69, no. 3, 2021. IF (JCR 2022) : **8.3**.

[6] **P. Mach**, Z. Becvar and T. Spyropoulos, " Coping with Spatial Unfairness and Overloading Problem in Mobile Networks via D2D Relaying, to appear in *IEEE Wireless Communications*, vol. 31, no. 1, Feb. 2024. IF (JCR 2022) : **12.9**.

[7] **P. Mach**, Z. Becvar, and M. Najla, "Joint Association, Transmission Power Allocation and Positioning of Flying Base Stations Considering Limited Backhaul", *IEEE Vehicular Technology Conference (IEEE VTC-Fall 2020)*, 2020.

[8] **P. Mach**, Z. Becvar, and M. Najla, "Power Allocation, Channel Reuse, and Positioning of Flying Base Stations with Realistic Backhaul," *IEEE Internet of Things Journal*, vol. 9, no. 3, 2022. IF (JCR 2022) : **10.6**.

[9] **P. Mach**, Z. Becvar, and M. Nikooroo, "Multi-hop Relaying with Mixed Half and Full Duplex Relays for Offloading to MEC," in Proc. *IEEE Global Communications Conference (Globecom)*, Kuala Lumpur, Malaysia, Dec. 2023.
Available online: https://arxiv.org/abs/2401.06908.

[10] E. Gures and **P. Mach**, "Joint Route Selection and Power Allocation in Multi-hop Cache-enabled Networks," in Proc. *IEEE Wireless Communications and Networking Conference (WCNC)*, Dubai, United Arab Emirates, April. 2024.
Available online: https://arxiv.org/abs/2401.09060.

B. Other selected publications (in chronological order)

Journal papers:

[1] **P. Mach**, Z. Becvar, and T. Vanek, "In-Band Device-to-Device Communication in OFDMA Cellular Networks: A Survey and Challenges," *IEEE Communications Surveys & Tutorials*, vol. 17, no. 4, pp. 1885-1922, 2015. IF (JCR 2022): **35.6**. **Highly cited paper (GS: 379 citations)**.

[2] **P. Mach** and Z. Becvar, "Mobile Edge Computing: A Survey on Architecture and Computation Offloading," *IEEE Communications Surveys & Tutorials*, vol. 19, no. 3, pp. 1628-1656, 2017. IF (JCR 2022): **35.6**. **Highly cited paper (GS: 2990 citations)**.

[3] **P. Mach** and Z. Becvar, "Energy-aware Dynamic Selection of Overlay and Underlay Spectrum Sharing for Cognitive Small cells," *IEEE Transactions on Vehicular Technology*, vol. 66, no. 5, pp. 4120-4132, 2017. IF (JCR 2022): **6.8**.

[4] M. Vondra, Z. Becvar, and **P. Mach**, "Vehicular network-aware route selection considering communication requirements of users for ITS," *IEEE Systems Journal*, vol. 12, no. 2, pp. 1239-50, 2018. IF (JCR 2022): **4.4**.

[5] J. Plachy, Z. Becvar, **P. Mach**, R. Marik and M. Vondra, "Joint Positioning of Flying Base Stations and Association of Users: Evolutionary-Based Approach," *IEEE Access*, vol. 7, pp. 11454-11463, 2019. IF (JCR 2022): **3.9**. **Highly cited paper (GS: 69 citations)**.

[6] M. Najla, **P. Mach**, and Z. Becvar, "Deep Learning for Selection between RF and VLC Bands in Device-to-Device Communication," *IEEE Wireless Communications Letters*, vol. 9, no. 10, pp/ 1763-1767, 2020. IF (JCR 2022): **6.3**.

[7] M. Najla, Z. Becvar, **P. Mach**, and D. Gesbert, "Predicting Device-to-Device Channels from Cellular Channel Measurements: A Learning Approach," *IEEE Transactions on Wireless Communications*, vol. 19, no. 11, pp. 7124-7138, 2020. IF (JCR 2022) : **10.4**.

[8] Z. Becvar, **P. Mach**, M. Elfiky, and M. Sakamoto, "Hierarchical Scheduling for Suppression of Fronthaul Delay in C-RAN with Dynamic Functional Split," *IEEE Communications Magazine*, vol. 59, no. 4, pp. 95-101, 2021. IF (JCR 2022) : **11.2**.

[9] M. Najla, Z. Becvar, **P. Mach**, and D. Gesbert, "Positioning and Association Rules for Transparent Flying Relay Stations," *IEEE Wireless Communication Letters*, vol. 10, no. 6, pp. 1276-1280, 2021. IF (JCR 2022) : **6.3**.

[10] **P. Mach** and Z. Becvar, "Device-to-Device Relaying: Optimization, Performance Perspectives, and Open Challenges towards 6G Networks," *IEEE Communications Surveys & Tutorials*, vol. 24, no. 3, pp. 1336-1393, 2022. IF (JCR 2022): **35.6**.

[11] Z. Becvar, M. Nikooroo and **P. Mach**, "On Energy Consumption of Airship-based Flying Base Stations Serving Mobile Users, *IEEE Transactions on Communications*, vol. 70, no. 10, 2022. IF (JCR 2022) : **8.3**.

[12] Z. Becvar, D. Gesbert, **P. Mach**, and M. Najla, "Machine Learning-based Channel Quality Prediction in 6G Mobile Networks," *IEEE Communications Magazine*, vol. 61, no. 7, 2023. IF (JCR 2022) : **10.4**.

[13] M. Elfiky, Z. Becvar, and **P. Mach**, "Allocation of Resources for HARQ Retransmission in Mobile Networks based on C-RAN," *IEEE Systems Journal*, early access. IF (JCR 2022) : **4.4**.

Conference papers:

[1] **P. Mach** and Z. Becvar, "Enhancement of Hybrid Cognitive Approach for Femtocells," *IEEE Vehicular Technology Conference (IEEE VTC-Spring 2015)*, 2015.

[2] Z. Becvar, M. Vondra, **P. Mach**, J. Plachy and D. Gesbert, "Performance of Mobile Networks with UAVs: Can Flying Base Stations Substitute Ultra-Dense Small Cells?," *European Wireless (EW 2017)*, 2017. **BEST PAPER AWARD.**

[3] **P. Mach**, Z. Becvar, M. Najla, and S. Zvanovec, "Combination of Visible Light and Radio Frequency Bands for Device-to-Device Communication," *IEEE International Symposium on Personal, Indoor and Mobile Radio Communications (IEEE PIMRC 2017), workshop on Coexisting Radio and Optical Wireless Deployments*, 2017.

[4] **P. Mach**, Z. Becvar and, A. Leshem, "Hybrid Spectrum Sharing for Cognitive Small Cells," *IEEE Wireless Communications and Networking Conference (IEEE WCNC 2018)*, 2018.

[5] Z. Becvar, M. Najla, and **P. Mach**, "Selection between Radio Frequency and Visible Light Communication Bands for D2D," *IEEE Vehicular Technology Conference (IEEE VTC-Spring 2018)*, 2018.

[6] **P. Mach**, Z. Becvar, and M. Najla, "Combined shared and dedicated resource allocation for Device-to-Device Communication," *IEEE Vehicular Technology Conference (IEEE VTC-Spring 2018)*, 2018.

[7] Z. Becvar, **P. Mach**, J. Plachy, and M.F.P. de Tuleda, "Positioning of Flying Base Stations to Optimize Throughput and Energy Consumption of Mobile Devices,", *IEEE Vehicular Technology Conference (IEEE VTC-Spring 2019)*, 2019.

[8] M. Najla, D. Gesbert, Z. Becvar, and **P. Mach**, "Machine Learning for Power Control in D2D Communication based on Cellular Channel Gains," *IEEE Global Communications Conference (IEEE Globecom 2019) workshop on Machine Learning for Wireless Communications*, 2019.

[9] Z. Becvar, **P. Mach**, and M. Nikooroo, "Reducing Energy Consumed by Repositioning of Flying Base Stations Serving Mobile Users," *IEEE Wireless Communications and Networking Conference (IEEE WCNC 2020)*, 2020.

[10] M. Najla, Z. Becvar, **P. Mach**, and D. Gesbert, "Integrating UAVs as Transparent Relays into Mobile Networks: A Deep Learning Approach," *IEEE International Symposium on Personal, Indoor and Mobile Radio Communications (IEEE PIMRC 2020)*, 2020.

[11] **P. Mach**, Z. Becvar, and J. Plachy, "Mitigation of Doppler Effect in High-speed Trains through Relaying," *IEEE Vehicular Technology Conference (IEEE VTC2022-Spring)*, 2022.

VIII. Appendix A

This appendix includes journal paper published in: **P. Mach**, Z. Becvar, and M. Najla, "Resource allocation for D2D communication with multiple D2D pairs reusing multiple channels," *IEEE Wireless Communication Letters*, vol. 8, no. 4, pp. 1008-1011, Aug. 2019. IF (JCR 2022) = **6.3**.

Resource Allocation for D2D Communication With Multiple D2D Pairs Reusing Multiple Channels

Pavel Mach, *Member, IEEE*, Zdenek Becvar, *Senior Member, IEEE*, and Mehyar Najla, *Student Member, IEEE*

***Abstract*—In this letter, the goal is to maximize sum capacity of device-to-device (D2D) communication through a reuse of each radio channel by multiple D2D pairs while each D2D pair can access multiple channels. Since existing approaches cannot be easily extended to enable reuse of multiple channels by multiple D2D pairs in scenario with a high interference among the D2D pairs, we propose a novel resource allocation consisting of two phases. In an initial phase, all available channels are assigned by the Hungarian algorithm so that each channel is occupied by just one D2D pair. In a reuse phase, multiple D2D pairs are sequentially added to the individual channels according to their priority expressed by channel quality and received interference from already added D2D pairs. The proposal significantly outperforms existing solutions and reaches close to theoretical upper bound capacity despite a very low complexity of the proposed algorithm.**

***Index Terms*—Device-to-device, channel allocation, capacity, multiple channels reuse.**

I. Introduction

DEVICE-TO-DEVICE (D2D) communication is a concept enabling a direct communication of user equipments (UEs) without a need to transmit data through a base station (BS) [1]. To fully benefit from the D2D concept, multiple D2D pairs should reuse each available channel and all D2D pairs should access multiple channels to maximize the spectrum usage.

The reuse of a single channel by more than one D2D pair underlying cellular communication is considered, e.g., [2]–[7]. These papers target to maximize the capacity of the D2D pairs while guaranteeing quality of service to the cellular UEs (CUEs). However, all these papers assume that each D2D pair can access at most one channel at a time. Although this assumption notably simplifies the channel allocation problem, a capacity gain introduced by the channel reuse is fairly limited. The use of more channels by single D2D pair is assumed in [8] and [9]. Still, in these papers, sharing of one channel by multiple D2D pairs is not possible due to the complexity of the resulting solution. The reuse of each channel by multiple D2D pairs while multiple channels can be exploited by each D2D pair is assumed in [10]. The authors propose a non-cooperative selfish game for the channel reuse. However, the game does not converge in realistic scenarios with the presence of mutual interference among D2D pairs. Hence, the solution is applicable only to scenarios with a very low number of the D2D pairs separated by large distances from each other.

As the papers [2]–[10] cannot be easily adapted to allow the D2D pairs communicating over multiple channels while reusing each channel by multiple D2D pairs in scenarios with interference among the D2D pairs, we introduce a novel two-phase channel allocation scheme. In an initial phase, each channel is allocated to one D2D pair by a common Hungarian algorithm. The core part of the proposed channel allocation scheme is a reuse phase that maximizes a sum D2D capacity through the reuse of multiple channels by multiple D2D pairs. The allocation of multiple D2D pairs to each channel is managed by a novel low complexity priority-based sequential algorithm. The algorithm adds the D2D pairs sequentially to the channels according to channel quality and interference from D2D pairs already occupying the channel. We also derive an optimal power allocation for the D2D pairs to show upper bound performance.

II. System Model

Let's consider a cellular network consisting of one BS, $\mathcal{N} = \{n_1, n_2, \ldots, n_N\}$ CUEs, and $\mathcal{M} = \{m_1, m_2, \ldots, m_M\}$ D2D pairs. Without loss of generality the uplink bandwidth is split into *N* orthogonal channels of an equal width (b_n) so that each channel is occupied by just one CUE (i.e., the CUE *n* accesses the channel *n*). The D2D pairs access the channels in an underlay mode [1] as all available channels are assumed to be occupied by the CUEs (i.e., heavy loaded BS is assumed). The channel occupancy by the D2D pair is defined by a binary parameter ϱ_m^n, where $\varrho_m^n = 1$ ($\varrho_m^n = 0$) means that the D2D pair *m* occupies (does not occupy) the channel *n*.

The signal to interference plus noise ratio (SINR) at the BS and the channel *n* is defined as:

$$\gamma_n^n = \frac{p_n^n g_{n,b}^n}{\sigma^2 + I_b^n + \sum_{m \in \mathcal{M}} \varrho_m^n p_m^n g_{m,b}^n}, \tag{1}$$

where p_n^n and p_m^n are the transmission powers of the CUE *n* and of the D2D transmitter (D2D-Tx) *m*, respectively; $g_{n,b}^n$ is the channel gain between the CUE *n* and the BS at the channel *n*; $g_{m,b}^n$ is the channel gain between the D2D-Tx *m* and the BS at the channel *n*; σ^2 is the noise; and I_b^n represents the inter-cell interference at the BS from the CUEs and the D2D pairs in adjacent cells using channel *n*. Note that we model the system with a single BS, but we still consider inter-cell interference from the neighboring cells as in the real networks. The SINR observed by the *m*-th D2D receiver (D2D-Rx) is:

$$\gamma_m^n = \frac{p_m^n g_{m,m}^n}{\sigma^2 + I_m^n + p_n^n g_{n,m}^n + \sum_{k \neq m} \varrho_k^n p_k^n g_{k,m}^n}, \tag{2}$$

Manuscript received February 11, 2019; accepted March 4, 2019. Date of publication March 7, 2019; date of current version August 21, 2019. This work was supported in part by the Czech Science Foundation under Grant GA17-17538S, and in part by the Grant Agency of Czech Technical University in Prague under Project SGS17/184/OHK3/3T/13. The associate editor coordinating the review of this paper and approving it for publication was G. Yu. *(Corresponding author: Pavel Mach.)*

The authors are with the Department of Telecommunication Engineering, Faculty of Electrical Engineering, Czech Technical University in Prague, 166 27 Prague, Czech Republic (e-mail: machp2@fel.cvut.cz; zdenek.becvar@fel.cvut.cz; najlameh@fel.cvut.cz).

Digital Object Identifier 10.1109/LWC.2019.2903798

where $g^n_{m,m}$ is the channel gain between the D2D-Tx *m* and the D2D-Rx *m* at the channel *n*; $g^n_{n,m}$ represents the channel gain between the CUE *n* and the D2D-Rx *m* at the channel *n*; $g^n_{k,m}$ stands for the channel gain between the D2D-Tx *k* and the D2D-Rx *m* at the channel *n*, and I^n_m is the inter-cell interference caused to the D2D-Rx *m* at the channel *n*.

III. Problem Formulation

Our goal is to maximize a sum D2D capacity (defined as a sum of capacities of all D2D pairs at all channels) while a certain capacity c^c_{min} is still guaranteed to the CUEs. Thus, the objective is formulated as:

$$\begin{aligned} \max \ & \sum_{n\in\mathcal{N}}\sum_{m\in\mathcal{M}} \varrho^n_m b_n log_2(1+\gamma^n_m) \\ \text{s.t. } & \text{a1: } b_n log_2(1+\gamma^n_n) \geq c^c_{min}, \forall n \in \mathcal{N} \\ & \text{a2: } p^n_n \leq P_{max}, \forall n \in \mathcal{N} \\ & \text{a3: } \sum_{n\in\mathcal{N}} p^n_m \leq P_{max}, \forall m \in \mathcal{M}, \end{aligned} \tag{3}$$

The constraint a1 guarantees that the capacity of the CUEs is at least c^c_{min} while the constraints a2 and a3 limit the total transmission power of the CUEs and D2D pairs, respectively. The a1 is guaranteed if $\sum_{m\in\mathcal{M}} \varrho^n_m p^n_m g^n_{m,b} \leq I^n_t$, where I^n_t is a maximum tolerable interference expressed as [2]:

$$I^n_t = \frac{p^n_n g^n_{n,b}}{2^{\frac{c^c_{min}}{b_n}} - 1} - \sigma^2 - I^n_b, \forall n \in \mathcal{N}. \tag{4}$$

Note that if the capacity of CUE *n* is below c^c_{min} even if no D2D pair occupies the channel *n*, I^n_t is set to 0.

IV. Proposed Channel and Power Allocation

The channel allocation for the D2D pairs is managed in two phases. In the initial phase, each channel is assigned to one D2D pair (denoted as a primary D2D pair). The purpose of the initial phase is to prepare a base for the novel reuse phase. In the reuse phase, multiple D2D pairs (denoted as secondary D2D pairs) can be added to each channel on top of the primary D2D pairs. Note that the D2D pair, which is in the role of the primary D2D pair at a specific channel can also be the secondary D2D pair at any other channel(s).

A. Initial Phase

In the initial phase, the objective is to assign all available channels to the D2D pairs so that each channel is occupied by one primary D2D pair. The allocation in the initial phase is done by the Hungarian algorithm that maximizes the capacity if only one D2D pair occupies each channel [11]. To exploit the Hungarian algorithm, the potential maximal capacity of all D2D pairs at all available channels (represented by matrix $C = \{c^n_m\}$) is calculated. The potential maximal capacity (c^n_m) of the D2D pair *m* at the channel *n* is determined as:

$$c^n_m = b_n log_2\left(1 + \frac{p^n_m g^n_{m,m}}{\sigma^2 + I^n_m + p^n_n g^n_{n,m}}\right), \tag{5}$$

To achieve the maximal capacity of the D2D pairs at each channel while guaranteeing a1, we set p^n_m in (5) as:

$$\frac{I^n_t}{g^n_{m,b}} = p^n_m \leq P_{max}, \forall n \in \mathcal{N}, \forall m \in \mathcal{M}, \tag{6}$$

After the matrix $C = \{c^n_m\}$ is obtained, the Hungarian algorithm assigns each channel to a single primary D2D pair. If $N>M$, the Hungarian algorithm is run $\lceil N/M \rceil$ times, as only *M* channels are allocated during each run of the algorithm. Consequently, some D2D pairs are primary D2D pairs at several channels to fully exploit all available radio resources. On the contrary, if $N \leq M$, the Hungarian algorithm is performed only once, and some D2D pairs may not access any channel as the primary D2D pair. The pairs that get no channel in the initial phase can still access channels as the secondary D2D pairs in the reuse phase.

B. Reuse Phase

The core part of the proposed scheme is the reuse phase. The objective of this phase is to maximize the sum D2D capacity through reusing each channel by multiple secondary D2D pairs. In general, adding new D2D pair(s) to the channel inevitably reduces the capacity of the D2D pairs already occupying the channel because of the interference originating from the newly added D2D pair(s) (see (2)). To guarantee the capacity of the D2D pairs (similarly as the capacity of the CUEs), the problem defined in (3) is extended as:

$$\begin{aligned} \max \ & \sum_{n\in\mathcal{N}}\sum_{m\in\mathcal{M}} \varrho^n_m b_n log_2(1+\gamma^n_m) \\ \text{s.t. } & \text{a1}\sim\text{a3 as defined in (3)} \\ & \text{a4: } \sum_{n\in\mathcal{N}} b_n log_2(1+\gamma^n_m) \geq c^d_{min}, \forall m \in \mathcal{M}, \end{aligned} \tag{7}$$

The constraint a4 ensures that the capacity of the D2D pairs over all channels is at least c^d_{min}. Thus, no additional D2D pairs can be added to the channel if the capacity of any D2D pair already using the channel is lower than c^d_{min}.

The channel reuse is done by the proposed low complexity Priority-Based Sequential Algorithm (PBSA) that adds secondary D2D pairs to individual channels sequentially. The order in which the secondary D2D pairs are added to the channel *n* is supposed to play an important role. The reason is that adding one secondary D2D pair can result in preventing further addition of another secondary D2D pair(s) (e.g., due to high interference generated among the secondary D2D pairs). The proposed PBSA adds the secondary D2D pairs in an order determined according to priority metric $\omega^n_{m'}$ defined as:

$$\omega^n_{m'} = p^n_{m'} g^n_{m',m'} - \sum_{m\in\mathcal{M}\setminus\{m'\}} \varrho^n_m p^n_m g^n_{m,m'}, \forall n \in \mathcal{N}, \tag{8}$$

where the first term corresponds to the signal strength received by the D2D-Rx from the D2D-Tx of the secondary D2D pair m' that is supposed to be added at the channel *n* and the second term is the sum of interference from the D2D pairs already assigned to the channel *n*. Note that the priority of the secondary D2D pair is higher if $\omega^n_{m'}$ is higher. It is worth to mention that the D2D-Rx measures the sum interference from all D2D pairs using the channel. Thus, there is no need to know channel gains to all D2D pairs and the required signaling to

manage the reuse phase is the same as if no reuse would be applied at all.

In order to enumerate $\omega^n_{m'}$ according to (8), the transmission powers of the D2D pairs at each channel need to be determined. Since the constraint a1 should be guaranteed during the whole reuse phase, the following condition should hold: $\sum_{m\in\mathcal{M}} x^n_m I^n_t \leq I^n_t$, where $x^n_m I^n_t = p^n_m g^n_{m,b}$ is the interference caused by the D2D pair *m* to the CUE *n*. To find the optimal D2D power allocation (i.e., to find optimal values of x^n_m), we define the objective function as:

$$f(\mathbf{X^n}) = \sum_{m\in\mathcal{M}} log_2\left(1 + \frac{\varrho^n_m \frac{x^n_m I^n_t}{g^n_{m,b}} g^n_{m,m}}{I^n_s + \sum_{k\neq m} \varrho^n_k \frac{x^n_k I^n_t}{g^n_{k,b}} g^n_{k,m}}\right), \tag{9}$$

where $I^n_s = \sigma^2 + I^n_m + p^n_n g^n_{n,m}$ and $\mathbf{X^n} = \{x^n_1, x^n_2, \ldots, x^n_M\}$. Then, the optimization problem is:

$$\begin{aligned} \min_{\mathbf{X^n}} \ & -f(\mathbf{X^n}) \\ \text{s.t.} \ & 0 \leq x^n_m \leq 1, \ \forall n \in \mathcal{N}, \ \forall m \in \mathcal{M} \\ & \sum_{m\in\mathcal{M}} x^n_m \leq 1, \ \forall n \in \mathcal{N} \end{aligned} \tag{10}$$

where both constraints ensure that a1 in (3) is fulfilled. We solve (10) by a sequential quadratic programming (SQP). In general, SQP solves a quadratic programming sub-problem at each iteration. During each iteration, an estimate of the Hessian of the Lagrangian is calculated via the Broyden–Fletcher–Goldfarb–Shanno (BFGS) formula (see more details in [12]). Due to relatively high complexity of SQP, we also propose "equal" power allocation (PBSA-equal) introducing no additional complexity to the channel allocation process since the power of the D2D pairs is set so that each D2D pair causes the same interference to the CUE (i.e., $x^n_m = 1/\sum_{m\in\mathcal{M}} \varrho^n_m, \forall x^n_m \in \mathbf{X^n}$).

After acquiring the $\mathbf{X^n}$, transmission power of the D2D pair *m* occupying the channel *n* is:

$$\frac{x^n_m I^n_t}{g^n_{m,b}} = p^n_m \leq P_{max}, \forall n \in \mathcal{N}, \forall m \in \mathcal{M}, \tag{11}$$

The allocation of channels in the reuse phase is described in Algorithm 1. First, $\Omega^n = \{\omega^n_1, \omega^n_2, \ldots, \omega^n_{M-1}\}$ is determined for all *N* channels according to (8). Then, the Ω^n is sorted according to $\omega^n_{m'}$ in descending order (line 4). Subsequently, the secondary D2D pair with the highest priority at the channel *n* (i.e., the D2D pair with max(ω^n)) is added to the channel *n* by setting $\varrho^n_{m'} = 1$ (line 5). Then, the transmission power p^n_m is updated for all D2D pairs occupying the channel according to (11) (line 6) and a new sum D2D capacity at the channel ($c^n_{m'}$) is calculated (line 7). If the sum D2D capacity is decreased by an inclusion of the secondary D2D pair m' (i.e., if $c^n_{m'} < c^n_{m'-1}$) or if a4 is not fulfilled, the secondary D2D pair is removed from the channel (i.e., $\varrho^n_{m'} = 0$). Otherwise, the secondary D2D pair starts reusing the channel and ω^n_m is updated for the D2D pairs that still can be added to this channel (line 11). This whole process (lines 2–14) is repeated for all secondary D2D pairs and for all available channels.

The complexity of the channel allocation in reuse phase is up to $\mathcal{O}(N(M-1))$ as ($M-1$) secondary D2D pairs can be added to *N* channels. Note that the complexity of channel allocation process is even lower than in related works (see [2], [7]). Further, the complexity of the optimal power allocation is, in the worst case, $\mathcal{O}(M^3KN)$, where M^3 corresponds to the maximal complexity of quadratic programming and *K* is the number of iterations of the sequential process. The complexity of "equal" power allocation is $\mathcal{O}(1)$.

Algorithm 1 Priority-Based Sequential Algorithm

1: determine $\Omega^n, \forall n \in \mathcal{N}$ acc. (8)
2: **for** n=1:N **do**
3: **for** m'=1:($M-1$) **do**
4: sort Ω^n in descending order (D2D pairs priority)
5: $\varrho^n_{m'} = 1$ (add D2D pair m' at channel n)
6: set $p^n_m \ \forall$ D2D pairs using channel n acc. (11)
7: $c^n_{m'} = \sum_{m\in M} \varrho^n_m b_n log_2(1+\gamma^n_m)$
8: **if** $c^n_{m'} < c^n_{m'-1}$ or a4 is not satisfied **then**
9: $\varrho^n_{m'} = 0$, $c^n_{m'} = c^n_{m'-1}$
10: **else**
11: update ω^n_m for D2D pairs not yet added
12: **end if**
13: **end for**
14: **end for**

TABLE I
PARAMETERS AND SETTINGS FOR SIMULATIONS

Parameter	Value
Simulation area	500x500 m
Number of CUEs/channels (N)	10
Number of D2D pairs (M)	2–20
Channel bandwidth (b_n)	2 MHz
Max. distance between D2D-Tx and D2D-Rx	50 m
Carrier frequency	2 GHz
Transmission power of CUEs (p^n_n)	24 dBm [10]
Max. DUE's transmission power at channel n (p^n_m)	10 dBm [10]
Number of simulation drops	200

V. PERFORMANCE ANALYSIS

The proposed scheme is evaluated by simulations. The BS is located in the middle of a simulation area. For each simulation drop, the positions of CUEs, D2D-Txs, and D2D-Rxs are generated randomly with uniform distribution. The maximum distance between D2D-Tx and D2D-Rx creating one D2D pair is set to 50 m. Hence, the position of the D2D-Tx is generated first and, then, the D2D-Rx is randomly dropped within the allowed maximum radius from the D2D-Tx. Moreover, the inter-cell interference at the BS (I^n_b) and the D2D-Rxs (I^n_m) is generated randomly according to Gamma distribution [13] with a mean value of -80 dBm. The channel gains between individual nodes are derived according to the models defined by 3GPP. Since our objective does not target an optimization of the CUEs' transmission power, we assume fixed transmission power p^n_n of the CUEs at each channel as in [10]. All major simulation parameters are summarized in Table I.

The results of the PBSA with the optimal power allocation (PBSA-opt) according to (10) and the PBSA-equal are compared with the proposed "random" algorithm, which exploits reuse, but does not consider the priority metrics (i.e., the secondary D2D pairs are added to the channels randomly). The performance of the proposed PBSA is also compared with

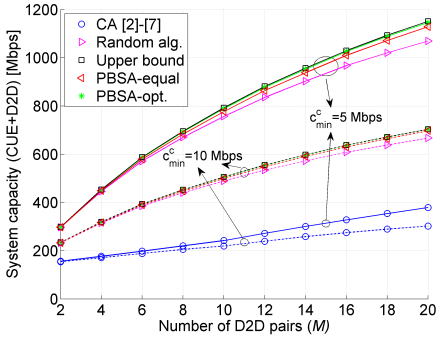

Fig. 1. System capacity depending on M for $c^d_{min} = 0$.

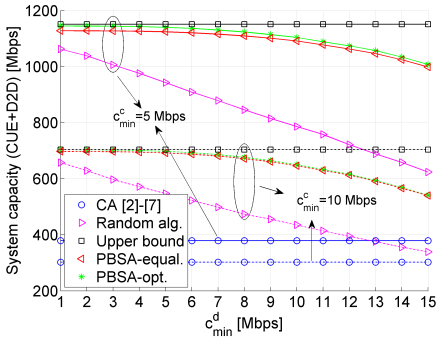

Fig. 2. System capacity depending on $c^d_{min} = 0$ for $M = 20$.

channel allocation (CA) based on [2]–[7] allowing to reuse each channel by multiple D2D pairs while only one channel can be exploited by each D2D pair. Then, we show a theoretical upper bound performance obtained by checking all possible D2D pair allocations to all channels (i.e., the optimal case) and with the D2D transmission power set to the optimal values according to (10). The complexity of the theoretical upper bound is $\mathcal{O}(N2^M)$. Note that we do not compare the proposed PBSA with the scheme in [10], since the non-cooperative game exploited in [10] does not converge if interference among the D2D pairs is high.

Fig. 1 illustrates the system capacity depending on the number of D2D pairs (M). Increasing c^c_{min} decreases the capacity of all algorithms. The reason is that the CUEs can tolerate less amount of interference for a higher c^c_{min} and, hence, I^n_t is decreased (see (4)). Fig. 1 further shows that the proposed PBSA-opt provides between 1.52 and 3.26 times higher capacity (depending on c^c_{min} and M) than the CA scheme based on [2]–[7]. These encouraging results demonstrate that the reuse of multiple channels by multiple D2D pairs results in a significant gain in capacity comparing to the CA [2]–[7], where each D2D pair can access only one channel. In addition, Fig. 1 demonstrates that the PBSA-opt reaches almost theoretical upper bound capacity (only 0.5% degradation). It is worth to mention that the performance of the PBSA-equal is at most 1.6% below that of the PBSA-opt. Thus, the equal power allocation can be applied in a real system instead of more complex optimal power allocation at the cost of only a slight decrease in the sum D2D capacity.

Fig. 1 also reveals an interesting fact: if $c^d_{min} = 0$ Mbps (no capacity is guaranteed to the D2D pairs), the order in which the secondary D2D pairs are added to the channel is not that critical. Hence, the PBSA does not outperform random adding of the D2D pairs significantly for $c^d_{min} = 0$ Mbps (up to 7.1% for 20 D2D pairs). However, Fig. 2 shows that performance gap between the random algorithm and the PBSA significantly increases with c^d_{min} (up to 61.5% for $c^d_{min} = 15$ Mbps). The reason is that in the case of random adding of the D2D pairs, even the D2D pair with the capacity slightly above c^d_{min} can be added to the channel at the beginning of the reuse phase. Then, other D2D pairs can be no longer allowed to reuse the same channel to guarantee c^d_{min}. Although the system capacity of PBSA (both -equal and -opt.) starts also decreasing for a higher c^d_{min}, this decrease is only marginal when compared to the random adding of the D2D pairs.

Since our main objective is to maximize the system capacity, $c^d_{min} \leq 10$ Mbps is recommended since the PBSA performance is still close to the upper bound. A specific c^d_{min} should be selected according to requirements and/or priority of individual D2D pairs at each channel.

VI. Conclusion

In this letter, we have proposed a novel low complexity resource allocation scheme maximizing sum D2D capacity. The scheme allows an efficient reuse of the channels by multiple D2D pairs while each D2D pair may access multiple channels. We show that the proposed allocation significantly outperforms the state-of-the-art approaches (increasing the sum D2D capacity at up to 3.26 times) and reaches close-to-optimum performance despite low (linear) complexity.

References

[1] A. Asadi, Q. Wang, and V. Mancuso, "A survey on device-to-device communication in cellular networks," *IEEE Commun. Surveys Tuts.*, vol. 16, no. 4, pp. 1801–1819, 4th Quart., 2014.
[2] W. Zhao and S. Wang, "Resource sharing scheme for device-to-device communication underlaying cellular networks," *IEEE Trans. Commun.*, vol. 63, no. 12, pp. 4838–4848, Dec. 2015.
[3] D. Ma, N. Wang, and X. Mu, "Resource allocation for hybrid mode device-to-device communication networks," in *Proc. WCSP*, 2016, pp. 1–5.
[4] Y. Li, M. C. Gursoy, and S. Velipasalar, "Joint mode selection and resource allocation for D2D communications under queueing constraints," in *Proc. IEEE INFOCOM WKSHPS*, vol. 20, no. 3, 2016, pp. 490–495.
[5] R. Wang, J. Zhang, S. H. Song, and K. B. Letaief, "QoS-aware joint mode selection and channel assignment for D2D communications," in *Proc. IEEE ICC*, 2016, pp. 1–6.
[6] M. C. Lucas-Estan and J. Gozalvez, "Distributed radio resource allocation for device-to-device communications underlaying cellular networks," *J. Netw. Comput. Appl.*, vol. 99, pp. 120–130, Dec. 2017.
[7] S. M. A. Kazmi *et al.*, "Mode selection and resource allocation in device-to-device communications: A matching game approach," *IEEE Trans. Mobile Comput.*, vol. 16, no. 11, pp. 3126–3141, Nov. 2017.
[8] Y. Qian, T. Zhang, and D. He, "Resource allocation for multichannel device-to-device communications underlaying QoS-protected cellular networks," *IET Commun.*, vol. 11, no. 4, pp. 558–565, Mar. 2017.
[9] R. Alihemmati, M. Dong, B. Liang, G. Boudreau, and S. H. Seyedmehdi, "Multi-channel resource allocation toward ergodic rate maximization for underlay device-to-device communications," *IEEE Trans. Wireless Commun*, vol. 17, no. 2, pp. 1011–1025, Feb. 2018.
[10] R. Yin *et al.*, "Joint spectrum and power allocation for D2D communications underlaying cellular networks," *IEEE Trans. Veh. Technol.*, vol. 65, no. 4, pp. 2182–2195, Apr. 2016.
[11] H. W. Kuhn, "The Hungarian method for the assignment problem," *Naval Res. Logistics Quart.*, vol. 2, nos. 1–2, pp. 83–97, Mar. 1955.
[12] S. S. Rao, *Engineering Optimization: Theory and Practice*. Hoboken, NJ, USA: Wiley, 2009.
[13] I. Viering, A. Klein, M. Ivrlac, M. Castaneda, and J. A. Nossek, "On uplink intercell interference in a cellular system," in *Proc. IEEE ICC*, 2006, pp. 2095–2100.

IX. Appendix B

This appendix includes conference paper presented at: M. Najla, Z. Becvar and **P. Mach**, "Sequential Bargaining Game for Reuse of Radio Resources in D2D Communication in Dedicated Modes," *IEEE Vehicular Technology Conference (IEEE VTC-Spring 2020)*, 2020.

Sequential Bargaining Game for Reuse of Radio Resources in D2D Communication in Dedicated Mode

Mehyar Najla, Zdenek Becvar, and Pavel Mach,
Faculty of Electrical Engineering, Czech Technical University in Prague
Technicka 2, 166 27 Prague, Czech republic
emails: {najlameh, zdenek.becvar, machp2}@fel.cvut.cz

***Abstract*—Device-to-device communication (D2D) is expected to accommodate high data rates and to increase the spectral efficiency of mobile networks. We focus on the dedicated mode where D2D pairs exploit channels that are different from the channels allocated to conventional cellular users. Such mode is suitable for scenarios of crowded areas with many D2D pairs where interference management between cellular and D2D users would be very complicated. We propose a novel solution that enables the reuse of multiple channels by multiple D2D pairs in order to increase the throughput of D2D users. The proposed channel reuse is facilitated via grouping D2D pairs into coalitions. The D2D pairs within the same coalition then mutually reuse the channels of each other. The coalitions are defined via sequential bargaining games played among the D2D pairs. The coalitions are created if individual D2D pairs involved in the game benefit from participation in the coalition. The proposed algorithm based on sequential bargaining reaches a throughput gain of $28-64\%$ comparing to the best performing existing algorithm.**

***Index Terms*—Device-to-device, Dedicated mode, Game theory, Resource allocation, Channel reuse.**

I. Introduction

Higher data rates and lower latencies are required to enable new services and to increase the number of connected devices in the mobile networks. These demands can be accommodated via a direct communication between user equipments (UEs) in proximity of each other, i.e., via Device-to-Device (D2D) communication [1], [2]. Two D2D UEs (DUEs) communicating with each other create a D2D pair. Contrary to the conventional cellular communication through a base station (denoted as gNB), the data is sent directly from a transmitting DUE (DUE_T) to a receiving DUE (DUE_R) without being relayed by the base station [3].

The DUEs can access radio channels in two modes: shared and dedicated [4]. In the shared mode, the DUEs are allowed to reuse the channels that are already allocated to common cellular UEs (CUEs) communicating via the gNB. Thus, the CUEs and the DUEs mutually interfere with each other. In contrast, the DUEs operating in the dedicated mode access only the channels that are not used by the CUEs. Hence, the DUEs do not interfere with the CUEs, but the spectral efficiency in the dedicated mode can be decreased due to the lower reuse of the channels [5]. Algorithms allocating channels for the DUEs can be classified into those that target channel allocation: i) solely for the shared mode (see, e.g., [6]–[14]); ii) solely for the dedicated mode (e.g., [15], [16]); and iii) combining both the shared and dedicated modes (e.g., [17], [18]).

Besides the selection of D2D mode, the spectral efficiency of the whole system is strongly influenced also by the reuse of the channels among the D2D pairs. The research works related to the reuse of the D2D channels can be classified into papers where: i) each D2D pair uses only one channel and the channel cannot be reused by any other D2D pair [6]–[16]; ii) multiple D2D pairs are allowed to reuse a single channel [7]–[9], [17], [18]; iii) more than one channel can be allocated for each D2D pair, but each D2D pair uses only one channel [10]–[12]; and iv) multiple D2D pairs can reuse multiple channels [13], [14].

The most generic case is, of course, the reuse of multiple channels by multiple D2D pairs. Both [13] and [14] addressing this general case target only the shared mode where the channel bandwidth and the number of channels are given by the CUE's allocation. However, the channel allocation schemes dealing with the shared mode cannot be easily extended to the dedicated mode due to two reasons. The first reason is that the shared mode assumes a D2D power allocation in order to protect the quality of service of the CUEs (see, e.g., [8], [10]–[14]). In contrast, the D2D pairs in the dedicated mode are not constrained by the CUEs and the D2D pairs are commonly supposed to transmit with maximum power (see, e.g., [15] and [16]). The second reason is that the channel allocation for D2D pairs in the shared mode is heavily influenced by the level of interference from the CUEs [9]. The interference from the CUEs affects the D2D pairs on individual channels differently due to various distances between the CUEs and the D2D pairs [6], [7], [17]. This is, however, not the case of dedicated mode where the allocation of channels depends only on the D2D pairs and on the interference among D2D pairs reusing the same channels. In the dedicated mode, the existing works are focused either on no-reuse resource allocation schemes ([15], [16]); or on the channel reuse only if the number of available channels is higher than the number of the D2D pairs ([17], [18]). However, none of these papers allows the reuse of multiple channels by multiple D2D pairs in the dedicated mode.

978-1-7281-5207-3/20/$31.00 ©2020 IEEE

In this paper, we focus on the maximization of the sum capacity of the D2D communication in the dedicated mode. The dedicated mode is preferred in scenarios with high density of the CUEs in small areas where a high interference among the CUEs and the D2D pairs would be extremely hard to manage [19]. We propose a novel solution that enables the reuse of multiple D2D channels by multiple D2D pairs in the dedicated mode to maximize the sum capacity of the D2D pairs. The proposed solution exploits sequential bargaining games to define coalitions of the D2D pairs mutually reusing multiple channels. We show that our proposed sequential bargaining solution leads to a significant improvement in the sum capacity of the D2D pairs when compared to related works. We also demonstrate the low complexity of our proposed algorithm allowing its implementation in real networks.

The rest of the paper is organized as follows. In Section II, the system model is described and the problem is formulated. In Section III, the proposed channel reuse scheme for D2D in dedicated mode is presented. The simulations results are discussed in Section IV. Last, Section V concludes the paper and outlines possible future research directions.

II. System model and problem formulation

In this section, we first describe the system model and, then, we formulate the problem, which is solved in the next sections of this paper.

A. System model

The model considers N D2D pairs deployed within a single gNB. The distance (d) between any DUE_T and any DUE_R creating a D2D pair is assumed to be no longer than a maximum distance d_{max} (i.e., $d \leq d_{max}$) guaranteeing a reliable D2D communication similarly as considered in, e.g., [20]–[22]. Thus, the scenario where the DUE_T and the DUE_R are not able to communicate directly and data is sent via the gNB (i.e., if $d > d_{max}$) is out of scope of this paper.

The whole communication bandwidth B is split into $K = N$ channels (as in [15] and [16]) to serve all N D2D pairs. Thus, the capacity $C_{n,k}$ of the n-th D2D pair at the k-th channel is defined as:

$$C_{n,k} = B_k log_2\left(1+\gamma_{n,k}\right) = B_k log_2\left(1+\frac{P_{n,k}\, g_{n,n}}{\sigma_k+\sum_{\substack{t\in N_k\\ t\neq n}} p_{t,k} g_{t,n}+I_d}\right) \quad (1)$$

where B_k is the bandwidth of the k-th channel, $\gamma_{n,k}$ is the signal to interference plus noise ratio (SINR) for the n-th D2D pair (D_n) at the k-th channel, $p_{n,k}$ is the transmission power of the n-th DUE_T at the k-th channel, $g_{n,n}$ is the channel gain between the n-th DUE_T and the n-th DUE_R, $p_{t,k}$ is the transmission power of the t-th DUE_T at the k-th channel, $g_{t,n}$ is the channel gain between the t-th DUE_T and the n-th DUE_R, I_d stands for the background interference received from adjacent cells, N_k represents the set of D2D pairs communicating at the k-th channel, and σ_k is the thermal noise affecting the k-th communication channel. The noise σ_k is calculated as $\sigma_k = \sigma_o B_k$, where σ_o is the white noise power spectral density on the carrier frequency. As we focus on the dedicated mode, the D2D pairs experience no interference from the CUEs, which communicate at separated channels. Thus, the CUEs are left out form the model. The maximal transmission power P_{max} of any D2D pair communicating over a set of reused channels K_n is divided equally among the $|K_n|$ channels so that $P_{n,k} = \frac{P_{max}}{|K_n|}$.

Initially, as in [15] and [16], each n-th D2D pair occupies the n-th channel with a bandwidth of $B_n = \frac{g_{n,n}}{\sum_{n=1}^{n=N} g_{n,n}} B$ without channel reuse. Consequently, before any reuse, every n-th D2D pair achieves the capacity $C_{n,n}^{nr}$ at its n-th dedicated channel, i.e., without neither reuse nor interference from other D2D pairs. Based on all $C_{n,n}^{nr}$, the minimal communication capacity that can be guaranteed to all D2D pairs even without reuse is defined as: $C_{min} = min\{C_{n,n}^{nr} \mid n \in \{1, ..., N\}\}$. Thus, C_{min} represents the minimum capacity that is guaranteed to every D2D pair disregarding whether the reuse is considered or not. Note that C_{min} depends on the number of D2D pairs, because the more D2D pairs are active, the narrower dedicated channel is available to each pair and, thus, a lower C_{min} can be guaranteed to the pairs.

Note that, although the DUEs communicate directly via D2D communication, the allocation of the channels and the communication control are assumed to be decided centrally by the gNB. Therefor, we consider that the channel state information (CSI) is reported periodically to the gNB and, thus, a full knowledge of CSI is assumed to be available in our system, like in [10],[11],[23]. Based on the CSI knowledge, the gNB is able to determine capacity and the channel reuse rules.

B. Problem formulation

The objective of this paper is to maximize the sum communication capacity of the D2D pairs in the dedicated mode by enabling the reuse of multiple channels by multiple D2D pairs. To determine which D2D pairs should mutually reuse their channels, we formulate the problem as a coalition structure generation problem [24]–[26]. To that end, we denote the set of L coalitions of the D2D pairs as $\mathbf{CS} = \{cs_1, cs_2, \ldots, cs_L\}$, where each coalition $cs_l \in \mathbf{CS}$ includes a subset of D2D pairs that mutually reuse all channels allocated to these D2D pairs in cs_l. Note that any D2D pair can belong only to a single coalition. As the global objective of this paper is to maximize the sum communication capacity of D2D pairs, the coalitions are formed so that the sum capacity of D2D pairs is maximized while the minimal capacity C_{min} is still guaranteed for all D2D pairs. Then, the problem is formulated as:

$$\mathbf{CS} = argmax \sum_{n=1}^{n=N} \sum_{k\in K_n} B_k log_2(1+\gamma_{n,k}) \quad (2)$$

$$\text{s.t.} \sum_{k\in K_n} B_k log_2(1+\gamma_{n,k}) \geq C_{min}\ \forall n \in \{1,2,...N\}$$

where the constraint ensures that the sum capacity of any D2D pair n over all channels K_n allocated to the n-th D2D pair

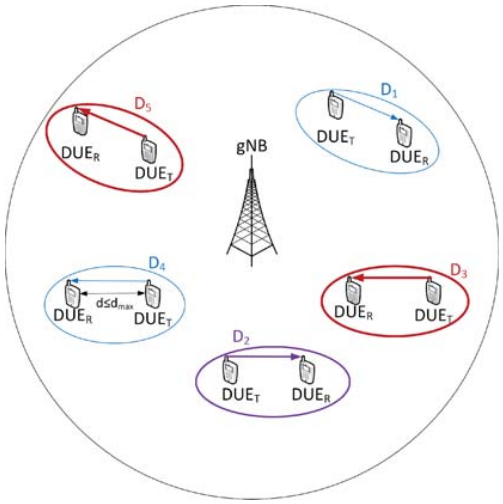

Fig. 1: An example of a coalition structure in a scenario with five D2D pairs, where $\mathbf{CS} = \{cs_1 = \{D_1, D_4\}, cs_2 = \{D_2\}, cs_3 = \{D_3, D_5\}\}$

(including reused channels within the coalition) is not below C_{min}.

Fig. 1 shows an example of five D2D pairs composing a coalition structure $\mathbf{CS}$ that is composed of three coalitions cs_1, cs_2 and cs_3 containing two, one and two D2D pairs, respectively.

Intuitively, we can expect that the D2D pairs that are far from each other have a higher probability to be in the same coalition based on the proposed coalition structure generation. However, finding such pairs simply based on the distance is a very complex problem as we have multiple D2D pairs and there are no limitations neither on how many D2D pairs can be in the same coalition nor on how many coalitions should be created. Thus, the coalition structure generation problem is NP-complete [26]. Moreover, the problem cannot be simply transformed to pure distance-based problem due to a consideration of mutual interference among the D2D pairs reusing the same channel.

III. The Proposed Channel Reuse Scheme

This section describes the novel channel reuse scheme. We propose a low-complexity algorithm solving coalition structure generation problem via sequential bargaining games.

The proposed solution based on the sequential bargaining allows multiple D2D pairs to reuse multiple channels. As a basement, we consider that every D2D pair occupies a single channel allocated initially without reuse (see [15] and [16]).

The proposed sequential bargaining process is defined as follows. First, a utility function is calculated for all possible coalitions of any two D2D pairs (D_i and D_j) in the system. The utility function is defined as:

$$U_{i,j} = \begin{cases} -1 & \text{if } C_{i,i} + C_{i,j} < C_{min} \quad (a) \\ -1 & \text{if } C_{j,i} + C_{j,j} < C_{min} \quad (b) \\ G_{i,j} & Otherwise \qquad\qquad (c) \end{cases} \tag{3}$$

where $C_{i,i}$ and $C_{i,j}$ are the capacities of the i-th D2D pair at the i-th and j-th channels, respectively. Similarly, $C_{j,i}$ and $C_{j,j}$ represent the capacities of the j-th D2D pair at the i-th and j-th channels, respectively. Note that D_i as well as D_j communicate over both channels k_i and k_j in parallel and at the same time. If the reuse would lead to a decrease in the capacity below C_{min} for either of the D2D pairs, the coalition is not created and the utility function $U_{i,j}$ is set to -1. Contrary, if both D2D pairs keep the capacity at least at C_{min} (i.e., neither (a) nor (b) in (3) is fulfilled), a gain $G_{i,j}$, introduced by the new coalition of the D2D pairs D_i and D_j, is calculated. The gain $G_{i,j}$ is understood as the gain in capacity due to mutual sharing of both channels (k_i and k_j) by both pairs (D_i and D_j). Therefore, the gain $G_{i,j}$ is defined as:

$$G_{i,j} = (C_{i,i} + C_{i,j} + C_{j,i} + C_{j,j}) - (C^{nr}_{i,i} + C^{nr}_{j,j}) \tag{4}$$

where $C^{nr}_{i,i}$ and $C^{nr}_{j,j}$ correspond to the capacities of the i-th and the j-th D2D pairs without channel reuse. The pairs D_i and D_j are willing to share their channels among each other if $U_{i,j}$ is positive, i.e., if $G_{i,j} > 0$.

The utility $U_{i,j}$ is obtained for all possible coalitions created by two pairs (i.e., $U_{i,j}$, $\forall D_i, D_j \in N$). We do not calculate utilities for more pairs to keep the complexity of the proposed scheme low. The individual utilities $U_{i,j}$ are, then, inserted into a bilateral utility matrix $\boldsymbol{U}$:

$$\boldsymbol{U} = \begin{bmatrix} 0 & \dots & U_{1,N} \\ \vdots & \ddots & \vdots \\ U_{N,1} & \dots & 0 \end{bmatrix} \tag{5}$$

From the structure of the utility function $U_{i,j}$ and from (4), we can see that the bilateral utility matrix is symmetric (i.e., $U_{i,j} = U_{j,i}$). Moreover, the diagonal values in $\boldsymbol{U}$ are set to 0 as D2D pairs cannot create a coalition with themselves. Since the D2D pairs should create coalition only if $U_{i,j} > 0$, the non-positive elements in (5) are omitted in the remainder of the process. This significantly reduces the complexity of the whole bargaining procedure, since the search space (i.e., number of possible combinations for the coalitions among the D2D pairs) is decreased. Then, the positive elements of $\boldsymbol{U}$ are sorted in a descending order taking into account that every couple of symmetric positive elements is considered as one element ($U_{i,j} = U_{j,i}$). The sorting serves further for the indication of the coalitions' creation priorities so that the coalitions yielding the highest gains are created preferentially.

The sorted positive elements $U_{i,j}$ from $\boldsymbol{U}$ represent a vector of sub-games (denoted as U^*) that are played sequentially over time in a way that one sub-game is played in every time step. The sub-game is played only between two D2D pairs (e.g., D_i and D_j) over their respective channels (k_i and

Algorithm 1 sequential bargaining algorithm to solve channel reuse problem for N D2D pairs

Estimate utility matrix $\boldsymbol{U}$ with size $N \times N$
Extract the positive utilities from the matrix $\boldsymbol{U}$
Sort positive utilities in descending order to a vector $\boldsymbol{U}^*$
Initialize $\mathbf{CS} = \{cs_1, .., cs_N\}$; $cs_i = \{D_i\}$, $\forall i \in \{1, ..., N\}$
for $s = 1 :$ length($\boldsymbol{U}^*$) **do**
  $\boldsymbol{U}^*(s) \sim U_{i,j}$ is sub-game between pairs D_i and D_j
  for every pair D_x from cs_x where $D_i \in cs_x$ **do**
    for every pair D_y from cs_y where $D_j \in cs_y$ **do**
      Determine $U_{x,y}$ from $\boldsymbol{U}^*$
    end for
  end for
  if $U_{x,y} > 0$, $\forall D_x \in cs_x$ and $\forall D_y \in cs_y$ **then**
    Update $\mathbf{CS}$ (i.e., replace cs_x and cs_y with cs_z)
  end if
end for

k_j) allocated in the initial phase. In this case, the coalition is simply created if both D_i and D_j agree to reuse their dedicated channels among each other. However, when some coalitions already exist, the sub-game is extended to all members of all related coalitions. Thus, if the pair D_i wants to join the coalition cs_x composed of two or more D2D pairs, the game is played between the pair D_i and all the D2D pairs already included in the coalition cs_x. The pair D_i joins the coalition cs_x if and only if all the D2D pairs in the cs_x agree, i.e., if $U_{i,j} > 0$, $\forall D_j \in cs_x$.

When all sub-games are finished, the coalitions of the D2D pairs are formed and all D2D pairs included in the same coalition reuse the multiple communication channels belonging to all D2D pairs in the coalition. The algorithm proposed for sequential bargaining-based channel reuse is summarized in Algorithm 1.

IV. Performance evaluation

Simulations in Matlab are carried out to evaluate the performance of the proposed resource allocation scheme and to compare it with competitive algorithms. To this end, simulation scenario and parameters are presented in the next subsections. Then, the competitive algorithms are introduced. Last, the simulation results are described and thoroughly discussed.

A. Simulation scenarios

We consider an area of 500×500 meters. The simulations are performed for 1000 drops. For each drop, the positions of N D2D pairs are generated uniformly within the area. The maximum distance between two devices of the same D2D pair (d_{max}) is set to a default value of 50 m in line with related works ([20]–[22]).

For the modeling of radio channel, we follow 3GPP recommendation for D2D communication defined in [27]. Hence, the path loss model is defined as $PL = 89.5 + 16log_2(d)$, where d is the distance between the transmitter and the receiver. Each D2D pair transmits with a maximum power $p_{max} = 20$ dBm. The background interference from neighboring cells I_d is the same for all D2D pairs at all channels in one drop, and it is modeled over drops randomly using a normal distribution with a mean value of -80 dBm and a standard deviation of 15 dBm. This level of interference from neighboring cells represents a high interference scenario, which can be expected in future mobile networks with dense small cell deployment. The detailed simulations' parameters are summarized in Table I.

TABLE I: Simulation parameters.

RF channel model parameters		
Parameter		Value
Carrier frequency	f_c	2 GHz
Bandwidth	B	20 MHz
Noise power spectral density	σ_o	-174 dBm/Hz
Interference level from neighboring cells	I_d	$\mathcal{N}(-80, 15)$ dBm
General parameters		
Parameter		Value
Number of D2D pairs	N	$10 - 100$
Max. transmission power of D2D pair	p_{max}	20 dBm
Max. distance between DUE_T and DUE_R	d_{max}	50 m

B. Competitive algorithms and performance metrics

To the best of our knowledge, there is no solution targeting the reuse of multiple channels by multiple D2D pairs in dedicated mode. Nevertheless, we compare our proposed algorithm (denoted as "Channel Reuse - SB") with schemes that target similar objectives or address similar problem. Thus, we compare the proposal with the following state of the art schemes:

1) *No reuse* [15],[16]: This scheme, designed for the dedicated mode, distributes the whole available bandwidth B among the D2D pairs in a way that the communication capacity is maximized while C_{min} is guaranteed to each D2D pair. However, the channels cannot be reused by the D2D pairs and each channel is occupied by just one pair.
2) *Single reuse* [17]: In this algorithm, the bandwidth is divided into several (in our case six, according to [17]) channels with equal bandwidths. Every channel is allocated to a single D2D pair (i.e. six D2D pairs are served). The Hungarian algorithm is implemented to solve a matching problem between the six channels and the unserved D2D pairs to enable D2D channel reuse. As defined in [17], up to two D2D pairs can reuse each channel. Thus, the solution allows twelve (2×number of channels) D2D pairs to be served, while the rest of the D2D pairs are provided with no resources. Even if this leads to unfairness among the D2D pairs, it also yields a high sum capacity as only the D2D pairs with high channel quality access the available channels.
3) *Empty channel protocol (ECP)* [18]: For this case, the bandwidth is also divided into several (in our case six according to [18]) channels with equal bandwidths. First, every channel is allocated to a single D2D pair (i.e. six D2D pairs are served). Then, empty channel protocol adds

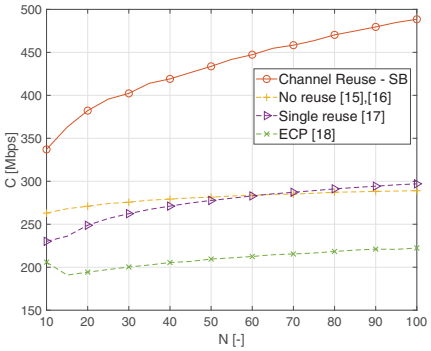

Fig. 2: Sum capacity of D2D pairs over number of D2D pairs for $d_{max} = 50\ m$.

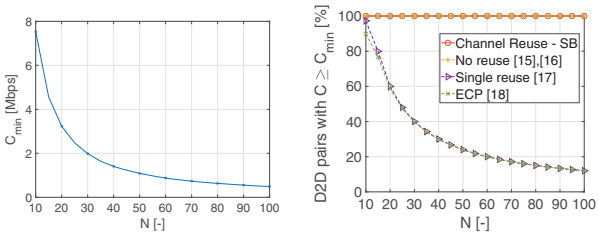

(a) (b)

Fig. 3: Minimum capacity C_{min} that can be guaranteed to all D2D pairs according to [15], [16] (a), and percentage of D2D pairs for which C_{min} is guaranteed by proposed and competitive algorithms (b).

the unserved D2D pairs to the channels so that all unserved D2D pairs reuse the channels already assigned to other D2D pairs. Note that D2D pairs are not allowed to exploit multiple channels simultaneously and only one channel can be used by every D2D pair. Still, each channel can be reused by multiple D2D pairs at the same time.

C. Simulation results

In this section, we compare the performance of the proposed channel reuse scheme with the above-mentioned competitive schemes by means of the sum capacity of D2D pairs defined as $C = \sum_{n=1}^{n=N} \sum_{k \in K_n} C_{n,k}$ and by the ratio of satisfied D2D pairs (i.e., D2D pairs with $C \geq C_{min}$). Further, we analyze feasibility of the proposed scheme via the number of the time steps corresponding to the number of bargaining sub-games needed.

1) Comparison of the proposed scheme with competitive schemes: Fig. 2 illustrates the impact of the number of D2D pairs on the sum capacity of all D2D pairs. The capacity is increasing for the proposed as well as for the competitive algorithms, because the inclusion of a new pair leads to a more efficient exploitation of radio resources over the simulation area. We can see that even for 100 D2D pairs the sum capacity of both No reuse and Single reuse gets only close to 300 Mbps while ECP reaches a sum capacity only slightly above 220 Mbps. The proposed scheme leads to a significant gain with respect to all competitive algorithms. The gain ranges from 28% to 69%, from 46% to 64%, and from 63% to 120% comparing to the No reuse, Single reuse, and ECP algorithms, respectively. The gain increases with the number of D2D pairs, since a higher number of D2D pairs leads to more opportunities for multiple reuse in case of our proposed scheme.

The proposed algorithm is designed to guarantee the minimal capacity C_{min} reached by the D2D pairs without channel reuse (see (2)). The C_{min} is determined according to [15] and [16], as described in Section II-A, and decreases with the number of D2D pairs N, as the bandwidth B is divided among a higher number of the D2D pairs as shown in Fig. 3a. In other words, as explained in Section II-A, Fig. 3a shows the minimum capacity C_{min} guaranteed to every D2D pair depending on the number of deployed D2D pairs disregarding whether the reuse is considered or not. Then, Fig. 3b shows the percentage of the D2D pairs for which the C_{min} is really delivered after the reuse. We can see that our proposed solution for channel reuse guarantees C_{min} to absolutely all D2D pairs. Thus, although every D2D pair is exposed to interference from other D2D pairs in the same coalition, there is no D2D pair that would experience throughput below C_{min}. Also No reuse algorithm (proposed in [15], [16]) can satisfy the C_{min} for all D2D pairs. In contrast, the Single reuse algorithm and the EPC cannot guarantee C_{min} to all D2D pairs due to the equal channel bandwidth allocated to the D2D pairs and due to the limited channel reuse.

2) Feasibility of the proposed scheme: The worst time complexity of Algorithm 1 is $O(N^2 logN)$, but the proposed algorithm is based on bargaining sub-games that are played sequentially over time. Thus, we investigate also the feasibility of the proposed scheme for real networks by the analysis of the convergence of the proposed algorithm. The number of time steps of the proposed algorithm over the number of D2D pairs N to reach 95% and 90% of the maximum capacities is illustrated in Fig. 4a and Fig. 4b, respectively. The figures confirm that reaching 95% and 90% of the maximum capacity is very quick even for a high number of D2D pairs. For realistic scenarios with, for example, 40 D2D pairs, only eight and six steps (bargaining sub-games) are needed in average to reach 95% and 90% of the maximum sum D2D capacity, respectively. Even for 100 D2D pairs (which is rather an extreme case for our considered area of 500×500 m), we still need only less than 12 and 9 time steps in average to reach 95% and 90% of the maximum capacity. This confirms the fast convergence of the proposed algorithm and its suitability for practical applications and implementation in real networks.

V. Conclusion

In this paper we have proposed a new channel reuse scheme for the D2D communication in dedicated mode allowing multiple pairs to reuse multiple channels. The channel reuse

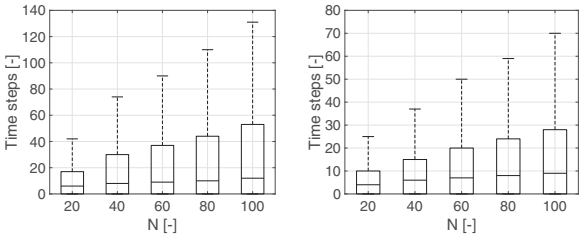

(a) (b)

Fig. 4: Number of time steps corresponding to number of bargaining sub-games required to reach 95% (a) and 90% (b) of the sum capacity of D2D pairs.

is presented as a coalition structure generation game where the D2D pairs composing one coalition mutually reuse the channels of each other. The coalition structure generation problem is solved by the proposed low complexity sequential bargaining algorithm. The simulation results show that the proposed channel reuse increases the sum capacity of D2D pairs by $28 - 64\%$ comparing to the best performing existing algorithm. In addition, although the interference is imposed among D2D pairs reusing the same channel, the minimal required capacity for each D2D pair is still guaranteed after the channel reuse.

The future work should focus on deriving the optimal coalition structure as an upper bound for the proposed channel reuse. In addition, a power allocation for each D2D pair over the reused channels should be investigated.

ACKNOWLEDGMENT

This work has been supported by grant No. GA17-17538S funded by Czech Science Foundation and by the grants of Czech Technical University in Prague No. SGS17/184/OHK3/3T/13.

REFERENCES

[1] M. N. Tehrani, at al., "Device-to-Device Communication in 5G Cellular Networks: Challenges, Solutions, and Future Directions," *IEEE Communications Magazine*, 52(5), pp. 86–92, 2014.

[2] P. Mach, at al., "In-band device-to-device communication in OFDMA cellular networks: A survey and challenges," *IEEE Communications Surveys & Tutorials*, vol. 17, no. 4, pp. 1885–1922, 2015.

[3] X. Huang, at al., "Dynamic femtocell gNB on/off strategies and seamless dual connectivity in 5G heterogeneous cellular networks," *IEEE Access*, vol. 6, pp. 21359–21368, 2018.

[4] D. Zhai, at al., "Energy-saving resource management for D2D and cellular coexisting networks enhanced by hybrid multiple access technologies," *IEEE Transactions on Wireless Communications*, 16(4), pp. 2678–2692, 2017.

[5] P. Mach, at al., "Combined Shared and Dedicated Resource Allocation for D2D communication," *IEEE 87th Vehicular Technology Conference (VTC-Spring)*, pp. 1–7, 2018.

[6] T. Liu, and G. Wang, "Resource allocation for device-to-device communications as an underlay using nash bargaining game theory," *2015 Information and Communication Technology Convergence (ICTC)*, pp. 366–371, 2015.

[7] S. A. Kazmi, at al., "Mode Selection and Resource Allocation in Device-to-Device Communications: A Matching Game Approach," *IEEE Transactions on Mobile Computing*, 16(11), pp. 3126-3141, 2017.

[8] W. Zhao, and S. Wang, "Resource sharing scheme for device-to-device communication underlaying cellular networks," *IEEE Transactions on Communications*, 63(12), pp. 4838–4848, 2015.

[9] R. Wang, at al. "Qos-aware joint mode selection and channel assignment for D2D communications," *IEEE International Conference on Communications (ICC)*, pp. 1–6, 2016.

[10] R. AliHemmati, at al., "Power Allocation for Underlay Device-to-Device Communication over Multiple Channelsular networks," *IEEE Transactions on Signal and Information Processing over Networks*, 4(3), pp. 467–480, 2018.

[11] R. AliHemmati, at al., "Multi-Channel Resource Allocation Toward Ergodic Rate Maximization for Underlay Device-to-Device Communications," *IEEE Transactions on Wireless Communications*, 17(2), pp. 1011–1025, 2018.

[12] Y. Qian, at al., "Resource allocation for multichannel device-to-device communications underlaying QoS-protected cellular networks," *IET Communications*, 11(4), pp. 558–565, 2017.

[13] P. Mach, at al.,, "Resource Allocation for D2D communication with Multiple D2D pairs reusing Multiple Channels," *IEEE Wireless Communications Letters*, 2019.

[14] R. Yin, at al., "Joint spectrum and power allocation for D2D communications underlaying cellular networks," *IEEE Transactions on Vehicular Technology*, 65(4), pp. 2182–2195, 2016.

[15] Y. Huang, at al., "Mode selection, resource allocation, and power control for D2D-enabled two-tier cellular network," *IEEE Transactions on Communications*, 64(8), pp. 3534–3547, 2016.

[16] C. H. Yu, at al., "Resource sharing optimization for device-to-device communication underlaying cellular networks," *IEEE Transactions on Wireless Communications*, 10(8), pp. 2752–2763, 2011.

[17] Y. Li, at al.,"Joint mode selection and resource allocation for D2D communications under queueing constraints," *IEEE Conference on Computer Communications Workshops (INFOCOM WKSHPS)*, pp. 490-495, 2016.

[18] D. Ma, at al.,"Resource allocation for hybrid mode device-to-device communication networks," *8th International Conference on Wireless Communications & Signal Processing (WCSP)*, pp. 1-5, 2016.

[19] J. Dai, at al., "Analytical modeling of resource allocation in D2D overlaying multihop multichannel uplink cellular networks," *IEEE Transactions on Vehicular Technology*, 66(8), pp. 6633–6644, 2017.

[20] M. Pischella, at al., "A Joint Multiplexing and Resource Allocation Algorithm for Asynchronous Underlay D2D Communications," *IEEE 87th Vehicular Technology Conference (VTC Spring)*, pp. 1–5, 2018.

[21] L. Melki, at al., "Interference management scheme for network-assisted multi-hop D2D communications," *IEEE 27th Annual International Symposium on Personal, Indoor, and Mobile Radio Communications (PIMRC)*, pp. 1–5, 2016.

[22] T. D. Hoang, at al., "Energy-efficient resource allocation for D2D communications in cellular networks," *IEEE Transactions on Vehicular Technology*, 65(9), pp. 6972–6986, 2016.

[23] W. Lee, at al., "Transmit Power Control Using Deep Neural Network for Underlay Device-to-Device Communication," *IEEE Wireless Communications Letters*, 8(1), pp. 141–144, 2019.

[24] T. Rahwan, and N. R. Jennings,"An improved dynamic programming algorithm for coalition structure generation," *Proceedings of the 7th international joint conference on Autonomous agents and multiagent systems*, vol. 3, pp. 1417–1420, 2008.

[25] T. Rahwan at al.,"An anytime algorithm for optimal coalition structure generation," *Journal of artificial intelligence research*, vol. 34, pp. 527–567, 2009.

[26] T. Rahwan at al.,"A Coalition structure generation: A survey," *Artificial Intelligence*, vol. 229, pp. 139–174, 2015.

[27] 3GPP TR 36.843, "Study on LTE device to device proximity services; Radio aspects," v12.0.1, Release 12, 2014.

X. Appendix C

This appendix includes journal paper published in: M. Najla, Z. Becvar, and **P. Mach**, "Reuse of Multiple Channels by Multiple D2D Pairs in Dedicated Mode: Game Theoretic Approach," *IEEE Transactions on Wireless Communications*, vol. 20, no. 7, pp. 4313-4327, July 2021. IF (JCR 2022) = **10.4**.

Reuse of Multiple Channels by Multiple D2D Pairs in Dedicated Mode: A Game Theoretic Approach

Mehyar Najla, *Member, IEEE*, Zdenek Becvar, *Senior Member, IEEE*, and Pavel Mach, *Member, IEEE*

***Abstract*— Device-to-device communication (D2D) is expected to accommodate high data rates and to increase the spectral efficiency of mobile networks. The D2D pairs can opportunistically exploit channels that are not allocated to conventional users in a dedicated mode. To increase the sum capacity of D2D pairs in the dedicated mode, we propose a novel solution that allows the reuse of multiple channels by multiple D2D pairs. In the first step, the bandwidth is split among D2D pairs so that each pair communicates at a single channel that guarantees a minimal capacity for each pair. Then, the channel reuse is facilitated via a grouping of the D2D pairs into coalitions. The D2D pairs within one coalition mutually reuse the channels of each other. We propose two approaches for the creation of the coalitions. The first approach reaches an upper-bound capacity by optimal coalitions determined by the dynamic programming. However, such approach is of a high complexity. Thus, we also introduce a low-complexity algorithm, based on the sequential bargaining, reaching a close-to-optimal capacity. Moreover, we also determine the transmission power allocated to each reused channel. Simulations show that the proposed solution triples the sum capacity of the state-of-the-art algorithm with the highest performance.**

***Index Terms*— Device-to-device, dedicated mode, game theory, resource allocation, channel reuse.**

I. Introduction

HIGH data rates and low latencies are required to enable new services and to increase the number of connected devices in the future mobile networks. To accommodate these demands, a direct communication between two user equipments (UEs) in proximity of each other, known as Device-to-Device (D2D) communication, is considered as a promising technology [1]–[3]. Two D2D UEs (DUEs), a transmitter (DUE_T) and a receiver (DUE_R), create a single D2D pair, within which the data is transmitted directly, i.e., without being relayed through a base station (in this paper, denoted as gNB in line with 3GPP terminology for 5G mobile networks) [4].

The D2D communication enables two possible modes: 1) a *shared mode* in which the D2D pairs reuse the resources allocated to common cellular UEs (CUEs) communicating via the gNB and 2) a *dedicated mode* in which the D2D pairs use dedicated resources that are not assigned to the CUEs [5], [6]. Although, the shared mode offers a higher spectral efficiency than the dedicated one, the higher efficiency is usually at the cost of highly complex solutions for the resource allocation and management. Moreover, the shared mode leads to a mutual interference among the CUEs and the DUEs. This interference can be too high and can vary frequently and significantly, especially in the case with a dense presence of the UEs. Consequently, the reliability of the communication cannot be easily guaranteed and overall quality of services (QoS) can be impaired due to the interference in the shared mode [7]. Thus, the DUEs with strict requirements on QoS should prefer the dedicated mode, which is suitable for the services that require highly reliable communication with a minimum risk of an unexpected interference from the CUEs. Concrete and up-and-coming examples of the use cases for the dedicated mode are the direct communication of vehicles or public safety communication. Then, an ultra-reliable communication with a guaranteed minimum communication capacity should be ensured. In the shared mode, however, interference might lead to the situations when such guarantee is simply not possible and the unreliability in the communication can have grievous consequences. Hence, the dedicated resources are commonly considered for the vehicular or public safety communications. Thus, in this paper, we focus on the dedicated mode for D2D communication.

One of the key challenges in the dedicated mode is the allocation of the available bandwidth to the D2D pairs. The authors in [8] and [9] present channel allocation schemes dividing a dedicated bandwidth to channels with different bandwidths so each D2D pair gets exactly one channel. In both [8] and [9], the optimal allocation is achieved for the case when the interference from other neighboring cells is nonexistent. However, in real networks, the interference from other cells always exists and we can expect the level of interference will even increase in the future due to the densification of mobile networks. Such inter-cell interference impacts the optimal channel allocation for the D2D pairs in the dedicated mode. Moreover, neither [8] nor [9] assume the reuse of each channel by more than one D2D pair resulting in a low spectral efficiency.

A simplified channel reuse in the dedicated mode is presented in [10]–[12]. Although all these studies consider that either two D2D pairs [10] or multiple D2D pairs [11], [12] can access the same channel, each D2D pair is allowed to occupy

Manuscript received June 3, 2019; revised November 20, 2019, March 27, 2020, July 2, 2020, and November 23, 2020; accepted February 1, 2021. Date of publication February 17, 2021; date of current version July 12, 2021. This work was supported by Czech Science Foundation under Grant GA17-17538S, by Ministry of Education, Youth and Sport of the Czech Republic under Grant LTT20004, and by Czech Technical University in Prague under Grants SGS17/184/OHK3/3T/13. The associate editor coordinating the review of this article and approving it for publication was L. Musavian. *(Corresponding author: Zdenek Becvar.)*

The authors are with the Faculty of Electrical Engineering, Czech Technical University in Prague, 166 27 Prague, Czechia (e-mail: najlameh@fel.cvut.cz; zdenek.becvar@fel.cvut.cz; machp2@fel.cvut.cz).

Color versions of one or more figures in this article are available at https://doi.org/10.1109/TWC.2021.3057825.

Digital Object Identifier 10.1109/TWC.2021.3057825

just one channel at any time. The papers [13]–[15] exploit the reuse of multiple channels by multiple D2D pairs to guarantee a minimal SINR for every D2D pair while using the minimal possible number of channels. In these works, however, the D2D pairs do not benefit fully from the reuse, as only a limited number of channels is used and the sum capacity is not maximized. In [16], the authors maximize the sum capacity of D2D pairs in the dedicated mode considering that the D2D pairs reuse all available channels. Nevertheless, the authors do not consider the constraint on the minimal capacity C_{min} that should be guaranteed to the individual D2D pairs. Thus, the solution proposed in [16] can lead to the situation when some D2D pairs end up with zero capacity as these are forbidden to transmit at any channel due to the interference caused to other D2D pairs. Note that the ideas presented in [13]–[16] cannot be easily extended to maximize the sum capacity and, at the same time, to guarantee C_{min}, since the capacity maximization under the constraint on C_{min} for every D2D pair requires completely different solutions.

In summary, the existing resource allocation methods for the dedicated mode either restrict the number of D2D pairs reusing a single channel (e.g., [8], [9]) or limit the number of channels that can be occupied by a single D2D pair (e.g., [10]–[12]). As an exception, the papers [13]–[16] allow the reuse of multiple channels by multiple D2D pairs in the dedicated mode. These papers target either the sum capacity maximization ([16]) or the individual minimal capacity (C_{min}) satisfaction ([13]–[15]). However, none of these papers maximizes the sum capacity while guaranteeing C_{min} to every D2D pair.

Despite our focus on the dedicated mode in this paper, we survey also research targeting the shared mode and we also summarize related works on the channel reuse not considering D2D communication at all in order to justify the novelty of our solution from a broader perspective. Most of the existing channel allocation algorithms in the shared mode assume a restriction on either the number of D2D pairs that can reuse a single channel [17]–[21] or the number of channels that can be occupied by each D2D pair [22]–[30]. An exception to these restrictions is represented by [31] and [32]. These papers allow the reuse of multiple channels by multiple D2D pairs in the shared mode. Nevertheless, the channel allocation approaches from [31] and [32] depend on the presence of the CUEs. In other words, the optimized utility function in [31] is convex only if the interference caused to the CUEs by the D2D pairs is taken into account. The utility function becomes non-convex if the dedicated mode is considered and the presented solution becomes infeasible. Similarly, in [32], the presented solution adds the D2D pairs sequentially to the channels, which are already occupied by the CUEs. Hence, the decision of the D2D pairs whether to communicate over the given channel or not is based on the interference from/to the CUEs. Moreover, when the D2D pair reuses the channel according to [32], the D2D pair sets its transmission power at this channel based on the allowed interference imposed by this D2D pair to the corresponding CUE. Considering this, the channel and power allocations in [32] essentially depend on the existence of the CUEs that are completely absent in the dedicated mode and can be absent even in the shared mode with (very realistic) situation when the CUEs do not occupy all channels.

Besides the work addressing the reuse of channels for D2D communication, ongoing research is focused also on multiple links communicating over multiple channels for other scenarios and concepts. For example, in [33], many-to-many matching game is exploited to allocate multiple channels to multiple cellular links (i.e., links from multiple UEs to the gNB) in non-orthogonal multiple access-based networks. Since the matching games generally fall into the category of non-cooperative games, every link aims to selfishly maximize its own capacity. Consequently, the matching approach does not guarantee any C_{min} to individual links. Although the cooperative "coalitions' formation games" are also used widely for the channel reuse problem, e.g., in cognitive femtocell networks [34] or in cloud radio access networks [35], these approaches allow the users in the coalition to reuse a single channel only. Moreover, both [34] and [35] cannot be simply extended to the case where the UEs can access multiple channels, because [34] considers the coalitions' creation problem in the partition form (different problem compared to channel reuse problem in D2D communication) and [35] solves the coalitions' formation problem with a predefined final number of coalitions, but this number is usually not known in advance as it should be an output of the optimization.

In our paper, we focus on the resource allocation in D2D dedicated mode and we propose a solution that allows the reuse of multiple channels by multiple D2D pairs to maximize the sum capacity while guaranteeing C_{min} to individual D2D pairs. The major contributions of the paper are summarized as follows:

- We present and solve the problem of reusing multiple channels by multiple pairs as a coalition structure generation problem in order to put the D2D pairs into disjoint coalitions in a way that all D2D pairs in the same coalition can reuse the channels of each other. We derive the optimal coalitions by means of the dynamic programming reaching a theoretical maximum sum capacity while each D2D pair is still guaranteed to receive at least C_{min}.
- Since the dynamic programming is of a high complexity, we also propose a sequential bargaining game to determine the coalitions of the D2D pairs mutually reusing multiple channels. The heuristic sequential bargaining-based approach is of a low complexity and reaches a close-to-optimal performance.
- In order to facilitate the channel reuse in an efficient way, we analytically derive the optimal initial channel bandwidth allocation for the D2D pairs in the dedicated mode if interference from other cells is considered.
- Furthermore, we analytically determine the optimal allocation of the DUEs' transmission power over the reused channels within the coalitions. Since the defined optimization problem for power allocation is not convex, we approximate the problem to the convex one and we discuss the assumptions under which this approximation is realistic.

- We demonstrate that the proposed solution combining the initial allocation of the bandwidth available to the D2D pairs, the novel reuse of multiple channels by multiple D2D pairs exploiting sequential bargaining game, and the proposed power allocation significantly outperforms state-of-the-art solutions and reaches close-to-optimal sum capacity of the D2D pairs. Moreover, we show that our proposed algorithm is of a low complexity and exhibits very short convergence time. This allows its implementation in real networks.

Note that a basic idea of the sequential bargaining solution for the coalitions' creation in its simplified version and without any optimization of bandwidth and power allocations is presented in our prior conference paper [36].

The rest of the paper is organized as follows. In Section II, the system model is described and the targeted problem is formulated. In Section III, the proposed resource allocation scheme for D2D communication in the dedicated mode is presented. The simulations results are discussed in Section IV. Last, Section V concludes the paper and outlines possible future research directions.

II. System Model and Problem Formulation

In this section, we first describe the system model and, then, we formulate the problem, which is solved later in the next sections of this paper.

A. System Model

In our model, N D2D pairs are uniformly deployed within an area. Each D2D pair is composed of one DUE_T and one DUE_R. The DUE_T and the DUE_R in a single D2D pair are fixed for a specific time interval (such as, e.g., a communication session during which the transmitter sends data to the receiver). This consideration is in line with the common purpose of the D2D communication when a high amount of data is transmitted from one device to another, as in, e.g., [37].

The whole bandwidth B dedicated for D2D communication is split into $K = N$ channels (as in [8] and [9]) to serve all N D2D pairs. The capacity of the n-th D2D pair at the k-th channel ($C_{n,k}$) is defined as:

$$\begin{aligned} C_{n,k} &= B_k log_2\left(1+\gamma_{n,k}\right) \\ &= B_k log_2\left(1+\frac{p_{n,k}\, g_{n,n}}{\sigma_o B_k + \sum_{\substack{t\in N_k \\ t\neq n}} p_{t,k} g_{t,n} + I_d}\right) \end{aligned} \quad (1)$$

where B_k is the bandwidth of the k-th channel, $\gamma_{n,k}$ is the signal to interference plus noise ratio (SINR) of the n-th D2D pair at the k-th channel, $p_{n,k}$ is the transmission power of the n-th DUE_T at the k-th channel, $g_{n,n}$ is the channel gain between the n-th DUE_T and the n-th DUE_R, $p_{t,k}$ is the transmission power of the t-th DUE_T at the k-th channel, $g_{t,n}$ is the channel gain between the t-th DUE_T and the n-th DUE_R, N_k represents the set of D2D pairs communicating at the k-th channel, σ_o is the white noise power spectral density [38], and I_d stands for the background interference received from adjacent cells. The background interference is measured by the receiver of each D2D pair and reported to the gNB. As this interference represents the sum interference from all sources (namely the interference from neighboring gNBs and UEs in other cells), it can be derived from RSRP/RSRQ reported even in a conventional network according to 3GPP. Note that we focus on the dedicated mode, where the D2D pairs experience no interference from the CUEs in the same cell. Consequently, the CUEs are not considered.

Without loss of generality, we define C_{min}, based on [8] and [9], as the minimal capacity that can be guaranteed to the D2D pair with the worst SINR if the total bandwidth is split among N D2D pairs proportionally to $g_{n,n}$ (i.e., $B_n = \frac{g_{n,n}}{\sum_{n=1}^{n=N} g_{n,n}}$). Taking this into consideration, C_{min} is defined as:

$$C_{min} = \frac{g_{n,n}^{min}}{\sum_{n=1}^{n=N} g_{n,n}} B\ log_2\left(1+\frac{P_{max}\, g_{n,n}^{min}}{\sigma_o \frac{g_{n,n}^{min}}{\sum_{n=1}^{n=N} g_{n,n}} B + I_d}\right) \quad (2)$$

where $g_{n,n}^{min}$ is the minimal channel gain among all D2D pairs, i.e., $g_{n,n}^{min} = min\{g_{i,i}\},\ \forall i = 1,\ldots,N$, and P_{max} is the maximal transmission power that can be used by the D2D pair over all channels. Note that P_{max} in (2) is considered in order to achieve the highest possible C_{min} that can be guaranteed to each D2D pair. The value of C_{min} decreases if the number of D2D pairs increases in order to serve all D2D pairs with at least C_{min}.

In our system model, we adopt the following assumptions:

Assumption 1: We consider that the distance d between the DUE_T and the DUE_R creating one D2D pair is at most equal to a maximal distance d_{max} (i.e., $d \leq d_{max}$) to guarantee a reliable D2D communication.

Assumption 2: We consider a fully controlled D2D communication, where the gNB is aware of the devices under its coverage and manages them. This is in line with the implementation of the D2D communication expected in 3GPP-based mobile networks, see, e.g., [42].

Assumption 3: We assume full knowledge of channel state information (CSI) in our system. Although full CSI knowledge can imply a high signaling overhead, such assumption is commonly adopted in many recent papers, e.g., [17], [18], [43]–[45]. Moreover, there are already works that relax this problem and allow to determine the channel gains among all D2D pairs at a very low cost, see for example, [46], where deep neural networks are exploited to predict the D2D channel gains with a very high accuracy with almost no additional overhead.

Assumption 4: We focus on a common interference-limited mobile network [47]–[49], where the interference is a key limiting factor and overrules the impact of noise. This allows to adopt the approximation $\sigma + I_d = I_d$ later in Appendix A.

B. Problem Formulation

The objective of this paper is to maximize the sum communication capacity of the D2D pairs in the dedicated mode while the minimum capacity is guaranteed to each D2D pair. The sum capacity is maximized by an efficient allocation of the communication channels and their reuse in such a way

that multiple channels can be reused by multiple D2D pairs. We denote the set of L coalitions of the D2D pairs as $\mathbf{CS} = \{cs_1, cs_2, \ldots cs_L\}$. Each coalition cs_l includes all D2D pairs that mutually reuse all channels allocated to all D2D pairs in cs_l. The coalitions are formed so that the sum capacity of the D2D pairs is maximized while the minimal capacity C_{min} of each D2D pair is still guaranteed. To improve the sum capacity, we also determine a vector $\mathbf{B}$ of the communication channels bandwidths for all N D2D pairs, i.e., $\mathbf{B} = \{B_1, B_2, \ldots, B_N\}$. To exploit the overall bandwidth allocated to each D2D pair (including reused channels) efficiently, we further find a set of vectors $\mathbf{P} = \{P_1, P_2, \ldots, P_N\}$, where every vector P_n contains the transmission powers of the n-th D2D pair at all channels allocated to this pair. Note that every vector P_n is of $|K_n|$ length, where K_n is the subset of channels allocated to the n-th D2D pair. Hence, K_n contains all channels of all D2D pairs, which are in the same coalition with the n-th pair. The optimization problem over $\mathbf{B}$, $\mathbf{CS}$, and $\mathbf{P}$ is then formulated as:

$$
\begin{aligned}
&\mathbf{B}^*, \mathbf{CS}^*, \mathbf{P}^* \\
&= \underset{\mathbf{B},\mathbf{CS},\mathbf{P}}{\operatorname{argmax}} \sum_{n=1}^{n=N} \sum_{k \in K_n} B_k log_2 \left(1 + \gamma_{n,k}\right) \\
&\quad \text{s.t.} \sum_{k \in K_n} B_k log_2(1+\gamma_{n,k}) \geq C_{min} \quad \forall n \in \{1, 2, \ldots N\} \quad (a) \\
&\qquad 0 < B_n \leq B \quad \forall n \in \{1, 2, \ldots N\} \quad (b) \\
&\qquad \sum_{n=1}^{n=N} B_n = B \quad (c) \\
&\qquad \sum_{k \in K_n} p_{n,k} = P_{max} \quad \forall n \in \{1, 2, \ldots N\} \quad (d)
\end{aligned} \tag{3}
$$

where $\mathbf{B}^*$, $\mathbf{CS}^*$, and $\mathbf{P}^*$ are the optimal $\mathbf{B}$, $\mathbf{CS}$, and $\mathbf{P}$, respectively. The constraint (a) ensures that the sum capacity of any D2D pair over all the channels allocated to this pair (including the reused channels within the coalition) is not below C_{min}, (b) limits the size of each channel with respect to the maximum available bandwidth B, (c) guarantees that the sum of all channel bandwidths is equal to B (i.e., that the dedicated spectrum is fully utilized to maximize the capacity), and (d) limits the sum transmission power of each D2D pair over all channels to the maximal allowed transmission power P_{max}.

The problem defined in (3) is a non-convex mixed integer non-linear programming (MINLP) as the coalitions' formation represents an integer programming problem [53] while the bandwidth allocation and the power allocation represent continuous non-integer variables. The MINLP problems are known to be NP-hard. Nevertheless, theoretically, the joint solution of problem (3) is numerically derivable via the common approach for solving MINLP problems, i.e., optimizing the continuous variables ($\mathbf{B}$ and $\mathbf{P}$) at all feasible settings of the discrete variables ($\mathbf{CS}$). The optimization of both continuous variables is an NLP problem that is solvable via the interior point method. However, the joint numerical solution is not practical due to its very high complexity and its feasibility only for very few D2D pairs, as previously mentioned. Therefore, in the next section, we solve the optimization problem from (3) by determining, sequentially, the bandwidth allocation, the coalitions' formation and the power allocation. However, later in Section IV, we still derive the joint numerical solution when few pairs are present, in order to prove that the proposed sequential solution introduces only minor losses in the performance compared to the joint solution.

III. The Proposed Resource Allocation Scheme

To solve the optimization problem from (3), we separate it into three sub-problems. First, we analytically derive the channel bandwidth allocated to each D2D pair in the initial phase (i.e., determination of $\mathbf{B}$). Second, we solve the coalitions' creation problem allowing the reuse of multiple channels by multiple D2D pairs (i.e., determination of $\mathbf{CS}$). The channel reuse problem is solved by the dynamic programming, which composes the optimal coalition structure and demonstrates an upper bound performance. However, the dynamic programming is of a high complexity, which makes it impractical for real networks. Thus, we propose also a low-complexity algorithm based on the sequential bargaining to handle the reuse. Third, we determine the power allocation for the D2D pairs at each channel (i.e., determination of $\mathbf{P}$). Note that, in the following subsections, the solutions solving the sub-problems of bandwidth allocation, coalitions' formation, and power allocation are denoted as $\mathbf{B}^{**}$, $\mathbf{CS}^{**}$, and $\mathbf{P}^{**}$, respectively.

A. Initial Allocation of Channel Bandwidth for Individual D2D Pairs

Before the channel reuse by D2D pairs takes place, each D2D pair is allocated with a dedicated channel of a certain bandwidth to guarantee the required channel capacity C_{min} for all D2D pairs. This channel can be then reused by other pairs in the main phase of the proposed approach (described in the next subsections). The sub-problem of optimizing $\mathbf{B}$ from the problem defined in (3) is reformulated as:

$$
\begin{aligned}
\mathbf{B}^{**} = \underset{\mathbf{B}}{\operatorname{argmax}} & \sum_{n=1}^{n=N} B_n log_2 \left(1 + \gamma_{n,n}\right) \\
\text{s.t. } & C_{n,n}^{nr} = B_n log_2 \left(1 + \gamma_{n,n}\right) \geq C_{min} \\
& \forall n \in \{1, 2, \ldots N\} \quad (a) \\
& (b), (c) \quad \text{taken from } (3)
\end{aligned} \tag{4}
$$

where $\gamma_{n,n} = \frac{p_{n,n}\, g_{n,n}}{\sigma_o B_n + I_d}$ is the SINR of the n-th D2D pair at the n-th dedicated channel with no-reuse and the constraint (a) ensures that the capacity of every n-th D2D pair at the n-th dedicated channel with no-reuse ($C_{n,n}^{nr}$) is, at least, equal to the minimal required capacity C_{min}. It is worth to mention that each D2D pair can transmit with P_{max} (i.e., $p_{n,n} = P_{max}$) at its allocated channel in this initial phase, because only one channel without reuse is exploited by each D2D pair and the interference among the D2D pairs is absent in this phase.

The solution of (4) for the case with no interference from the adjacent cells (i.e., with $I_d = 0$) is derived in [8] and [9]. However, in a realistic case with a dense deployment of cells and a high density of communicating UEs, the interference I_d

is significant with respect to the noise and cannot be neglected. In such case, the solution proposed in [8] and [9] is not optimal. Thus, we determine the optimal allocation of the bandwidth for the channel assigned to each D2D pair initially (without channel reuse) in the following proposition.

Proposition 1: Considering the background interference from the adjacent cells I_d, the optimal allocation of the bandwidth B_n to the n-th channel assigned to the n-th D2D pair guaranteeing the fulfillment of C_{min} for all D2D pairs is:

$$B_n = \frac{C_{min}}{log_2\left(1+\frac{P_{max}g_{n,n}}{\sigma_o \frac{g^{min}_{n,n}}{\sum_{n=1}^{n=N} g_{n,n}} B + I_d}\right)} \tag{5}$$

Proof: The proof of Proposition 1 is in Appendix A. ■

If $\sum_{n=1}^{n=N} B_n < B$ after the channel allocation, the rest of the bandwidth is added to the channel of the D2D pair with the highest $g_{n,n}$ in order to maximize the sum capacity of the D2D pairs as defined in (4). Consequently, the highest capacity in the initial allocation phase is achieved by the D2D pair with the best channel quality similarly like in [8] and [9]. Then, with a high probability, this particular D2D pair forms a coalition with other pairs during the generation of the coalition structure (as described in the next subsection). Thus, the above-mentioned assignment of the rest of the bandwidth is beneficial for other D2D pairs as their capacity can be significantly enhanced as well by joining the coalition, which contains the D2D pair with the highest $g_{n,n}$.

The initial resource allocation is centrally managed by the gNB based on the knowledge of the channel quality of all D2D pairs in a similar way as assumed, e.g., in [17], [18], or [43].

B. Optimal Coalition Structure Generation for Channel Reuse

After the initial channel bandwidth allocation to the D2D pairs, the reuse of channels is implemented. To determine which D2D pairs should mutually reuse their channels, we formulate the problem of coalitions' formation. The problem is understood as a coalition structure generation problem in game theory [51]–[53]. For any set of players, the coalition structure is a set of coalitions $\mathbf{CS}= \{cs_1, cs_2, \ldots, cs_L\}$ such that each element $cs_l \in \mathbf{CS}$ is the set of players composing one coalition. Note that each player can belong only to a single coalition. For our channel reuse case, the problem is to find the coalition structure over N D2D pairs in such a way that the D2D pairs in each coalition mutually reuse the channels of each other. Based on this, our goal is to find the coalition structure that maximizes the sum capacity of D2D pairs while guaranteeing the minimal capacity required by each pair. Consequently, the sub-problem of optimizing **CS**, from the problem defined in (3), is written as:

$$\mathbf{CS}^{**} = \underset{\mathbf{CS}}{\operatorname{argmax}} \sum_{n=1}^{n=N} \sum_{k\in K_n} B_k log_2\left(1+\gamma_{n,k}\right)$$
$$\text{s.t. } (a)-(d) \text{ taken from } (3) \tag{6}$$

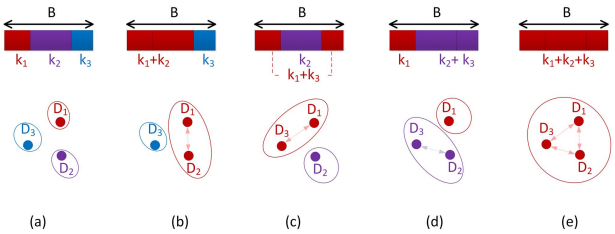

Fig. 1. The possible coalitions' creation for three D2D pairs. Note that the dashed arrows represent the interference introduced by the channel reuse.

Fig. 1 illustrates the channel reuse problem presented as a coalition structure generation with an example of three D2D pairs (i.e., three players' coalition structure game). The example represents all possible coalitions created for the problem of three D2D pairs. Note that the D2D pairs within the same coalition transmit at the same time over all channels of all D2D pairs in the same coalition. For example, if three D2D pairs create one coalition (as in Fig. 1e), all these D2D pairs transmit over all three channels simultaneously and mutually interfere with each other. The D2D pairs in different coalitions are supposed to transmit at the same time, but at different channel(s), thus no interference occurs among the different coalitions.

To find the optimal solution for the problem defined in (6) and to determine the optimal structure of the coalitions, the dynamic programming [53], [54] is a suitable solution. In the dynamic programming, the values of a gain function V for each possible coalition cs_x composed of X D2D pairs (where $X \in \{1, 2, \ldots, N\}$) should be calculated. However, the problem defined in (6) is different from the general coalition structure generation problems due to the constraint (a). Therefore, in order to solve (6), the gain function should take the constraint (a) into account to guarantee C_{min} for each D2D pair even after the channel reuse. Thus, we build up the gain function $V(cs_x)$ of the coalition cs_x, which is composed of X D2D pairs, as follows:

$$V(cs_x) = \begin{cases} C_{cs_x} & \text{if } C_{D_y} > C_{min},\ \forall D_y \in cs_x \\ 0 & \text{otherwise} \end{cases} \tag{7}$$

where C_{cs_x} is the sum capacity of all D2D pairs in the coalition cs_x mutually reusing the channels of all D2D pairs in cs_x, and C_{D_y} is the sum capacity of the D2D pair D_y over the communication channels, including the reused channels, in cs_x (note that D_y represents the y-th D2D pair from the coalition cs_x). Note that to calculate (7), the transmission powers of the D2D pairs over the reused channels are optimized based on subsection III-D presented later in this paper.

The dynamic programming-based solution is of a high complexity as the general complexity of dynamic programming is $\mathcal{O}(3^N)$, where N is the number of D2D pairs. Thus, such solution is not practical for the real networks and we propose a low-complexity algorithm in the next subsection to solve the coalitions' creation problem.

C. Low-Complexity Channel Reuse Based on Sequential Bargaining

In this subsection, we describe the proposed low-complexity algorithm for the channel reuse to solve (6). The proposed solution is based on the sequential bargaining allowing multiple D2D pairs to reuse multiple channels simultaneously. This reuse is enabled by the fact that all D2D pairs in the same coalition always use all channels allocated to them previously during the initial allocation phase (as shown in Fig. 1e). Moreover, all channels in the coalition are used simultaneously by all D2D pairs in that particular coalition.

Before the proposed sequential bargaining process is initiated, we calculate the utilities for all possible coalitions of any two D2D pairs (D_i and D_j) in the system. The utility function is defined as:

$$U_{i,j} = \begin{cases} -\infty & \text{if } C_{i,i} + C_{i,j} < C_{min} \\ -\infty & \text{if } C_{j,i} + C_{j,j} < C_{min} \\ G_{i,j} & \text{otherwise} \end{cases} \quad (8)$$

where $C_{i,i}$ ($C_{j,i}$) and $C_{i,j}$ ($C_{j,j}$) are the capacities of the i-th (j-th) D2D pair at the i-th and j-th channels, respectively. If the reuse would lead to a decrease in the capacity below C_{min} for any of the D2D pairs, the coalition is not allowed and the utility function $U_{i,j}$ is set to $-\infty$, see (8). In contrast, if both D2D pairs keep the capacity at least at C_{min}, a gain $G_{i,j}$ introduced by the new coalition of the pairs D_i and D_j, even if it is negative, is calculated as:

$$G_{i,j} = (C_{i,i} + C_{i,j} + C_{j,i} + Cj, j) - (C_{i,i}^{nr} + C_{j,j}^{nr}) \quad (9)$$

where $C_{i,i}^{nr}$ and $C_{j,j}^{nr}$ correspond to the capacities of the i-th and j-th D2D pairs without channel reuse (see Section III-A). Note that from the structure of the utility function $U_{i,j}$ and from (9), we observe that $U_{i,j} = U_{j,i}$.

Remark 1: If the D2D pairs D_i and D_j form togther one coalition, the communication channel k_i is reused by the pair D_j while the pair D_i reuses the channel k_j. In other words, both D_i and D_j communicate over both channels k_i and k_j at the same time.

Remark 2: Since the utility $U_{i,j}$ in (8) is calculated for any two D2D pairs D_i and D_j creating one coalition and accessing the two shared channels k_i and k_j assigned originally to each of them, the transmission powers $p_{i,i}$, $p_{i,j}$, $p_{j,i}$, and $p_{j,j}$ that are required to derive $U_{i,j}$ are calculated as $p_{x,y} = \frac{B_y}{B_x+B_y} P_{max}$, where x and y stand for either i or j to represent all four powers $p_{i,i}$, $p_{i,j}$, $p_{j,i}$, and $p_{j,j}$. For more details on the power allocation, please refer to the proposed power allocation derived later in Section III-D).

After obtaining the individual utilities $U_{i,j}$, these are inserted into a bilateral utility matrix $\boldsymbol{U}$:

$$\boldsymbol{U} = \begin{bmatrix} -\infty & \dots & U_{1,N} \\ \vdots & \ddots & \vdots \\ U_{N,1} & \dots & -\infty \end{bmatrix} \quad (10)$$

where the diagonal elements are set to $-\infty$ (i.e., $U_{i,i} = -\infty$). The reason for setting $U_{i,i} = -\infty$ is that the diagonal elements contain the utilities of the i-th D2D pair making a coalition with itself. Such coalition is automatically disregarded as, in principal, a D2D pair cannot make any new coalition with itself. The reason why we do not set the diagonal values simply to "0" is that in some special cases even the coalitions with slightly negative utilities can be initially created as long as C_{min} is guaranteed. In contrast, the elements $U_{i,j}$ equal to $-\infty$ (i.e., the elements for which C_{min} is not guaranteed as well as all diagonal elements) are omitted in the reminder of the process, because these should not lead to the creation of any coalition. This way, the complexity of the whole bargaining process is significantly decreased, as the search space (i.e., the number of the possible coalition structures among the D2D pairs) is reduced.

After all the entries in $\boldsymbol{U}$ equal to $-\infty$ are removed, the rest of the elements are sorted in a descending order taking into account that every couple of symmetric elements is considered as one element ($U_{i,j} = U_{j,i}$). The sorting serves further to indicate the priorities for coalitions' creation so that the coalitions yielding the highest capacity gains are created preferentially. This ordering is motivated by the fact that a higher bilateral utility represents, in our case, a lower interference among two D2D pairs. Thus, these D2D pairs are expected to end up in the same coalition also in the case of optimal coalitions created by the dynamic programming. Hence, it is likely that the proposed low-complexity solution leads to a close-to-optimal performance.

The sorted elements $U_{i,j}$ from $\boldsymbol{U}$ represent a vector of sub-games (denoted as $\boldsymbol{U}^*$) that are played sequentially over time in the way that one sub-game is played in every time step. Consequently, when the sub-game s is played, the coalition structure $\mathbf{CS_s}$ is created resulting in the sum capacity $C_{\mathbf{CS_s}}$. At the beginning of the algorithm, the sub-game is played only between two D2D pairs (e.g., D_i and D_j) over their respective channels (k_i and k_j) allocated in the initial phase. In this case, the coalition is simply created if both D_i and D_j agree to reuse their dedicated channels among each other. However, when some coalitions already exist, the sub-game is extended to all members of all related coalitions. Thus, if the pair D_i wants to join the coalition cs_x composed of two or more other D2D pairs, the sub-game s is played between the pair D_i and all the D2D pairs already included in the coalition cs_x. The pair D_i joins the coalition cs_x if and only if the pair D_i as well as all pairs in cs_x agree. Each D2D pair D_j agrees to accept the pair D_i into cs_x if the capacity of the pair D_j is not lower than C_{min} and if the sum capacity of the D2D pairs composing $\mathbf{CS_s}$ is higher than the sum capacity of the D2D pairs composing $\mathbf{CS_{s-1}}$ (i.e., if $C_{\mathbf{CS_s}} > C_{\mathbf{CS_{s-1}}}$); where $\mathbf{CS_{s-1}}$ is the coalition structure created in the previous sub-game $s-1$ with the sum capacity of $C_{\mathbf{CS_{s-1}}}$.

Furthermore, to get closer to the creation of the optimal coalitions, we enhance the proposed sequential bargaining process by testing to create larger coalitions even if the coalitions of two pairs are not beneficial (i.e., $C_{\mathbf{CS_s}} < C_{\mathbf{CS_{s-1}}}$). Thus, we try the coalitions of three pairs even if the previous coalitions with two pairs can lead to a decreased performance. In other words, if the creation of the coalitions with any two pairs leads to a negative gain (all bilateral utilities are negative), the two D2D pairs playing the first sub-game in the sorted utilities are forced to test the reuse of their channels

even if the sum capacity is decreased. Then, the rest of the sub-games are played out normally as described before and the D2D pair is added only if the sum capacity of D2D pairs is increased. This way, we keep the possibility of making coalitions with more than two D2D pairs and we prevent the possibility that the algorithm gets stuck in local optima.

In the last step, the formed coalition structure $\mathbf{CS_s}$ is compared with two other coalition structures: i) $\mathbf{CS_{all}} = cs_1$ where all D2D pairs create one coalition cs_1 and reuse all the channels; ii) $\mathbf{CS_0} = \{cs_1, \ldots, cs_N\}$ where each D2D pair represents a stand-alone coalition and no channel reuse is exploited (i.e., the initial allocation from Section III-A). Among the three coalition structures $\mathbf{CS_s}$, $\mathbf{CS_{all}}$, and $\mathbf{CS_0}$, the one that reaches the highest sum capacity of D2D pairs is chosen. Note that the sum capacity of $\mathbf{CS_{all}}$ is set to zero if $\mathbf{CS_{all}}$ does not guarantee C_{min} for all D2D pairs. There are two reasons for the inclusion of this last step. The first reason is a potential consequence of the special case (described in previous paragraph) when all elements of (10) are negative and the sum capacity decrement is acceptable in the first sub-game. This sum capacity decrement makes it necessary to compare the sum capacity in the final formed coalition structure $\mathbf{CS_s}$ with the sum capacity achieved by the initial allocation (i.e., $C_{\mathbf{CS_0}}$), in order to guarantee that $C_{\mathbf{CS_s}} > C_{\mathbf{CS_0}}$. The second reason is, generally, the very low probability of reaching the coalition structure where all D2D pairs reuse all of the available channels (i.e., $\mathbf{CS_{all}}$) through the played sub-games. Nevertheless, with a very low density of D2D pairs, the probability that the D2D pairs can reuse all the channels and compose one coalition is higher. Thus, selecting the best-performing coalition structure among $\mathbf{CS_s}$ and $\mathbf{CS_{all}}$ can further improve the performance.

The above-described algorithm for the sequential bargaining-based channel reuse is summarized in Algorithm 1. The algorithm is supposed to run centrally at the gNB (as explained in Section II.A). Thus, no special synchronization between the D2D links is needed with respect to the common D2D communication fully controlled by the network [2], because all the D2D pairs within the coalition use all the channels of each other at the same time. Note that within every step from the previously described coalitions' formation solution, the capacities are calculated (line 8 from Algorithm 1) with the optimized transmission power allocation derived in the following subsection III-D.

Algorithm 1 Sequential Bargaining Algorithm to Solve Channel Reuse Problem for N D2D Pairs

1: Estimate utility matrix $\boldsymbol{U}$ with size $N \times N$
2: Eliminate utilities equal to $-\infty$ from the matrix $\boldsymbol{U}$
3: Sort remaining utilities in descending order into vector $\boldsymbol{U^*}$
4: Initialize $\mathbf{CS_0} = \{cs_1, \ldots, cs_N\}$; $cs_i = \{D_i\}$, $\forall i \in \{1, \ldots, N\}$
5: **for** $s = 1 : \text{length}(\boldsymbol{U^*})$ **do**
6: Sub-game is played between pairs $D_i \in cs_x$ and $D_j \in cs_y$ where $U_{i,j} \equiv \boldsymbol{U^*}(s)$
7: Update $\mathbf{CS_s}$ (i.e., merge cs_x and cs_y into one coalition cs_z)
8: Estimate all $\sum_{k \in K_n} B_k log_2(1 + \gamma_{n,k})$ $\forall n \in \{1, ...N\}$ and corresponding $C_{\mathbf{CS_s}}$
9: **if** $\exists n \in \{1, ...N\} : \sum_{k \in K_n} B_k log_2(1 + \gamma_{n,k}) < C_{min}$ **or** $C_{\mathbf{CS_s}} < C_{\mathbf{CS_{s-1}}}$ **then**
10: **if** $\exists s \; : \; \boldsymbol{U^*(s)} > 0$ **or** $s \neq 1$ **then**
11: $\mathbf{CS_s} = \mathbf{CS_{s-1}}$
12: **end if**
13: **end if**
14: **end for**
15: **if** in $\mathbf{CS_{all}}$ $\exists n \in \{1, ...N\} : \sum_{k \in K_n} B_k log_2(1 + \gamma_{n,k}) < C_{min}$ **then** $C_{\mathbf{CS_{all}}} = 0$
16: **end if**
17: $\mathbf{CS_s} = \{\mathbf{CS_s} \in \{\mathbf{CS_s}, \mathbf{CS_{all}}, \mathbf{CS_0}\} : C_{\mathbf{CS_s}} = max(C_{\mathbf{CS_s}}, C_{\mathbf{CS_0}}, C_{\mathbf{CS_{all}}})\}$

D. Power Allocation to Channels

In this subsection, we aim to optimize the power allocation and set the transmission power of every D2D pair at every channel allocated to this pair based on the created coalition structure. We take into account the maximum power budget for each D2D pair to fulfill the constraint (d) in (3) and (6). The problem of power allocation is non-convex. Thus, an iterative method is required to solve such problem. However, any iterative method would increase the time complexity of the overall resource allocation scheme. Thus, we relax the problem from the maximization of the sum capacity to the maximization of individual capacity of each D2D pair. In other words, the transmission power of each D2D pair at each individual channel allocated to this pair is set in a selfish way so that the sum capacity of every single D2D pair is maximized.

The problem of maximizing the sum capacity of the D2D pair D_n over all $|K_n|$ channels reused by this pair D_n is formulated as:

$$\max(C_n) = \max \left(\sum_{k \in K_n} B_k log_2 \left(1 + \frac{p_{n,k} g_{n,k}}{\sigma_o B_k + \sum_{\substack{t \in N_k \\ t \neq n}} p_{t,k} \, g_{t,k} + I_d} \right) \right)$$
$$\text{s.t.} \sum_{k \in K_n} p_{n,k} = P_{max} \quad (a) \tag{11}$$

The optimization problem (11) is, still, unsolvable analytically as the transmission power setting of other pairs is not known. However, the DUE_T and the DUE_R of the same D2D pair are typically close to each other and, consequently, the channel between the DUE_T and the DUE_R is of a high quality (i.e., high SINR). Moreover, the coalitions' formation algorithm is interference-aware and, hence, minimizes the mutual interference among the D2D pairs. These reasons allow to expect $\gamma_{n,k} \gg 1$ and, hence, to adopt the approximation $log_2(1+\gamma_{n,k}) \approx log_2(\gamma_{n,k})$ for the derivation of the analytical solution of the previous optimization problem (11). Note that this approximation is very common for the scenarios with a "high SINR regime" (as considered in this paper), see for example [8]. Thus, the problem of maximizing C_n is

simplified to:

$$\max(C_n) = \max\left(\sum_{k\in K_n} B_k log_2 \left(\frac{p_{n,k}g_{n,k}}{\sigma_o B_k + \sum_{\substack{t\in N_k \\ t\neq n}} p_{t,k}\, g_{t,k} + I_d}\right)\right)$$
$$\text{s.t.} \sum_{k\in K_n} p_{n,k} = P_{max} \quad (a) \tag{12}$$

The maximization problem in (12) is a convex constrained optimization problem and its solution is determined using the Lagrangian method as:

$$p_{n,k} = \frac{B_k}{\sum_{k\in K_n} B_k} P_{max} \tag{13}$$

This sub-optimal solution maximizes the individual capacity of every D2D pair selfishly. The relaxation from maximizing the sum capacity to maximizing the individual capacity of individual pairs is justified by the fact that the coalitions are formed to suppress the interference among the D2D pairs belonging to one coalition and interfering to each other. This interference suppression allows to perform the power allocation for every D2D pair independently with only minor losses in terms of the sum capacity, as confirmed via simulations in Section IV. In addition to the sum capacity maximization, C_{min} is guaranteed to be satisfied by Algorithm 1 via lines 9-11, where C_{min} satisfaction is continuously checked.

By deriving the transmission powers of all D2D pairs over all the corresponding channels based on (13), a sub-optimal power allocation ($\mathbf{P}^{**}$) is reached. The transmission power $p_{n,k}$ defined in (13) is inserted to (9) for the determination of the gains $G_{i,j}$ and to derive the bilateral utilities $U_{i,j}$ in (8) (see *Remark 2* in Section III-C).

IV. Performance Evaluation

The simulations are carried out in Matlab to evaluate the performance of the proposed resource allocation scheme and to compare it with the competitive algorithms. To this end, the simulation scenario and parameters are presented in the next subsection. Then, the competitive algorithms and performance metrics are defined. Last, the simulation results are presented and discussed.

A. Simulation Scenarios

We consider an area of $500\times500\ m^2$. The simulation results are averaged out over 1000 simulation drops. For each drop, N DUE_T are uniformly distributed within the area. The position of the DUE_R for each D2D pair is generated with respect to the position of the DUE_T to guarantee that the distance between the transmitter and the receiver is not higher than d_{max}. The distance between the transmitter and the receiver is randomly generated with the uniform distribution between 0 and d_{max}. The angle of the receiver with respect to the transmitter is also uniformly generated between 0° and 360°. The number of D2D pairs remains the same for all 1000 drops, but we run different 1000 drops for every tested value of N from 5 to 50.

TABLE I
Simulation Parameters

Parameter		Value
Carrier frequency	f_c	2 GHz
Bandwidth	B	20 MHz
Noise power spectral density	σ_o	−174 dBm/Hz
Interference level from neighboring cells	I_d	$\mathcal{N}(-80, 15)$ dBm
Number of D2D pairs	N	5 – 100
Maximal transmission power of D2D pair	P_{max}	20 dBm
Default maximal distance between DUE_T and DUE_R	d_{max}	50 m ([39]–[41])

Note that the CUEs are not considered as these operate in a different band in case of the dedicated mode as explained in Section II-A.

For the modeling of radio channel, we follow 3GPP recommendation for D2D communication defined in [42]. Hence, the path loss model is defined as $PL = 89.5 + 16log_2(d)$, where d is the distance between the transmitter and the receiver. The maximal transmission power for every D2D pair is set to $P_{max} = 20$ dBm. The background interference from neighboring cells I_d is modeled randomly for each drop following a normal distribution with a mean value of -80 dBm and a standard deviation of 15 dB. This level of interference from neighboring base stations represents a high interference scenario, which can be expected in future mobile networks with dense small cells deployment [50]. The detailed parameters of the simulations are summarized in Table I.

B. Competitive Algorithms and Performance Metrics

To the best of our knowledge, there is no solution targeting the reuse of multiple channels by multiple D2D pairs in the dedicated mode with the goal of maximizing the sum capacity of D2D pairs and guaranteeing the minimal capacity for each individual D2D pair. Nevertheless, we compare our proposed algorithm with the schemes that target similar objectives or address similar problem. Thus, the proposed resource allocation algorithm, encompassing the initial channel bandwidth allocation (derived in Section III-A), the channel reuse algorithm (Section III-B and III-C), and the proposed power allocation (Section III-D), is compared with the following state-of-the-art schemes:

1) *No reuse* [8], [9]: This scheme, designed for the dedicated mode, distributes the whole available bandwidth B among the D2D pairs in the way that communication capacity is maximized while C_{min} is guaranteed to each D2D pair. However, the channels cannot be reused by the D2D pairs and each channel is occupied by just one pair. Note that the channel allocation in [8] and [9] is not optimal if there is background interference I_d as considered in our case.
2) *Single reuse* [10]: In this algorithm, the total bandwidth is divided into several channels with equal bandwidths (we consider six channels as in [10]). Every channel is allocated to a single D2D pair, i.e., six D2D pairs are served. The Hungarian algorithm is implemented to solve a matching problem between the six channels and the unserved D2D pairs to enable the D2D channel reuse. As defined in [10], up to two D2D pairs can

reuse each channel. Thus, the solution allows twelve ($2\times$number of channels) D2D pairs to be served, while the rest of the D2D pairs are provided with no resources. Even if this leads to an unfairness among the D2D pairs, it also yields a high capacity for the served D2D pairs as only those having a high channel quality between DUE_T and DUE_R access the available channels.

3) *Empty channel protocol (ECP)* [11]: For this case, the total bandwidth is also divided into several channels with equal bandwidth (in our case six channels as in [11]). First, every channel is allocated to a single D2D pair (i.e., six D2D pairs are served). Then, empty channel protocol adds the unserved D2D pairs to the channels so that all unserved D2D pairs reuse the channels already assigned to other D2D pairs. Note that the D2D pairs are not allowed to exploit multiple channels simultaneously and only one channel can be used by every D2D pair. Still, each channel can be reused by multiple D2D pairs at the same time.

The performance of the proposed and competitive algorithms is assessed by means of the sum capacity of D2D pairs defined as $C = \sum_{n=1}^{n=N} \sum_{k \in K_n} C_{n,k}$. We also investigate the percentage of satisfied D2D pairs, that is, the D2D pairs for which the minimal capacity is granted (i.e., the percentage of the D2D pairs with $C \geq C_{min}$).

C. Simulation Results

In this section, we first compare the performance of the proposed resource allocation scheme with the competitive state-of-the-art algorithms. Then, we analyze thoroughly the proposed scheme and we show the added value of the individual sub-parts of the proposal.

1) Comparison of the Proposed Scheme With Competitive Algorithms: In this subsection, we compare the performance of the full proposed resource allocation scheme, containing the initial bandwidth allocation, channel reuse based on sequential bargaining (SB), and proposed power allocation (denoted as "Proposal with SB (Alg. 1)"), with all above-mentioned competitive algorithms. Additionally, we derive the optimal sequential solution, where the optimal bandwidths are allocated to the channels, the optimal channels are allocated to the D2D pairs via the dynamic programming (i.e., the optimal coalitions are created) (Section III-B), and finally, the transmission powers are allocated to the D2D pairs based on (13) (denoted as "Proposal - optimum"). Although the optimal solution is not practical due to the high complexity of the dynamic programming, it is used as a benchmark for our scheme as it achieves the maximal possible sum capacity. In addition, we also test the performance of the sub-optimal greedy algorithm for the creation of the coalitions with a complexity equal to $\mathcal{O}(N^3)$. The greedy algorithm outlined for a general coalitions' creation in [55] is modified to guarantee C_{min} and we combine it with the initial channel allocation and the power allocation of our proposed scheme. Hence, we denote the algorithm as "Proposal with m-greedy").

Fig. 2 illustrates the impact of the number of D2D pairs on the sum capacity of all D2D pairs. The capacity is increasing for the proposed as well as competitive algorithms with more D2D pairs in the system despite the fact that the interference among D2D pairs increases. The reason for this is the fact that C_{min} naturally decreases with the increasing number of D2D pairs (as explained in Section II-A), such that C_{min} can be always guaranteed. The decrease in C_{min} with the increasing number of D2D pairs allows all pairs to contribute to their sum capacity and, hence, increase it. This is, however, expected as the coalitions are created in a way that decreases the interference among pairs.

We see that the sum capacity of all three competitive schemes saturates quickly and reaches approximately 223 Mbps (ECP), 297 Mbps (Single reuse), and 294 Mbps (No reuse) for 50 D2D pairs. The proposal with sequential bargaining leads to a significant gain with respect to all competitive algorithms. The gain ranges from 20% to 200%, from 55% to 297%, from 55% to 295%, when compared to the No reuse, Single reuse, ECP algorithms, respectively. The gain of the proposal with respect to the existing solutions increases with the number of D2D pairs, since a higher number of D2D pairs leads to more opportunities for the multiple reuse in case of our proposed scheme. Note that the proposal with m-greedy, also, outperforms the existing solutions, but its sum capacity is from 2% to 13% below the sequential bargaining approach. Besides, Fig. 2 also shows the performance of the proposal with the optimal coalitions' creation by the dynamic programming. Due to the very high complexity, we cannot show results for more than ten D2D pairs as the results cannot be obtained in a realistic time frame. The difference between the optimal coalition structure derived by dynamic programming and the low-complexity sequential bargaining approach is negligible (1.2% for 10 D2D pairs) and the low-complexity solution reaches almost optimal performance. Note that such a good performance of the proposed sequential bargaining with respect to the optimum is thanks to the sorting of the bilateral utilities in descending order and, also, allowing the creation of the coalitions with negative utilities if no bilateral utility is positive, see Section III.C. Fig. 2 also proves that our proposed sequential solution reaches a sum capacity very close to the joint numerical solution (derived as explained in Section II-B for up to eight D2D pairs only due to its very high complexity). The sum capacity of the "Proposal - Optimum" and the "Proposal with SB (Alg. 1)" is only less than 3% and 4%, respectively, below the provided joint numerical solution.

Furthermore, we investigate the impact of the maximum distance between the DUE_T and DUE_R (i.e., d_{max}) on the sum capacity in Fig. 3 for $N = 10$. It is obvious that the longer d_{max} is, the lower sum capacity is observed. The reason for such behavior is that the signal between the DUE_T and the DUE_R is more attenuated for a larger d_{max} and the D2D communication becomes less efficient. Figure 3 also shows that the proposal with sequential bargaining outperforms all competitive algorithms significantly and also overcomes the proposal with m-greedy. The gain introduced by the proposed algorithm with sequential bargaining ranges from 16.4% to 180%, from 53% to 166%, and from 73% to 187% in comparison to the No reuse, Single reuse, and ECP algorithms,

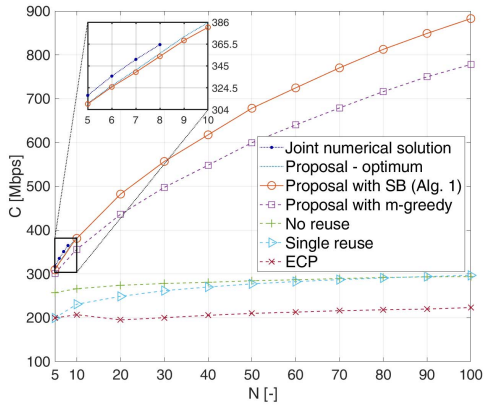

Fig. 2. Sum capacity of D2D pairs over number of D2D pairs for $d_{max} = 50$ m.

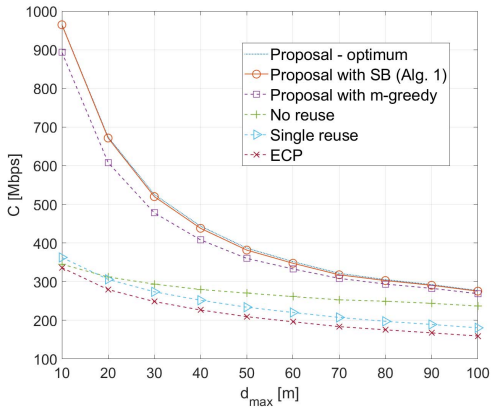

Fig. 3. Sum capacity of D2D pairs over maximum distance between transmitting and receiving device within D2D pair and for $N = 10$.

respectively. The proposal with m-greedy reaches from 2% to 10% lower sum capacity with respect to the sequential bargaining. The gain is less significant for a larger d_{max} as the interference among D2D pair is more significant with respect to the useful signal and the possibility of sharing communication channels decreases. From Fig. 3, we further see that the proposed low-complexity algorithm with sequential bargaining reaches almost the optimal capacity obtained by the dynamic programming disregarding d_{max}.

The proposed algorithm is designed to guarantee the minimal capacity C_{min} to all D2D pairs (see (3)). The minimal capacity C_{min} is derived as the capacity that is guaranteed to all D2D pairs in the case of no reuse (according to [8] and [9] as explained in (2) in Section II-A). The minimal capacity C_{min} decreases with the number of D2D pairs N, since the bandwidth B is divided among a higher number of D2D pairs (see Fig. 4a). In Fig. 4b, we verify the fulfillment of the constraint on C_{min}. The proposals with optimal coalitions, sequential bargaining as well as with m-greedy guarantee C_{min} for every D2D pair over all investigated numbers of D2D pairs in all simulation drops. Thus, although every D2D pair is exposed to interference from other D2D pairs in the same coalition, there is no D2D pair that experiences a capacity below C_{min}. Note that there is no difference between the percentage of the satisfied D2D pairs for the proposed algorithm with optimal coalitions' creation and sequential bargaining-based coalitions' creation. Also No reuse algorithm (proposed in [8] and [9]) satisfies C_{min} for all D2D pairs. In contrast, the Single reuse algorithm and the EPC do not guarantee C_{min} to all D2D pairs due to the equal channel bandwidth allocation and limited channel reuse.

2) Analysis of the Proposed Resource Allocation Scheme: In this subsection, we analyze the impact of individual sub-parts of the proposed scheme on the sum capacity of D2D pairs and the contribution of individual sub-parts to the gains achieved with respect to the competitive algorithms. To that end, we show the impact of the following individual sub-parts of the proposed algorithm:

1) *Proposal - opt. BW*: Illustrates the gain of stand-alone proposed initial channel bandwidth allocation for scenario with the background interference (Section III-A) while no channel reuse is considered. This way we show the impact of interference on the bandwidth allocation with respect to [8] and [9], where the authors neglect this interference.
2) *Proposal - reuse only*: Performance of the stand-alone proposed channel reuse (Section III-C) is demonstrated on the top of the channel bandwidth allocation according to [8], [9], i.e., if the n-th D2D pair has the bandwidth $B_n = \frac{g_{n,n}}{\sum_{n=1}^{n=N} g_{n,n}} B$ while the transmitting power among all channels is distributed equally.
3) *Proposal - reuse with opt. BW*: One can expect that the consideration of interference for the bandwidth allocation can influence also the efficiency of the reuse phase. Thus, we present this scheme in order to demonstrate the contribution of the derived initial bandwidth allocation (i.e., combined Section III-A and Section III-C). As this algorithm also assumes the equal power allocation over all channels, the gain of the proposed power allocation over channels is illustrated by the difference between this algorithm and the proposal with sequential bargaining.

For the sake of Fig. 5 clarity, we do not show the performance of the optimal coalitions' creation and we depict only the No reuse algorithm [8], [9], which serves as a basis for the bandwidth allocation performance. We see that a high gain ranging from 19.5% to 106% with respect to No reuse algorithm is introduced by the reuse of multiple channels by multiple D2D pairs (as proposed in Section III-C, in Fig. 5 labeled as "Proposal - reuse only"). The gain is a result of the proposed reuse of channels by the D2D pairs whenever it is beneficial. In addition, Fig. 5 also shows that the gain introduced by the proposed initial bandwidth allocation considering the background interference (in Fig. 5 depicted as "Proposal - opt. BW" and derived in Section III-A) with respect to the same approach disregarding the interference (i.e., No reuse according to [8] and [9]) introduces only a gain of up to 8.1% for $N = 50$. However, if the proposed

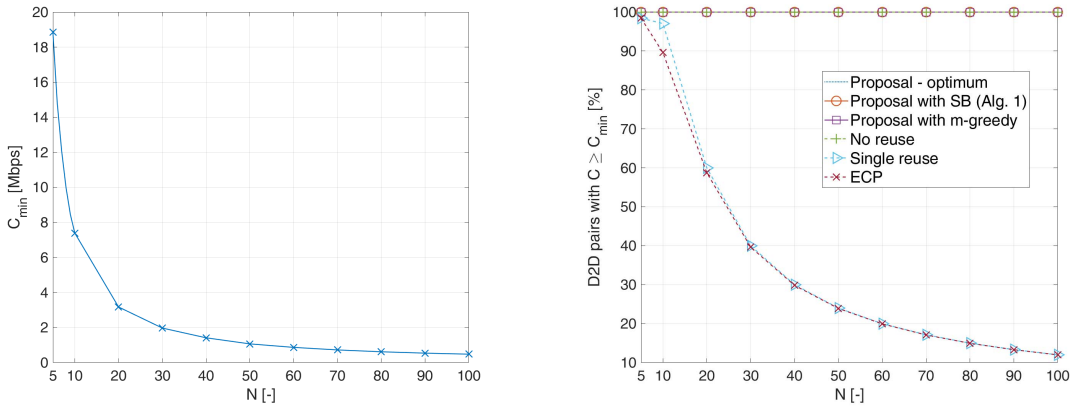

(a) (b)

Fig. 4. Minimum capacity C_{min} that can be guaranteed to all D2D pairs according to (2) (a), and percentage of D2D pairs for which C_{min} is guaranteed (b).

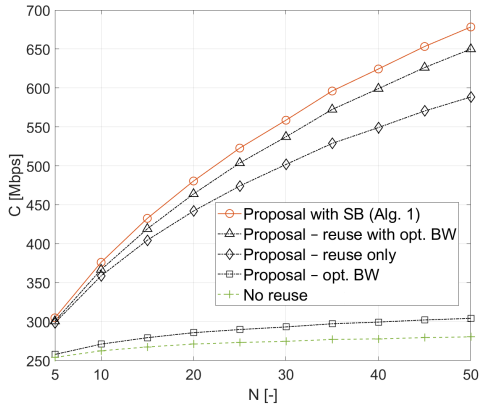

Fig. 5. Impact of individual subparts of proposed algorithm (bandwidth allocation, channel reuse, power allocation) on sum capacity of D2D pairs ($d_{max} = 50\ m$).

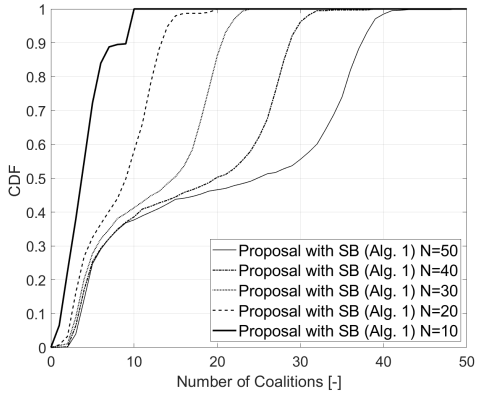

Fig. 6. CDF of number of coalitions created by the sequential bargaining for different numbers of D2D pairs.

initial bandwidth allocation considering interference is applied together with the proposed reuse ("Proposal - reuse with opt. BW" in Fig. 5), the synergy effect of both leads to an additional gain of up to 22.5% added on the top of the reuse gain. The reason for such gain of the proposed initial bandwidth allocation applied together with the reuse is that the bandwidths of the individual channels are derived with respect to the background interference. If the interference from the adjacent cells is neglected for the bandwidth allocation, the reuse phase is impaired by the non-optimal bandwidth allocation and, consequently, some well-performing coalitions are not established.

The impact of the proposed power allocation (determined in Section III-D) is represented by the difference between two top lines in Fig. 5 ("Proposal with SB (Alg. 1)" and "Proposal - reuse with opt. BW"). The additional gain with respect to No reuse (up to 8.6%) is a result of the power allocation over the channels assigned to each D2D pair taking into account the inequality among the bandwidths of these channels.

In addition to the analysis of the impact of individual subparts of the proposed algorithm, we also give more insight into the size of the resulting coalitions. Cumulative distribution function of the number of coalitions resulting from the proposed sequential bargaining game (see Section III-C) is depicted in Fig. 6. In roughly 40% of the cases, less than ten coalitions are created disregarding the number of pairs. This relatively low number of coalitions indicates that there is a high probability that multiple D2D pairs reuse the channels of other D2D pairs. The figure shows that at least one coalition is composed of more than one D2D pair (i.e., the channel(s) are reused) in 90%, 99%, and 100% of the cases for $N = 10$, $N = 20$, and $N > 20$, respectively. In other words, almost always, the number of created coalitions is lower than the number of D2D pairs N, thus, multiple D2D pairs reuse multiple channels. Note that each D2D pair represents one coalition if this D2D pair communicates only at its dedicated channel without reuse.

3) Feasibility of the Proposed Scheme: The worst case time complexity of Algorithm 1 is $\mathcal{O}(N^2 log N)$, since the bilateral utility matrix $\boldsymbol{U}$ in (10) is of $N \times N$ size and its entries

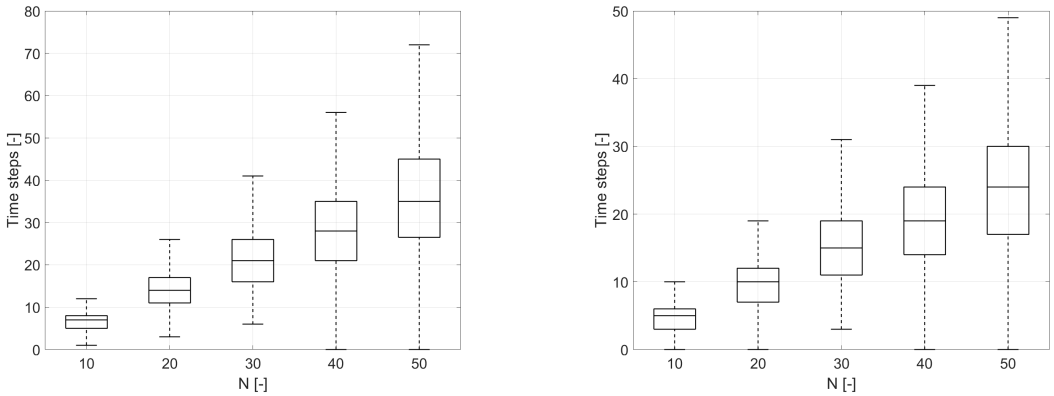

Fig. 7. Number of time steps corresponding to number of bargaining sub-games required to reach 95% (a) and 90% (b) of the sum capacity of D2D pairs.

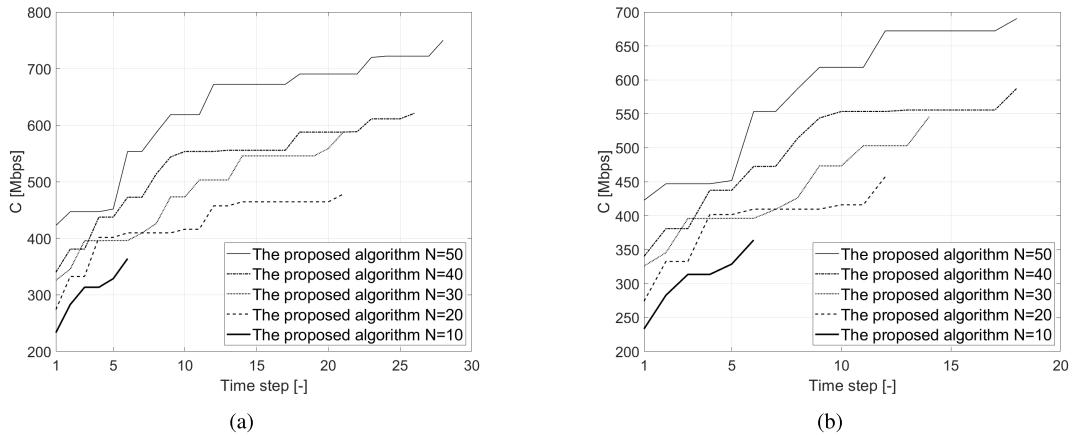

Fig. 8. Example of evolution of sum capacity over time steps in one drop for different number of D2D pairs N. The endpoint for each line illustrates the step when 95% (a) and 90% (b) of sum D2D capacity is reached.

are sorted in descending order (sorting of n elements results in the complexity $\mathcal{O}(nlog(n))$. Nevertheless, the proposed algorithm is based on the bargaining sub-games that are played sequentially over time. Thus, we investigate also the feasibility of the proposed scheme for real networks by analyzing the convergence of the proposed algorithm. The number of time steps of the proposed algorithm over the number of D2D pairs N to reach 95% and 90% of the maximum capacities is illustrated in Fig. 7a and Fig. 7b, respectively. The figures confirm that reaching 95% and 90% of the maximum capacity is quick even for a high number of D2D pairs. For realistic scenarios with, for example, 20 D2D pairs, only 14 and 10 steps (bargaining sub-games) are performed in average to reach 95% and 90% of the maximum sum D2D capacity, respectively. Even for 50 D2D pairs (which is rather an extreme case for an area of 500×500 m), only 35 and 24 time steps in average are carried out to reach 95% and 90% of the maximum capacity. Note that the complexity of dynamic programming is 3^N, thus, the complexity of the sequential bargaining-based solution is negligible.

We also show a step-by-step increase in the sum capacity of D2D pairs after each sub-game is played out for selected samples of results in Fig. 8. The capacity is increasing steeply during the first steps and promptly converges close to the maximum. Even after very first steps, the gain with respect to the best performing competitive solution is significant (up to 281.5 Mbps in average for No reuse [8], [9] as shown in Fig. 2). The low number of time steps and the steep growth of the sum capacity over the time steps, demonstrated in Fig. 7 and Fig. 8, confirm the feasibility of the proposed solution for the real-world mobile networks.

V. Conclusion

In this paper we have proposed a new resource allocation scheme allowing multiple pairs to reuse multiple channels for the D2D communication in the dedicated mode. The proposed resource allocation scheme encompasses an initial bandwidth allocation, channel reuse, and power allocation over the reused channels. The channel reuse is presented as a

coalition structure generation problem, where the D2D pairs composing one coalition reuse the channels dedicated to each other. The coalition structure generation problem is optimally solved by the algorithm based on dynamic programming. As the dynamic programming is of a high complexity, we also develop a low-complexity sequential bargaining algorithm solving the reuse problem while reaching close-to-optimal sum capacity of D2D pairs. The performance analysis shows that the sum capacity of D2D pairs is significantly increased by the proposed resource allocation scheme compared to the existing algorithms. In addition, although the interference is imposed among D2D pairs reusing the same channel, the minimal required capacity for each D2D pair is still guaranteed after the channel reuse.

A potential future direction should aim at a power control among D2D pairs in every coalition in order to further increase the spectral efficiency. Another topic for further study is the allocation of resources when the multiple channels are used by multiple D2D pairs without the requirement on forcing the D2D pairs to reuse their channels only mutually while still guaranteeing the minimal capacity to each D2D pair.

APPENDIX A

To solve the problem of channel bandwidth presented in (4), we adopt the approximation $log_2(1+\gamma_{n,n}) \approx log_2(\gamma_{n,n})$ like in Section III-D and under the same assumptions. By applying this approximation into sub-problem (4) and after several simple mathematical operations, the objective function from (4) is rewritten as:

$$\begin{aligned}\sum_{n=1}^{n=N} B_n log_2\left(1+\frac{p_{n,n}\, g_{n,n}}{\sigma_o B_n + I_d}\right) &= \sum_{n=1}^{n=N} log_2\left(\frac{p_{n,n}\, g_{n,n}}{\sigma_o B_n + I_d}\right)^{B_n} \\ &= log_2 \prod_{n=1}^{n=N}\left(\frac{p_{n,n}\, g_{n,n}}{\sigma_o B_n + I_d}\right)^{B_n} \end{aligned} \quad (14)$$

We target an interference-limited network, see Section II-A, allowing us to assume that $\sigma_n + I_d \approx I_d$. Hence, the objective function of (4) presented in (14) is simplified to:

$$log_2 \prod_{n=1}^{n=N}\left(\frac{p_{n,n}\, g_{n,n}}{I_d}\right)^{B_n} \quad (15)$$

By the integration of (15) into (4) and by substituting $p_{n,n}$ by P_{max} in the objective function according to the constraint (d) in (4), the sub-problem (4) is presented as:

$$\begin{aligned} \mathbf{B}^{**} = argmax\, log_2 \prod_{n=1}^{n=N}\left(\frac{P_{max}\, g_{n,n}}{I_d}\right)^{B_n} \\ \text{s.t. } B_n log_2\left(\frac{P_{max}\, g_{n,n}}{I_d}\right) \geq C_{min} \\ \forall n \in \{1,2,\dots N\} \quad (a) \\ 0 < B_n \leq B \quad \forall n \in \{1,2,\dots N\} \quad (b) \\ \sum_{n=1}^{n=N} B_n = B \quad (c) \end{aligned} \quad (16)$$

The constraint (a) ensures that the approximated capacity of every n-th D2D pair on the n-th dedicated channel with no-reuse is higher than the minimal capacity C_{min}. The constraints (b) and (c) are the same constraints as described in (4).

The maximization of any function $f = log_2(f')$ can be solved by maximizing f'. The problem (16) is in a form of $\text{argmax}[(a_1)^{B_1}(a_2)^{B_2}\dots(a_N)^{B_N}]$, where $a_1, a_2, \dots, a_N$ are constants. Thus, taking into account the constraints (b) and (c), maximizing (16) is achieved by assigning the maximum possible part of the bandwidth to the D2D pair with the maximal a_n. In other words, the D2D pair with the highest $g_{n,n}$ is granted with the maximal allowed part of the dedicated bandwidth. However, the constraint (a) should be also satisfied. We are able to guarantee C_{min} if any n-th D2D pair is allocated with a channel of a bandwidth equal to $B_n = \frac{C_{min}}{log_2\left(1+\frac{P_{max}\, g_{n,n}}{\sigma_{max}+I_d}\right)}$, where σ_{max} is the highest possible expected noise at the channel with the bandwidth B_n. The noise σ_{max} is, then, estimated as follows. The D2D pair with the lowest channel quality (i.e., the pair with $g_{n,n}^{min}$) is allocated with a channel of a bandwidth $\frac{g_{n,n}^{min}}{\sum_{n=1}^{n=N} g_{n,n}} B$ to guarantee C_{min}. Thus, any other n-th D2D pair requires less bandwidth to guarantee C_{min}, since the channel gain of the n-th D2D pair is always higher than $g_{n,n}^{min}$. Thus, the noise at the channel of the n-th D2D pair with the bandwidth B_n is at most equal to the noise at the channel dedicated to the D2D pair with the lowest channel quality (i.e., $\sigma_n = \sigma_n B_n \leq \sigma_o \frac{g_{n,n}^{min}}{\sum_{n=1}^{n=N} g_{n,n}} B = \sigma_{max}$). Hence, the bandwidth of the channel dedicated for any n-th D2D pair always guaranteeing C_{min} is:

$$B_n = \frac{C_{min}}{log_2\left(1+\frac{P_{max} g_{n,n}}{\sigma_o \frac{g_{n,n}^{min}}{\sum_{n=1}^{n=N} g_{n,n}} B + I_d}\right)} \quad (17)$$

This concludes the proof.

REFERENCES

[1] M. N. Tehrani, M. Uysal, and H. Yanikomeroglu, "Device-to-device communication in 5G cellular networks: Challenges, solutions, and future directions," *IEEE Commun. Mag.*, vol. 52, no. 5, pp. 86–92, May 2014.

[2] P. Mach, Z. Becvar, and T. Vanek, "In-band device-to-device communication in OFDMA cellular networks: A survey and challenges," *IEEE Commun. Surveys Tuts.*, vol. 17, no. 4, pp. 1885–1922, 4th Quart., 2015.

[3] A. Asadi, Q. Wang, and V. Mancuso, "A survey on device-to-device communication in cellular networks," *IEEE Commun. Surveys Tuts.*, vol. 16, no. 4, pp. 1801–1819, 4th Quart., 2014.

[4] X. Huang, S. Tang, Q. Zheng, D. Zhang, and Q. Chen, "Dynamic femtocell gNB On/Off strategies and seamless dual connectivity in 5G heterogeneous cellular networks," *IEEE Access*, vol. 6, pp. 21359–21368, 2018.

[5] D. Zhai, M. Sheng, X. Wang, Z. Sun, C. Xu, and J. Li, "Energy-saving resource management for D2D and cellular coexisting networks enhanced by hybrid multiple access technologies," *IEEE Trans. Wireless Commun.*, vol. 16, no. 4, pp. 2678–2692, Apr. 2017.

[6] P. Mach, Z. Becvar, and M. Najla, "Combined shared and dedicated resource allocation for D2D communication," in *Proc. IEEE 87th Veh. Technol. Conf. (VTC Spring)*, Jun. 2018, pp. 1–7.

[7] J. Dai, J. Liu, Y. Shi, S. Zhang, and J. Ma, "Analytical modeling of resource allocation in D2D overlaying multihop multichannel uplink cellular networks," *IEEE Trans. Veh. Technol.*, vol. 66, no. 8, pp. 6633–6644, Aug. 2017.

[8] Y. Huang, A. A. Nasir, S. Durrani, and X. Zhou, "Mode selection, resource allocation, and power control for D2D-enabled two-tier cellular network," *IEEE Trans. Commun.*, vol. 64, no. 8, pp. 3534–3547, Aug. 2016.

[9] C.-H. Yu, K. Doppler, C. B. Ribeiro, and O. Tirkkonen, "Resource sharing optimization for device-to-device communication underlaying cellular networks," *IEEE Trans. Wireless Commun.*, vol. 10, no. 8, pp. 2752–2763, Aug. 2011.

[10] Y. Li, M. C. Gursoy, and S. Velipasalar, "Joint mode selection and resource allocation for D2D communications under queueing constraints," in *Proc. IEEE Conf. Comput. Commun. Workshops (INFOCOM WKSHPS)*, Apr. 2016, pp. 490–495.

[11] D. Ma, N. Wang, and X. Mu, "Resource allocation for hybrid mode device-to-device communication networks," in *Proc. 8th Int. Conf. Wireless Commun. Signal Process. (WCSP)*, Oct. 2016, pp. 1–5.

[12] Y. Zhang, C.-Y. Wang, and H.-Y. Wei, "Incentive compatible overlay D2D system: A group-based framework without CQI feedback," *IEEE Trans. Mobile Comput.*, vol. 17, no. 9, pp. 2069–2086, Sep. 2018.

[13] D. H. Lee, K. W. Choi, W. S. Jeon, and D. G. Jeong, "Resource allocation scheme for device-to-device communication for maximizing spatial reuse," in *Proc. IEEE Wireless Commun. Netw. Conf. (WCNC)*, Apr. 2013, pp. 112–117.

[14] W. Zhibo, T. Hui, and C. Nannan, "Clustering and power control for reliability improvement in Device-to-Device networks," in *Proc. IEEE Globecom Workshops (GC Wkshps)*, Dec. 2013, pp. 573–578.

[15] Z.-Y. Yang and Y.-W. Kuo, "Efficient resource allocation algorithm for overlay D2D communication," *Comput. Netw.*, vol. 124, pp. 61–71, Sep. 2017.

[16] A. Abrardo and M. Moretti, "Distributed power allocation for D2D communications Underlaying/Overlaying OFDMA cellular networks," *IEEE Trans. Wireless Commun.*, vol. 16, no. 3, pp. 1466–1479, Mar. 2017.

[17] R. AliHemmati, B. Liang, M. Dong, G. Boudreau, and S. H. Seyedmehdi, "Power allocation for underlay device-to-device communication over multiple channels," *IEEE Trans. Signal Inf. Process. over Netw.*, vol. 4, no. 3, pp. 467–480, Sep. 2018.

[18] R. AliHemmati, M. Dong, B. Liang, G. Boudreau, and S. H. Seyedmehdi, "Multi-channel resource allocation toward ergodic rate maximization for underlay device-to-device communications," *IEEE Trans. Wireless Commun.*, vol. 17, no. 2, pp. 1011–1025, Feb. 2018.

[19] Y. Qian, T. Zhang, and D. He, "Resource allocation for multichannel device-to-device communications underlaying QoS-protected cellular networks," *IET Commun.*, vol. 11, no. 4, pp. 558–565, Mar. 2017.

[20] Y. Xiao, K.-C. Chen, C. Yuen, Z. Han, and L. A. DaSilva, "A Bayesian overlapping coalition formation game for device-to-device spectrum sharing in cellular networks," *IEEE Trans. Wireless Commun.*, vol. 14, no. 7, pp. 4034–4051, Jul. 2015.

[21] M. Hasan and E. Hossain, "Distributed resource allocation for relay-aided device-to-device communication under channel uncertainties: A stable matching approach," *IEEE Trans. Commun.*, vol. 63, no. 10, pp. 3882–3897, Oct. 2015.

[22] A. Asheralieva, "Bayesian reinforcement learning-based coalition formation for distributed resource sharing by device-to-device users in heterogeneous cellular networks," *IEEE Trans. Wireless Commun.*, vol. 16, no. 8, pp. 5016–5032, Aug. 2017.

[23] S. Maghsudi and S. Stanczak, "Channel selection for network-assisted D2D communication via no-regret bandit learning with calibrated forecasting," *IEEE Trans. Wireless Commun.*, vol. 14, no. 3, pp. 1309–1322, Mar. 2015.

[24] Y. Li, D. Jin, J. Yuan, and Z. Han, "Coalitional games for resource allocation in the device-to-device uplink underlaying cellular networks," *IEEE Trans. Wireless Commun.*, vol. 13, no. 7, pp. 3965–3977, Jul. 2014.

[25] A. Asheralieva, T. Q. S. Quek, and D. Niyato, "An asymmetric evolutionary Bayesian coalition formation game for distributed resource sharing in a multi-cell device-to-device enabled cellular network," *IEEE Trans. Wireless Commun.*, vol. 17, no. 6, pp. 3752–3767, Jun. 2018.

[26] J. Kim, S. Kim, J. Bang, and D. Hong, "Adaptive mode selection in D2D communications considering the bursty traffic model," *IEEE Commun. Lett.*, vol. 20, no. 4, pp. 712–715, Apr. 2016.

[27] T. Liu and G. Wang, "Resource allocation for device-to-device communications as an underlay using Nash bargaining game theory," in *Proc. Int. Conf. Inf. Commun. Technol. Converg. (ICTC)*, Oct. 2015, pp. 366–371.

[28] S. M. A. Kazmi *et al.*, "Mode selection and resource allocation in device-to-device communications: A matching game approach," *IEEE Trans. Mobile Comput.*, vol. 16, no. 11, pp. 3126–3141, Nov. 2017.

[29] W. Zhao and S. Wang, "Resource sharing scheme for device-to-device communication underlaying cellular networks," *IEEE Trans. Commun.*, vol. 63, no. 12, pp. 4838–4848, Dec. 2015.

[30] R. Wang, J. Zhang, S. H. Song, and K. B. Letaief, "QoS-aware joint mode selection and channel assignment for D2D communications," in *Proc. IEEE Int. Conf. Commun. (ICC)*, May 2016, pp. 1–6.

[31] R. Yin, C. Zhong, G. Yu, Z. Zhang, K. K. Wong, and X. Chen, "Joint spectrum and power allocation for D2D communications underlaying cellular networks," *IEEE Trans. Veh. Technol.*, vol. 65, no. 4, pp. 2182–2195, Apr. 2016.

[32] P. Mach, Z. Becvar, and M. Najla, "Resource allocation for D2D communication with multiple D2D pairs reusing multiple channels," *IEEE Wireless Commun. Lett.*, vol. 8, no. 4, pp. 1008–1011, Aug. 2019.

[33] B. Di, L. Song, and Y. Li, "Sub-channel assignment, power allocation, and user scheduling for non-orthogonal multiple access networks," *IEEE Trans. Wireless Commun.*, vol. 15, no. 11, pp. 7686–7698, Nov. 2016.

[34] T. LeAnh, N. H. Tran, S. Lee, E.-N. Huh, Z. Han, and C. S. Hong, "Distributed power and channel allocation for cognitive femtocell network using a coalitional game in partition-form approach," *IEEE Trans. Veh. Technol.*, vol. 66, no. 4, pp. 3475–3490, Apr. 2017.

[35] B. Zhang, X. Mao, J.-L. Yu, and Z. Han, "Resource allocation for 5G heterogeneous cloud radio access networks with D2D communication: A matching and coalition approach," *IEEE Trans. Veh. Technol.*, vol. 67, no. 7, pp. 5883–5894, Jul. 2018.

[36] M. Najla, Z. Becvar, and P. Mach, "Sequential bargaining game for reuse of radio resources in D2D communication in dedicated mode," in *Proc. IEEE 91st Veh. Technol. Conf. (VTC-Spring)*, May 2020, pp. 1–6.

[37] J. Huang, S. Wang, X. Cheng, and J. Bi, "Big data routing in D2D communications with cognitive radio capability," *IEEE Wireless Commun.*, vol. 23, no. 4, pp. 45–51, Aug. 2016.

[38] *Evolved Universal Terrestrial Radio Access (E-UTRA); Physical layer; Measurements*, document 3GPP TS 36.214, v10.1.0, Rel.10, 2011.

[39] M. Pischella, R. Zakaria, and D. Le Ruyet, "A joint multiplexing and resource allocation algorithm for asynchronous underlay D2D communications," in *Proc. IEEE 87th Veh. Technol. Conf. (VTC Spring)*, Jun. 2018, pp. 1–5.

[40] L. Melki, S. Najeh, and H. Besbes, "Interference management scheme for network-assisted multi-hop D2D communications," in *Proc. IEEE 27th Annu. Int. Symp. Pers., Indoor, Mobile Radio Commun. (PIMRC)*, Sep. 2016, pp. 1–5.

[41] T. D. Hoang, L. B. Le, and T. Le-Ngoc, "Energy-efficient resource allocation for D2D communications in cellular networks," *IEEE Trans. Veh. Technol.*, vol. 65, no. 9, pp. 6972–6986, Sep. 2016.

[42] *Study on LTE Device to Device Proximity Services; Radio Aspects*, document 3GPP TR 36.843, v12.0.1, Rel. 12, 2014.

[43] W. Lee, M. Kim, and D.-H. Cho, "Transmit power control using deep neural network for underlay device-to-device communication," *IEEE Wireless Commun. Lett.*, vol. 8, no. 1, pp. 141–144, Feb. 2019.

[44] M. R. Mili, A. Khalili, N. Mokari, S. Wittevrongel, D. W. K. Ng, and H. Steendam, "Tradeoff between ergodic energy efficiency and spectral efficiency in D2D communications under Rician fading channel," *IEEE Trans. Veh. Technol.*, vol. 69, no. 9, pp. 9750–9766, Sep. 2020.

[45] O. Yazdani, M. Monemi, and G. Mirjalily, "Fast globally optimal transmit antenna selection and resource allocation scheme in mmWave D2D networks," *IEEE Trans. Mobile Comput.*, early access, Jul. 14, 2020, doi: 10.1109/TMC.2020.3009183.

[46] M. Najla, Z. Becvar, P. Mach, and D. Gesbert, "Predicting device-to-device channels from cellular channel measurements: A learning approach," *IEEE Trans. Wireless Commun.*, vol. 19, no. 11, pp. 7124–7138, Nov. 2020.

[47] P. S. Bithas, K. Maliatsos, and F. Foukalas, "An SINR-aware joint mode selection, scheduling, and resource allocation scheme for D2D communications," *IEEE Trans. Veh. Technol.*, vol. 68, no. 5, pp. 4949–4963, May 2019.

[48] S. Joshi and R. K. Mallik, "Coverage and interference in D2D networks with Poisson cluster process," *IEEE Commun. Lett.*, vol. 22, no. 5, pp. 1098–1101, May 2018.

[49] J. Sun, T. Zhang, X. Liang, Z. Zhang, and Y. Chen, "Uplink resource allocation in interference limited area for D2D-based underlaying cellular networks," in *Proc. IEEE 83rd Veh. Technol. Conf. (VTC Spring)*, May 2016, pp. 1–6.

[50] J. G. Andrews *et al.*, "What will 5G be?" *IEEE J. Sel. Areas Commun.*, vol. 32, no. 6, pp. 1065–1082, Jun. 2014.

[51] N. Changder, S. Aknine, and A. Dutta, "An effective dynamic programming algorithm for optimal coalition structure generation," in *Proc. IEEE 31st Int. Conf. Tools with Artif. Intell. (ICTAI)*, vol. 3, Nov. 2019, pp. 1417–1420.
[52] T. Rahwan, S. D. Ramchurn, N. R. Jennings, and A. Giovannucci, "An anytime algorithm for optimal coalition structure generation," *J. Artif. Intell. Res.*, vol. 34, pp. 527–567, Apr. 2009.
[53] T. Rahwan, T. P. Michalak, M. Wooldridge, and N. R. Jennings, "Coalition structure generation: A survey," *Artif. Intell.*, vol. 229, pp. 139–174, Dec. 2015.
[54] F. Cruz *et al.*, "Coalition structure generation problems: Optimization and parallelization of the IDP algorithm in multicore systems," *Concurrency Comput., Pract. Exper.*, vol. 29, no. 5, p. e3969, Mar. 2017.
[55] A. Farinelli, M. Bicego, F. Bistaffa, and S. D. Ramchurn, "A hierarchical clustering approach to large-scale near-optimal coalition formation with quality guarantees," *Eng. Appl. Artif. Intell.*, vol. 59, pp. 170–185, Mar. 2017.

Mehyar Najla (Member, IEEE) is currently pursuing the Ph.D. degree with the Department of Telecommunication Engineering, Czech Technical University in Prague, Czech Republic. In 2016, he joined the 5Gmobile research lab at the Czech Technical University in Prague focusing on research related to future mobile networks. He was/is involved in several national research projects focused on combination of radio frequency and visible light communication for device-to-device communication, machine learning for wireless networks, and mobile networks with flying base stations. In 2019, he was on an internship at EURECOM, France. He has coauthored more than 10 conference and journal papers. His research interests include radio resource management in mobile networks, device-to-device communication, hybrid radio frequency and visible light communication systems, machine learning for prediction and optimization in mobile networks, game theoretic techniques for resource allocation in wireless networks and optimization of mobile networks with flying base stations.

Zdenek Becvar (Senior Member, IEEE) received the M.Sc. and Ph.D. degrees in telecommunication engineering from Czech Technical University in Prague, Czech Republic, in 2005 and 2010, respectively. He is an Associate Professor with the Department of Telecommunication Engineering, Czech Technical University in Prague, Czech Republic. From 2006 to 2007, he joined the Sitronics Research and Development center in Prague focusing on speech quality in VoIP. Furthermore, he was involved in research activities of Vodafone Research and Development center at Czech Technical University in Prague in 2009. He was on internships at Budapest Politechnic, Hungary (2007), CEA-Leti, France (2013), and EURECOM, France (2016, 2019). From 2013 to 2017, he was a representative of the Czech Technical University in Prague in ETSI and 3GPP standardization organizations. In 2015, he founded 5Gmobile research lab at CTU in Prague focusing on research towards 5G and beyond mobile networks. He has published 4 book chapters and more than 70 conference or journal papers. He works on development of solutions for future mobile networks with special focus on optimization of mobility and radio resource management, energy efficiency, device-to-device communication, edge computing, C-RAN, self-optimization, and architecture of radio access networks.

Pavel Mach (Member, IEEE) received the M.Sc. and Ph.D. degree in telecommunication engineering from Czech Technical University in Prague, Czech Republic, in 2006 and 2010, respectively. In 2006 and 2007, he joined the Sitronics Research and Development center in Prague focusing on emerging mobile technologies and he was involved in research activities of Vodafone Research and Development center at Czech Technical University in Prague from 2005 to 2008. He is currently a Senior Researcher in 5G mobile lab founded in 2015 at CTU in Prague focusing on 5G and beyond mobile networks. He was involved in several European projects such as FP6 FIREWORKS, FP7 ROCKET, FP7 FREEDOM, and FP7 TROPIC. He was/is principal investigator in national research projects focused on allocation of radio resources to cognitive small cells and combination of device-to-device communication with visible light communication. He has published three book chapters, more than 60 conference or journal papers, and 1 patent. He was on internship in EURECOM, France, in 2019. His current research areas include radio resource management for device-to-device communication, new techniques for dynamic functional split for C-RAN based network architectures, positioning of flying mobile base stations, and mobile edge computing.

XI. Appendix D

This appendix includes conference paper presented at: **P. Mach**, Z. Becvar and T. Spyropoulos, "Incentive Mechanism and Relay Selection for D2D Relaying in Cellular Networks, *IEEE Global Communications Conference (IEEE Globecom 2019)*, 2019.

Incentive Mechanism and Relay Selection for D2D Relaying in Cellular Networks

Pavel Mach[1], Zdenek Becvar[1], Thrasyvoulos Spyropoulos[2]
[1]Czech Technical University in Prague, Czech republic, emails: {machp2, zdenek.becvar}@fel.cvut.cz
[2]EURECOM, Sophia-Antipolis, France, email: spyropou@eurecom.fr

***Abstract*—The performance of the cell edge users (CUEs) can be improved if they transmit their data via suitable relay UEs (RUEs) exploiting device-to-device (D2D) communication. The critical aspect of the whole relaying concept is to offer convenient incentives for the RUEs to motivate them to act as relays. The contribution of this paper is twofold. First, we propose a new incentive mechanism for the RUEs that can exploit certain amount of resources allocated to the CUE. Depending on the preferences of users, the CUEs/RUEs can benefit from relaying in terms of capacity enhancement, reduction of energy consumption or both. In this respect, we provide a detailed analysis on how and when relaying is of benefit for both sides. Second, we propose a low-complexity greedy relay selection algorithm incorporating the incentive mechanism that increases capacity up to 32.1% and/or reduces energy consumption by up to 36.1% when compared to state-of-the-art schemes. Moreover, we show that the greedy approach gives close-to-optimal performance.**

***Index Terms*—device-to-device, relaying, incentives, energy consumption, relay selection.**

I. Introduction

Device-to-device (D2D) communication is seen as an effective approach to increase the capacity of contemporary mobile networks by allowing a direct communication of two devices in proximity, if data is available locally, in one device [1]. Such D2D communication can be further exploited for various relaying purposes [2]: (i) to improve the capacity of another device, by creating an additional D2D link with it (see, e.g., in [3]-[7]), (ii) to extend cell coverage, as the UEs out of coverage can communicate with a base station (BS) via the relay UE (RUE) [8]), and (iii) to enhance the capacity of cell-edge UEs (CUEs) that experience a low channel quality from the BS. Note that the last scenario is often referred to as a UE-to-Network relay scenario, since the RUE relays data between the UE and a network infrastructure.

Relaying via inactive UEs: A number of works targeting UE-to-Network scenarios consider using only inactive RUEs, namely RUEs that are not transmitting/receiving their own data at that moment. While in [9]-[12] the objective is to enhance the capacity of the CUEs, the authors in [13] exploit the UE-to-Network scenario to minimize their energy consumption. Even though the transmission power of the CUEs in [13] is decreased, *this approach poses an important disadvantage to the inactive RUE, whose energy consumption gets increased in the process.* Thus, the RUE may not be willing to act as a relay due to the selfish nature of most users. This observation gets only more aggravated if one further considers the additional reception energy consumption for relaying, neglected in the above works.

Relaying via active UEs: The use of active RUEs instead of inactive ones is assumed in [14][15]. In [14], the authors aim to minimize a total transmission energy via the Hungarian method. However, similar to [13], reception energy for relaying is not accounted for and transmission energy of the RUEs can in fact be increased. In [15], a UE can change its role from UE to RUE and vice versa, on a time slot basis. Specifically, in one time slot the UE can chose to be a regular UE and receive data from the BS, while in another time slot the UE acts as an RUE and relays data of another UE with a weak signal from the BS.

Relaying incentives: Although all these works show very promising gains by the use of UE relaying, the critical issue for the UE-to-network concept is to properly motivate some UEs to act as relays, in the first place. The main obstacle, which threatens the entire D2D relaying concept, is the potential reduction of battery life-time of the RUEs. Despite this fact, only a small number of related works focus on incentive mechanism for relays, and these are largely inconclusive. For example, the authors in [15] suggest an incentive mechanism based on virtual currency [16], where the RUEs are rewarded with a small additional amount of virtual currency if they act as relays. The received currency is then used by UEs to pay other UEs for relaying services. The mechanism is, however, not flexible and all RUEs get the same amount of virtual currency disregarding how much data they relay and/or how much energy is spent by them due to relaying. A similar approach is considered in [17], where a token-based incentive mechanism is proposed. A UE that receives help from an RUE pays that RUE with a token. The token can be used by the RUE in the future when asking for help itself. However, such token-based approaches are plagued by two key shortcomings: (i) it is hard to estimate whether the potential future gain (from earning a token or some currency) outweighs the immediate energy cost of relaying; (ii) unless channel characteristics *and* traffic demand is uniformly distributed among all UEs over time, token-based mechanisms can lead to deadlocks.

Contributions: In this paper we propose a flexible relaying framework, where the active UEs can perform *incentive-aligned* relaying for other active CUEs. The first key contribution is a novel incentive mechanism where the RUEs are *guaranteed to benefit* in terms of capacity enhancement, reduction of energy consumption (considering not only transmission

978-1-7281-0962-6/19/$31.00 ©2019 IEEE

energy but also reception energy), or combination of both. To the best of our knowledge, this is the first work considering a combination of capacity enhancement and energy reduction to motivate relays. Unlike [15][17], the RUE experiences the immediate benefit at the moment of relaying, not in the future, which avoids both shortcomings mentioned earlier. Specifically, an RUE capacity increase can be achieved by handing over a part of the resources allocated for the CUE communication with the BS to the RUE; the latter then can use these to transmit more of its own data. Conversely, an energy reduction for RUE is accomplished by decreasing the RUEs' transmission power to transmit the same amount of data (which is of course possible given that the RUE resources now are more). At the same time, the CUEs *still* profits from relaying, despite using fewer available resources than before, due to superior channel quality of the D2D link, compared to the CUE's direct link to the BS. Given this incentive mechanism that ensures all CUEs and RUEs participating in a D2D link will mutually benefit, our second key contribution is a low-complexity greedy algorithm that is able to select among the various ("win-win") relaying options, towards maximizing network-wide performance. What is more, we provide a sketch of prove that this algorithm has a constant approximation ratio to the optimal performance, in theory, and almost always close-to-optimal performance in practice.

The rest of the paper is structured as follows. The next section describes the system model. Then, the proposed incentive mechanism for the RUEs is introduced in Section 3 and the relay selection algorithm in Section 4. Section 5 describes our simulation scenario and demonstrates the effectiveness of the proposed framework in terms of system capacity and energy consumption of the UEs. The last section gives our conclusion and sketches future work directions.

II. System Model

We consider a scenario with multiple cells, potentially interfering with each other (i.e., reuse factor of 1). For the sake of simplicity we focus on the performance of one such cell. Without loss of generality, we consider the uplink direction, where energy consumption of the UEs is critical. However, the proposed idea can be easily applied also to downlink direction. In order to maximize the overall system capacity and/or minimize the energy consumption of the UEs, we assume that the UEs with favorable channels to the BS can relay data of the CUEs. The CUE is understood as an UE with a bad channel quality to the BS as shown in Fig. 7. The CUE and RUE create a D2D pair where the CUE is the transmitter while the RUE is the receiver. Since the RUE is supposed to be an active UE, it transmits both its own data and data received from the CUE to the BS. Similarly as in [14] we consider that the RUE is allowed to provide relay service only for one CUE at the time. The case of multiple CUEs per RUE is part of future work.

The BS has a bandwidth B at its disposal. Without loss of generality, the bandwidth is split into N orthogonal uplink channels so that each UE is assigned one channel with a size

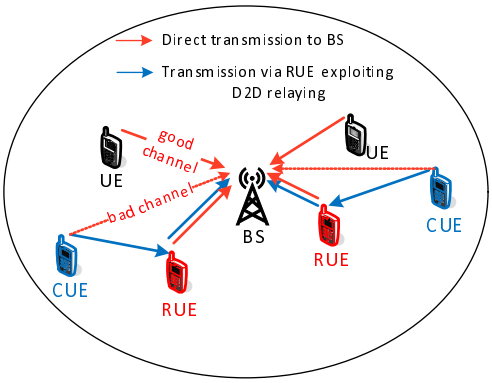

Fig. 1: System model.

equal to B/N. In general, the signal to interference plus noise ratio (SINR) between the transmitter (i.e., UE, CUE, or RUE) and the receiver (RUE or BS) is expressed as:

$$\gamma_{t,r} = \frac{p_t g_{t,r}}{B_n(\sigma_0 + I_{s,0})}, \tag{1}$$

where p_t is the transmission power of the transmitter, $g_{t,r}$ represents the channel gain between the transmitter and the receiver, B_n stands for channel bandwidth, and σ_0 is the noise spectrum density per Hz. Even though we study the impact of the D2D relaying in the single cell scenario, interference from adjacent cells, $I_{s,0}$, is considered like in real network.

The part of the proposed incentive mechanism is the energy reduction at the side of the RUEs (and potentially at the CUEs as well). The energy consumed by the UE due to transmission/reception of data is calculated according to well established empirical model defined in [18]. The total energy consumption of the UE by transmission/reception (in J) is:

$$E = P_{Tx} t_{Tx} + P_{Rx} t_{Rx}, \tag{2}$$

where P_{Tx} and P_{Rx} represent a power consumption of the UE per second while transmitting and receiving, respectively, and t_{Tx}/t_{Rx} stands for the transmission/reception time.

III. Proposed Incentive Mechanism

The incentive for the UE to become a RUE is: 1) an increase of RUE's capacity, 2) a decrease of RUE's energy consumption, or 3) a combination of both. Which option is selected depends on the RUE's preferences. As sketched earlier, the increased capacity/decreased energy consumption of the RUE is feasible by transferring some resources from the CUE to the RUE. This is elaborated in Fig. 2. Without relaying (left part of Fig. 2), the CUE and potential RUE use orthogonal channels (e.g., frequency division). If the RUE serves as a relay for the CUE, the resources (e.g., bandwidth) of the CUE (B_C) and RUE (B_R) are aggregated and accessed in a time division manner as shown in right part of Fig. 2. The CUE sends its data to the RUE in the first part of the time

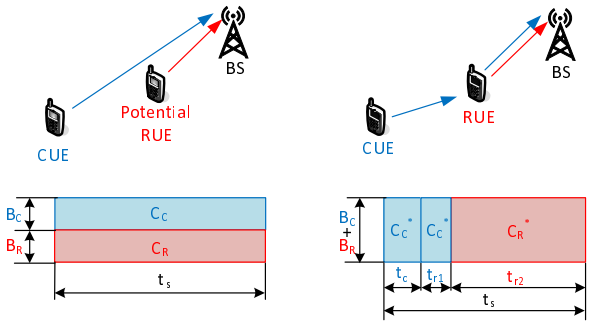

Fig. 2: Channel allocation for CUE and RUE in case of no relaying (left) and with relaying (right).

slot (t_c). In the second part of the time slot the RUE transmits the CUE's data (t_{r1}). Finally, it transmits its own data for the remainder of the slot (t_{r2}). The choice of these parameters (t_c, t_{r1}, t_{r2}) will decide if and how much the CUE and RUE gain from such a relaying arrangement, in terms of capacity or energy. Note also that this protocol can be used by UEs allowing only for half duplex. The following two subsections provide a detailed analysis of this mechanism.

A. Analysis of capacity gain

To analyze when relaying is profitable for both the CUE and the RUE in terms of capacity, we first derive the baseline capacity of a CUE and a potential RUE, when there is no relaying. The capacity of the CUE and RUE during each time slot is expressed as:

$$C_C = B_C log_2\left(1+\frac{p_c g_{c,b}}{B_C\left(\sigma_0+I_{s,0}\right)}\right)t_s = K_1 t_s, \quad (3)$$

$$C_R = B_R log_2\left(1+\frac{p_r g_{r,b}}{B_R\left(\sigma_0+I_{s,0}\right)}\right)t_s = K_2 t_s, \quad (4)$$

where p_c and p_r is the transmission power of the CUE and RUE, respectively, $g_{c,b}$ is the channel gain between the CUE and BS, and $g_{r,b}$ is channel gain between the RUE and BS.

Now, the capacity of the CUE and RUE if the relaying is applied can be expressed as:

$$C_C^* = 2B_C log_2\left(1+\frac{p_c g_{c,r}}{2B_C\left(\sigma_0+I_{s,0}\right)}\right)t_c = K_3 t_c, \quad (5)$$

$$C_R^* = 2B_C log_2\left(1+\frac{p_r g_{r,b}}{2B_C\left(\sigma_0+I_{s,0}\right)}\right)(t_s-t_c-t_{r1}) = \\ = K_4(t_s-t_c-t_{r1}) = K_4(t_s-t_c)-K_3 t_c, \quad (6)$$

where $g_{c,r}$ is the channel gain between the CUE and RUE. Notice that $K_3 t_c = K_4 t_{r1}$ as the amount of data transmitted by the CUE and then retransmitted by the RUE is the same. Then, the relative gain of the CUE (α) and RUE (β) is:

$$\alpha = \frac{K_3 t_c}{K_1 t_s}, \quad (7)$$

$$\beta = \frac{K_4(t_s-t_c)-K_3 t_c}{K_2 t_s}, \quad (8)$$

For $\alpha > 1$ ($\beta > 1$), the CUE (RUE) benefits from the relaying. However, for $\alpha < 1$ ($\beta < 1$), the CUE (RUE) would lose in terms of capacity and the relaying does not make sense from the CUE's (RUE's) point of view in such case.

It is clear that increasing α (the relative gain for the CUE), by increasing t_c (the duration of D2D transmission) would reduce β (the relative gain for the RUE) and vice versa. Our goal is thus to find a range of t_c values for which both α and β are higher than 1. The lower bound of the t_c ($t_{c,min}$) is for the case where the CUE has exactly the same capacity as if without relaying (i.e., if $\alpha = 1$). The upper bound of the t_c ($t_{c,max}$) represents a case where $\beta = 1$. Consequently, the feasible interval for t_c can be expressed as:

$$t_{c,min} = \frac{K_1 t_s}{K_3} < t_c < \frac{(K_4-K_2)\,t_s}{K_3+K_4} = t_{c,max} \quad (9)$$

were $t_{c,min}$ is derived from (7) for $\alpha = 1$ and $t_{c,max}$ is obtained from (8) for $\beta = 1$. The (9) holds if $\beta > 1$ for $\alpha = 1$. Otherwise, relaying is not allowed since either CUE, RUE or both would experience capacity degradation in case of relaying. Also note that if $\alpha = 1$ (i.e., for $t_{c,min}$), we obtain upper bound capacity.

Proof. Lets assume that $t_{c,min}$ is increased by Δt_c (i.e., $t_c = t_{c,min} + \Delta t_c$). Then, the CUE capacity in (5) is increased by $\Delta C_C^* = K_3 \Delta t_c$. Simultaneously, the RUE capacity in (6) is decreased by $\Delta C_R^* = -K_4 \Delta t_c - K_3 \Delta t_c$. Thus any increase of $t_{c,min}$ by Δt_c leads to overall decrease of capacity equal to $\Delta C_C^* + \Delta C_R^* = -K_4 \Delta t_c$. □

To further increase the capacity of the RUE while keeping the same t_c, the RUE is optionally allowed to increase its transmission power provided that: 1) the constraint on maximal allowed transmission power (p_{max}) is not violated and 2) the energy consumption of the RUE in case of relaying (E_R^*) is lower or the same as if relaying would not be applied (E_R). This capacity "boost" is possible due to the fact that the energy consumption during data reception (i.e., during t_c interval) is lower than during transmission over period of $t_{r1} + t_{r2}$. Notice that the CUEs are not allowed to "boost" their own capacity in the same way since the capacity gain of the RUEs would be inevitably reduced.

The maximum capacity boost can be expressed as:

$$C_B = 2B_C log_2\left(\frac{2B_C\left(\sigma_0+I_{s,0}\right)+p_{r'} g_{r,b}}{2B_C\left(\sigma_0+I_{s,0}\right)+p_r g_{r,b}}\right)(t_s-t_c), \quad (10)$$

where $p_{r'} = \min(p_r^*, p_{max})$ and p_r^* is the transmission power for which $E_R = E_R^*$. Thus, C_B represents an absolute gain

of the RUE, which transmits with $p_{r'}$ instead of p_r.

B. Analysis of energy consumption reduction

The capacity gain of either the CUE or RUE obtained by proper selection of t_c can be further fully or partly sacrificed to decrease energy consumption. Notice that the reduction of energy consumption can also be seen as second part of incentive mechanism for the RUEs. This option can be interesting for the CUE/RUE that does not need to increase its capacity (or only marginal increase is needed) while prolonging battery life-time is of more interest. The reduction of energy consumption is achieved by a decrease of transmission power provided that the capacity would not be decreased below C_C and C_R, respectively. To determine a feasible range of energy consumption reduction by adaptation of transmission power, the absolute gain of the CUE is derived first from (3) and (5):

$$G_C = C_C^* - C_C = \\ = 2B_C log_2\left(1+\frac{p_c g_{c,r}}{2B_C\left(\sigma_0+I_{s,0}\right)}\right)t_c - K_1 t_s, \quad (11)$$

and, similarly, the absolute gain of the RUE is obtained from (4) and (6) as:

$$G_R = C_R^* - C_R = \\ = 2B_C log_2\left(1+\frac{p_r g_{r,b}}{2B_C\left(\sigma_0+I_{s,0}\right)}\right)(t_s - t_c) - K_3 t_c - K_2 t_s \quad (12)$$

Then from (11) and (12), we can express p_c and p_r as:

$$p_c = \frac{2B_C(\sigma_0+I_{s,0})(2^{\frac{\rho G_C + K_1 t_s}{2B_C t_c}}-1)}{g_{c,r}} \quad (13)$$

$$p_r = \frac{2B_C(\sigma_0+I_{s,0})(2^{\frac{\rho G_R + K_3 t_c + K_2 t_s}{2B_C (t_s - t_c)}}-1)}{g_{r,b}} \quad (14)$$

were $\rho =< 0,1 >$ represents a parameter indicating a decrease of G_C and G_R, respectively.

Obviously, if $\rho = 1$, no energy reduction is achieved and the CUE/RUE does not reduce its transmission power at all (i.e., $p_{c,max}/p_{r,max}$ in (13) and (14) is applied). In this case, the capacity of the system is maximized. Contrary, the maximum energy reduction is observed for $\rho = 0$ as the whole capacity gain of the CUE/RUE is sacrificed to minimize energy consumption. Then, the CUE/RUE transmits with minimal transmission power ($p_{c,min}/p_{r,min}$). The value of ρ can be set individually for each user according to his/her preferences and can be dynamically changed as needed.

IV. Proposed relay selection

So far, we have identified potential D2D pairs based on their ability to both benefit from relaying in terms of capacity enhancement and/or reduction of energy consumption. For example, in the former case of capacity increase (Section III.A), a CUE could get matched with any RUE for which the feasible t_c region, as defined in (9), is non-empty, as both UEs could benefit. However, given multiple RUE options for each CUE, and multiple CUEs that would potentially prefer the same RUE, an algorithm is needed to efficiently select among the feasible pairs.

Our objective is to select CUE-RUE pairs, among the feasible ones, so as to maximize the total capacity gain across the BS, given equal energy consumption for every RUE (i.e., if maximal capacity boost defined in Section III.B is considered). Take notice that by maximizing total capacity gain, we can also achieve maximal energy savings since p_c/p_r can be decreased more significantly if capacity gain is higher (see (13) and (14)). To select individual CUE-RUE pairs we define a potential gain matrix $\mathbf{G}^p$ as follows:

$$\mathbf{G}^p = \begin{bmatrix} 0 & \dots & G^p_{1,N} \\ \vdots & \ddots & \vdots \\ G^p_{N,1} & \dots & 0 \end{bmatrix} \quad (15)$$

where $G^p_{i,j} \in \mathbf{G}^p$, the capacity gain introduced if the i-the CUE exploits the j-th RUE, is expressed as:

$$\mathrm{G}^p_{i,j} = \begin{cases} G_{C,i} + G_{R,j} + C_{B,j} & \text{if } G_{C,i} \geq 0 \text{ and } (G_{R,j} + C_{B,j}) \geq 0 \\ 0 & \text{if } G_{C,i} < 0 \text{ or } (G_{R,j} + C_{B,j}) < 0 \end{cases} \quad (16)$$

where $G_{C,i}$ and $G_{R,j}$ is the relaying gain of the i-th CUE and j-th RUE, respectively, and $C_{B,j}$ is maximal capacity boost of j-th RUE. The $G^p_{i,j}$ is positive if both the CUE and RUE experience non-negative capacity gain in case of relaying. If this would not be the case, $G^p_{i,j}$ is set to 0. Moreover, the diagonal values of $\mathbf{G}^p$ are also set to 0 as the UE cannot act as its own relay.

To keep the complexity of relay selection reasonably low, each CUE can use only one RUE and, at the same time, each RUE can relay data only for one CUE. Thus, we introduce a control variable $x_{ij} \in \{0,1\}$, where $x_{ij} = 1$ means that i-th CUE is matched to j-th RUE. Then, the objective of relay selection is to maximize the sum relaying gain formulated as:

$$\begin{aligned} \underset{x_{ij}}{\text{maximize}} \quad & \sum_i \sum_j x_{ij} \cdot G^p_{i,j} \\ \text{s.t.} \quad & \text{a)} \ \sum_j x_{ij} \leq 1, \forall i \\ & \text{b)} \ \sum_i x_{ij} \leq 1, \forall j \end{aligned} \quad (17)$$

where a) and b) constraints ensure that each CUE attach to at most one RUE and that each RUE serves up to one CUE.

Due to a) and b) constraints, one-to-one matching problem needs to be solved. While this is an integer program (so, generally hard) it can in fact be solved using the Hungarian

Algorithm 1 Greedy relay selection

1: Derive $G^p_{i,j} \in \mathbf{G}^p, \forall i,j \in \{1,\dots,N\}$
2: **while** $\max(G^p_{i,j}) > 0$ **do**
3: $\quad \{i,j\} \leftarrow \max(G^p_{i,j})$
4: $\quad$ Create D2D pair from i-th CUE and j-th RUE
5: $\quad$ Set i-th column in $\mathbf{G}^p$ to 0
6: $\quad$ Set j-th row in $\mathbf{G}^p$ to 0
7: **end while**

method [19]. However, the Hungarian algorithm is characterized by relatively high complexity ($O(N^3)$). As a result, we show the performance achieved by Hungarian algorithm as a benchmark and propose a greedy algorithm for the relay selection shown in Algorithm 1.

The selection of relays by our greedy algorithm proceeds as follows. At the beginning, $G^p_{i,j} \in \mathbf{G}^p, \forall i,j \in \{1,N\}$ is calculated according to (16) as shown in line 1. Based on the $\mathbf{G}^p$, the D2D pair for relaying is established by the i-th CUE and the j-the RUE that yield the highest capacity gain (lines 3, 4). In other words, indexes i and j corresponding to the maximum gain in whole $\mathbf{G}^p$ (over all rows and columns) defines the CUE and its selected RUE, respectively. Then, the i-th column and j-th row in $\mathbf{G}^p$ matrix containing the maximum value of the gain is set to zero to ensure constraints a) and b) in (17) (lines 5, 6). The whole process is repeated (i.e., lines 2-7) until all values in $\mathbf{G}^p$ are zeroed out.

The following lemma states that the greedy algorithm provides a worst-case approximation guarantee to the optimal. Due to space limitations, we only give a brief sketch of proof here. Note that in the simulation results, the greedy algorithm actually performs much closer to the optimal.

Theorem 1. *The optimization problem of (17) is monotone submodular in the control variables x_{ij}, subject to an intersection of matroid constraints. As a result, the proposed greedy algorithm is guaranteed to provide a $\frac{1}{3}$ approximation ratio to the optimal.*

Sketch of proof. The $G^p_{i,j}$ are independent of each other, since the D2D pairs have orthogonal resources. Hence, every time a new pair is added, the objective of (17) increases. Furthermore, assume that the subset of selected pairs is A and we add next pair $\{i,j\}$. Assume further another set of selected D2D pairs $A \subset B$. Then $\{i,j\}$ will either have the same $G^p_{i,j}$ value, or will be 0, if that i or j have already been assigned in B. This satisfies the submodularity requirement. Finally, it is easy to see that the first set of constraints defines a matroid (max of one item per row) and the second set is another matroid (max of one item per column). The approximation result then follows (see e.g. [20]). □

V. Simulations

Simulations, performed in MATLAB, are done for 1000 random scenarios. Within each scenario, up to 100 UEs are uniformly distributed in the simulation area with a size of 500x500 m. The results are then averaged out over all scenarios. The models for calculation of channel gains between individual nodes is in line with 3GPP [20]. The simulation parameters are summarized in Table 1.

TABLE I: Parameters and settings for simulations

Parameter	Value
Carrier frequency	2 GHz
Simulation area	500x500 m
Number of CUEs (N)	10-100
Bandwidth available at BS in uplink (B)	20 MHz
Channel bandwidth initially allocated to UE	B/N MHz
Max. transmission power of UE, CUE, RUE	23 dBm
Noise spectral density (σ_0)	-173 dBm/Hz
Average interference from adjacent cells ($I_{s,0}$)	-140 dBm/Hz
Height of BS/UE antenna	30/1 m
Number of simulation scenarios	1000

The performance of the proposed incentive mechanism is demonstrated for two relay selection schemes: (i) the Hungarian method that selects the CUE-RUE pairs optimally (labeled as "Proposal-optimal") and (ii) greedy relay selection based on Algorithm 1 (Proposal-greedy). We also show the performance of a baseline scheme without relaying (labeled in figures as "No relaying"). Lastly, we compare the proposed method with a state-of-the-art scheme based on [15] that also considers active RUEs, but proposes a different allocation

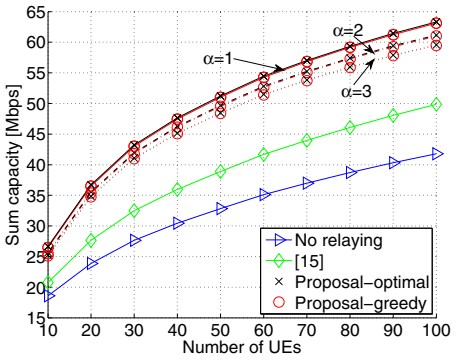

Fig. 3: Sum system capacity ($\rho = 1$).

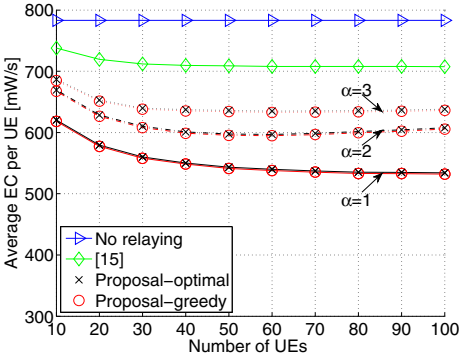

Fig. 4: Average energy consumption per UE ($\rho = 1$).

scheme beneficial solely for the CUEs while offering inflexible incentives for the RUEs based on virtual currency.

Figure 3 analyzes the performance of the proposed algorithm for various number of UEs while energy consumption of the RUEs is the same as without relaying (i.e., if $E_R = E_R^*$). The highest sum capacity is reached by the proposed scheme while $\alpha = 1$ (all capacity gain goes to the RUEs) since this corresponds to the upper bound performance (see Section III.A). The capacity gain with respect to "no relaying" case and [15] is up to 55.7% and 32.1%, respectively. The gain of our proposed scheme over [15] is achieved due to flexible incentive mechanism, where the RUEs give consent to relaying only if they have immediate profit (i.e., higher capacity in this case). With increasing α, the capacity gain of the proposed scheme is slightly decreasing as more data needs to be retransmitted by the RUEs. Nevertheless, it is important to note that even the stricter requirement to increase capacity of the CUEs by three times to form a relay link ($\alpha = 3$), still allows significant gains for the RUEs (and overall), up to 48.1% and 26.2% comparing to "no relaying" and [15]. Fig. 3 further demonstrates that the greedy algorithm gives close-to-optimal performance as the gap between optimal and greedy algorithm is always less than 0.8% (notice that the curves for optimal and greedy algorithm are basically overlapping).

Figure 4 shows the average energy consumption per UE while energy consumption of the RUEs is the same as in the case without relaying. The energy consumption slightly decreases with the number of UEs since the more CUEs can exploit D2D link the more beneficial D2D pairing is achieved (i.e., more notable shortening of CUEs transmission interval). The most significant energy reduction is attained for the proposed scheme considering $\alpha = 1$, i.e., reduction down to 68% (compared to no relaying) and 75% (compared to [15]). With increasing α, however, the energy saving is less prominent as fewer number of RUEs is willing to relay data of the CUEs due to their increasing requirements. The higher reduction of energy consumption in case of our proposed scheme comparing to [15] is, in general, owning to the fact that the CUEs transmit the whole time slot in the latter case.

Figures 5-7 shed light on the performance of the proposal

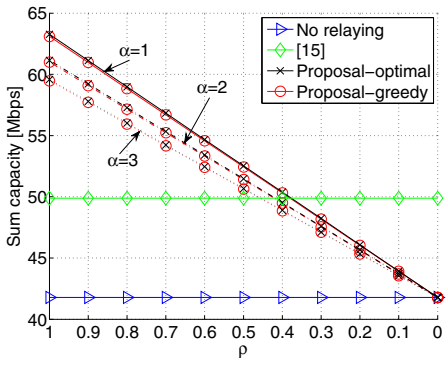

Fig. 5: Sum system capacity ($\rho = 1$).

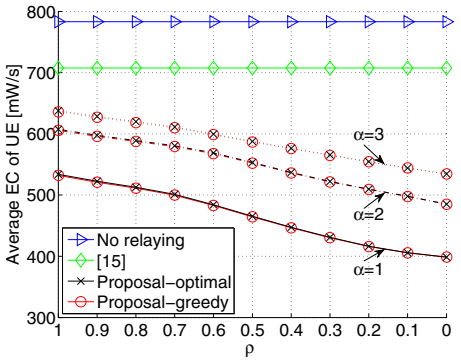

Fig. 6: Average energy consumption per UE ($\rho = 1$).

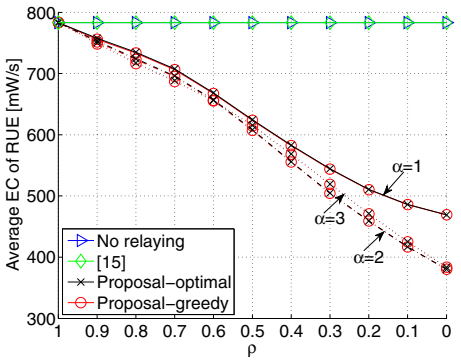

Fig. 7: Average energy consumption per RUE ($\rho = 1$).

if the whole (or at least part) of the capacity gain is sacrificed in order to reduce energy consumption of the UEs (relating to the incentive mechanism of Section III.B). Obviously, the more capacity gain is given up by the UEs the more energy reduction is possible. Thus, the highest reduction of energy consumption is achieved for $\rho = 0$ when the whole gain is translated to energy reduction (see Fig. 6 and Fig. 7). In such case, the proposed scheme is able to nearly half the overall energy consumption with respect to "no relaying" case, provided that $\alpha = 1$. But even for $\alpha = 3$ the energy reduction is around 30%. On top of this, the proposal significantly outperforms [15] in terms of energy reduction while guaranteeing the same capacity gain. For example, if $\alpha = 1$ and $\rho = 0.4$, the capacity of both schemes equals but the energy consumption of the proposed scheme is decreased by 36.1% with respect to [15].

Figure 7 analyzes more closely the possible energy savings experienced solely by the RUEs. The highest reduction of energy consumption is interestingly achieved by $\alpha = 2$ and $\alpha = 3$. This phenomenon occurs due to the fact that for $\alpha = 1$ some of the RUEs perform relaying even though their capacity gain is low. Consequently, the transmission power of such RUEs can be decreased only negligibly resulting in minimal overall energy savings. Contrary, if $\alpha > 1$, the D2D connections with low gains for the RUEs are eliminated in

the relay selection process and only the ones yielding the high capacity gains are exploited.

VI. Conclusions

In this paper, we have proposed a novel incentive mechanism for the D2D relaying in the UE-to-Network relaying scenario. The UE is motivated to perform relaying for the cell edge UE by getting more radio resources taken from the CUE. This way, the capacity of both the CUE and RUE can be improved significantly. The incentive mechanism also enables reducing the CUE/RUE energy consumption depending on users preferences. Second, we propose a low-complexity relay selection algorithm incorporating this new incentive mechanism. We have shown that the relay selection reaches close-to-optimal performance and provides up to 32.1% capacity boost and/or reduces energy consumption by up to 36.1% when compared to state-of-the-art scheme.

As for future work to address, the relay should be allowed to perform relaying services for multiple cellular users.

Acknowledgment

This work has been supported by Grant No. GA17-17538S funded by Czech Science Foundation.

References

[1] A. Asadi, et al., "A Survey on Device-to-Device Communication in Cellular Networks," *Comunn. Surveys Tuts.*, 16(4), 1801-1819, 2014.

[2] P. Mach, Z. Becvar, and T. Vanek, "In-Band Device-to-Device Communication in OFDMA Cellular Networks: A Survey and Challenges," *Comunn. Surveys Tuts.*, 17(4), 1885-1922, 2015.

[3] S. Dang, G. Chen, and J. P. Coon, "Outage Performance Analysis of Full-Duplex Relay-Assisted Device-to-Device Systems in Uplink Cellular Networks," *IEEE Trans. Veh. Technol.*, 66(5), 4506-4510, 2017.

[4] T. Liu, J. C. S. Lui, X. Ma, and H. Jiang, "Enabling Relay-Assisted D2D Communication for Cellular Networks: Algorithm and Protocols," *IEEE Internet of Things Journal*, 5(4), 3136-3150, 2018.

[5] S. Dang, G. Chen, and J. P. Coon, "Multicarrier Relay Selection for Full-Duplex Relay-Assisted OFDM D2D Systems," *IEEE Transactions on Vehicular Technology*, 67(8), 7204-7218, 2018.

[6] J. Sun, Z. Zhang, Ch. Xing, and H. Xiao, "Uplink Resource Allocation for Relay-Aided Device-to-Device Communication," *IEEE Transactions on Intelligent Transportation Systems*, 19(12), 3883-3892, 2018.

[7] B. Klaiqi, X. Chu, and J. Zhang, "Energy- and Spectral-Efficient Adaptive Forwarding Strategy for Multi-Hop Device-to-Device Communications Overlaying Cellular Networks," *IEEE Transactions on Wireless Communications*, 17(9), 5684-5699, 2018.

[8] L.Wang, et al., "Interference Constrained Relay Selection of D2D Communication for Relay Purpose Underlaying Cellular Networks," *in Proc. 8th Int. Conf. WiCOM, Netw. Mobile Comput*, 1-5, 2012.

[9] J. Deng, Alexis A. Dowhuszko, R. Freij, O. Tirkkonen, "Relay Selection and Resource Allocation for D2D-Relaying under Uplink Cellular Power Control," *Globecom worskshop*, 2015.

[10] J. Zhao, et al, "Two-Level Game for Relay-Based Throughput Enhancement via D2D Communications in LTE Networks," *IEEE ICC*, 2016.

[11] J. Gui and J. Deng, "Multi-Hop Relay-Aided Underlay D2D Communications for Improving Cellular Coverage Quality," *IEEE Access*, Volume 6, 14318-14338, 2018.

[12] X. Xu, J. Wang, and X. Tao, "Analytical Modeling for Caching Enabled UE-to-Network Relay in Cellular Networks," *IEEE Access*, Volume 6, 51061-51068, 2018.

[13] J. Wang, et al, "Analytical Modeling of Mode Selection for UE-to-Network Relay Enabled Cellular Networks with Power Control," *IEEE ICC*, 2018.

[14] S. Zhang, et al, "Energy Efficient Uplink Transmission for UE-to-Network Relay in Heterogeneous Networks," *IEEE PIMRC*, 2017.

[15] Z. Zhu, et al, "Time Reusing in D2D-Enabled Cooperative Networks," *IEEE Trans. Wireless Commun.* , 17(5), pp. 3185-3200, 2018.

[16] G. Iosifidis, L. Gao, J. Huang, and L. Tassiulas, "Efficient and Fair Collaborative Mobile Internet Access," *IEEE/ACM Trans. Netw.*, 25(3), pp. 13861400, 2017.

[17] N. Mastronarde, et al, "Learning Relaying Strategies in Cellular D2D Networks with Token-Based Incentives," *IEEE Globecom Wkshps*, 2013.

[18] M. Lauridsen, L. Nol, T.B. Sorensen, and P. Mogensen, "An Empirical LTE Smartphone Power Model with a View to Energy Efficiency Evolution", *Intel Technol. J.*, 18(1), 172193, 2014.

[19] H. Kuhn, "The Hungarian Method for the Assignment Problem, *Naval Res. Logist. Quart.*, 2(1), 8397, Mar. 1955.

[20] A. Krause, D. Golovin, "Submodular Function Maximization," Tractability, 3, 71-104, 2011.

[21] 3GPP TR 36.843 "Study on LTE Device to Device Proximity Services," (Release 12), V12.0.1, 2014.

XII. Appendix E

This appendix includes journal paper published in: **P. Mach**, T. Spyropoulos and Z. Becvar, "Incentive-based D2D Relaying in Cellular Networks, *IEEE Transactions on Communications*, vol. 69, no. 3, 2021. IF (JCR 2022) = **8.3**.

Incentive-Based D2D Relaying in Cellular Networks

Pavel Mach, *Member, IEEE*, Thrasyvoulos Spyropoulos, *Member, IEEE*, and Zdenek Becvar, *Senior Member, IEEE*

***Abstract*— Device-to-device (D2D) relaying is a concept, where some users relay data of cell-edge users (CUEs) experiencing a bad channel quality to a base station. While this research topic has received plenty of attention, a critical aspect of the D2D relaying remains a selfish nature of the users and their limited willingness to relay data for others. Thus, we propose a scheme to identify potential candidates for the relaying and provide a sound incentive to these relaying users (RUEs) to motivate them helping other users. First, we provide a detailed theoretical analysis showing when and if the relaying is beneficial for the CUE(s) and related RUE. Second, to choose among all possible incentive-compliant relaying options, we formulate the optimal CUE-to-RUE matching problem maximizing a network-wide performance. Since the optimal solution is hard to obtain for a high number of users, we propose a low-complexity greedy algorithm and prove its constant worst-case approximation guarantees to the optimum. Finally, we derive a closed-form expression for a fair allocation of the resources among the CUEs and the RUEs. The proposed framework more than doubles the users' capacity and/or reduces the energy consumption by up to 87% comparing to existing incentive-based relaying schemes.**

***Index Terms*— Device-to-device, relaying, incentives, relay selection, submodularity, worst-case guarantees.**

I. Introduction

DEVICE-TO-DEVICE (D2D) communication is seen as a way to increase the capacity and energy efficiency of contemporary mobile networks by allowing a direct communication of two devices in proximity [1], [2]. The D2D communication can be exploited also for various relaying purposes [3], [4], such as: (i) relaying of data between two D2D users (see, e.g., in [5]–[9]), (ii) extending a cell coverage so that the user equipment (UE) out of coverage can communicate with a base station (BS) via a relay UE (RUE) [10]), or (iii) enhancing the capacity of the UEs with a low channel quality to the BS if the UE is shadowed by an obstacle or located at the cell edge.

A number of works targeting scenario with the relaying of data from cell-edge UEs (CUEs) to the BS consider only the relaying via the RUEs that are not transmitting/receiving their own data at that moment. For example, the objective in [11]–[14] is to enhance the capacity of the CUEs and the authors in [15] minimize the energy consumption of the CUEs. All schemes considering inactive RUEs, however, pose an important disadvantage to the RUEs, whose energy consumption is increased in the process. Thus, *the RUE has no motivation to act as the relay* due to the selfish nature of most of the users. This observation gets even more aggravated if the energy spent for a reception of data by the RUE from the CUEs, neglected in the above works, is also considered. The use of the active RUEs instead of the inactive ones is assumed in [16], where the authors aim to minimize the transmission energy of the RUEs and the CUEs via the Hungarian algorithm. However, similar to [15], the reception energy for relaying is not considered, hence, even this solution may increase the overall energy consumption of the RUEs.

Although [11]–[16] show very promising gains introduced by the D2D relaying, none of them targets a problem of motivating the UEs to act as the RUEs and spend their own energy for the relaying of data form other UEs. One way to motivate the UEs to perform the relaying is considered in [17], [18], where a *token-based incentive* mechanism is proposed. In this concept, the UE that receives a help from any idle RUE pays with a token to that RUE. The token can be used by the RUE in the future when the RUE asks for the help itself. A similar approach to the one with tokens is considered also in [19]–[21], where the authors suggest a *virtual currency-based incentive* mechanism. The RUEs are rewarded with a virtual currency (or a credit) whenever they act as the relays. The received currency is then used by the UEs to pay to other UEs for the relaying services in the future. Other works motivate the users to act as the relays by means of *social-aware incentives*. In [22], the authors explore a social relationship among the users and assume that close friends are more likely to relay the data for each other. Along similar lines, in [23], the authors propose *contract theory-based incentives*, where the users prefer to help their friends rather than strangers. An incentive mechanism for the relaying considering also an energy efficiency is proposed in [24], where the relays are rewarded with a longer transmission time, thus, reducing their energy consumption.

A. Drawbacks of Existing Incentives Schemes

Although all incentive-based works significantly contributes to the problem of the UEs' motivation acting as the relay, they still have following drawbacks. The token/currency-based approaches [17]–[21] are plagued by two key shortcomings: (i) it is hard to estimate if the potential future gain (from earning a token or some currency) outweighs the immediate energy cost of the relaying; (ii) unless radio channel characteristics and traffic demands are uniformly distributed among all UEs

Manuscript received May 15, 2020; revised October 7, 2020 and November 19, 2020; accepted November 29, 2020. Date of publication December 4, 2020; date of current version March 17, 2021. The associate editor coordinating the review of this article and approving it for publication was X. Chen. *(Corresponding author: Pavel Mach.)*

Pavel Mach and Zdenek Becvar are with the Faculty of Electrical Engineering, Czech Technical University in Prague, 166 36 Prague, Czech Republic (e-mail: machp2@fel.cvut.cz; zdenek.becvar@fel.cvut.cz).

Thrasyvoulos Spyropoulos is with EURECOM, 06410 Sophia Antipolis, France (e-mail: spyropou@eurecom.fr).

Color versions of one or more figures in this article are available at https://doi.org/10.1109/TCOMM.2020.3042461.

Digital Object Identifier 10.1109/TCOMM.2020.3042461

over time, the token-based mechanisms can lead to deadlocks. The main drawback of the social-aware incentive approaches [22], [23] is: (i) there may not be any available friends in vicinity or (ii) the exploitation of only the friends for relaying is usually far from the optimal in terms of the communication capacity.

Moreover, none of the above-mentioned incentive-based approaches addresses the problem of an increased energy consumption of the RUEs. Although [24] tackles the energy consumption, it neglects the additional energy required for the data reception at the relay. However, the reception energy eventually increases the overall energy consumption. Besides, the works trying to incentivize the RUEs *restricts the number of CUEs exploiting each RUE to one*, thus, fairly limits a potential of the whole D2D relaying concept. On top of that, these works either do not address a critical problem of the relay selection ([19], [21]) or *no performance guarantees are given* for the proposed relay selection schemes ([17], [18], [20], [22]–[24]).

B. Contributions

Motivated by the drawbacks of the above-mentioned papers, we propose a flexible incentive-based relaying framework that guarantees *immediate* rewards for the RUE as well as for *all* CUEs exploiting the RUE. The contributions can be summarized as follows:

- We provide a detailed theoretical analysis showing when and if the matching of one or more CUEs with the RUE is beneficial in terms of the capacity, energy, or both. While the CUEs benefit due to a superior relaying channel quality, the RUE profits, as it can exploit a part of the CUE(s) resources for its own transmission.
- We formulate an optimal CUE-to-RUE matching problem to determine the relaying groups maximizing the network-wide performance. As the optimal solution is hard to obtain for a high number of UEs, we also propose a low-complexity greedy algorithm and we prove that the proposed greedy approach has a constant worst-case approximation guarantees to the optimum.
- We find a closed-form expression for the allocation of resources among the UEs in the relaying group to ensure a fairness among the CUEs and the RUE in terms of absolute or relative gains.

This work is an extended version of our prior paper [25], where we outline the general idea and indicate a performance for the case with just one CUE relaying via single RUE.

The rest of the paper is structured as follows. The next section describes the system model. Section III outlines the proposed incentive framework. A theoretical analysis on a capacity gain and potential energy savings is given in Section IV. Section V formulates an optimal CUE-to-RUE matching problem, describes a low-complexity greedy algorithm and discusses its submodularity properties. Section VI gives closed-form expression for fair resource allocations of all users within D2D relaying group. Section VII analyzes the effectiveness of the proposed incentive framework. The last section gives our conclusions.

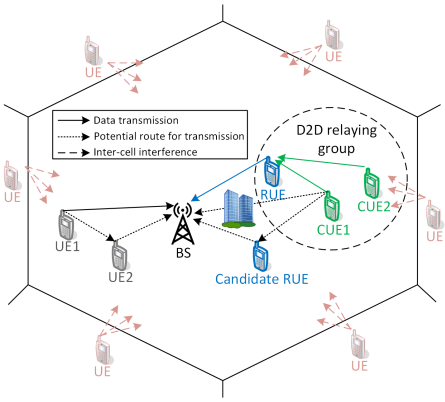

Fig. 1. Example of system model for Urban scenario where: (i) UE1 transmits data directly as a matching of UE1 with UE2 is not beneficial and (ii) CUE1 and CUE2 selects to relay data via the RUE, thus creating D2D relaying group.

II. System Model

We consider an urban scenario with multiple cells and multiple UEs, as shown in Fig. 1. Every UE is already associated with a BS, and CUEs in the cell can only be paired with the RUEs in the same cell.[1] Hence, we can focus the description of our scheme on a single cell, where interference from nearby cells is included in the physical layer model, as is common in other related works (see, e.g., [26]–[28]). We focus on the uplink, where the energy consumption of the UEs is critical. Although the proposed idea can be applied also to downlink, it would require notable changes to the overall concept and a novel solution that goes beyond the scope of this paper. The BS serves N active UEs that are randomly distributed in the cell. The UEs with favorable channels to the BS can relay data of the CUEs. The CUE is defined as the UE with a bad channel quality to the BS due to either its far distance to the BS or an obstacle in the communication path. Each CUE and its serving RUE, thus, create a D2D pair where the CUE plays the role of a transmitter while the RUE act as a receiver.

A. Physical Layer Model

The BS has a bandwidth B at its disposal. The bandwidth is split into N orthogonal uplink channels so that each UE is assigned with one channel of a bandwidth B_n. The signal to interference plus noise ratio (SINR) between any transmitter (i.e., UE, CUE, or RUE) and any receiver (RUE or BS) is expressed as:

$$\gamma_{t,r} = \frac{p_t g_{t,r}}{B_n(\sigma_0 + I_{s,r})}, \tag{1}$$

where p_t is the transmission power of the transmitter, $g_{t,r}$ represents the channel gain between the transmitter and the receiver, σ_0 is the noise spectrum density per Hz, and $I_{s,r}$ is the sum interference from the adjacent cells at the receiver.

B. Energy Consumption Model

A part of the proposed incentive mechanism is the energy reduction at the side of the RUEs (and potentially at the CUEs as well). The energy consumed by the UE due to

[1] We defer the problem of the user association to future work.

the transmission/reception of data is derived according to a well-established empirical model defined in [29]. In both uplink (transmission) and downlink (reception), the power consumption consists of the signal processing parts P_T^{bb} and P_R^{bb}, the radio communication parts P_T^{rf} and P_R^{rf}, and a consumption of the communication circuitry P_T^{on} and P_R^{on}. The powers consumed by the transmission (P_T) and the reception (P_R) are, then, defined as:

$$P_T = P_T^{bb} + P_T^{rf} + P_T^{on}, \tag{2}$$

$$P_R = P_R^{bb} + P_R^{rf} + P_R^{on}, \tag{3}$$

where the exact values and the calculation of individual parameters is in line with [29]. The total energy consumption of the UE by the transmission/reception (in J) is then a sum of both components weighed by the transmission time t_T and the reception time t_R:

$$E = P_T t_T + P_R t_R. \tag{4}$$

C. Assumptions

We adopt several assumptions and key distinctions of the proposed scheme: (i) the RUEs are assumed to be *active* and, thus, are expected to transmit their own data, in addition to the CUE data to be relayed; this is not the case in most of the related works, where only idle RUEs are considered, (ii) our scheme allows for multiple CUEs to be attached to the same RUE, provided that all CUEs and the RUEs can benefit from the relaying (this is contrary to, e.g., [11]–[23]), (iii) the CUE can use only one RUE at a time, although there might exist cases, where using more than one RUE by some CUEs might offer further benefits, this would come at a significant protocol complexity and our preliminary analysis suggests the benefits to be minimal, and (iv) we assume full knowledge of channel state information (CSI) similarly as in number of the recent studies (see, e.g., [30], [31]). Note that, there is no need to exchange CSI among all transmitters to select an appropriate relay for the CUEs in our proposal, as the potential RUEs should be in a relative proximity to the CUEs. Thus, only a relatively small subset of nearby UEs of the CUE should be considered as a set of the potential relays for which CSI should be known. Also, [32] shows that deep neural networks are able to predict the channel between any two D2D users with a high accuracy only from the users' cellular channels (i.e., channels from the user to the base station(s)). Such solution works even for none line of sight communication and in a scenario with dynamic objects (vehicles, etc.). Thus, the signaling cost is significantly reduced down to a negligible level. Note that the impact of an inaccurate CSI prediction can result in a suboptimal selection of the relays for some of the CUEs and to a subsequent degradation in the performance. Thus, we analyze the impact of the inaccurate CSI in Section VII.

III. High Level Overview of Proposed Incentive Framework for D2D Relaying

A motivation of the users relay data for others is a crucial aspect of the D2D relaying concept. In our proposed framework, any active UE that becomes the RUE can enjoy immediate benefit in terms of: (i) an increase in the capacity, (ii) a decrease in the energy consumption, or (iii) a combination of both. Any of these three options is selected according to the RUE's personal preferences. Of course, the CUEs should benefit from the relaying in the same way as the RUE.

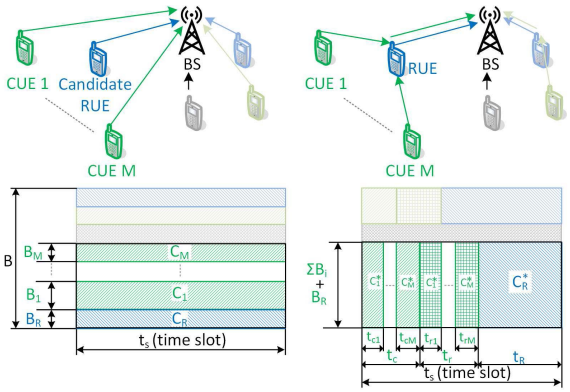

Fig. 2. Example of channel allocation in case without relaying (left) and with relaying (right). Figure highlights one reference D2D relaying group with one RUE and M CUEs.

The increased capacity or the decreased energy consumption of the RUE is feasible by rendering a part of the radio resources of the CUE to the RUE. This is illustrated in Fig. 2 for one potential RUE and M CUEs. Without relaying (left part of Fig. 2), all UEs use orthogonal channels within each time slot (t_s). Via these channels, the data is sent directly to the BS. Then, the baseline capacity of the i-th CUE (C_i) and the candidate RUE (C_R) without relaying during each time slot is expressed as:

$$C_i = B_i log_2 \left(1 + \frac{p_i g_{i,b}}{B_i \left(\sigma_0 + I_{s,r}\right)}\right) t_s, \tag{5}$$

$$C_R = B_R log_2 \left(1 + \frac{p_r g_{r,b}}{B_R \left(\sigma_0 + I_{s,r}\right)}\right) t_s, \tag{6}$$

where B_i and B_R are the bandwidths allocated initially by the BS to the i-th CUE and the potential RUE, respectively, p_i and p_r represent the transmission powers of the i-th CUE and the RUE, respectively, $g_{i,b}$ stands for the channel gain between the i-th CUE and the BS, and $g_{r,b}$ corresponds to the channel gain between the RUE and the BS.

If the candidate RUE starts to actually relay data for the CUEs, the resources of the CUEs and the RUE are aggregated and accessed in a time division manner as shown in the right part of Fig. 2. Note that if the relaying would be done fully in a frequency division manner, the RUEs should be able to receive and send data simultaneously. This would, however, assume that the RUEs are able to work in full duplex, while we assume only more practical half-duplex devices. Also note that the whole proposed concept is seen rather as OFDMA, where the transmissions of the UEs are separated in both frequency and time (see the right part of Fig. 2, where the D2D relaying groups work in the time division manner while the D2D relaying groups are separated with respect to each other and also to other UEs in the frequency division manner).

For each D2D relaying group, the whole transmission interval t_s (e.g., a time slot) is split into three separated parts.

The CUEs transmit their data to the RUE at the beginning of each time slot, the CUE 1 during the slot t_{c1}, the CUE 2 during the slot t_{c2}, and so forth, one after the other. The total duration of this part is $t_c = \sum_{i=1}^{M} t_{ci}$. In the second part, the RUE transmits (relays) the data of the CUEs. The data of the i-th CUE is relayed during t_{ri} and other CUEs follows again one after the other with the overall time duration equal to $t_r = \sum_{i=1}^{M} t_{ri}$. Finally, in the last part, the RUE transmits its own data during t_R. In the case of relaying, the capacity of the i-th CUE (C_i^*) and the RUE (C_R^*) is defined as:

$$C_i^* = B_s log_2\left(1 + \frac{p_i g_{i,r}}{B_s\left(\sigma_0 + I_{s,r}\right)}\right) t_{ci}, \tag{7}$$

$$C_R^* = B_s log_2\left(1 + \frac{p_r g_{r,b}}{B_s\left(\sigma_0 + I_{s,r}\right)}\right)\left(t_s - \sum_{i=1}^{M}(t_{ci} + t_{ri})\right), \tag{8}$$

where $B_s = B_R + \sum_{i=1}^{M} B_i$ is the aggregated channel bandwidth of the D2D relaying group, and $g_{i,r}$ corresponds to the channel gain between the i-th CUE and the RUE.

Obviously, the setting of t_{ci}, t_{ri}, and t_R parameters influence the relaying gain experienced by the CUEs and the RUE. To that end, we analyze when and if all involved parties within the relaying group benefit from the relaying in Section IV. Then, in Section V, we formulate the optimal group formation and we propose the greedy approach leading to a close-to-optimal performance. Finally, we derive closed-form expressions for the fair allocation of resources within the formed relaying groups in Section VI.

IV. Analysis of Relaying Gain

This section analyzes first when the relaying is profitable for the RUE and the CUEs in terms of the capacity and, then, it discuss a possible reduction in the energy consumption.

A. Capacity Gain

Taking (5)-(8) into mind, the relative gain of the i-th CUE (α_i) and the RUE (β), resulting from the appointment of the RUE as the relay for the i-th CUE, is defined as:

$$\alpha_i = \frac{C_i^*}{C_i} = \frac{K_i^* t_{ci}}{K_i t_s}, \tag{9}$$

$$\beta = \frac{C_R^*}{C_R} = \frac{K_R^*\left(t_s - \sum_{i=1}^{M}(t_{ci} + t_{ri})\right)}{K_R t_s}. \tag{10}$$

where $K_i = B_i log_2(1 + \frac{p_i g_{i,b}}{B_i(\sigma_0 + I_{s,r})})$ and $K_R = B_R log_2(1 + \frac{p_r g_{r,b}}{B_R(\sigma_0 + I_{s,r})})$ for the i-th CUE and the RUE, respectively. Moreover, the use of K_i^* and K_R^* refer to the case when the relaying is applied, analogously as in (7) and (8).

For $\alpha_i > 1$, the i-th CUE benefits from the relaying. Similarly, for $\beta > 1$, the RUE benefits from the relaying. As a matter of fact, the relaying is of interest if it is mutually beneficial for the CUEs and the RUE, i.e., if both $\alpha_i > 1$ ($\forall i \in \mathcal{M} = \{m_1, m_2, \ldots, m_M\}$ and $\beta > 1$. However, increasing α_i (the relative gain for the i-th CUE) by extending t_{ci} (the duration of D2D transmission) reduces β (the relative gain for the RUE) and vice versa. In this respect, the following lemma defines the condition for which all UEs within the D2D relaying group benefit from the relaying.

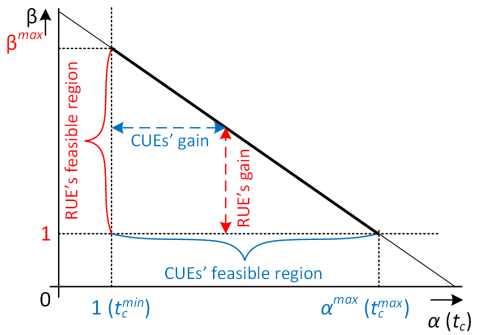

Fig. 3. Illustrative example of the feasible operational regions of RUE and CUEs, where all involved UEs benefits from relaying. Note that β^{max} and α^{max} are achieved for $\alpha = 1$ and $\beta = 1$, respectively.

Lemma 1: All M CUEs and the RUE in any D2D relaying group benefit from the relaying in terms of capacity, if:

$$\sum_{i=1}^{M} \frac{K_i}{K_i^*} t_s < \sum_{i=1}^{M} t_{ci} < \frac{(K_R^* - K_R) t_s}{K_R^*} - \sum_{i=1}^{M} t_{ri}, \tag{11}$$

while $t_{ci} > t_{ci}^{min}$, $\forall i \in \mathcal{M}$, where t_{ci}^{min} is the time allocation interval for which the i-th CUE has the relative gain $\alpha_i = 1$.

Proof: See proof in Appendix A.1. ■

After t_{ci} is obtained for all CUEs according to Lemma 1, t_{ri} and t_R are derived as:

$$t_{ri} = \frac{K_i^*}{K_R^*} t_{ci}, \ \forall i \in \mathcal{M}, \tag{12}$$

$$t_R = t_s - \sum_{i=1}^{M} t_{ci} - \sum_{i=1}^{M} t_{ri}. \tag{13}$$

It turns out that t_c^{min} (and respective allocation of the time resources) also maximizes the total capacity of the given D2D relaying group while assigning t_c^{max} minimizes the total capacity. In this respect, we formulate the following lemma.

Lemma 2: The upper bound on the total capacity is achieved for the case when each i-th CUE attached to the RUE is allocated with t_{ci}^{min}, i.e., if $t_{ci} = t_{ci}^{min}$, $\forall i \in \mathcal{M}$. Contrary, if $t_c = t_c^{max} = \sum_{i=1}^{M} t_{ci}^{max}$, the lower bound on the total capacity improvement is achieved by the relaying.

Proof: See proof in Appendix A.2. ■

All the values of $\sum_{i=1}^{M} t_{ci}$ in between the boundaries defined by (11) *do improve the total capacity of the D2D relaying group*. This is illustrated in Fig. 3, which shows a feasible operational region (depending on allocation of t_c), where the RUE and the CUEs gain in terms of the capacity.

B. Energy Consumption Reduction

In practice though, we want to properly incentivize the RUEs and the CUEs to form the relaying group as the relaying itself can cost also an additional energy consumed by the RUE. In fact, the energy consumption can be reduced by a decrease in the transmission power. This option can be attractive especially for the users who do not need to increase their capacity (or only marginal increase is needed) while prolonging a battery life-time of the UE is of more interest. This inevitably reduces the capacity gain of the CUE/RUE

obtained by the allocation of t_{ci} as described above. Thus, we allow to decrease the transmission power at the cost of a full or a partial reduction in the capacity gain obtained by the relaying. Nonetheless, the capacity should not be decreased below C_i or C_R as the capacity of the UEs still should not drop below their original respective capacities.

On the other hand, if the users do not care much about the energy consumption (e.g., if the device is plugged in the electricity or if the device is fully charged), the transmission power can be optionally increased to further enhance the capacity. This option is feasible since the proposed allocation scheme partly reduces the energy consumption simply by adopting the relaying. Note that this is due to the fact that the transmission time of the UEs is reduced by switching from the frequency division manner to the time division (see Fig. 2). This optional power "boost", however, can be applied only if the following conditions hold: (i) the constraint on the maximal allowed transmission power (P_{max}) is not violated and (ii) the energy consumption of the UE in the case of relaying (E_R^*) is not higher than the energy consumption before the relaying is adopted (E_R). Also note that only the RUEs are allowed to increase their capacity by the power boost, since the power boost of the CUEs capacity inevitably negatively affects the gain of the RUE (i.e., t_{r1} would be increased and, thus, t_R would be decreased). The maximum capacity gain of the RUE due to the boosting of the transmission power, while above-mentioned constrains are fulfilled, is defined by the following lemma.

Lemma 3: The maximum capacity gain of the RUE due to the capacity boost is expressed as:

$$G_B = B_s log_2 \left(\frac{B_s \left(\sigma_0 + I_{s,0}\right) + p_r^B g_{r,b}}{B_s \left(\sigma_0 + I_{s,0}\right) + p_r g_{r,b}} \right) \left(t_s - t_c\right), \quad (14)$$

where p_r^B represents the RUE's boosted transmission power calculated as $p_r^B = min(p_r^*, P_{max})$, and p_r^* is the transmission power for which $E_R = E_R^*$.

Proof: See proof in Appendix A.3. ∎

Now, the feasible energy consumption reduction is directly proportional to the transmission power of the UE and depends on the limits within which the CUEs or the RUE can transmit. Thus, the following lemma defines allowable range of any i-th CUE and the RUE, respectively.

Lemma 4: The allowable range of the transmission power of the i-th CUE and the RUE (considering also possible power boost in case of the RUEs) are expressed as:

$$\kappa_i \left(2^{\frac{K_i t_s}{B_s t_{ci}}} - 1\right) \leq p_i \leq \kappa_i \left(2^{\frac{\rho G_i + K_i t_s}{B_s t_{ci}}} - 1\right), \quad (15)$$

$$\kappa_R \left(2^{\frac{K_R t_s + \sum_{i=1}^{M} K_i^* t_{ci}}{B_s (t_s - \sum_{i=1}^{M} t_{ci})}} - 1\right) p_r \leq \kappa_R \left(2^{\frac{\rho(G_R + G_B) + K_R t_s + \sum_{i=1}^{M} K_i^* t_{ci}}{B_s (t_s - \sum_{i=1}^{M} t_{ci})}} - 1\right), \quad (16)$$

where $\kappa_i = \frac{B_s(\sigma_0 + I_{s,0})}{g_{i,r}}$ and $\kappa_R = \frac{B_s(\sigma_0 + I_{s,0})}{g_{r,b}}$, $G_i = C_i^* - C_i$ stands for the absolute gain of the i-th CUE, $G_R = C_R^* - C_R$ represents the absolute gain of the RUE, and $\rho = \langle 0, 1 \rangle$ represents the parameter indicating a decrease in G_i and G_R, respectively.

Proof: See proof in Appendix A.4. ∎

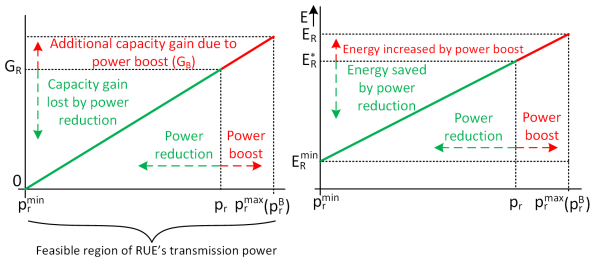

Fig. 4. Illustrative example of the feasible transmission power regions for the RUE and its impact on achieved capacity gain (left figure) and energy consumption (right figure).

An illustrative example of the feasible region of the RUE's transmission power and its impact on the capacity gain and the energy consumption is shown in Fig. 4 (note that the similar figure applies for the CUEs as well, just without the power boost). Fig. 4 shows that there is a trade-off between the capacity gain and the energy consumption. If p_r is decreased, the energy consumption of the RUE is decreased while the capacity gain due to relaying is lowered. If p_r is increased, the relaying capacity gain is increased at the cost of a higher energy consumption.

V. Incentive-Aligned Relaying Groups Formation

So far, we have analyzed conditions when the UEs in the D2D relaying group benefit from the relaying in terms of the capacity enhancement and/or the reduction in the energy consumption. For example, in the case of the capacity increase, any i-th CUE can get matched with any RUE for which the feasible region of t_{ci}, as defined in (11), is non-empty, since both the RUE and the CUEs benefit. Given multiple RUE options for each CUE and multiple CUEs that potentially prefer the same RUE, an algorithm is needed to efficiently select among the feasible CUE-RUE combinations.

To select an individual CUE-RUE pairs and, thus, create individual D2D relaying groups, we define the matrix $\mathbf{G}^p$ of the potential gains where $G_{i,j}^p \in \mathbf{G}^p$ is the capacity gain introduced if the i-the UE would exploit the j-th UE as the relay is expressed as:

$$G_{i,j}^p = \begin{cases} G_i + G_R + G_B, & \text{if } G_i \geq 0 \text{ and } (G_R + G_B) \geq 0 \\ 0, & \text{if } G_i < 0 \text{ or } (G_R + G_B) < 0 \end{cases} \quad (17)$$

The capacity gain is composed of the absolute gain of the i-th CUE (G_i), the absolute gain of the RUE (G_R), and also of the capacity boost set in line with Lemma 3 (G_B). Note that G_i is calculated as a difference between C_i^* and C_i and G_R is derived as a difference between C_R^* and C_R as explained in Lemma 4. Both G_i and G_R depend on the allocation of the transmission intervals for the CUEs (i.e., t_{ci}) and the RUE (i.e., t_{ri} and t_R). In this regard, t_{ci} is determined first according to the expected gain of the i-th CUE (α_i). For example, in case of the upper bound, α_i is set to 1 and t_{ci} is calculated via (9). If t_{ci} is within the allowable interval

guaranteeing benefit to both the CUE and the RUE (as defined by Lemma 1), t_{ri} and t_R are calculated according to (12) and (13), respectively. The $G^p_{i,j}$ is positive if both the CUE and the RUE experience a non-negative capacity gain in case of the relaying. If the CUE and/or RUE would experience a negative capacity gain, $G^p_{i,j}$ is set to 0. The diagonal values of $\mathbf{G}^p$ are also set to 0 as the UE cannot act as its own relay.

Our objective is then to select the CUE-RUE pairs among the feasible combinations of the CUEs and the RUEs, so as to maximize the relaying gain and, consequently, also the sum total capacity of the system. As the solution differs for the case where just single CUE is allowed to be attached to each RUE (i.e., if $M = 1$) and the case where multiple CUEs can exploit the same relay ($M > 1$), we first focus on a single-CUE case. Then, we contemplate necessary modifications to extend the problem to the multi-CUE case.

A. Single-CUE Case

In single-CUE per RUE case, each CUE can use only one RUE and, at the same time, each RUE can relay data only for one CUE. Thus, the objective is formulated as:

$$\begin{aligned} \underset{x_{ij}}{\text{maximize}} \ & \sum_i \sum_j x_{ij} G^p_{i,j} \\ \text{s.t. a)} \ & \sum_j x_{ij} \leq 1, \quad \forall i \\ \text{b)} \ & \sum_i x_{ij} \leq 1, \quad \forall j \end{aligned} \tag{18}$$

where $x_{ij} \in \{0, 1\}$ is the control variable indicating whether the i-th CUE is matched with j-th RUE ($x_{ij} = 1$) or not ($x_{ij} = 0$), the constraint a) ensures that each CUE attaches to at most one RUE, and the constraint b) guarantees that each RUE serves up to one CUE.

Due to a) and b) constraints, one-to-one matching problem should to be solved. While this is an integer program (so, generally hard) it can, in fact, be optimally solved using the Hungarian algorithm [33]. However, the Hungarian algorithm is characterized by a relatively high complexity ($\mathcal{O}(N^3)$). As a result, we show the performance achieved by Hungarian algorithm as a benchmark and we propose a low-complexity sub-optimal greedy algorithm with the worst-case approximation guarantees to the optimal solution.

The selection of the relays by our greedy algorithm is described in Algorithm 1. At the beginning, $G^p_{i,j} \in \mathbf{G}^p, \forall i, j \in \{1, \ldots, N\}$ is calculated according to (17) as shown in line 1. Based on the $\mathbf{G}^p$, the D2D pair for relaying is established by the i-th CUE and the j-the RUE that yields the highest capacity gain (lines 3, 4). In other words, indexes i and j corresponding to the maximum gain in the whole $\mathbf{G}^p$ (over all rows and all columns) defines the CUE and its selected RUE, respectively. Then, the i-th row and j-th column in $\mathbf{G}^p$ matrix containing the maximum value of the gain is set to zero to ensure the constraints a) and b) in (18) (lines 5, 6). The whole process is repeated (i.e., lines 2-7) until all values in $\mathbf{G}^p$ are zeroed out.

The complexity of the proposed Algorithm 1 is in the worst case $\mathcal{O}(N^2 \log N)$. The reason is that Algorithm 1 initially checks N^2 entries in $\mathbf{G}^p$, selects the one with the highest value, and remove one row and one column from $\mathbf{G}^p$. In the next rounds, the algorithm respectively checks $(N-1)^2$, $(N-2)^2$, and so on till 1 entry in $\mathbf{G}^p$. Still, even for relatively small numbers of the UEs (up to 100 UEs), the complexity of the proposed greedy algorithm is significantly lower comparing to the complexity of the Hungarian algorithm. Consequently, Algorithm 1 offers a good trade-off between the complexity and the performance, which is close-to-optimal, as demonstrated, e.g., in [34], [35] and later in the simulations results.

Algorithm 1 Incentive-Aligned Relaying Groups Formation

1: Derive $G^p_{i,j} \in \mathbf{G}^p, \forall i, j \in \{1, \ldots, N\}$
2: **while** $\max(G^p_{i,j}) > 0$ **do**
3: $\quad \{i, j\} \leftarrow \max(G^p_{i,j})$
4: $\quad$ Create D2D pair from i-th CUE and j-th RUE
5: $\quad$ Set i-th row in $\mathbf{G}^p$ to 0
6: $\quad$ Set j-th column in $\mathbf{G}^p$ to 0
7: **end while**

The following theorem states that the greedy algorithm (Algorithm 1) provides a worst-case approximation guarantee to the optimal. Note that, in the simulation results, the greedy algorithm actually performs much closer to the optimal.

Theorem 5: The optimization problem of (18) is monotone submodular in the control variables x_{ij}, subject to an intersection of matroid constraints. As a result, the proposed Algorithm 1 is guaranteed to provide a $\frac{1}{3}$ approximation ratio to the optimal.

Proof: See proof in Appendix B.1. ■

B. Multi-CUE Case

This subsection discusses the more general case when the constrain b) in (18) is relaxed and multiple CUEs can exploit the same RUE. Then, the problem in (18) is rewritten as:

$$\begin{aligned} \underset{x_{ij}}{\text{maximize}} \ & \sum_i \sum_j x_{ij} G^p_{i,j} \\ \text{s.t. a)} \ & \sum_j x_{ij} \leq 1, \quad \forall i \end{aligned} \tag{19}$$

Contrary to (18), (19) cannot be solved optimally by the Hungarian algorithm, since this is a many-to-one matching problem while the Hungarian algorithm is applicable only to one-to-one matching problems. Moreover, the order in which the CUEs are assigned to the RUE matters. The reason is that, by selecting any i-th CUE to use the j-th RUE, the channel bandwidth available for the j-th RUE is increased by adding the channel bandwidth of the i-th CUE to this particular D2D relaying group (see Fig. 2). This implies a need to recalculate the remaining positive gains in the j-th column of $\mathbf{G}^p$. Hence, a different ordering in which the CUEs are added may result in a different grouping and a different performance.

The optimal solution can be derived by the full search, i.e., by trying all possible combinations of the matching of the CUEs with the RUEs. The full search, however, checks $\frac{K!}{(K-L)!}$ possible combinations, where K is the number of positive elements in the initially created $\mathbf{G}^p$ and L is the number of CUEs that can initially be attached to at least one RUE (i.e., the number of CUEs with at least one positive

Algorithm 2 Optimal Algorithm for Multi-CUE case

1: Identify all positive $G^p_{i,j} \in \mathbf{G}^p$ that cannot be selected together
2: Divide $\mathbf{G}^p$ into S sub-matrices
3: Check all combinations in each sub-matrix
4: Select the matching in each sub-matrix maximizing gain
5: Select the matching among all sub-matrices max. gain

entry in $\mathbf{G}^p$). Unfortunately, there is no way to find the optimal solution for higher number of UEs due to excessive number of combinations to be checked. To this end, we outline a way that is able to notably decrease the number of combinations to be checked while still obtaining the optimal matching.

The optimal algorithm reducing the number of combinations is described in the following five subsequent steps (see Algorithm 2). First, all the positive entries in the $\mathbf{G}^p$ matrix that cannot be selected together are identified. More specifically, since the CUEs cannot exploit multiple number of RUEs, at most only one positive entry in each i-th row of $\mathbf{G}^p$ can be selected. Second, the matrix $\mathbf{G}^p$ is divided into S sub-matrices in such a way that each sub-matrix contains only the positive entries, which can be selected together. This way we avoid checking the combinations that are not allowed. Also, if there is only one positive entry in the i-th row, this entry is included in each sub-matrix. In the third step, all matching combinations in each created sub-matrix are checked separately. Due to second step, each CUE can be matched with just one RUE in each sub-matrix. Consequently, the matching can be done separately also for each RUE (i.e., for each row in each sub-matrix), since the matching of the CUEs to the RUE affects only other CUEs that are already attached to (or to be potentially attached) to the same RUE. Then, in the fourth step, the matching combination yielding the highest gain is selected for each sub-matrix. Finally, the matching yielding the highest gain out of these matching combinations is selected. Despite a reduced complexity of Algorithm 2 with respect to the full search, the optimal solution still cannot be obtained for a very high numbers of the UEs. Hence, we show the optimal solution only for up to 24 UEs and propose an alternative greedy low-complexity algorithm solving (19).

The greedy algorithm for the multi-CUE case is based on Algorithm 1 proposed for the single-CUE case. Still, we need to make a modification of line 6. Thus, instead of setting all remaining positive entries in the j-th column in $\mathbf{G}^p$ to 0, these are updated. More specifically, we recalculate potential gain of any CUE with the positive entry in the j-th column. This update is necessary, since the CUEs attached to the j-th RUE (and the j-th RUE itself as well) exploit a wider channel bandwidth containing individual bandwidths of each CUE attached to the same RUE, as explained above. Consequently, by matching any new CUE with this RUE, the potential gain by adding yet another CUE to this particular D2D relaying group is decreased as σ_0 and $I_{s,0}$ is increased with the use of wider channel. Moreover, t_{ci} and t_{ri} of the CUEs already matched with the j-th RUE are updated as well after the new CUE is added to this D2D relaying group, together with the transmission time of this particular RUE (t_R).

The complexity of the modified Algorithm 1 for the multi-CUE case is, in the worst case, $\mathcal{O}(\frac{N^3+N^2}{2})$. The algorithm goes first through N^2 entries, selects the highest one, and deletes the row. Then, the algorithm subsequently searches over $N(N-1)$, $N(N-2)$, till N entries in $\mathbf{G}^p$. Thus, the complexity is derived as $\mathcal{O}(N^2+N(N-1)+\cdots+N) = \mathcal{O}(N^2 + N\sum_{i=1}^{N-1} i) = \mathcal{O}(\frac{N^3+N^2)}{2})$. Note that while the greedy algorithm for the multi-CUE case can be solved in a polynomial time, the optimal solution cannot be solved in the polynomial time.

While the greedy algorithm for the multi-CUE case is similar to the single-CUE one, the approximation guarantee(s) it gives depend on some additional network parameters. In the following results, we consider some important sub-cases.

Lemma 6: Assume that every UE has an equal bandwidth B allocated, and a maximum of M CUEs per RUE is allowed. Assume further that the initial $\mathbf{G}^p$ matrix contains only the candidate CUE-RUE pairs for which $G^p_{i,j} \geq 0$ if the CUE and the RUE bandwidth is B and $M \cdot B$, respectively. Then, the modified greedy algorithm again achieves a $\frac{1}{3}$ approximation.

Proof: See proof in Appendix B.2 ■

Remark 1: We remind the reader that the initial matrix $\mathbf{G}^p$ contains only candidate pairs who can benefit from the relaying in a one-to-one situation (i.e., a positive gain from the relaying can be achieved for both). The additional assumptions in Lemma 6, hence, only refer to such pairs, and not any CUE-RUE pair (whose channel can be arbitrarily bad), and thus are satisfied in most scenarios.

Remark 2: Other approximation algorithms, besides the greedy one, can be used for our optimization problem (e.g., continuous relaxation and pipage rounding [36]). These, however, give worse approximation guarantees for polymatroid constraints, like the ones we have in our optimization problem (i.e., $\frac{0.38}{p}$ approximation for p matroids [37]). Moreover, there exists significant recent literature in the field of accelerated greedy [38] or stochastic greedy schemes [39] that can further improve the running time of basic greedy. We see as an advantage of our analytical contribution that such improvements are applicable. However, the actual investigation of such refinements, we believe, is orthogonal to this work and beyond the scope of the paper.

VI. Derivation of Fair Resource Allocation

In this section, we address a fair allocation of the communication resources *within the same D2D relaying group* (i.e., for all CUEs connected to the same RUE). There is no requirement on the fairness among different RUE groups (and neither should be), which might even implement different fairness policies to be agreed upon by the participants. This fairness is achieved by an appropriate allocation of the resources during the time slot among the CUEs and the RUE (i.e., by the allocation of t_{ci}, t_{ri}, and t_R).

We follow two common fair allocation principles, where the CUEs and the RUE have either: (i) the same relative capacity gain (this can be also interpreted as a proportional fairness)

or (ii) the same absolute capacity gain. The following two lemmas give closed-form expressions on the time allocation for the CUEs (i.e., t_{ci}) resulting in the same relative and absolute gains of all M CUEs and RUE within the same relaying group.

Lemma 7: The same relative capacity gain for each member of the D2D relaying group is achieved if:

$$t_{ci} = \frac{K_1^* K_i}{K_1 K_i^*} t_{c1}, \tag{20}$$

where t_{c1} is derived as:

$$t_{c1} = \frac{K_1 K_R^* t_s}{K_R K_1^* + K_1(K_1^* + K_R^*) + K_1^* K_R^* \left(\sum_{i=2}^{M} (\frac{K_i}{K_i^*} + \frac{K_i}{K_R^*})\right)}. \tag{21}$$

The (21) has a solution always if β is increased by creating any i-th CUE-RUE pair, i.e., if the i-th CUE does not degrade the capacity of the RUE for $\alpha_i = 1$.

Proof: See proof in Appendix C.1. ■

When t_{ci} is obtained for all CUEs relaying via the same RUE as described above, t_{ri} with t_R are derived according to (12) and (13), respectively.

Lemma 8: The same absolute capacity gain for each member of the D2D relaying group is achieved if:

$$t_{ci} = \frac{K_1^* t_{c1} - K_1 t_s + K_i t_s}{K_i^*}. \tag{22}$$

where t_{c1} is calculated as:

$$t_{c1} = \frac{\left(M K_1 - K_R + K_R^* + K_R^* \sum_{i=2}^{M} (\frac{K_1 - K_i}{K_i^*} - \frac{K_i}{K_R^*})\right) t_s}{(M+1) K_1^* + K_R^* + K_1^* K_R^* \sum_{i=2}^{M} \frac{1}{K_i^*}}. \tag{23}$$

The (23) has a solution always if $G_R > 0$ for the case when $G_i = 0,\ \forall i \in \mathcal{M}$.

Proof: See proof in Appendix C.2. ■

When t_{ci} is obtained for all CUEs relaying via the same RUE, t_{ri} and t_R are again derived according to (12) and (13), respectively.

VII. Simulations

This section first describes a simulation setup for an evaluation of the proposed incentive framework. Also existing competitive incentive schemes related to our work are introduced. Then, we present the simulation results and discuss the gains with respect to the existing schemes.

A. Simulation Setup

The simulations, performed in MATLAB, are run for 1000 random drops. Within each drop, up to 100 UEs are uniformly distributed in the simulation area with the size of 500×500 m. The results are then averaged out over all drops. Without lose of generality, we consider that the BS splits the available bandwidth among the UEs equally in the simulations. The channel models between the UEs and the BS and among the individual UEs are in line with 3GPP considering the outdoor-to-outdoor environment [40]. The simulations are performed for an urban scenario, where possible obstacles between any transmitter and any receiver can turn a line of sight (LoS) communication into a non line of sight (NLoS). The probability of LoS is determined according to 3GPP for Urban Macrocell scenario, where the probability of LoS decreases with the distance between the transmitter and the receiver [41]. If there is the NLoS communication between any two nodes, 20 dB is added to the link attenuation representing an obstacle. As we consider a multicell environment, we model the inter-cell interference at any receiver randomly according to Gamma distribution (see [42]). The simulation parameters are summarized in Table I.

TABLE I
Parameters and Settings for Simulations

Parameter	Value
Carrier frequency	2 GHz
Simulation area	500x500 m
Number of UEs (N)	10-100
Bandwidth available at BS in uplink (B)	20 MHz
Max. transmission power of UE, CUE, RUE	23 dBm
Noise spectral density (σ_0)	-173 dBm/Hz
Mean interference from adjacent cells ($I_{s,0}$)	-140 dBm/Hz
Height of BS/UE antenna	30/1 m
Number of simulation drops	1000

The performance of the proposed framework is demonstrated for several proposed relaying groups formation schemes: (i) greedy selection following Algorithm 1, where only one CUE can exploit single RUE (denoted as "*Greedy: M=1*"), (ii) greedy selection where multiple CUEs can exploit the same RUE ("*Greedy: M>1*"), (iii) Hungarian algorithm that is able to find the optimal relaying groups for the single CUE per RUE case ("*Optimal: M=1*"), and (iv) optimal scheme defined in Algorithm 2 for the multi-CUE case ("*Optimal: M>1*"). Note that the optimal scheme for the multi-CUE case is shown only for up to 24 UEs due to its huge complexity.

The proposed incentive framework is confronted with other two existing types of the incentive-based schemes for the D2D relaying. The first type is based on the token/virtual currency incentives, where the CUEs enhance their capacity while the RUEs receive tokens or some virtual credits to perform the relaying as proposed in [19]–[21] (see Introduction section for more details). We label this type of schemes as "*T/VC incentives*". The second type is based on the social-aware incentives, where the relaying is done only by friends as other UEs are not willing to perform the relaying due to selfish nature of the users, see, e.g., [22], [23]. We label this type as "*SA incentives*". We also show a baseline scheme without relaying ("*No relaying*") demonstrating the relaying gain introduced by our proposal and by competitive schemes.

B. Simulation Results

The simulation results are divided into three parts: i) showing the potential maximum capacity gain achieved by the proposal, ii) analyzing a trade-off between the capacity gain and the energy consumption reduction, and iii) investigating the performance of our proposal if the gain is shared fairly among the UEs within the same D2D relaying group, as derived in Section VI.

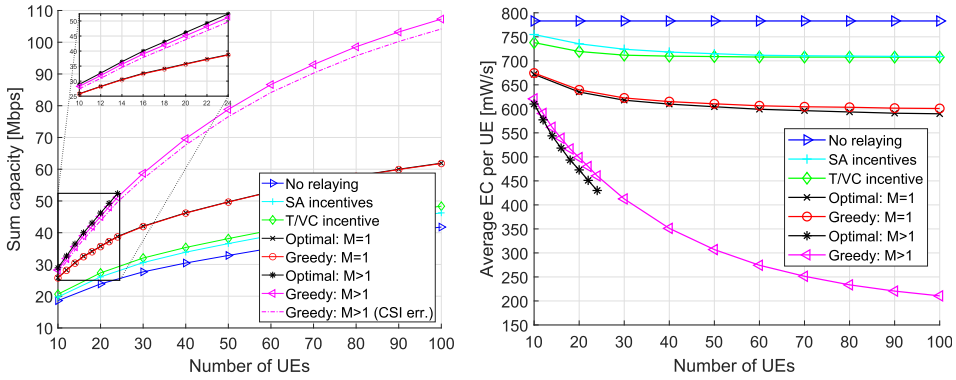

Fig. 5. Performance of the proposal depending on the number of UEs in terms of sum capacity (a) and average energy consumption per UE (b) ($\rho = 1$).

1) Evaluation of Potential Maximum Capacity Gain: Fig. 5a illustrates that the sum capacity increases with the number of UEs as the probability of finding a suitable RUE for each CUE is generally higher with the more deployed UEs. The highest sum capacity is always reached by the proposed greedy algorithm, which allows multiple CUEs to connect to single RUE (*Greedy: M>1*). The proposed *Greedy: M>1* improves the sum capacity by up to 156.8%, 132%, and 121.9% comparing to *No relaying*, *SA incentives*, and *T/VC incentives*, respectively. The gain of *Greedy: M>1* over *SA incentives* is due to the fact that more relaying options are available in the case of the proposed *Greedy: M>1*. Similarly, the gain with respect to *T/VC incentives* is achieved thanks to the proposed flexible incentive mechanism, where the RUEs give a consent to the relaying only if the RUEs have an immediate profit (i.e., reach a higher capacity in this case). The gain of the proposal is more significant if the RUE is exploited by multiple CUEs. However, even the case permitting only one CUE per RUE (*Greedy: M=1*) outperforms *No relaying*, *SA incentives*, and *T/VC incentives* by 47.9%, 33.6%, by 27.8% for 100 UEs.

Fig. 5a also demonstrates that the proposed Greedy algorithm reaches a close-to-optimal performance for both single- and multi- CUE per RUE cases. The performance gap between the Optimal and Greedy selection of relays for the single-CUE case is less than 0.5% (the curves for optimal and greedy algorithms overlap). Although the performance gap between the Optimal and Greedy algorithms for the multi-CUE case increases, this gap is still below 2.4%. These encouraging results confirm the fact that the greedy algorithms are known to give a close-to-optimal performance in practical scenarios.

Last, Fig. 5a also investigates the impact of the inaccurate CSI estimation on the performance of *Greedy: M>1* (labeled as *Greedy: M>1 (CSI err.)*). Note that the channel gain estimation error is selected randomly and varies between -10% and 10% with respect to a real channel gain. Despite this rather high channel estimation error, the decrease in the sum capacity is only up to 2.9%. This confirms a robustness of the proposed scheme against the channel estimation errors and it validates its suitability even for the practical applications.

Fig. 5b shows the average energy consumption per UE. The energy consumption decreases with the number of UEs, as more number of the CUEs exploit the RUEs. The most significant energy consumption reduction is attained by the proposed *Greedy: M>1* scheme, which enables the energy consumption reduction by up to 73.1%, 70.3%, and 70.2% comparing to *No relaying*, *SA incentives*, *T/VC incentives*, respectively. The reason for such a notable reduction in the energy consumption is that multiple CUEs can be attached to the same RUE and, thus, the transmission intervals of the CUEs are significantly reduced with respect to the other schemes. Note that the more CUEs are attached to the RUE the shorter transmission intervals of the CUEs are as a wider channel bandwidth is utilized by the CUEs and the RUE, especially for a higher number of the UEs in the cell as the number of CUEs relaying data via the same RUE increases. Still, even the simplified proposed scheme *Greedy: M=1* reduces the energy consumption by up to 23.3% comparing to *No relaying*, up to 15.3% comparing to *SA incentives*, and up to 15.1% comparing to *T/VC incentives*. Note that the gap between the proposed Optimal and Greedy schemes is small and the proposed Greedy scheme reduces the energy consumption by up to 1% (for the single-CUE case) and up to 6.4% (for the multi-CUE case) less then the optimum.

2) Trade-Off Between Relaying Capacity Gain and Energy Consumption Reduction: This subsection a sheds light on the performance of the proposal if a part of the capacity gain introduced by the proposed relaying is sacrificed in order to reduce the energy consumption of the UEs via the power reduction described in Section IV. Note that the results are for 100 UEs in the system, thus, the performance of *Optimal: M>1* cannot be shown due to its complexity. As expected, if ρ decreases the sum capacity of the proposal decreases as well, since more capacity gain is transformed to the reduction in the energy consumption (see Fig. 6a). Hence, for $\rho = 0$, the proposal performs as if there would be no relaying and the whole capacity gain is translated to the energy savings.

Fig. 6b illustrates the impact of varying ρ on the average energy consumption of the UEs. The proposal (both for single- and multi- CUE case) reduces the energy consumption more significantly for a lower ρ. Hence, when compared to Fig. 5b, the proposed *Greedy M>1* algorithm further reduces the energy consumption from 73.1% to 87.6%, from 70.3% to 86.3%, and from 70.2% to 86.2% with respect to *No relaying*, *SA incentives*, and *T/VC incentives*, respectively, for $\rho = 0$.

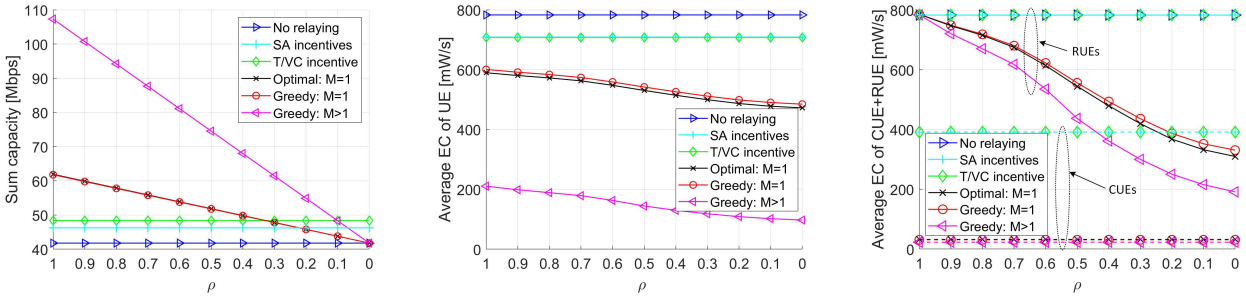

Fig. 6. Impact of transmission power reduction on sum capacity (a) and average energy consumption of all UEs (b) and energy consumption of CUEs and RUEs (c) (100 UEs).

Even if *Greedy M=1* algorithm is not able to offer such notable energy savings as *Greedy M>1*, it still significantly outperforms *No relaying*, *SA incentives*, and *T/VC incentives* up to 38.1%, 31.6%, and 31.5%, respectively.

Fig. 6c analyzes the energy savings experienced by the CUEs and the RUEs separately. The RUEs benefit notably in terms of the energy consumption reduction if ρ is decreased. More specifically, *Greedy: M>1* and *Greedy: M=1* reduce the energy consumption roughly by up to 75.6% and 57.7%, respectively, comparing to both competitive incentive schemes. On the contrary, there is no further reduction in the energy consumption of the CUEs resulting from a decreasing ρ. This is due to the fact that Fig. 6c depicts the case for $\alpha_i = 1$, $\forall i$, i.e., the CUEs experience no gain in terms of the capacity. Thus, there is no relaying capacity gain to be sacrificed by the CUEs as in the case of the RUEs. Still, we observe that the CUEs significantly lower the energy consumption by 97.1% with respect to *No relaying* and by 94.1% with respect to both *SA incentives* and *T/VC incentives*. The reason for such a huge energy consumption reduction is that the CUEs notably minimize their transmission intervals if the proposed relaying is applied.

Now, we demonstrate the energy savings introduced by the proposed *Greedy: M>1* algorithm with respect to all competitive schemes in Fig. 7. In this figure, we illustrate the energy savings achieved by the proposed relaying for the case when the proposed *Greedy: M>1* reaches the same capacity as individual competitive schemes. The proposed *Greedy: M>1* performs the same in terms of the capacity as *No relaying*, *SA incentives*, and *T/VC incentives* for $\rho = 0$, $\rho = 0.07$, and $\rho = 0.1$, respectively, see Fig. 6a. For these values of ρ, *Greedy: M>1* algorithm reduces the energy consumption of the UEs by 87.6%, 85.9%, and 85.6% comparing to *No relaying*, *SA incentives*, and *T/VC incentives*, respectively. The energy saving of only CUEs is 97.1% comparing to *No relaying* and 94.1% comparing to both incentive schemes. Finally, the energy savings of the RUEs is 75.6%, 73.7%, and 72.5% in comparison to *No relaying*, *SA incentives*, and *T/VC incentives*, respectively. The results above demonstrate that our proposal is able to significantly decrease the energy consumption while offering the same capacity as the competitive schemes.

3) Fair Resource Allocation: This subsection studies the impact of the proposed fair allocation derived in Section VI.

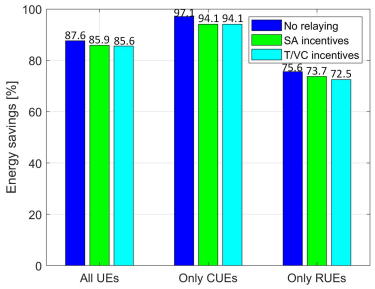

Fig. 7. Energy consumption savings reached by proposed algorithm *Greedy:M>1* with respect to competitive schemes if ρ is set so that individual competitive schemes reach the same sum capacity as the proposal (see Fig. 6a).

We analyze the performance for three allocation cases: (i) upper bound performance in terms of the sum capacity (achieved if $\alpha_i = 1$, $\forall i$); (ii) fair allocation ensuring the same relative gain for the UEs within the same D2D relaying group, i.e., $\alpha_i = \beta$, $\forall i$, labeled as *Fair (relative)*, and (iii): fair allocation guaranteeing the same absolute gain, i.e., $G_{Ci} = G_R$, $\forall i$, labeled as *Fair (absolute)*.

Fig. 8 shows that even the fair allocation introduces a significant improvement with respect to the existing works. If the goal is to guarantee the same relative gains for all CUEs and the RUE within one relaying group, the sum capacity gain with respect to *No relaying*, *SA incentives*, and *T/VC incentives* is 149.9%, 125.8%, and 116%, respectively (Fig. 8a). Even if the same absolute gain is ensured for all UEs within the relaying group, the proposed scheme is still superior to the competitive ones and its gain is at least 91.6% (see Fig. 8a).

From the energy savings perspectives, both fair resource allocations within the relaying group offer a similar energy savings as the *Upper bound*. More specifically, the fair allocation results in the energy savings equal to 85.2% (if the same relative gains are ensured) and 82.8% (if the absolute gains are guaranteed) with respect to *T/VC incentives*, which is the best performing competitive scheme. Note that slightly lower energy savings achieved by the *Fair (absolute)* comparing to the *Upper bound* and the *Fair (relative)* is a result of the fact that improving the performance of the poorly performing UEs by the *Fair (absolute)* allocation costs too many resources, which cannot be exploited by the UEs that can use these resources more efficiently.

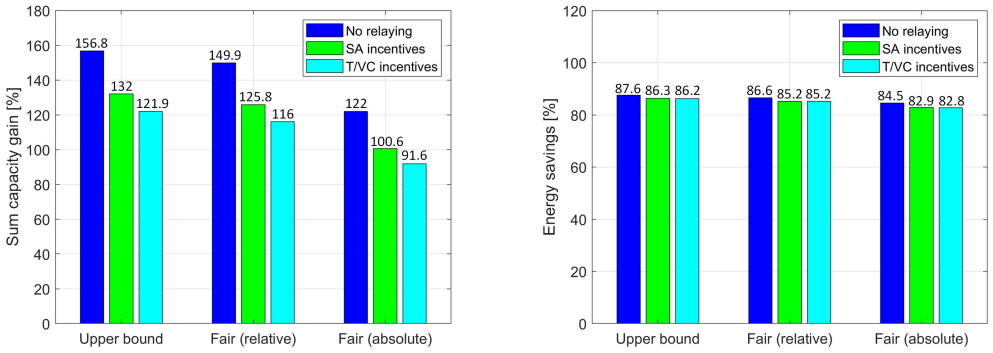

(a) The sum capacity gain ($\rho = 1$). (b) Energy savings ($\rho = 0$).

Fig. 8. Analyzes of fair resource allocation of proposed *Greedy: M>1* over competitive schemes (100 UEs).

TABLE II
SUMMARY OF KEY NOTATIONS

Notation	Description
N	Number of UEs and channels
M	Number of CUEs attached to the RUE
$\gamma_{t,r}$	SINR between any transmitter (TX) and receiver (RX)
P_{max}	Maximum transmission power of UE
$g_{t,r}$	Channel gain between any TX and RX
p_t, p_i, p_r	Transmission power of any TR, i-th CUE, and RUE
p_r^B	Boosted transmission power of RUE
p_r^*	Transmission power of RUE for which $E_R = E_R^*$
σ_0	Noise spectral density
$I_{s,r}$	Mean sum interference from adjacent cells at RX
p_T^{bb}, p_R^{bb}	Power consumption of processing parts at TX and RX
p_T^{rf}, p_R^{rf}	Power consumption of comm. parts at TX and RX
p_T^{on}, p_R^{on}	Power consumption of comm. circuitry at TX and RX
P_T, P_R	Power consumption of TX and RX
E	Total energy consumption of the UE
E_R, E_R^*	Energy consumption of the RUE w/o and with relaying
t_T, t_R	Transmission and reception time
t_s	Duration of a time slot
t_{ci}, t_{ri}, t_R	Transmission time of i-th CUE, of RUE on behalf of i-th CUE, and RUE
B	Bandwidth (BW) available at the BS
B_i, B_R, B_s	Channel BW of i-th CUE, RUE, and aggregated BW
C_i, C_R	Capacity of i-th CUE and RUE w/o relaying
C_i^*, C_R^*	Capacity of i-th CUE and RUE with relaying
K_i, K_R	Normalized capacity of i-th CUE and RUE w/o relaying
K_i^*, K_R^*	Normalized capacity of i-th CUE and RUE with relaying
α_i, β	Relative relying gain of i-th CUE and RUE
G_i, G_R	Absolute relaying gain of i-th CUE and RUE
G_B	The maximum gain of the RUE by capacity boost
$\mathbf{G}^p$	Matrix with potential relaying gains
$G_{i,j}^p$	Relaying gain if i-th CUE is attached to j-th RUE
$x_{i,j}$	Control variable indicating if i-th CUE uses j-th RUE

VIII. CONCLUSION

In this paper, we have proposed a novel incentive framework for the D2D relaying to motivate the UEs to relay the data of the cell edge UEs. The UEs are motivated to perform the relaying via a natural increase in their own capacity and/or a decrease in the energy spent for communication. We have proven that the proposed low-complexity greedy algorithm handling the relay selection for the CUEs is of a submodular nature giving the worst-case approximation guarantees to the optimal performance. Furthermore, we have derived a closed-form expression for the fair allocation of the resources among the RUE and the CUEs exploiting this RUE. We have demonstrated that the proposed scheme reaches a close-to-optimal performance and is able to more than double the capacity and/or reduce the energy consumption by roughly up to 87% when compared to the existing incentive-based relaying schemes.

APPENDIX A

1. Proof of Lemma 1

The minimum allowable value for t_c (denoted as t_c^{min}), is that for which the capacity of every CUEs relaying through the same RUE is exactly the same as its original capacity without the relaying, i.e., $\alpha_i = 1$, $\forall i \in \mathcal{M}$. Thus, using (9) and considering $\alpha_i = 1$, we obtain:

$$t_c^{min} = \sum_{i=1}^{M} t_{ci}^{min} = \frac{K_1}{K_1^*} t_s + \cdots + \frac{K_M}{K_M^*} t_s = \sum_{i=1}^{M} \frac{K_i}{K_i^*} t_s, \quad (24)$$

The maximum value of t_c (denoted as t_c^{max}) is given when $\beta = 1$, i.e., the CUEs gains an additional capacity while the RUE is as good as without relaying (i.e., loses no capacity). The t_c^{max} is derived from (10) considering $\beta = 1$ as:

$$t_c^{max} = \sum_{i=1}^{M} t_{ci} = \frac{(K_R^* - K_R) t_s}{K_R^*} - \sum_{i=1}^{M} t_{ri}, \quad (25)$$

From (24) and (25), we derive the operational region of t_c as:

$$\sum_{i=1}^{M} \frac{K_i}{K_i^*} t_s < \sum_{i=1}^{M} t_{ci} < \frac{(K_R^* - K_R) t_s}{K_R^*} - \sum_{i=1}^{M} t_{ri}, \quad (26)$$

2. Proof of Lemma 2

Let's assume that any t_{ci}^{min} is increased by Δt_{ci} so that $t_{ci} = t_{ci}^{min} + \Delta t_{ci}$. Then, the i-th CUE capacity in (7) is increased by $\Delta C_i^* = K_i^* \Delta t_{ci}$. Simultaneously, the RUE capacity in (8) is decreased by $\Delta C_R^* = -K_R^* \Delta t_{ci} - K_R^* \Delta t_{ri} = -K_R^* \Delta t_{ci} - K_i^* \Delta t_{ci}$. We can substitute $K_R^* \Delta t_{ri}$ for $K_i^* \Delta t_{ci}$ as the amount of data relayed by the RUE on behalf of the i-th CUE is the same as the data send by the CUE during t_{ci}. Thus, any increase in t_{ci}^{min} by Δt_{ci} leads to an overall decrease in the capacity equal to $\Delta C_i^* + \Delta C_R^* = -K_R^* \Delta t_{ci}$. As a result, t_c^{min} corresponds to the upper bound capacity.

It is easy to see, following the same reasoning as above, that for any decrease in t_c^{max} by Δt_{ci}, the total capacity is always increased by $K_R^* \Delta t_{ci}$. Consequently, allocating t_c^{max} to the CUEs corresponds to the lower bound capacity.

3. Proof of Lemma 3

The maximum gain by the power boost can be calculated as a ratio of the RUE's capacity if transmitting with p_r^B (i.e., transmission power if the power boost is applied) to the case when only p_r is utilized (i.e., no power boost). Consequently, taking (8) into account and assuming that the RUE transmits over $t_s - \sum_{i=1}^{M} t_{ci}$ time interval, we can calculate G_B in the following way:

$$\begin{aligned} G_B &= B_s log_2\left(1+\frac{p_r^B g_{r,b}}{B_s\left(\sigma_0+I_{s,0}\right)}\right)(t_s-t_c) \\ &\quad - B_s log_2\left(1+\frac{p_r g_{r,b}}{B_s\left(\sigma_0+I_{s,0}\right)}\right)(t_s-t_c) \\ &= B_s log_2\left(\frac{B_s\left(\sigma_0+I_{s,0}\right)+p_r^B g_{r,b}}{B_s\left(\sigma_0+I_{s,0}\right)}\right)(t_s-t_c) \\ &\quad - B_s log_2\left(\frac{B_s\left(\sigma_0+I_{s,0}\right)+p_r g_{r,b}}{B_s\left(\sigma_0+I_{s,0}\right)}\right)(t_s-t_c) \\ &= B_s log_2\left(\frac{B_s\left(\sigma_0+I_{s,0}\right)+p_r^B g_{r,b}}{B_s\left(\sigma_0+I_{s,0}\right)+p_r g_{r,b}}\right)(t_s-t_c). \end{aligned} \quad (27)$$

4. Proof of Lemma 4

To determine an allowable range of the transmission power, we first derive an absolute gain of each particular UE. Specifically, the absolute gain of the i-th CUE is determined from (5) and (7) as:

$$G_i = C_i^* - C_i = B_s log_2\left(1+\frac{p_i g_{i,r}}{B_s\left(\sigma_0+I_{s,0}\right)}\right)t_{ci} - K_i t_s, \quad (28)$$

and, similarly, the absolute gain of the RUE is obtained from (6) and (8) as:

$$\begin{aligned} G_R + G_B &= C_R^* - C_R + G_B \\ &= B_s log_2\left(1+\frac{p_r g_{r,b}}{B_s\left(\sigma_0+I_{s,0}\right)}\right)(t_s - \sum_{i=1}^{M} t_{ci}) \\ &\quad - \sum_{i=1}^{M} K_i^* t_{ci} - K_R t_s, \end{aligned} \quad (29)$$

Then, (28) and (29) is rearranged in the following way:

$$\frac{\rho G_i + K_i t_s}{B_s t_{ci}} = log_2\left(1+\frac{p_i g_{i,r}}{B_s\left(\sigma_0+I_{s,0}\right)}\right), \quad (30)$$

$$\frac{\rho(G_R+G_B)+\sum_{i=1}^{M} K_i^* t_{ci} + K_R t_s}{B_s(t_s - \sum_{i=1}^{M} t_{ci})} = log_2\left(1+\frac{p_r g_{r,b}}{B_s\left(\sigma_0+I_{s,0}\right)}\right), \quad (31)$$

Finally, from (30) and (31), we express p_i and p_r as:

$$p_i = \kappa_i(2^{\frac{\rho G_i + K_i t_s}{B_s t_{ci}}} - 1), \quad (32)$$

$$p_r = \kappa_R(2^{\frac{\rho(G_R+G_B)+K_R\cdot t_s+\sum_{i=1}^{M} K_i^* t_{ci}}{B_s(t_s-\sum_{i=1}^{M} t_{ci})}} - 1), \quad (33)$$

From (32) and (33), we see that if $\rho = 0$, the CUE/RUE sacrifice the whole capacity gain in order to reduce the energy consumption and the CUE and the RUE transmit with the minimal transmission power. Contrary, if $\rho = 1$, no energy reduction is achieved and the CUE/RUE does not reduce its transmission power at all. Thus, the maximal transmission power is used.

APPENDIX B

1. Proof of Theorem 5

The elements $G_{i,j}^p$ are independent of each other, since the D2D pairs have orthogonal resources. Hence, every time a new pair is added, the gain increases. Furthermore, assume that the subset of the selected pairs is A and we add the next pair $\{i,j\}$. Assume further another set of the selected D2D pairs $A \subset B$. Then $\{i,j\}$ either have the same $G_{i,j}^p$ value, or is 0, if that i or j have already been assigned in B. This satisfies the submodularity requirement [43]. Finally, it is easy to see that the first set of constraints defines a matroid (max of one item per row) and the second set is another matroid (max of one item per column). It is known that a greedy algorithm yields an approximation ratio of $\frac{1}{(p+1)}$, when the constraints are the intersection of p matroids (or in general, a p-system independent constraint) [44]. Hence, given that we have 2 matroids for our problem this gives a $\frac{1}{3}$ approximation for the greedy algorithm.

2. Proof of Lemma 6

The objective is submodular using the similar arguments as in Theorem 5. As more and more pairs are selected, each gain $G_{i,j}^p$ either becomes 0 (the i-th CUE has already been assigned to an RUE) or is decreased (the j-th RUE has already been assigned some other CUEs, so the gain for the i being associated to the j is smaller. The additional condition, that of $G_{i,j}^p \geq 0$ if the CUE bandwidth, where B and the RUE $M \cdot B$, ensures the objective's monotonicity, even if the RUE ends up serving the maximum number (M) of the CUEs. Finally, the constraint set is again an intersection of the matroids, leading to the same approximation ratio as in Theorem 5, the difference being that the optimal value now cannot be obtained in polynomial time.

APPENDIX C

1. Proof of Lemma 7

The same relative gain of the CUEs and the RUE is guaranteed if $\alpha_1 = \alpha_2 = \cdots = \alpha_M = \beta$. Thus, using (9), we can write:

$$\frac{K_1^* t_{c1}}{K_1 t_s} = \frac{K_2^* t_{c2}}{K_2 t_s} = \cdots = \frac{K_M^* t_{cM}}{K_M t_s} = \beta. \quad (34)$$

Hence, (20) is easily derived from (34). Then, we determine t_{c1}. Considering that $\alpha_1 = \beta$, the following is derived from (9) and (10) by applying several simple math operation:

$$\frac{K_1^* K_R}{K_1} t_{c1} = K_R^* t_s - K_R^* \sum_{i=1}^{M} t_{ci} - K_R^* \sum_{i=1}^{M} t_{ri}. \quad (35)$$

Taking into account that $K_R^* \sum_{i=1}^{M} t_{ri} = \sum_{i=1}^{M} K_i^* t_{ci}$ (i.e., the RUE retransmits the same amount of the CUEs' data as the amount of data transmitted by the CUEs to the RUE) and substituting all t_{ci} in (35) using (20), we can write:

$$\begin{aligned} \frac{K_1^* K_R}{K_1} t_{c1} &= K_R^* t_s - K_R^* t_{c1} - \frac{K_1^* K_R^*}{K_1} \sum_{i=2}^{M} \frac{K_i}{K_i^*} t_{c1} \\ &\quad - K_1^* t_{c1} - \sum_{i=2}^{M} \frac{K_1^* K_i}{K_1} t_{c1}. \end{aligned} \quad (36)$$

Finally, t_{c1} is derived according to (21). The rest of t_{ci} is calculated from (20) via inserting t_{c1} obtained in (21).

2. Proof of Lemma 8

The same absolute gain for all UEs is guaranteed when $G_1 = \cdots = G_M = G_R$, that is, if:

$$K_1^* t_{c1} - K_1 t_s = K_M^* t_{cM} - K_M t_s = G_R \tag{37}$$

Equation (22) is again derived from (37). Then, analogously to the case with the same relative gains, we first determine t_{c1} and the rest of t_{ci} is calculated by (22) afterwards. Thus, we need to fulfill the following:

$$K_1^* t_{c1} - K_1 t_s = K_R^* \left(t_s - \sum_{i=1}^{M} (t_{ci} + t_{ri}) \right) - K_R t_s. \tag{38}$$

Equation (38) is rewritten exploiting (22) and considering that $K_R^* \sum_{i=1}^{M} t_{ri} = \sum_{i=1}^{M} K_i^* t_{ci}$ as:

$$\begin{aligned} &K_1^* t_{c1} - K_1 t_s \\ &\quad = K_R^* \left(t_s - t_{c1} - \sum_{i=2}^{M} \frac{K_1^* t_{c1} - K_1 t_s + K_i \cdot t_s}{K_i^*} \right) \\ &\qquad - K_1^* t_{c1} - \sum_{i=2}^{M} (K_1^* t_{c1} - K_1 t_s + K_i t_s) - K_R t_s. \end{aligned} \tag{39}$$

From (39), we finally express t_{c1} as presented in (23). Subsequently, any t_{ci} is calculated according to (22).

ACKNOWLEDGMENT

This work was supported by project No. LTT18007 funded by Ministry of Education, Youth and Sports, Czech Republic.

REFERENCES

[1] A. Asadi, Q. Wang, and V. Mancuso, "A survey on device-to-device communication in cellular networks," *IEEE Commun. Surveys Tuts.*, vol. 16, no. 4, pp. 1801–1819, 4th Quart., 2014.

[2] D. Wen, G. Yu, and L. Xu, "Energy-efficient mode selection and power control for device-to-device communications," in *Proc. IEEE Wireless Commun. Netw. Conf.*, Doha, Qatar, Apr. 2016, pp. 1–7.

[3] P. Mach, Z. Becvar, and T. Vanek, "In-band device-to-device communication in OFDMA cellular networks: A survey and challenges," *IEEE Commun. Surveys Tuts.*, vol. 17, no. 4, pp. 1885–1922, 4th Quart., 2015.

[4] O. A. Amodu, M. Othman, N. K. Noordin, and I. Ahmad, "Relay-assisted D2D underlay cellular network analysis using stochastic geometry: Overview and future directions," *IEEE Access*, vol. 7, pp. 115023–115051, 2019.

[5] S. Dang, G. Chen, and J. P. Coon, "Outage performance analysis of full-duplex relay-assisted device-to-device systems in uplink cellular networks," *IEEE Trans. Veh. Technol.*, vol. 66, no. 5, pp. 4506–4510, May 2017.

[6] T. Liu, J. C. S. Lui, X. Ma, and H. Jiang, "Enabling relay-assisted D2D communication for cellular networks: Algorithm and protocols," *IEEE Internet Things J.*, vol. 5, no. 4, pp. 3136–3150, Aug. 2018.

[7] S. Dang, G. Chen, and J. P. Coon, "Multicarrier relay selection for full-duplex relay-assisted OFDM D2D systems," *IEEE Trans. Veh. Technol.*, vol. 67, no. 8, pp. 7204–7218, Aug. 2018.

[8] J. Sun, Z. Zhang, C. Xing, and H. Xiao, "Uplink resource allocation for relay-aided device-to-device communication," *IEEE Trans. Intell. Transp. Syst.*, vol. 19, no. 12, pp. 3883–3892, Dec. 2018.

[9] B. Klaiqi, X. Chu, and J. Zhang, "Energy- and spectral-efficient adaptive forwarding strategy for multi-hop device-to-device communications overlaying cellular networks," *IEEE Trans. Wireless Commun.*, vol. 17, no. 9, pp. 5684–5699, Sep. 2018.

[10] L. Wang, T. Peng, Y. Yang, and W. Wang, "Interference constrained relay selection of D2D communication for relay purpose underlaying cellular networks," in *Proc. 8th Int. Conf. Wireless Commun., Netw. Mobile Comput.*, Shanghai, China, Sep. 2012, pp. 1–5.

[11] J. Deng, A. A. Dowhuszko, R. Freij, and O. Tirkkonen, "Relay selection and resource allocation for D2D-relaying under uplink cellular power control," in *Proc. IEEE Globecom Workshops (GC Wkshps)*, San Diego, CA, USA, Dec. 2015, pp. 1–6.

[12] J. Zhao, K. K. Chai, Y. Chen, J. Schormans, and J. Alonso-Zarate, "Two-level game for relay-based throughput enhancement via D2D communications in LTE networks," in *Proc. IEEE Int. Conf. Commun. (ICC)*, Kuala Lumpur, Malaysia, May 2016, pp. 1–6.

[13] J. Gui and J. Deng, "Multi-hop relay-aided underlay D2D communications for improving cellular coverage quality," *IEEE Access*, vol. 6, pp. 14318–14338, 2018.

[14] X. Xu, J. Wang, and X. Tao, "Analytical modeling for caching enabled UE-to-network relay in cellular networks," *IEEE Access*, vol. 6, pp. 51061–51068, 2018.

[15] J. Wang, X. Xu, X. Tang, S. Zhang, and X. Tao, "Analytical modeling of mode selection for UE-to-network relay enabled cellular networks with power control," in *Proc. IEEE Int. Conf. Commun. Workshops (ICC Workshops)*, Kansas City, MO, USA, May 2018, pp. 1–6.

[16] S. Zhang, X. Xu, M. Sun, X. Tang, and X. Tao, "Energy efficient uplink transmission for UE-to-network relay in heterogeneous networks," in *Proc. IEEE PIMRC*, Montreal, QC, Canada, Oct. 2017, pp. 1–7.

[17] N. Mastronarde, V. Patel, J. Xu, and M. van der Schaar, "Learning relaying strategies in cellular D2D networks with token-based incentives," in *Proc. IEEE Globecom Workshops (GC Wkshps)*, Atlanta, GA, USA, Dec. 2013, pp. 1–7.

[18] N. Mastronarde, V. Patel, and L. Liu, "Device-to-device relay assisted cellular networks with token-based incentives," in *Proc. IEEE Int. Conf. Commun. Workshop (ICCW)*, London, U.K., Jun. 2015, p. 698.

[19] Z. Zhu, S. Jin, Y. Yang, H. Hu, and X. Luo, "Time reusing in D2D-enabled cooperative networks," *IEEE Trans. Wireless Commun.*, vol. 17, no. 5, pp. 3185–3200, May 2018.

[20] Q. Xu, Z. Su, and S. Guo, "A game theoretical incentive scheme for relay selection services in mobile social networks," *IEEE Trans. Veh. Technol.*, vol. 65, no. 8, pp. 6692–6702, Aug. 2016.

[21] Q. Shen, W. Shao, and X. Fu, "D2D relay incenting and charging modes that are commercially compatible with B2D services," *IEEE Access*, vol. 7, pp. 36446–36458, 2019.

[22] Y. Li, Z. Zhang, H. Wang, and Q. Yang, "SERS: Social-aware energy-efficient relay selection in D2D communications," *IEEE Trans. Veh. Technol.*, vol. 67, no. 6, pp. 5331–5345, Jun. 2018.

[23] P. Yang, Z. Zhang, J. Yang, and X. Wang, "Incorporating user willingness in contract-based incentive mechanism for D2D cooperative data forwarding," *IEEE Access*, vol. 6, pp. 54927–54937, 2018.

[24] Q. Sun, L. Tian, Y. Zhou, J. Shi, and X. Wang, "Energy efficient incentive resource allocation in D2D cooperative communications," in *Proc. IEEE Int. Conf. Commun.*, London, U.K., Jun. 2015, pp. 1–6.

[25] P. Mach, Z. Becvar, and T. Spyropoulos, "Incentive mechanism and relay selection for D2D relaying in cellular networks," in *Proc. IEEE Global Commun. Conf. (GLOBECOM)*, Waikoloa, HI, USA, Dec. 2019, pp. 1–7.

[26] A. Ramezani-Kebrya, M. Dong, B. Liang, G. Boudreau, and S. H. Seyedmehdi, "Robust power optimization for device-to-device communication in a multi-cell network under partial CSI," in *Proc. IEEE Int. Conf. Commun. (ICC)*, Paris, France, May 2017, pp. 1–6.

[27] B. V. R. Gorantla and N. B. Mehta, "Allocating multiple D2D users to subchannels with partial CSI in multi-cell scenarios," in *Proc. IEEE Int. Conf. Commun. (ICC)*, Shanghai, China, May 2019, pp. 1–6.

[28] B. V. R. Gorantla and N. B. Mehta, "Resource and computationally efficient subchannel allocation for D2D in multi-cell scenarios with partial and asymmetric CSI," *IEEE Trans. Wireless Commun.*, vol. 18, no. 12, pp. 5806–5817, Dec. 2019.

[29] M. Lauridsen, L. Noël, T. B. Sørensen, and P. Mogensen, "An empirical LTE smartphone power model with a view to energy efficiency evolution," *Intel Technol. J.*, vol. 18, no. 1, pp. 172–193, Mar. 2014.

[30] M. R. Mili, A. Khalili, N. Mokari, S. Wittevrongel, D. W. K. Ng, and H. Steendam, "Tradeoff between ergodic energy efficiency and spectral efficiency in D2D communications under rician fading channel," *IEEE Trans. Veh. Technol.*, vol. 69, no. 9, pp. 9750–9766, Sep. 2020.

[31] O. Yazdani, M. Monemi, and G. Mirjalily, "Fast globally optimal transmit antenna selection and resource allocation scheme in mmWave D2D networks," *IEEE Trans. Mobile Comput.*, early access, Jul. 14, 2020, doi: 10.1109/TMC.2020.3009183.

[32] M. Najla, Z. Becvar, P. Mach, and D. Gesbert, "Predicting device-to-device channels from cellular channel measurements: A learning approach," *IEEE Trans. Wireless Commun.*, vol. 19, no. 11, pp. 7124–7138, Nov. 2020.

[33] H. Kuhn, "The hungarian method for the assignment problem," *Nav. Res. Logistics Quart.*, vol. 2, no. 1, pp. 83–97, Mar. 1955.
[34] A. Krause, A. Singh, and C. Guestrin, "Near-optimal sensor placements in Gaussian processes: Theory, efficient algorithms and empirical studies," *J. Mach. Learn. Res.*, vol. 9, no. 2, pp. 235–284, 2008.
[35] D. Tsigkari and T. Spyropoulos, "An approximation algorithm for joint caching and recommendations in cache networks," 2020, *arXiv:2006.08421*. [Online]. Available: http://arxiv.org/abs/2006.08421
[36] A. A. Ageev and M. I. Sviridenko, "Pipage rounding: A new method of constructing algorithms with proven performance guarantee," *J. Combinat. Optim.*, vol. 8, no. 3, pp. 307–328, Sep. 2004.
[37] C. Chekuri, J. Vondrak, and R. Zenklusen, "Submodular function maximization via the multilinear relaxation and contention resolution schemes," in *Proc. 43rd ACM Symp. Theory Comput. (STOC)*, San Jose, CA, USA, Jun. 2011, pp. 783–792.
[38] M. Minoux, "Accelerated greedy algorithms for maximizing submodular set functions," in *Optimization Techniques*, in Lecture Notes in Control and Information Sciences, vol. 7, J. Stoer, Eds. Berlin, Germany: Springer, 1978, pp. 234–243.
[39] B. Mirzasoleiman, A. Badanidiyuru, A. Karbasi, J. Vondrak, and A. Krause, "Lazier than lazy greedy," in *Proc. Artif. Intell. Conf.*, Austin, TX, USA, 2015, pp. 1812–1818.
[40] *Study on LTE Device to Device Proximity Services*, document TR 36.843, 3GPP, 2014.
[41] *Evolved Universal Terrestrial Radio Access (E-UTRA), Further Advancements for E-UTRA Physical Layer Aspects*, document TR 36.814, 3GPP, 2017.
[42] I. Viering, A. Klein, M. Ivrlac, M. Castaneda, and J. A. Nossek, "On uplink intercell interference in a cellular system," in *Proc. IEEE Int. Conf. Commun.*, Istanbul, Turkey, Jun. 2006, pp. 2095–2100.
[43] A. Krause and D. Golovin, "Submodular function maximization," in *Tractability: Practical Approaches to Hard Problems*. Cambridge, U.K.: Cambridge Univ. Press., Feb. 2011, pp. 71–104.
[44] G. Calinescu, C. Chekuri, M. Pál, and J. Vondrák, "Maximizing a monotone submodular function subject to a matroid constraint," *SIAM J. Comput.*, vol. 40, no. 6, pp. 1740–1766, Jan. 2011.

Pavel Mach (Member, IEEE) received the M.Sc. and Ph.D. degrees in telecommunication engineering from the Czech Technical University in Prague, Czech Republic, in 2006 and 2010, respectively. In 2006 and 2007, he joined Sitronics R&D Center, Prague, focusing on emerging mobile technologies and was involved in research activities of Vodafone R&D Center, Czech Technical University, Prague, from 2005 to 2008. He is currently a Senior Researcher with the 5G Mobile Lab, CTU, Prague, in 2015, focusing on 5G and beyond mobile networks. He was involved in several European projects such as FP7 ROCKET, FP7 FREEDOM, and FP7 TROPIC. He has published more than 60 conference or journal papers, including two patents on scheduling in C-RAN.

Thrasyvoulos Spyropoulos (Member, IEEE) received the Diploma degree in electrical and computer engineering from the University of Athens, and the Ph.D. degree from the University of Southern California. He was a Post-Doctoral Researcher with INRIA and then a Senior Researcher with ETH Zürich. He is currently a Professor at EURECOM, Sophia Antipolis. He was a recipient of the Best Paper Award in IEEE SECON 2008 and IEEE WoWMoM 2012, and runner-up for ACM Mobihoc 2011 and IEEE WoWMoM 2015.

Zdenek Becvar (Senior Member, IEEE) received the M.Sc. and Ph.D. degrees in telecommunication engineering from the Czech Technical University in Prague, Czech Republic, in 2005 and 2010, respectively. He is currently an Associate Professor with the Department of Telecommunication Engineering, Czech Technical University in Prague. From 2006 to 2007, he joined Sitronics R&D Center, Prague, focusing on speech quality in VoIP. Furthermore, he was involved in research activities of Vodafone R&D Center, Czech Technical University in Prague, in 2009. He was on internships at Budapest Politechnic, Hungary, in 2007; CEA-Leti, France, in 2013; and EURECOM, France, in 2016 and 2019. From 2013 to 2017, he was a representative of the Czech Technical University in Prague in ETSI and 3GPP standardization organizations. In 2015, he founded 5Gmobile Research Lab at CTU in Prague, focusing on research towards 5G and beyond mobile networks. He has published four book chapters and more than 70 conference or journal papers.

XIII. Appendix F

This appendix includes journal paper published in: **P. Mach**, Z. Becvar and T. Spyropoulos, "Coping with Spatial Unfairness and Overloading Problem in Mobile Networks via D2D Relaying, to appear in *IEEE Wireless Communications*, vol. 31, no. 1, Feb. 2024 IF (JCR 2022) = **12.9**.

ACCEPTED FROM OPEN CALL

Coping with Spatial Unfairness and Overloading Problem in Mobile Networks via D2D Relaying

Pavel Mach, Zdenek Becvar, and Thrasyvoulos Spyropoulos

Abstract

Device-to-device (D2D) relaying is able to increase the network capacity, enhance the network coverage, or mitigate the interference to legacy cellular transmissions. These benefits are even emphasized if a proper incentives are offered to the users to motivate them to act as relays. We first survey the state-of-the-art incentives to show that despite a proper incentivization, the benefits from relaying are enjoyed typically only by the users directly involved in relaying, that is, either those in favorable locations to act as relays or those exploiting such relays to improve their performance. Nevertheless, many users, who are not satisfied with their quality of service (QoS), may not profit from D2D relaying due to their unfavorable locations. Besides, the current incentive mechanisms are not able to alleviate the overloading of the base station (BS) without violating QoS of already admitted users. Thus, to cope with the spatial unfairness and the overloading of BSs, we propose resource allocation framework extending D2D relaying benefits also to the users not directly involved in the relaying process. The proposed framework enables efficient reuse of radio resources and takes inspiration from economy concept of taxes. Moreover, it gives an opportunity to the users distributing spared radio resources to increase their virtual monetary gain, reputation, or even helping other users depending on mutual social relationships. The simulations demonstrate that the proposed concept improves the ratio of satisfied users and/or maximizes the number of newly admitted users for which the BS would not have radio resources otherwise.

Introduction

Device-to-device (D2D) communication is seen as a convenient way to increase the capacity and the energy efficiency of contemporary mobile networks [1]. At its inception more than a decade ago, the sole intended purpose of D2D communication was to send data directly between any two devices in proximity, thus bypassing a base station (BS) and saving radio resources in the process.

As D2D communication progressively matured, it has found additional intriguing use-cases and applications, such as content sharing and caching [2, 3]. Moreover, D2D communication can be exploited for relaying purposes (also known as D2D relaying) in order to increase the performance of users experiencing a low channel quality to/from the BS. Besides, D2D relaying can augment multi-casting/broadcasting services [4], facilitate a load balancing among adjacent BSs [5], or improve the computation offloading to edge servers [6]. Consequently, D2D relaying is a very useful tool for the existing 5G and the emerging 6G networks.

One of the crucial challenges for D2D relaying, however, is to ensure a *willingness* of the users *to offer relaying services* to other users, who are often complete strangers. This willingness can hardly be taken granted, given that devices used for relaying, such as smartphones or IoT devices, can suffer from an additional energy consumption. Similarly, even the users exploiting relaying services should be convinced to entrust their data to the intermediate relaying users. In this regard, several incentive strategies have been proposed throughout the years taking an inspiration from economy [7, 8], social aspects [9, 10], or reputation [11, 12]. Besides, an attractive option to motivate the relaying users is to give him/her some additional radio resources [13].

The existing incentive mechanisms typically provide benefits, in terms of capacity increase and/or energy consumption decrease, solely to the users *directly* involved in relaying, that is, to the users assisted by the relaying users and to the relaying users themselves. Still, there are users with a low channel quality to the BS that, unfortunately, cannot enjoy the benefits of relaying simply because no suitable relay is in their vicinity. Consequently, Quality of Service (QoS) requirements of these "unlucky" users with low-quality channels to the BS cannot be met due to this spatial unfairness. Besides, the existing incentive solutions are not able to alleviate an overloading problem, when the BS is not able to admit any new users without violating QoS of the already admitted users.

In this article, we first overview recent incentive approaches for D2D relaying maximizing the benefits of the users directly involved in D2D relaying. Then, to increase the number of users benefiting from D2D relaying, primarily those users who are not satisfied with their QoS or cannot

Digital Object Identifier:
10.1109/MWC.012.2200236

Pavel Mach and Zdenek Becvar are with Czech Technical University in Prague, Faculty of Electrical Engineering, Czech Republic; Thrasyvoulos Spyropoulos is with EURECOM, France.

be admitted by the BS due to its overloading, we propose a novel resource allocation framework. The proposed framework builds upon the existing incentive mechanisms but it enables to extend the benefits of D2D relaying also to the users not directly involved in relaying itself. In particular, we propose to:

- *Reuse* resources allocated to D2D links (i.e., links between the users) by the cellular links
- *Tax* resources earned or saved by the users benefiting directly from relaying
- *Sell* the earned (or saved) resource to other users to convert the relaying gain into monetary gain, increased reputation, or to help others with strong mutual social relationship

Subsequently, the resources obtained from these mechanisms are distributed to the users not directly involved in relaying. We also discuss various optimization, implementation, and feasibility aspects of each proposed mechanism allowing their smooth and efficient implementation into mobile networks. Finally, we show that the proposed framework increases significantly the number of users satisfied with QoS and/or allows to admit many new users to be served even if the network is highly overloaded.

Overview of Incentive Strategies for D2D Relaying

This section discusses the most prominent incentive strategies giving benefits to the users directly participating in relaying (Fig. 1). Moreover, we outline key properties each incentive mechanism should support and describe the common approaches to reach mutual agreement among cooperating users.

Virtual Currency-Based Incentives

One family of incentives motivating the users to relay data is based on a virtual currency. The virtual currency can be represented by tokens paid to the users providing the relaying services [7]. The tokens are initially distributed by the network to the users. Afterwards, the token is given to the user whenever he/she agrees on the relaying service provisioning. The received tokens can be exploited by the relaying users in the future, when these users require some relaying service themselves. The potential problem with tokens is that the relaying users receive one token for relaying service disregarding the amount of relayed data or the relaying time/consumed energy. To remedy this problem, the relaying users can be paid in "credits" that can easily factor the amount of relayed data, capacity improvement, or simply duration of the relaying service [8].

Social Relationship-Based Incentives

The social relationship-based incentives build on the assumption that the users tend to interact preferentially with the people to whom they have some social tie, such as close friends, relatives, or co-workers [9]. The relationships can be modeled as a weighted graph, where the vertices correspond to individual users while the edges represent a "social closeness" between them. To define strength of the social tie, a specific weight to each connection (edge) is assigned [10] (Fig. 1). Based on such graph, the one subset of users prefer to act as relays for other subset of users with whom they have close social ties. It is reasonable to assume that social peers are willing to relay each other's traffic without any (monetary) cost or, at least, with some discount depending on the level of social trust [9].

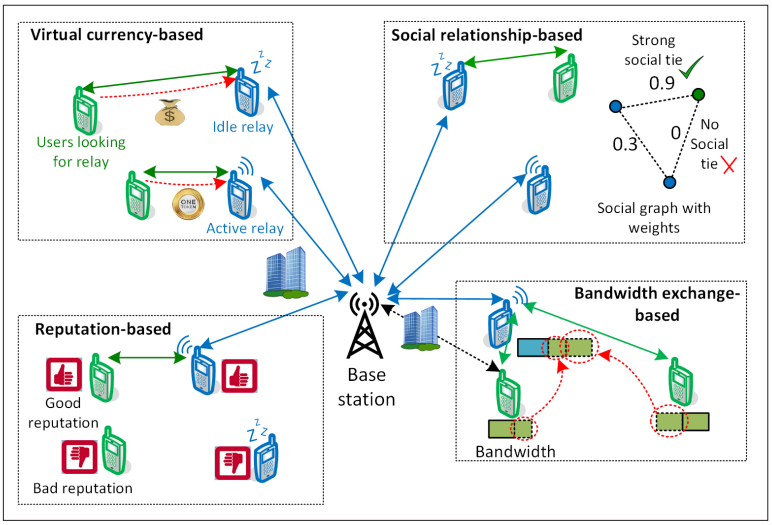

FIGURE 1. State-of-the-art incentive strategies for D2D relaying.

Reputation-Based Incentives

The relaying users can also be motivated via a reputation-based approach [11]. The users have either "bad" or "good" reputation, determined by the BS on a regular basis. Intuitively, the users with "good" reputation get help easily from others when they are in a need of relaying. Contrary, the users known to refuse helping others have hard times to find anyone volunteering to relay data due to "bad" reputation. Moreover, the BS is able to detect whether the relaying users send data at the appointed intervals and it assigns the reputation accordingly [11]. The binary reputation score, however, may not be sufficient to reflect the current users' behavior. Consequently, more flexible reputation is based on YouTube or Facebook "like" button, where the reputation is increased (or decreased) by 1 (or 0.5) if the users are satisfied (or not satisfied) with relaying [12].

Bandwidth Exchange-Based Incentives

All previous incentive mechanisms are based on an indirect reciprocity, where the relaying users benefit in the *future*. The bandwidth exchange-based incentives, on the contrary, gives an *immediate* benefit to the relaying users. The immediate benefit is represented by some part of the channel/resource blocks or more transmission opportunities [13] (Fig. 1). Hence, there is no risk in terms of the uncertainty whether the current relaying cost is outweighed by a reward in the future. The additional radio resources are, then, exploited by the relaying user to both relay data of other user(s) and to boost its own capacity and/or reduce the relay's energy consumption [13].

Properties of Incentive Mechanisms

All incentive concepts described in previous subsections should ensure *individual rationality* and *incentive compatibility*. The former one guaran-

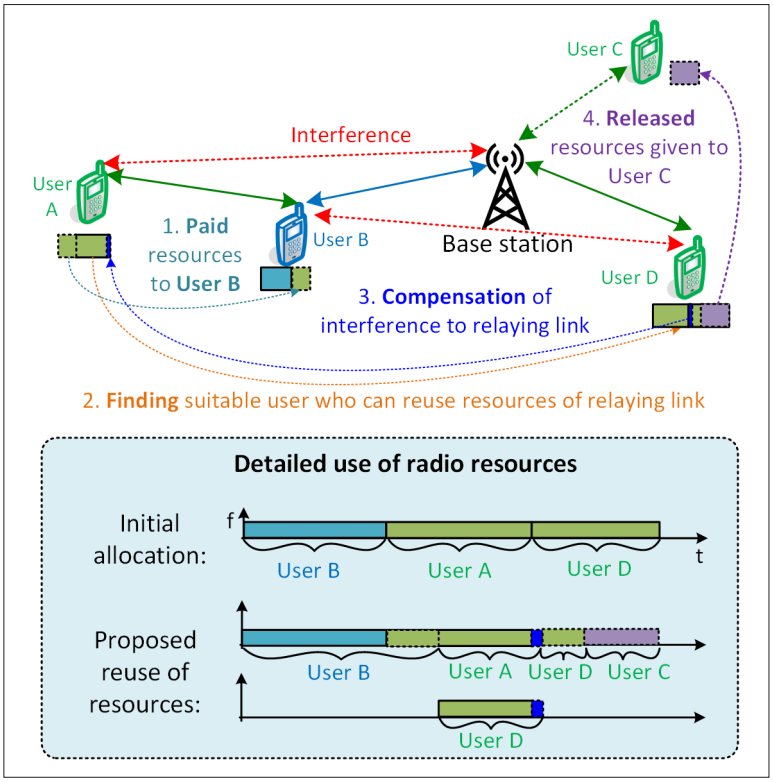

FIGURE 2. Illustrative principle of resources reuse by cellular link. After Users A and B become involved in D2D relaying, User D reuses resources of User A who is, at the same time, compensated by a part of resources initially allocated to User D. Then, the remaining resources initially allocated to User D are split to two parts; first part remain to user D to ensure his/her satisfaction while the second part is assigned to User C.

tees that all involved participants can benefit from relaying, that is, the relaying cost in terms of the payment for relaying service or additional energy consumption of the relaying users does not outweigh the relaying gain [14]. The latter one, then, ensures that every participant in relaying maximizes his/her own gain if acting according to their real and true preferences [10, 14].

Moreover, each incentive mechanism should ensure that all users participating in relaying are satisfied by finding a proper trade-off between the relaying gain and the relaying cost. The common approach to solve this challenge is to apply *auction mechanism*, where the buyers in the auction submit bids and corresponding prices they are willing to pay. Subsequently, the auctioneer selects winning buyers to maximize social welfare [10]. Besides, *contract theory* is often applied so that the users select contracts to maximize their own utility [14]. Lastly, also *game theory*, such as indirect reciprocity game adopted in [11], is commonly exploited to stimulate the users' cooperation.

Proposed Framework

The incentive mechanisms described in the previous section are able to motivate the relaying users and, thus, all users directly participating in D2D relaying can fully enjoy its benefits. Unfortunately, there are still many users unable to meet their QoS requirements due to their poor channel quality to the BS while incapable to capitalize on D2D relaying concept due to their disadvantageous locations with respect to other users in proximity. Besides, the existing incentive approaches cannot help users that would like to access the BS that is currently overloaded. To extend the benefits of D2D relaying to these users, we propose a framework encompassing three mechanisms:

- Reusing of resources allocated to D2D links
- Taxing
- Selling of resources.

While the first two are managed by the BS, the last mechanism gives a more free hand to the users themselves to decide to whom the resources are assigned.

Reuse of D2D Relaying Links Resources by Cellular Links

The main idea of the first mechanism is to reuse the resources allocated to the relaying links by the cellular users communicating directly with the BS. The proposed process of reuse is summarized in following four consecutive steps (Fig. 2).

In the first step, the user searching for relay (User A in Fig. 2) makes a deal with the relaying user (User B). In line with the bandwidth exchange-based incentives, User B gets a part of the resources from User A. Consequently, User B is able to both forward data of User A to/from the BS and to increase own capacity or save energy due to decreased transmission power. The exact determination of the amount of resources to be delegated to User B is out of scope of this article, but let's assume that both users benefit (e.g., resources can be allocated in a way that the relaying gain of both is the same [13]).

In the second step, the BS finds a suitable cellular user who can reuse resources allocated to the relaying link (i.e., the link between User A and User B in Fig. 2). By intuition, the reuse of relaying link's resources by the cellular user inevitably results in the interference to/from the cellular communication from/to D2D communication (Fig. 2). Nevertheless, interference from (or to) User A to (or from) the BS is usually not significant as the channel quality between these two is low. In fact, the low channel quality between User A and the BS is the main reason why relaying is initiated in the first place. Further, one can observe that interference from (to) User B to (from) User D depends strongly on the channel quality between these two. Thus, the ideal candidate cellular user to reuse the resources of the relaying link is the one that is far from the relaying user to mitigate interference imposed by the relay to the cellular user in downlink or vice versa in uplink.

Even though the interference to the relaying link is insignificant, there may be still a slight degradation in D2D relaying link quality. Consequently, during the third step, a part of the resources initially allocated to User D (i.e., the cellular user reuses resources of the relaying link) are assigned by the BS to D2D relaying link to compensate the interference generated to this user by the reuse.

In the last step, the resources initially allocated to User D are split into two parts. The first part of the resources is exploited by User D to satisfy his/her requirements. This is beneficial especially if User D cannot find any suitable relaying users and, at the same time, he/she has a weak channel to the BS. Then, the rest of the resources of User D are released and given to other user(s) (User C in Fig. 2).

Optimization, Implementation, and Feasibility Aspects: To maximize the benefit from the reuse, a selection of the users reusing the resources of individual relaying links should be optimized to minimize the interference between the cellular and D2D communications. The optimization problem can be understood as a selection of pairs, each composed from one user reusing resources of one relaying link. This corresponds to one-to-one matching problem solvable *optimally* in polynomial time by Hungarian algorithm [13].

Besides, to enable reuse of the resources, interference links should be known by the BS. While the interference between the BS and any user (e.g., User A in Fig. 2) is available via conventional channel estimation, the derivation of interference among users (e.g., User B and User D) can be demanding in terms of signaling, especially if there are many cellular users potentially reusing resources of many relaying links. Fortunately, the channel between any two users may be predicted with a high accuracy using deep neural networks [15], resulting in no or only very low signaling overhead.

Taxing Resources Earned Through Relaying

The application of only reuse mechanism may not always be sufficient to increase the number of users benefiting indirectly from relaying. To this end, we come up with the second mechanism, where the resources saved/earned by the users directly involved in relaying are taxed in a similar way as the taxes imposed by the government to its citizen. The principle of the taxation mechanism is summarized into three steps (Fig. 3).

The first step is analogous to the one utilized in the reuse mechanism, that is, in the establishing of D2D relaying link(s). Then, during the second step, the BS imposes a tax on both the resources earned by the relaying user (i.e., the resources obtained by User B) and the resources saved by the user exploiting relay (User A) due to superior channel quality between those two. This way, pool with taxed resources is created at the BS. Finally, the BS distributes the taxed resources from this pool to the users in a need, that is, to the users with either unfavorable channel quality to the BS that are not able to find any relay (User D) or even to the new users that cannot be served otherwise due to a high load of the BS (User C).

Optimization, Implementation, and Feasibility Aspects: The taxing mechanism should be properly optimized to maximize the revenue coming from taxed resources. A low tax rate results in small benefits coming to the users not involved in relaying. In contrast, a high tax rate may discourage the users to act as the relays resulting in small revenues going to the BS and in a subsequent decrease in the relaying gain. In theory, there is an optimum tax rate maximizing total tax revenue, as indicated by well-known Laffer curve. In practice, the optimum tax rate is very hard, if not impossible, to be determined due to its very complex nature and unpredictable people/users' behavior. Thus, we suggest to follow common taxing mechanisms based on either flat or progressive tax rate self-optimized via machine learning (e.g., by reinforcement learning).

To determine the taxes, the BS should be aware of the amount of resources obtained from relaying in the first place. Since the BS handles the resource allocation, it knows exactly the amount of both the earned resources by the relaying users and the saved resources by the users exploiting relays. Hence, the BS can determine the amount to be taxed by itself without any additional required signaling cost.

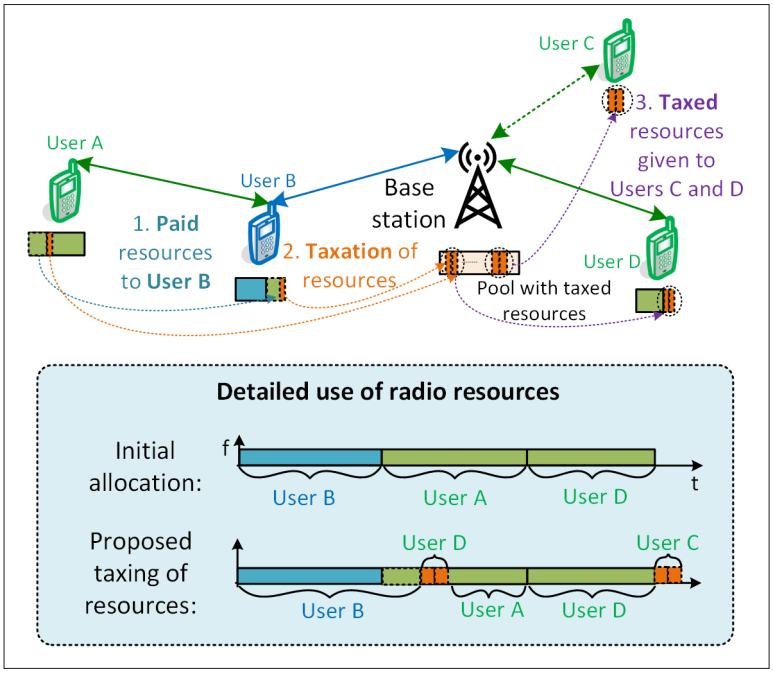

FIGURE 3. Illustrative principle of the concept of taxing resources obtained from relaying. The resources earned (saved) by User B (User A) via relaying are taxed by the BS and distributed to User D to improve his/her capacity. Moreover, taxed resources from other relaying users are given to User C who could not be served by the BS otherwise.

Selling of Resources Saved/Earned Through Relaying

The last piece of the puzzle forming the proposed framework is to sell and/or give resources obtained via relaying to other users that are still either not satisfied with provided services while no feasible relaying user is in their vicinity or have no resources at all due to high load of the BS. The whole mechanism can be summarized into the following subsequent steps (Fig. 4).

The first step consists again in the establishment of D2D relaying link between User A and User B. During the second step, some of the resources earned by User B for the provisioning of relaying services can be sold to other user(s) exploiting the auction mechanism and to obtain credits/tokens. These earned credits/tokens can be exploited in the future to pay the relaying services, similarly as in the case of virtual currency-based incentives. Further, the users may also give a helping hand to other users with whom they have close social ties. In fact, this approach can be seen as another way to motivate the users to relay data for others. For example, User B in Fig. 4 is willing to help to User D who is his/her friend. Since User B cannot relay data for User D due to an unfavorable mutual location, he/she decides to relay data for User A instead. Subsequently, User B gives (or sells with some discount) resources obtained from User A to User D. This way, User B is motivated to act as the relaying user to User A in order to help User C. Finally, in line with the reputation-based incentives, the resources can be also given freely to other

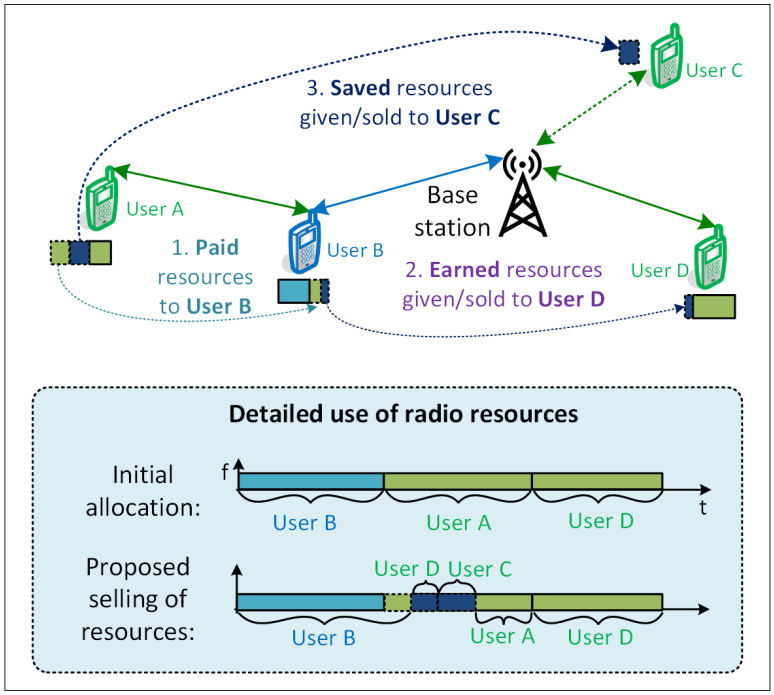

FIGURE 4. Illustrative principle of the proposed selling of resources saved/earned by the users benefiting directly from relaying. User A saves part of his/her resources due to relaying and these saved resources are sold or given to User C for whom the BS has no resources at all. Similarly, User B gives/sells certain portion of earned resources to User D who is able to enhance performance.

users to increase their own reputation.

To further maximize the number of users benefiting from relaying, even User A can sell/give some saved resources in the same way as the relaying user himself/herself during the third step (e.g., to User C in Fig. 4). Of course, this option is feasible only if: User A would experience a higher gain than required, for example, if the channel quality between cooperating users is very high, and the resources of User A are not reused by other cellular user to avoid unpredictable rise in the interference.

Optimization, Implementation, and Feasibility Aspects: To maximize the amount of resources sold to the users in need, the auction mechanism should be optimized. The optimal auction maximizing the social welfare can exploit Vickrey-Clarke-Groves (VCG) mechanism, which is, however, of a high complexity. As an alternative to VCG, various game theory-based auction mechanisms can be adopted with the goal to find an equilibrium. In such games, there are: a set of players (i.e., buyers and the sellers of resources), a set of actions available to each player, and a payoff vector for the particular action being taken. Then, the goal is to maximize the payoff for each player during the game.

To make the auction feasible for practical networks, the BS should play the role of an auctioneer mediating the whole process during which the users offer the resources and sell them to the highest bidder. The auction mechanism generates signaling overhead coming from submitting of bids and offers to the auctioneer (i.e., the BS) and, then, announcing the results of the auction to individual users. Fortunately, this overhead is negligible if a simple bidding language is adopted. Moreover, the signaling overhead can be further reduced by, for example, concurrent bidding pattern, where each buyer has only one chance to make a bid.

Cooperation of Individual Proposed Mechanisms

Although the individual mechanisms can work as stand-alone solutions, the maximum gain is observed if all three are integrated together and are performed in the following steps:

Step 1: The BS employs the mechanism enabling reuse of resources of newly formed D2D links by the cellular users. This, subsequently, allows to release some additional resources from the cellular users.

Step 2: To acquire even more resources, the taxing is enforced by the BS on the resources obtained through D2D relaying provided that enough resources are gained via such relaying.

Step 3: The obtained resources remaining to the users after the taxation can be further distributed to the users still not satisfied with their QoS by *selling* mechanism. Note that, as explained earlier, the users whose resources are reused by other cellular users are forbidden to sell their resources to avoid unpredictable interference (e.g., User A in Fig. 2 cannot dispense part of his/her resources, as these are reused by User B).

Moreover, our proposal is complementary to D2D load balancing approaches [5] so that our framework is envisioned to be a "first phase" in coping with the overloading at a single-cell level. If some of the cells would still be overloaded, the load balancing operating at a multi-cell level is initiated in the "second phase."

Evaluation of Proposed Framework

Now, we outline the simulation scenario and we evaluate the gain of the proposed concept.

Simulation Scenario

The evaluation of proposed framework is done in Matlab. We assume 50 active users randomly located in an area with size of 500x500 m. Without loss of generality, the BS initially splits the available bandwidth (20 MHz) equally among all active users. We assume time division relaying to support low-complexity half-duplex relays (note that the proposed framework can be also extended to full-duplex relaying). The relaying users first receive data in a specific time slot and at certain frequency resources, for example, represented by resource blocks. Then, the received data is re-transmitted to the BS in the next resource blocks. The reception/transmission time is derived in line with [13]. The relay selection is done in a greedy manner, commonly used for this purpose (e.g., [13]) to maximize the relaying gain.

The simulation emulates an urban scenario with obstacles potentially obstructing the communication path between any transmitter and any receiver. In case of none line-of-sight communication, additional 20 dB attenuation of the signal is considered. We consider a multicell-like environment with the inter-cell interference at any receiver generated randomly according to Gamma distribution (see more detail in [13]).

To evaluate our proposal, we assume that the selection of cellular users reusing the resources of individual D2D links is done by Hungarian algorithm to achieve maximum gain} in terms of saved resources. In addition, the users are taxed only if

the relaying gain is above certain threshold in order not to discourage them from relaying. Hence, the users whose capacity is not improved enough (i.e., if their QoS requirements are not met) are not taxed at all. Otherwise, the users are obliged to pay 20% of their earned/saved resources to the BS. Finally, the users that are satisfied with the capacity improvement and still have some resources left after the taxing either sell them to other unsatisfied users and/or give these unused resources to a close friend(s).

To see the added value of our proposed framework, we confront its performance with the baseline scheme proposed in [13] representing current state-of-the-art, where only the users directly involved in D2D relaying benefit. We also discuss and analyze the performance of individual mechanisms when working both as stand-alone solutions or together.

The proposed framework either improves the performance of currently active users not involved in D2D relaying or allows to admit new users if the BS is overloaded. Thus, the proposed concept is evaluated for the following two objectives.

Objective 1 — Maximize the ratio of the users satisfied with their QoS: The users are assumed to be satisfied with their QoS if their capacity is improved by a specific value varying between 5% to 50%.

Objective 2 — Maximize the number of newly admitted users: All resources obtained through the proposed framework are only exploited to admit new users to the network. The capacity requirements of each newly admitted user is generated randomly.

Simulation Results and Discussion

Now let's investigate performance of the proposed framework for *Objective 1*. From Fig. 5, we observe that the ratio of satisfied users decreases if the required capacity improvement increases. This is understandable behavior due to the following facts: there are less resources coming from the proposed framework, as the users directly involved in relaying should be satisfied first; and the users ask for more additional resources to satisfy their QoS requirements. If each mechanism works as a stand-alone solution, the highest gain with respect to the baseline scheme is accomplished by the selling mechanism (up to 18.5%). Still, even the reuse or taxing mechanisms working separately outperform the baseline scheme by more than 13% and 15%, respectively, if the required capacity increase to ensure QoS is below 10%. If the required capacity increase to satisfy the QoS rises to 50%, however, the gain of reuse, taxing, and selling mechanism with respect to baseline decreases to 3.8%, 3.3%, and 9%, respectively. To make the gain of the proposal even more interesting, all three proposed mechanisms should work together resulting in a gain up to 20.7% with respect to the baseline scheme. The benefit of the full proposal is promising especially if the QoS requirements increase as it outperforms baseline nearly by 19% even if users require capacity boost equal to 50% to meet their QoS.

Figure 6 illustrates the percentage of newly admitted users facilitated by the proposed framework (Objective 2). It is worth to mention that no new users are served by the BS in case of the baseline scheme, as there are no released resources for the newly arrived users. Again, we observe similar trends as in Fig. 5 and the percentage of newly served users decreases with an increase in the required capacity improvement, since there are less resources available for these new users. Only in case of the reuse mechanism, the ratio of newly served users is actually slightly increasing and outperforming taxing mechanism if required capacity increase becomes high. This phenomenon occurs due to the fact that more resources are, in general, allocated to the users assisted by the relays to serve their needs. Thus, more resources may be reused by the cellular users and, subsequently, also more resources are released by them. Figure 6 demonstrates that, compared to the baseline, reuse, taxing, and selling mechanisms can increase the number of newly admitted users by up to 10%, 13.8%, and 22.1%, respectively. If all proposed mechanisms work together, the number of newly served users increases even up to 30.9% with respect to the baseline.

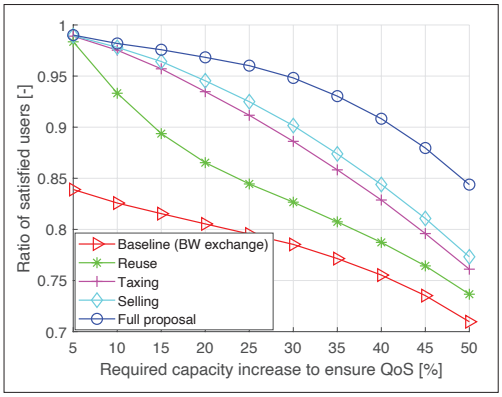

FIGURE 5. Ratio of satisfied users in relation to the required capacity improvement to ensure QoS (Objective 1).

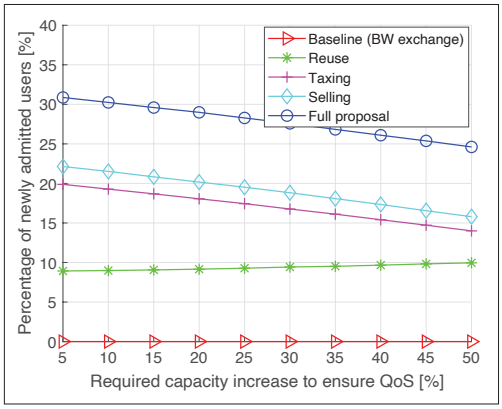

FIGURE 6. Percentage of newly admitted users over the required capacity improvement to ensure QoS (Objective 2).

Conclusion

In this article, we have first surveyed key state-of-the-art incentive approaches motivating the users to render the relaying services for others. Existing incentive approaches are able to improve performance of only those users that are directly involved in relaying while there are still remaining users that are not able to reap the benefits from relaying. To

this end, we have proposed resource allocation framework, build upon existing incentives, so that the users not being directly involved in D2D relaying also benefit}. We have demonstrated the proposed framework notably increases the number of users satisfied with their QoS and/or increases the number of users that could not be admitted otherwise due to the overloaded network.

In the future, the proposed framework can be jointly optimized with load balancing to further improve users' QoS and/or to make the network even more robust against the overloading problem.

Acknowledgment

This work was supported by project no. LTT 20004 funded by Ministry of Education, Youth and Sports, Czech Republic.

References

[1] F. Jameel *et al.*, "A Survey of Device-to-Device Communications: Research Issues and Challenges," *IEEE Commun. Surveys Tuts.*, vol. 20, no. 3, 2018, pp. 2133–68.
[2] C. Yi, S. Huang, and J. Cai, "An Incentive Mechanism Integrating Joint Power, Channel and Link Management for Social-Aware D2D Content Sharing and Proactive Caching," *IEEE Trans. Mobile Comput.*, vol. 17, no. 4, Apr. 2018, pp. 789–802.
[3] X. Xu, J. Wang, and X. Tao, "Analytical Modeling for Caching Enabled UE-to-Network Relay in Cellular Networks," *IEEE Access*, vol. 6, 2018, pp. 51,061–68.
[4] K. Wu and M. Jiang, "Joint Resource Efficiency Optimisation for Overlay Device-to-Device Retransmissions," *Proc. IEEE 85th Vehicular Technology Conf.*, Sydney, NSW, Australia, June 2017, pp. 1–5.
[5] J. Liu *et al.*, "Device-to-Device Communications Achieve Efficient Load Balancing in LTE-Advanced Networks," *IEEE Wireless Commun.*, vol. 21, no. 2, Apr. 2014, pp. 57–65.
[6] J. Peng *et al.*, "D2D-Assisted Multi-User Cooperative Partial Offloading, Transmission Scheduling and Computation Allocating for MEC," *IEEE Trans. Wireless Commun.*, vol. 20, no. 8, Aug. 2021, pp. 4858–73.
[7] N. Mastronarde *et al.*, "To Relay or Not to Relay: Learning Device-to-Device Relaying Strategies in Cellular Networks," *IEEE Trans. Mobile Comput.*, vol. 15, no. 6, June 2016, pp. 1569–85.
[8] Z. Zhu *et al.*, "Time Reusing in D2D Enabled Cooperative Networks," *IEEE Trans. Wireless Commun.*, vol. 17, no. 5, 2018, pp. 3185–3200.
[9] M. Wu *et al.*, "Dynamic Socially-Motivated D2D Relay Selection With Uniform QoE Criterion for Multi-Demands," *IEEE Trans. Commun.*, vol. 68, no. 6, 2020, pp. 3355–68.
[10] W. Sun *et al.*, "Social-Aware Incentive Mechanisms for D2D Resource Sharing in IIoT," *IEEE Trans. Ind. Electron.*, vol. 16, no. 8, 2020, pp. 5517–26.
[11] Y. Gao, Y. Chen, and K. J. Ray Liu, "Cooperation Stimulation for Multiuser Cooperative Communications Using Indirect Reciprocity Game," *IEEE Trans. Commun.*, vol. 60, no. 12, 2012, pp. 3650–61.
[12] P. K. Mishra, A. K. Mishra, and S. Tripathi, "Relay Selection Scheme for Dynamic Network Scenario in Multi-hop D2D Communication," *Proc. ICCCS*, Singapure, 2019.
[13] P. Mach *et al.*, "Incentive-Based D2D Relaying in Cellular Networks," *IEEE Trans. Commun.*, vol. 69, no. 3, 2021, pp. 1775–88.
[14] F. Seifhashemi, B. S. Ghahfarokhi, and N. Moghim, "Mobility-Aware Incentive Mechanism for Relaying D2D Communications," *Computer Commun.*, vol. 2022, Aug. 2022, pp. 361–77.
[15] M. Najla *et al.*, "Predicting Device-to-Device Channels from Cellular Channel Measurements: A Learning Approach," *IEEE Trans. Wireless Commun.*, vol. 19, no. 11, Nov. 2020, pp. 7124–38.

Biographies

Pavel Mach received M.Sc. and Ph.D. in Telecommunication Engineering from the Czech Technical University in Prague, Czech Republic in 2006 and 2010, respectively. He is a senior researcher in 6G mobile research lab at CTU in Prague. He has been involved in several European projects (e.g., FREEDOM, TROPIC). He has published more than 70 conference or journal papers and is the co-inventor of several U.S. patents.

Zdenek Becvar received M.Sc. and Ph.D. in Telecommunication Engineering from the Czech Technical University (CTU) in Prague, Czech Republic in 2005 and 2010, respectively. He is a Full Professor at the Department of Telecommunication Engineering at CTU. He was on visiting researcher and/or professor at Budapest Politechnic, Hungary (2007), CEA-Leti, France (2013), and EURECOM, France (2016, 2019, 2023). From 2013 to 2017, he was a representative of the CTU in 3GPP/ETSI. His research is oriented on a development of future mobile networks (5G, beyond 5G, 6G) with special focus on optimization of radio resource and mobility management, edge computing, C-RAN, and architecture of mobile networks.

Thrasyvoulos Spyropoulos received the Diploma degree in electrical and computer engineering from the National Technical University of Athens, Greece, and the Ph.D. degree in electrical engineering from the University of Southern California. He was a Post-Doctoral Researcher with INRIA, and then a Senior Researcher with the Swiss Federal Institute of Technology (ETH) Zurich. He is currently a Professor with EURECOM, Sophia-Antipolis. He was a recipient of the Best Paper Award from IEEE SECON 2008 and IEEE WoWMoM 2012, and runner-up for ACM Mobihoc 2011, IEEE WoWMoM 2015 and 2021.

XIV. Appendix G

This appendix includes conference paper presented at: **P. Mach**, Z. Becvar, and M. Najla, "Joint Association, Transmission Power Allocation and Positioning of Flying Base Stations Considering Limited Backhaul", *IEEE Vehicular Technology Conference (IEEE VTC-Fall 2020)*.

2020 IEEE 92nd Vehicular Technology Conference (VTC2020-Fall) | 978-1-7281-9484-4/20/$31.00 ©2020 IEEE | DOI: 10.1109/VTC2020-Fall49728.2020.9348784

Joint Association, Transmission Power Allocation and Positioning of Flying Base Stations Considering Limited Backhaul

Pavel Mach, Zdenek Becvar, Mehyar Najla
Department of Telecommunication Engineering, Faculty of Electrical Engineering
Czech Technical University in Prague
Technicka 2, 166 27 Prague, Czech Republic
{machp2, zdenek.becvar, najlameh}@fel.cvut.cz

***Abstract*—An integration of flying base stations (FlyBSs) into future mobile network allows to manage scenarios with a highly varying density and requests of user equipments (UEs). While this research topic has received plenty of attention, a backhaul link quality (i.e., the link between a static base station and FlyBS) is either fully disregarded or oversimplified. Nevertheless, to exploit radio resources efficiently, the backhaul link and an access link (i.e., the link between the FlyBS and UE) should be managed together. Thus, in this paper, we introduce a novel power efficient and backhaul-aware association of the UEs to either the FlyBSs or the SBSs to maximize the sum capacity of all UEs. The association of UEs is managed joinlty with the transmission power allocation and the UEs are associated according to the transmission power required at the FlyBSs to serve the UEs and the benefits observed by each UE if it is associated to the particular base station. In this regard, we derive a closed-form expression for the optimal allocation of the FlyBSs' transmission power to individual UEs to exploit the radio resources at backhaul and access links efficiently. Then, the proposed framework is enhanced by a re-positioning of the FlyBSs and a subsequent re-allocation of the transmission power at the FlyBSs to further improve the overall sum capacity. The simulations show that our proposal significantly increases the sum capacity of the UEs (from 19.6% to 135.3%) with respect to state of the art schemes.**

***Index Terms*—Flying base station, association of users, positioning, backhaul, capacity, transmission power**

The integration of flying base stations (FlyBSs) into mobile networks is a feasible way to cope with a high density of users and a dynamicity of the network [1]. The FlyBS acts as a relay between a conventional terrestrial static base station (SBS) and a user equipment (UE). In such scenario, the UEs receive/transmit data from/to the FlyBS over an access link and the FlyBS relays the UEs' data to/from the SBS via a backhaul link.

The incorporation of the FlyBSs into future mobile networks introduces many challenges [2] spanning over a coverage maximization by the FlyBSs [3][4], optimal deployment of FlyBSs [5][6], UEs' association [7]-[10], or various radio resource management problems, such as power control and resource allocation [11]-[14]. A majority of the existing works, however, *neglect the backhaul link* between the FlyBSs and the SBSs. Nevertheless, the backhaul link significantly influences a performance of the solutions developed for the above-mentioned challenges.

The maximization of the communication capacity by means of FlyBS's positioning while considering the backhaul with a limited capacity is addressed in [15] and [16]. However, both [15] and [16] assume the backhaul with a predefined fixed capacity R, which is independent of the FlyBS's position. Unfortunately, such assumption is not realistic as the capacity of the backhaul directly depends on an allocated bandwidth and a channel quality. Thus, the capacity should be a function of the FlyBS's position.

The limited backhaul between the FlyBS and the SBS is also considered in [17], where the authors focus on a joint optimization of the FlyBS's position and the bandwidth allocation to the UEs. The authors assume the backhaul is implemented over dedicated radio resources. Thus, the SBS may have no resources available for the FlyBSs if the network load is high and all resources are consumed by the UEs associated directly to the SBS. The paper also does not address the association of the UEs as just one FlyBS is assumed and all UEs are associated to this particular FlyBS.

An approach for the allocation of the radio resources both at the backhaul and access links of the FlyBS is introduced in [18]. The authors build on the integrated access and backhaul (IAB) networks concept proposed by 3GPP [19]. By adopting IAB, the backhaul, access, and direct links (i.e., links between UEs and SBS) share the whole available bandwidth. The main objective of the paper is to manage the interference among all these links by the UEs association, the power control at backhaul and access links, and the placement of FlyBSs. Nevertheless, if the backhaul quality is below the threshold (defined by signal to noise plus interference ratio, SINR), no transmission at the access link is allowed and the FlyBS is not exploited at all. In addition, the positioning of FlyBS is done via particle swarm optimization, which suffers in real world implementation from its long convergence and a high energy overhead for testing new positions to generate a new

This work was supported by the Czech Science Foundation (GACR) under Grant P102-18-27023S.

978-1-7281-9484-4/20/$31.00 ©2020 IEEE

population [7].

Main contributions: In this paper, we propose a *backhaul-aware* framework for the association of UEs, power allocation at the FlyBSs, and positioning of the FlyBSs with the objective to maximize sum capacity of the UEs. Unlike [15][16] we assume a realistic case where the backhaul capacity depends on the FlyBS's position. Also, none of the work considering limited backhaul of the FlyBSs ([15]-[18]) ensures that the capacity at backhaul and access links is equal. Thus, the resources are not used by the FlyBSs efficiently as either backhaul or access link is always underutilized (i.e., either bakchaul or access link acts as a bottleneck).

The contributions of the paper are summarized as follows:

- We propose a joint power-efficient association of the UEs and allocation of the transmission power to these UEs at the FlyBS. The proposed association takes into account both the potential gain experienced by the UEs associated to individual SBSs or FlyBSs and the transmission power consumed by the FlyBSs to serve all associated UEs.
- We derive a closed-form expression for the optimal transmission power allocation at the FlyBSs ensuring the same capacity at the backhaul and access links. This maximizes the capacity offered by the FlyBSs while simultaneously minimizes the FlyBSs' transmission power. If the transmission power would be at a lower level, the access links become a bottleneck in the transmission. Contrary, if the transmission power would be higher, the capacity is not improved as the backhaul link is a bottleneck instead.
- We propose a low complexity re-positioning of the FlyBSs, which have some remaining transmission power budget after the association to further boost the sum capacity provided by these FlyBSs.
- Via simulations, we demonstrate that the proposed scheme is able to outperform all competitive schemes by up to 135.3%.

The rest of the paper is organized as follows. The next section introduces the system model and formulates the addressed problem. Section III describes, in detail, the proposed joint power allocation and association of the UEs at the FlyBSs. Moreover, the re-positioning of the FlyBSs and the re-allocation of their transmission power is outlined in this section. Simulation scenario and discussion of simulation results is delivered in Section IV. Section V concludes the paper and contemplates possible future research directions.

I. System Model and Problem Formulation

In this section, we outline the system model for the proposed framework and, then, the problem is formulated.

A. System model

We consider a multicell scenario, where a reference cell is surrounded by K adjacent cells $\mathcal{K} = \{k_1, k_2, \ldots, k_K\}$ managed by K neighboring SBSs (see Fig. 1). The reference cell is served by one SBS and M FlyBSs defined by the set $\mathcal{M} = \{m_1, m_2, \ldots, m_M\}$. The positions of the FlyBSs are defined as $\mathbf{V} = \{v_1, v_2, \ldots, v_M\}$, where $v_m \in \mathbb{R}^3$ and $m \in \mathcal{M}$ represents the position of the m-th FlyBS. Then, N UEs in the set $\mathcal{N} = \{n_1, n_2, \ldots, n_N\}$ are associated either to the SBS or to one of the FlyBSs.

The SBS has a bandwidth B that is split to N channels so that each active UE is assigned with one channel. We focus on the downlink communication, where the SBS transmits data to the UEs. The capacity of the n-th UE served directly by the SBS is expressed as:

$$C_n^D = B_n log_2 \left(1 + \frac{p_s g_{s,n}}{B_n \sigma + \sum\limits_k p_k g_{k,n}}\right) \tag{1}$$

where B_n corresponds to the channel bandwidth allocated to the n-th UE, p_s is the transmission power of the SBS over B_n, p_k is the transmission power of the interfering k-th neighboring SBS, $g_{s,n}$ represents the channel gain between the SBS and the n-th UE, σ corresponds to the noise spectral density, and $g_{k,n}$ is the channel gain between the interfering k-th neighboring SBS and the n-th UE.

Due to the scarcity of available radio spectrum, the FlyBSs have no channel(s) dedicated for either the backhaul link (between the SBS and the FlyBS) or the access link (between the FlyBS and the UEs) as considered in [17]. Instead, both the backhaul and access links are facilitated by the channels that are initially assigned to the UEs by the SBS. If any n-th UE is connected to the m-th FlyBS, the m-th FlyBS relays data for the n-th UE solely over the n-th channel (see Fig. 1). Note that the FlyBS works in full duplex as it is able to receive new data from the SBS while it transmits already received data to the UE simultaneously. Then, the backhaul channel capacity between the SBS and m-th FlyBS is determined as:

$$C_{m,n}^B = B_n log_2 \left(1 + \frac{p_s g_{s,m}}{B_n \sigma + \sum\limits_k p_k g_{k,m}}\right) \tag{2}$$

where $g_{s,m}$ stands for the channel gain between the SBS and m-th FlyBS and $g_{k,m}$ is the channel gain between the k-th neighboring SBS causing the interference to the m-th FlyBS. Similarly, the capacity at the access channel between the m-th FlyBS and the n-th UE is expressed as:

$$C_{m,n}^A = B_n log_2 \left(1 + \frac{p_{m,n} g_{m,n}}{B_n \sigma + \sum\limits_k p_k g_{k,n} + p_s g_{s,n}}\right) \tag{3}$$

where $p_{m,n}$ is the transmission power allocated by the m-th FlyBS for the transmission of data to the n-th UE and $g_{m,n}$ represents the channel gain between m-th FlyBS and n-th UE. When compared to the backhaul link, the access link is interfered also by the SBS as the SBS transmits at the same channels as the FlyBS (see Fig. 1). Notice that the position of the m-th FlyBS impacts both $C_{m,n}^B$ (affecting $g_{s,m}$) and $C_{m,n}^A$ (affecting $g_{m,n}$). Hence, the positioning must be done with respect to both.

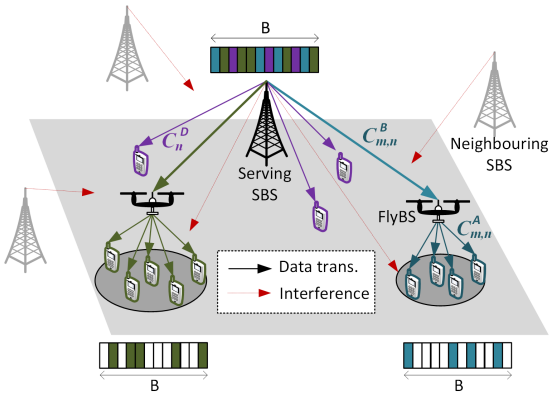

Fig. 1: Illustrative example of system model.

To determine whether the UEs are attached directly to the SBS or through one of the FlyBSs, we introduce the association control variable $x_{m,n}$. If $x_{m,n} = 1$ the n-th UE is attached to the m-th FlyBS while $\sum_m x_{m,n} = 0$ represents the case when the n-th UE is connected directly to the SBS (i.e., the UE is connected to no FlyBS). Consequently, the capacity of the n-th UE is expressed as:

$$C_n = \begin{cases} C_n^D & \text{if } \sum_m x_{m,n} = 0 \\ \sum_m \min(x_{m,n} C_{m,n}^B, x_{m,n} C_{m,n}^A) & \text{if } \sum_m x_{m,n} = 1 \end{cases} \tag{4}$$

As shown in (5) the capacity of the n-th UE connected through the m-th FlyBS is the minimum of $C_{m,n}^B$ and $C_{m,n}^A$, since even if one of these links provides a higher capacity, the other link still poses a bottleneck.

B. Problem formulation

The objective of the paper is to maximize the sum capacity of the UEs via the association of the UEs to either the FlyBSs or the SBS, transmission power allocation at the FlyBSs, and the subsequent re-positioning of the FlyBSs, while taking both backhaul and access links into account. The objective is formulated as:

$$\begin{aligned} &\underset{x_{m,n},\mathbf{V}}{\text{argmax}} && \sum_n C_n \\ &\text{s.t.} && \text{a) } \sum_n p_{m,n} \leq P_{max}, \forall m \in \mathcal{M} \end{aligned} \tag{5}$$

where the constraint a) guarantees that the sum transmission power allocated to all UEs connected to the same FlyBS does not exceed the maximum power budget P_{max} that is available at the FlyBSs. Note that C_n in the problem formulation is a function of both the UEs' association (defined by $x_{m,n}$) and the FlyBSs' position $\mathbf{V}$.

II. Proposed Scheme

In this section, we outline the proposed backhaul-aware framework maximizing the sum capacity of the UEs via the UEs' association and the allocation of transmission power at the FlyBS considering both the backhaul as well as access links. The proposed framework incorporates two steps. During the first step, the transmission power allocation at the FlyBSs and the association of the UEs are handled jointly. Then, in the second step, the capacity of the UEs associated to the FlyBS is maximized by an additional re-positioning of the FlyBSs and a consequent re-allocation of the transmission power. Both steps are described in detail in the following subsections.

A. Joint power-efficient allocation and association of the UEs

This subsection describes the joint allocation of the power for transmission of the FlyBS to the individual UEs and the association of the UEs to the FlyBSs. To maximize the capacity of the system, the UEs should be associated to the FlyBS, which results in the highest gain compared to the case when the UEs stay attached to the SBS. In order to determine an increase in the capacity if any UE is associated to any FlyBS, we first enumerate an association gain. The association gain experienced by the n-th UE exploiting the m-th FlyBS instead of the SBS is defined as a difference between the capacity achieved by the UE through the FlyBS and the capacity if the UE stays connected directly to the SBS. The association gain is, thus, defined as:

$$G_{m,n} = \min(C_{m,n}^B, C_{m,n}^A) - C_n^D \tag{6}$$

The association gains among all UEs and all FlyBSs are inserted into the association gain matrix $\mathbf{G}$, defined as:

$$\mathbf{G} = \begin{bmatrix} G_{1,1} & \dots & G_{1,N} \\ \vdots & \ddots & \vdots \\ G_{M,1} & \dots & G_{M,N} \end{bmatrix} \tag{7}$$

The association of the UEs to the FlyBS is of a benefit only if $G_{m,n} > 0$. In the opposite case, the UE should not be connected to the FlyBS as its capacity would be decreased.

When the FlyBS relays data over the n-th channel, the achieved association gain is limited either by the backhaul or the access link as the minimum capacity of both is considered ($\min(C_{m,n}^B, C_{m,n}^A)$ in (6)). Thus, whenever $C_{m,n}^B$ and $C_{m,n}^A$ differ, the resources are not used efficiently as one of the links is underutilized. Since the capacity at the backhaul is given by the transmission power of the SBS and the bandwidth of the corresponding channel to the FlyBS, the FlyBS is not able to affect the backhaul capacity for its current position. On the contrary, the capacity at the access link depends on the transmission power allocation at the FlyBS. The closed-form expression for the optimal transmission power allocation at the FlyBSs is defined in the following lemma.

Lemma 1. *The optimal transmission power allocated by the m-th FlyBS for the communication with the n-th UE is:*

$$p_{m,n} = \frac{\left(2^{\frac{C_{m,n}^B}{B_n}} - 1\right)\left(B_n \sigma + \sum_k p_s g_{k,n} + p_s g_{s,n}\right)}{g_{m,n}} \tag{8}$$

Proof. To optimize the capacity of the n-th UE associated to the m-the FlyBS, the transmission power $p_{m,n}$ should be set to such value that the access link capacity is the same as the

capacity at the backhaul link (i.e., $C^B_{m,n} = C^A_{m,n}$). If $p_{m,n}$ would be set to a lower level, the access link is the bottleneck decreasing the achievable association gain. If $p_{m,n}$ would be set to a higher level, the backhaul becomes the bottleneck and the FlyBS wastes its transmission power unnecessarily. To obtain the optimal $p_{m,n}$ for which $C^B_{m,n} = C^A_{m,n}$, we substitute $C^A_{m,n}$ by $C^B_{m,n}$ in (3). Thus, (3) is rewritten to:

$$C^B_{m,n} = B_n log_2 \left(1 + \frac{p_{m,n} g_{m,n}}{B_n \sigma + \sum_k p_s g_{k,n} + p_s g_{s,n}}\right) \quad (9)$$

Then, after several math operations, (9) is rewritten as:

$$2^{\frac{C^B_{m,n}}{B_n}} - 1 = \frac{p_{m,n} g_{m,n}}{B_n \sigma + \sum_k p_s g_{k,n} + p_s g_{s,n}} \quad (10)$$

After that, the transmission power $p_{m,n}$ of the m-th FlyBS for the n-th UE is expressed from (10) directly in the form as in (8). This concludes the proof. □

Now, lets discuss the association of UEs. A natural way for the UEs' association to one of the FlyBS is to select the FlyBS yielding the highest association gain as expected in related works. Nevertheless, this option does not have to maximize the sum capacity in a long run as it does not take the transmission power allocation, as derived in (8), into account. For example, the UEs with a low channel quality to the SBS should be always associated preferentially to the FlyBSs as these UEs experience a high association gain due to their low initial capacity C^D_n (see (6)). Nevertheless, if these particular UEs have also the channels to the FlyBS of a low quality (reflected by a low channel gain $g_{m,n}$), a significant amount of the FlyBS's transmission power budget is required to serve these UEs (see (8)). Consequently, only a limited number of the UEs is served by the FlyBS and the overall gain introduced by the FlyBSs is also limited in existing solutions.

In this regard, we propose a power efficient association scheme reflecting both the potential association gain and the relative amount of the transmission power necessary to serve the UE by the FlyBS. To this end, we define a power efficiency metric η representing a ratio between the association gain (expressed in (6)) and the transmission power needed at the FlyBS to serve the UEs (defined in (8)). Hence, for the n-th UE associated to the m-th FlyBS, the power efficiency metric $\eta_{m,n}$ is calculated as:

$$\eta_{m,n} = \frac{G_{m,n}}{p_{m,n}} \quad (11)$$

The UEs with a high value of η are served by the FlyBSs preferentially as these UEs experience, in general, a high association gain while the FlyBS consumes only a relatively low portion of its total transmission power budget to serve these UEs.

The joint power allocation and the UEs' association is described in Algorithm 1. At the beginning, the values of $\eta_{m,n}$ are obtained for all UEs and all FlyBSs according to (11) and inserted into matrix $\boldsymbol{\eta}$ defined as:

$$\boldsymbol{\eta} = \begin{bmatrix} \eta_{1,1} & \cdots & \eta_{1,N} \\ \vdots & \ddots & \vdots \\ \eta_{M,1} & \cdots & \eta_{M,N} \end{bmatrix} \quad (12)$$

Algorithm 1 Joint power allocation and association

1: Derive $\eta_{m,n}$, $\forall m, n$, create matrix $\boldsymbol{\eta}$
2: **while** $\max(\eta_{m,n}) > 0$ **do**
3: $\{m, n\} \leftarrow \max(\eta_{m,n})$
4: Update $\sum_n p_{m,n}$ if n-th UE assoc. to m-th FlyBS
5: **if** $\sum_n p_{m,n} \leq P_{max}$ **then**
6: $x_{m,n} = 1$ (UE associated to FlyBS)
7: set n-th row in $\boldsymbol{\eta}$ to 0
8: **else**
9: $\eta_{m,n} = 0$
10: **end if**
11: **end while**

Next, the maximum value in $\boldsymbol{\eta}$ is found as this represents the highest ratio between the relaying gain and the power required to serve the UEs by the given FlyBS (see line 3 in Algorithm 1). The m-th FlyBS checks if the sum transmission power for all served UEs (including the n-th UE currently being associated) does not exceed the transmission power budget of the m-th FlyBS. If the FlyBS has enough transmission power budget to serve this UE (i.e., if $\sum_n p_{m,n} \leq P_{max}$), the n-th UE is associated to the m-th FlyBS (indicated by setting $x_{m,n} = 1$, see line 6 in Algorithm 1). Then, all $\eta_{m,n}$ in the n-th row in $\boldsymbol{\eta}$ are set to 0 as this particular UE cannot be associated to any other FlyBS (line 7). Nevertheless, if the m-th FlyBS does not have enough transmission power budget to serve the n-th UE, this particular UE is not associated to the FlyBS and $\eta_{m,n}$ is set to 0. The lines 2-11 in Algorithm 1 are repeated as long as there is at least one positive value in $\boldsymbol{\eta}$. When the Algorithm 1 is completed all UEs with at least one positive entry in $\boldsymbol{\eta}$ are associated to one of the FlyBSs.

B. Re-positioning of FlyBSs and re-allocation of transmission power

After the association of the UEs to the FlyBSs and the transmission power allocation, the capacity is further increased by the FlyBSs re-positioning. Since the transmission power of the SBS is assumed to be fixed, the only option to increase the sum capacity of the UEs associated to the FlyBS is to move the FlyBS "closer" to the SBS to improve the backhaul link quality[1]. Of course, if the backhaul quality improves, more power should be allocated by the FlyBSs to individual UEs at the access links, because: i) more data is received

[1]Moving the FlyBSs farther from the SBS (i.e., generally closer to the UEs) can reduce the transmission power of the FlyBSs due to an increased access link quality. Then, however, sum capacity is decreased as backhaul link is degraded. Since the main objective of this paper is to maximize the sum capacity, we leave this option for potential future work where a trade-off between capacity gain and power consumption should be studied in detail.

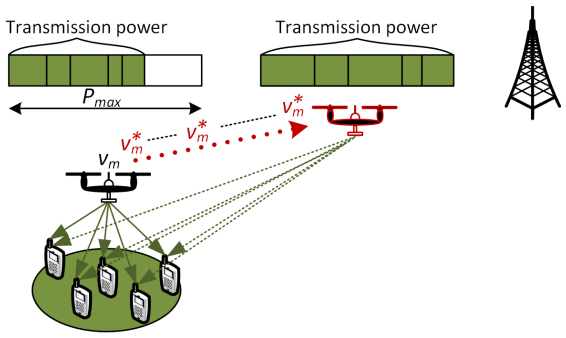

Fig. 2: Principle of joint FlyBSs re-positioning and re-allocation of transmission power.

via the backhaul as it becomes of a higher quality, thus, more data should be transmitted via the access links to ensure $C^B_{m,n} = C^A_{m,n}$ in line with Lemma 1 and ii) the quality of access links to the UEs is degraded as the FlyBSs moves away from its original position. The FlyBS should move to the position where the sum capacity of the UEs served by the FlyBS is maximized and, at the same time, the whole transmission power budget of the FlyBS should be consumed as shown in Fig. 2 (i.e., $\sum_n p_{m,n} = P_{max}, \forall m$).

To re-position the FlyBSs, we adopt a low-complexity approach in which the FlyBS moves along the straight line directly towards the SBS as a high increment in the capacity gain is expected in this direction. Thus, the new position is found promptly. The illustrative example of the FlyBS's movement is shown in Fig. 2. The FlyBS progressively updates its position from the starting position v_m (determined, e.g., by K-means) to the new position v^*_m in the direction to the SBS. The FlyBS updates its positions as long as its transmission power is lower than the maximal transmission power budget P_{max}.

The algorithm for the FlyBS re-positioning and the transmission power re-allocation is described in Algorithm 2. Since the positioning of each FlyBS is done in a distributed manner by every FlyBS, we describe the algorithm for the m-th FlyBS. First, the FlyBS moves to the new position v^*_m in the straight direction towards the SBS (line 2). Then, the SBS updates the transmission power allocation for all served UEs according to Lemma 1 (line 3). In the next step, the sum capacity at the backhaul and access links is calculated according to (2) and (3), respectively (line 4). The process is repeated as long as the FlyBS has enough transmission budget to ensure that $\sum_n C^B_{m,n} = \sum_n C^A_{m,n}$.

Algorithm 2 FlyBS repositioning and power reallocation

1: **while** $\sum_n p_{m,n} < P_{max}$ & $\sum_n C^B_{m,n} = \sum_n C^A_{m,n}$ **do**
2: Move FlyBS to new position v^*_m
3: Update $p_{m,n}, \forall n$ UEs at m-th FlyBS for v^*_m
4: Calculate $\sum_n C^B_{m,n}$ and $\sum_n C^A_{m,n}$ for v^*_m
5: **end while**

III. Simulations

This section describes the simulation scenario and competitive schemes to which our proposal is compared. Then, we present and discuss the simulation results.

A. Simulation scenario and competitive schemes

The performance of the proposed scheme is evaluated in MATLAB. We consider a reference cell with a size of 500x500m with one serving SBS deployed in the middle. Moreover, eight SBSs are located in the adjacent cells in the same way as the serving SBS in the reference cell. Note that the adjacent SBSs are considered as sources of inter-cell interference to the reference cell. In the simulation area, N UEs are uniformly deployed. We assume, without loss of generality, that the SBS splits the available bandwidth equally among all UEs, i.e., each channel is of a bandwidth $B_n = B/N$. Note that even a non-equal channel bandwidth can be adopted by the proposed scheme without any modifications.

The UEs are associated either to the serving SBS or to one of the FlyBS. The initial positions of the FlyBSs are determined with respect to the location of the UEs within each drop by K-means as in [20]. The channel gains between individual nodes (i.e., between the FlyBSs and the UEs, between the SBS and the UEs, and between the SBS and the FlyBSs) are modeled in line with the path loss models from [21] considering 2 GHz carrier frequency. The simulation is repeated 1000 times with random positions of the UEs and corresponding FlyBSs positions. The simulation results are then averaged out over all these drops. The simulation parameters are summarized in Table I.

The proposed scheme is confronted with three state-of-the-art schemes. The first scheme incorporates K-means-based algorithm [20], which determines the positions of the FlyBSs optimally with respect to the distance between the FlyBSs and UEs. The second scheme optimizes the UEs association and the FlyBSs positions only with respect to the quality of the access links while the backhaul link is disregarded (in figures with result labeled as w/o BA", standing for without backhaul awareness). Finally, we also show the performance of the scheme exploiting the proposed power allocation and positioning of the FlyBSs, but considering that the UEs are greedily associated to the FlyBSs yielding the highest

TABLE I: Parameters and settings for simulations

Parameter	Value
Carrier frequency	2 GHz
Simulation area	500x500 m
Number of adjacent SBSs (K)	8
Number of FlyBSs (M)	2-10
Number of UEs in reference cell (N)	10-100
Bandwidth available at SBS in downlink (B)	20 MHz
Channel bandwidth initially allocated to UE	B/N MHz
Max. transmission power of SBS and FlyBSs	20-30 dBm
Noise spectral density (σ_0)	-174 dBm/Hz
Height of SBS/FlyBSs/UEs antenna	30/30/1 m
Number of simulation scenarios	1000

association gain while neglecting the amount of transmission power needed to serve these UEs (labeled as "Greedy"). This way, we illustrate the efficiency of the proposed power efficient association scheme. We do not compare our proposal with other "backhaul-aware" schemes as these either address different problem [17][18] or limit the backhaul capacity in a simple way [15][16] and, thus, comparison is neither feasible nor fair. Note that we investigate also the performance if no FlyBSs are deployed, but we do not show this capacity in the figures to make them easier to read, because the capacity for such case is constant for all investigate metrics and equals to 46.7 Mpbs.

B. Simulations results

Fig. 3 illustrates the performance of the individual schemes for a varying number of the UEs in the simulation area. The proposed scheme significantly outperforms all competitive solutions. The sum capacity achieved by the proposal decreases with an increasing number of the UEs. This is due to the fact that more deployed UEs share individual FlyBSs and, hence, the FlyBSs have less degree of freedom during the re-positioning. Consequently, the FlyBSs stay further from the SBS resulting in a lower backhaul capacity. However, this decrease is notable only for a low number of the UEs and, then, the sum capacity becomes saturated if roughly 50 and more UEs are deployed. The saturation of the sum capacity results from a compensation of the initial decrease in the capacity by the fact that generally more UEs benefit from the FlyBSs deployment. Similar trend is observed also for the Greedy association of the UEs, which exploits the proposed power allocation and re-positioning of FlyBSs while association is done only with respect to the association gain. Nevertheless, the Greedy reaches between 22.1% and 42% lower sum capacity than the proposed scheme. K-means algorithm leads also to a small degradation in the sum capacity with an increasing number of the UEs. This degradation is less notable as the K-means already performs significantly worse than the proposal disregarding the numbers of UEs and the proposal increases the sum capacity by 47% – 59.7% comparing to the K-means.

Fig. 3 also illustrates that state-of-the-art the w/o BA scheme displays a bit different trend with respect to all previous schemes. First, the sum capacity achieved by the w/o BA slightly increases with the number of UEs and, then, saturates at about 50 UEs. The reason for this behavior is that more UEs enjoy a higher capacity due to deployed FlyBSs. Still, the performance of the w/o BA is lower (for low number of UEs) or only slightly higher (for more than 50 UEs) even than the performance of Greedy scheme. The proposed scheme outperforms the w/o BA significantly and the gain introduced by the proposal varies from 35.1% (for medium to high number of UEs) to 52.2% (for low number of UEs).

The impact of the number of deployed FlyBSs on the performance is depicted in Fig. 4. Again, the proposal is able to significantly outperform K-means (from 49.6% to 135.3%), w/o BA (from 35.6% to 116.1%), as well as Greedy (from 40.9% to 82.3%) schemes. The optimization done solely according to the access links (i.e., w/o BA) results in a slight decrease in the sum capacity with a growing number of the FlyBSs. The reason is that with more FlyBSs in the area, the FlyBSs generally stay "closer" to the UEs, but "farther" from the SBS as the backhaul is ignored. Consequently, the backhaul capacity is degraded and becomes the limiting factor. Similarly, if the positioning and the association are done by the K-means, there is no observable gain in the sum capacity with an increasing number of the FlyBSs, since the backhaul links act as the bottleneck. Contrary, both the proposed and Greedy schemes capitalize on a denser deployment of the FlyBSs as the FlyBSs' re-positioning closer to the SBS results in a higher quality backhaul. Still, in case of the Greedy scheme, the FlyBSs can be re-positioned only slightly towards the SBS as the power budget of the FlyBSs is mostly depleted during the association, which does not consider the power efficiency of the associated UEs. Hence, the re-positioning of the FlyBSs is limited as well for the Greedy scheme.

Fig. 5 investigates the impact of the maximal power budget P_{max} available at the FlyBSs on the sum capacity of all UEs. The proposal is again able to significantly outperform K-means, w/o BA, and Greedy schemes by 23.1% to 66%, 19.6% to 49.3%, and 24.1% to 53.1%, respectively. This

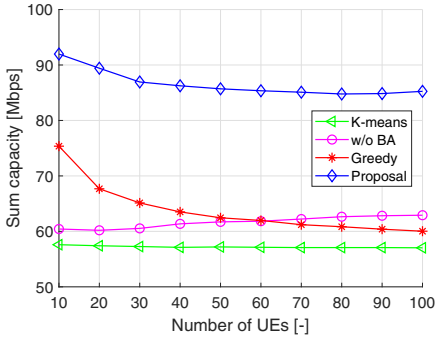

Fig. 3: Sum capacity depending on the number of active UEs ($P_{max} = 27$ dBm, $M = 4$).

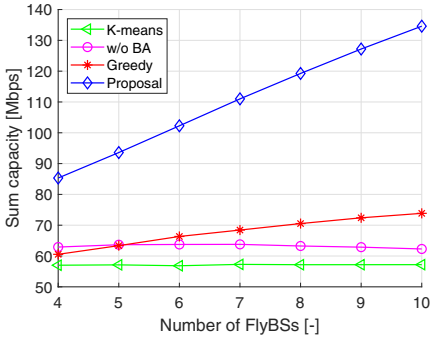

Fig. 4: Sum capacity depending on the number of FlyBSs ($P_{max} = 27$ dBm, $N = 100$).

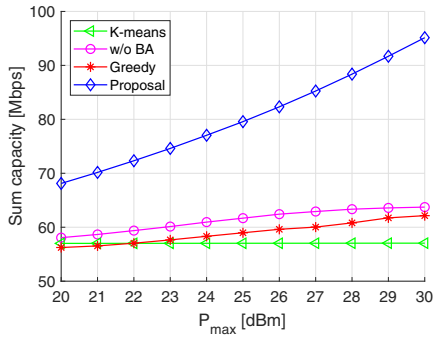

Fig. 5: Sum capacity depending on P_{max} of the FlyBSs ($N = 100$, $M = 4$).

performance gap between the proposal and the competitive schemes becomes wider with increasing P_{max}. The reason is that the FlyBSs can move generally closer to the SBS due to re-positioning as the FlyBSs have a higher remaining transmission power budget. Hence, the capacity at the backhaul improves with P_{max} as well. Although the FlyBSs can be re-positioned closer to the SBS with increasing P_{max} also for the Greedy, the FlyBS movement is fairly limited for the Greedy as most of the FlyBSs' transmission power budget is already allocated during the association process. Contrary to the Greedy and the proposal, the sum capacity of the w/o BA and the K-means increases with P_{max} only a little, as the backhaul capacity acts as the bottleneck disregarding a high capacity at the access links.

IV. Conclusions

In this paper, we have introduced a backhaul-aware framework for the power efficient association of the UEs and the FlyBSs' positioning. The framework itself is composed of two consecutive steps. In the first step, the UEs are associated to the FlyBSs considering the transmission power of the FlyBSs and the transmission power at the FlyBSs is allocated to the individual UEs so that the capacity at the backhaul and access links is the same. Such power allocation guarantees an efficient exploitation and no wasting of radio resources at the backhaul and access links. In the second step, the FlyBSs are re-positioned to further improve the sum capacity. The simulation results demonstrate that the proposed framework significantly outperforms competitive schemes (from 19.6% up to 135.3%) in a wide range of scenarios spanning from a low number of UEs and FlyBSs to a high number of UEs and FlyBSs.

The potential future research should be focused on more sophisticated re-positioning of the FlyBSs. Moreover, the possibility to reuse backhaul resources by several less interfering FlyBSs can further enhance the capacity.

References

[1] Y. Zeng, et al., "Wireless communications with unmanned aerial vehicles: Opportunities and challenges," *IEEE Communications Magazine*, 54(5), pp. 36–42, 2016.

[2] M. Mozaffari, W. Saad, M. Bennis, Y.-H. Nam, and M. Debbah, "A Tutorial on UAVs for Wireless Networks: Applications, Challenges, and Open Problems," *IEEE Communications Surveys and Tutorials*, 21(3), pp. 2334-2360, 2019.

[3] L. Ruan, et al. "Energy-Efficient Multi-UAV Coverage Deployment in UAV Networks: A Game-Theoretic Framework", *China Communications*, 15(10), 2018.

[4] M. Alzenad, A. El-Keyi, and H. Yanikomeroglu, "3-D placement of an unmanned aerial vehicle base station for maximum coverage of users with different QoS requirements," *IEEE Wireless Communication Letters*, 7(1), pp. 38–41, 2018.

[5] X. Zhong, Y. Guo, N. LI, and S. Li, "Deployment Optimization of UAV Relays for Collecting Data From Sensors: A Potential Game Approach," *IEEE Access*, Vol. 7, 2019.

[6] X. Zhong, Y. Guo, N. Li, and Y. Chen, "Joint Optimization of Relay Deployment, Channel Allocation, and Relay Assignment for UAVs-Aided D2D Networks," *IEEE ACM/IEEE Transactions on Networking*, Early access, 2020.

[7] J. Plachy, Z. Becvar, P. Mach, R. Marik, and M. Vondra, "Joint positioning of Flying Base stations and Association of Users: Evolutionary-based approach," *IEEE Access*, pp. 11454–11463, 2019.

[8] H. El Hammouti, M. Benjillali, B. Shihada, and M.-S. Alouini, "Distributed Mechanism for Joint 3D Placement and User Association in UAV-Assisted Networks," *IEEE WCNC*, 2019.

[9] H. El Hammouti, M. Benjillali, B. Shihada, and M.-S. Alouini, "Learn-As-You-Fly: A Distributed Algorithm for Joint 3D Placement and User Association in Multi-UAVs Networks," *IEEE Transactions on Wireless Communications*, 18(12), pp. 5831-5844, 2019.

[10] X. Xi, et al., "Joint User Association and UAV Location Optimization for UAV-Aided Communications," *IEEE Wireless Communications Letters*, 8(6), pp. 1688-1691, 2019.

[11] X. Liu and N. Ansari, "Resource Allocation in UAV-Assisted M2M Communications for Disaster Rescue," *IEEE Wireless Communications Letters*, 8(2), pp. 580-583, 2019.

[12] S. Yan, M. Peng, and X. Cao, "A Game Theory Approach for Joint Access Selection and Resource Allocation in UAV Assisted IoT Communication Networks," *IEEE Internet of Things Journal*, 6(2), pp. 1663-1674, 2019.

[13] M. Nikooroo, Z. Becvar, "Optimizing Transmission and Propulsion Powers for Flying Base Stations," *IEEE WCNC 2020*.

[14] J. Cui, Y. Liu, and A. Nallanathan, "Multi-Agent Reinforcement Learning-Based Resource Allocation for UAV Networks," *IEEE Transactions on Wireless Communications*, 19(2), pp. 729-743, 2020.

[15] E. Kalantari, M. Z. Shakir, H. Yanikomeroglu, and A. Yongacoglu, "Backhaul-aware Robust 3D Drone Placement in 5G+ Wireless Networks," *IEEE ICC WKSHP*, 2017.

[16] E. Kalantari, I. Bor-Yaliniz, A. Yongacoglu, and H. Yanikomeroglu, "User association and bandwidth allocation for terrestrial and aerial base stations with backhaul considerations," *IEEE PIMRC*, 2017.

[17] C. T. Cicek, H. Gultekin, B. Tavli, and H. Yanikomeroglu, "Backhaul-Aware Optimization of UAV Base Station Location and Bandwidth Allocation for Profit Maximization," arXiv:1810.12395v2, 2020.

[18] A. Fouda, A. S. Ibrahim, I. Guvenc, and M. Ghosh, "Interference Management in UAV-Assisted Integrated Access and Backhaul Cellular Networks," *IEEE Access*, Vol. 7, 2019.

[19] Technical Specification Group Radio Access Network, Study on Integrated Access and Backhaul, document 3GPP TR38.874 v16.0.0, Dec. 2018.

[20] B. Galkin, at al., "Deployment of UAV-mounted access points according to spatial user locations in two-tier cellular networks," *Wireless Days (WD)*, pp. 1–6, 2016.

[21] YD. Bultitude at al., "T. IST-4-027756 WINNER II D1. 1.2 V1. 2 WINNER II Channel Models," Tech. Rep., Tech. Rep. 2007.

XV. Appendix H

This appendix includes journal paper published in: **P. Mach**, Z. Becvar, and M. Najla, "Power Allocation, Channel Reuse, and Positioning of Flying Base Stations with Realistic Backhaul," *IEEE Internet of Things Journal*, vol. 9, no. 3, 2022. IF (JCR 2022) = **10.6**.

Power Allocation, Channel Reuse, and Positioning of Flying Base Stations With Realistic Backhaul

Pavel Mach, *Member, IEEE*, Zdenek Becvar, *Senior Member, IEEE*, and Mehyar Najla, *Student Member, IEEE*

***Abstract*—While the integration of flying base stations (FlyBSs) into future mobile networks has received plenty of attention, a backhaul link (i.e., the link between a static base station and the FlyBS) is often either fully disregarded or oversimplified. However, the backhaul link and an access link between the FlyBS and users should be managed together to exploit radio resources efficiently. Thus, we introduce a novel framework considering the FlyBSs with a realistic backhaul to maximize the sum capacity of the users. First, we propose a scheme for an association of the users and a transmission power allocation. Thus, we derive a closed-form expression for the optimal allocation of the FlyBSs' transmission power to individual users to utilize the radio resources at the backhaul and access links in an efficient way. Second, we develop an algorithm for a repositioning of the FlyBSs and a reallocation of the FlyBSs' transmission power to further improve the overall sum capacity. Third, we design a scheme reusing the access links by multiple users in the coalitions to reduce the FlyBSs' transmission power. The reduced transmission power allows to further increase the sum capacity of the users via an additional repositioning of the FlyBSs. Alternatively, the reduced transmission power also lowers the level of interference experienced by the underlying devices not communicating via the FlyBSs. Our proposal increases the sum capacity of the users by up to 60% while suppressing the interference to the underlying devices by up to 7.7 dB compared to the state-of-the-art schemes.**

***Index Terms*—Association of users, backhaul, channel reuse, coalitions, flying base station (FlyBS), positioning, power allocation.**

I. Introduction

THE INTEGRATION of the flying base stations (FlyBSs) into mobile networks is a feasible way to cope with the high density of users and dynamicity of the network [1]. The FlyBS acts as a relay between a conventional terrestrial static base station (SBS) and a user equipment (UE). In such a scenario, the UEs receive/transmit data from/to the FlyBS over an access link and the FlyBS relays the UEs' data to/from the SBS via a backhaul link.

The incorporation of the FlyBSs into future mobile networks introduces many challenges [2] spanning over a coverage maximization by the FlyBSs [3], [4], a deployment of the FlyBSs [5]–[8], a UEs' association [9]–[12], or various radio resource management problems, such as power control or resource allocation [13]–[16]. A majority of the existing works, however, *neglect the backhaul link* between the FlyBSs and the SBSs. Still, the backhaul link significantly influences a performance of the solutions developed for the above-mentioned challenges.

The maximization of the communication capacity by means of the FlyBS's positioning while considering the backhaul with a limited capacity is addressed in [17] and [18]. Nevertheless, both [17] and [18] assume the backhaul with a predefined fixed capacity, which is independent of the FlyBS's position. Unfortunately, such an assumption is not realistic as the capacity of the backhaul directly depends on an allocated bandwidth and the backhaul's channel quality. Hence, the backhaul capacity should naturally be a function of the FlyBS's position.

The backhaul using out-band frequencies is considered in [19]–[22]. Gapeyenko *et al.* [19] provided a novel mathematical framework capturing essential features of a millimeter-wave (mmWave) backhaul in an urban environment. The mmWave backhaul is also considered in [20], where an integrated satellite-drone network is exploited. An analysis of several out-band types of the backhaul using 3.5 and 60-GHz spectrum is presented in [21]. An investigation of the backhaul exploiting an optical spectrum for emergency situations is performed in [22]. In general, the out-band frequencies for the backhaul of the FlyBSs lead to less efficient exploitation of the spectrum (lower spectrum reuse factor). Moreover, the out-band frequencies might not be under the direct control of the mobile operators and it can be hard to guarantee sufficient backhaul capacity. Besides, both mmWaves and optical waves are highly susceptible to abrupt channel fluctuations.

The backhaul links facilitated by the in-band frequencies are assumed in [23]–[33]. Chowdhury *et al.* [23] optimized the 3-D trajectory and antenna pattern of a single FlyBS moving between two points. Although the paper assumes the backhaul between the FlyBS and the SBS is limited, it does not optimize the backhaul capacity in any way. In [24], bandwidth allocation, power allocation, and trajectory of the single FlyBS are optimized in order to maximize the minimum capacity among all users to guarantee fairness. Similarly as in [23], the backhaul limitation is considered only as a constraint while no optimization with respect to the access links is pursued in [24]. The optimization of the single FlyBS's trajectory is also addressed in [25]. The authors determine the optimal

Manuscript received February 25, 2021; revised April 13, 2021; accepted June 7, 2021. Date of publication June 10, 2021; date of current version January 24, 2022. This work was supported by the Czech Science Foundation under Grant P102-18-27023S. *(Corresponding author: Pavel Mach.)*

The authors are with the Department of Telecommunication Engineering, Faculty of Electrical Engineering, Czech Technical University in Prague, 166 27 Prague, Czech Republic (e-mail: machp2@fel.cvut.cz; zdenek.becvar@fel.cvut.cz; najlameh@fel.cvut.cz).

Digital Object Identifier 10.1109/JIOT.2021.3088287

duration of uplink and downlink transmissions and allocate the transmission power. Then, the authors solve a partial computation offloading and transmission power optimization related to the FlyBS and the SBS. Finally, the FlyBS trajectory is found by successive convex optimization.

Cicek *et al.* [26] focused on the joint optimization of the FlyBS's position and the bandwidth allocation to the UEs. The authors assume the backhaul is implemented over the radio resources not consumed by the UEs. Thus, the SBS may have no resources available for the FlyBSs if the network load is high and all resources are consumed by the UEs associated directly to the SBS. The paper also does not address the association of the UEs since only one FlyBS is assumed and all UEs are associated to this particular FlyBS. The paper [27] studies jointly the placement of FlyBSs, the users' association, and the bandwidth allocation. The association of users and the placement of FlyBSs are done depending on the users' classification into two groups: 1) delay-sensitive users and 2) delay-tolerant users. The objective, then, is to solve the above problem while minimizing the total transmission power at the FlyBSs. Although the backhaul link is considered to be limited, the backhaul capacity is only a constraint and the authors do not optimize the access and backhaul links together. The paper [28] proposes the positioning of a single FlyBS, the bandwidth allocation, and the transmission power allocation for full-duplex FlyBS exploiting nonorthogonal multiple access (NOMA). Similarly as in [27], the main objective is to minimize the transmission power of the FlyBS while guaranteeing the minimum capacity of the users.

In order to efficiently reuse radio resources at the backhaul and the access links of the FlyBSs, an integrated access and backhaul (IAB) concept, proposed by 3GPP [29], is considered in [30]–[33]. In [30], the main objective is to minimize the transmission power of the single FlyBS while meeting the rate requirements of the UEs. The objective is achieved by the placement of the FlyBS and an allocation of the transmission power at the backhaul and access links. The FlyBSs placement, the UEs association, and the bandwidth allocation are proposed in [31]. The paper, however, disregards the transmission power allocation, which is crucial in IAB, where the access and backhaul links reuse the same resources. The main objective of [32] and [33] is to manage the interference among the access and backhaul links by the association of the UEs, the power control at the backhaul and access links, and the positioning of the FlyBSs. Nevertheless, if the backhaul quality is below a threshold (defined by signal-to-noise-plus-interference ratio, SINR), no transmission at the access link is allowed and the FlyBS is not exploited at all.

None of the papers assuming the limited/constrained backhaul [17]–[33], however, guarantees that the access and backhaul links are of an equal capacity. Thus, the resources either at the access or backhaul links are not utilized efficiently. The goal to ensure the same capacity at the access and backhaul links is considered in [34], where the authors maximize the capacity of indoor users with poor channel conditions to the SBSs. The UEs' uplink transmission power is optimally split between the transmissions to the SBS and to the FlyBS in a way that one part is used for the users' transmission to the SBS and the second part is used for the users' transmission to the FlyBS. Then, the position of the FlyBS is optimized with respect to the access channels and considering the optimal power setting at the UEs. The paper assumes only one FlyBS; thus, it addresses neither the association of UEs to the FlyBSs nor the reuse of the access channels.

Main Contributions: In this article, we propose a *backhaul-aware* framework for the association of the UEs, the power allocation at the FlyBSs, the positioning of the FlyBSs, and the reuse of the access links by multiple UEs with an overall objective to maximize the sum capacity of the UEs. Unlike [17] and [18], we assume a realistic case, where the backhaul capacity depends on the FlyBS's position. Also, all works considering the limited backhaul of the FlyBSs [17]–[33] do not consider the backhaul and access links fully jointly. Consequently, the resources at the backhaul and access links are still exploited inefficiently and either the backhaul or the access link is underutilized and acts as a bottleneck. The backhaul and access links are optimized jointly in [34]; however, the paper is focused on the uplink and optimizes the transmission power of the UEs and the position of the FlyBS with respect to the access channels only. Moreover, as the paper assumes only single FlyBS, the association of the UEs to the multiple FlyBSs and the reuse of the access links are not addressed in [34]. In addition, the works adopting the IAB concept [30]–[33] assume that the FlyBSs always reuse all access links, thus generating a significant interference. With respect to this approach, we reuse the access links in a controlled way only if the reuse is of benefit for the individual UEs. Consequently, the interference introduced by the FlyBSs is significantly suppressed.

The contributions of the article are summarized as follows.

1) We derive a closed-form expression for the optimal transmission power allocation at the FlyBSs ensuring the same capacity at the backhaul and access links. Furthermore, we formulate the association of the UEs to the FlyBSs as a matching problem and we propose a greedy algorithm to solve it. We show that the proposed greedy algorithm reaches optimum or close-to-optimum performance.
2) We propose a repositioning of the FlyBSs to further boost the sum capacity provided by these FlyBSs. First, we solve the repositioning problem by the high complexity Nelder–Mead simplex algorithm to show the upper bound performance. Then, we propose a low-complexity algorithm suitable even for an urban environment, as the trajectory of the FlyBS considers various obstacles, such as buildings.
3) We propose a scheme reusing the access links among the UEs by means of a coalition structure generation to decrease the allocated transmission power at the FlyBS. The reduced transmission power facilitates either a further increase in the sum capacity of the UEs (via an additional repositioning of the FlyBSs) or a decrease in interference generated to the various underlying devices not exploiting the FlyBSs. We solve the problem of the coalition structure generation optimally by the dynamic programming and, subsequently,

we also propose a low-complexity algorithm suitable for practical applications.

4) Via extensive simulations, we demonstrate that the proposed scheme outperforms all competitive schemes by up to 60% in terms of the sum UE capacity and reduces the transmission power of the FlyBSs by up to 64% resulting in a suppression of interference by up to 7.7 dB.

This article is an extension of our prior work [35], where only a basic idea of the novel concept is presented.

The remainder of the article is organized as follows. The next section introduces the system model and formulates the problem. Section III describes the proposed optimal power allocation and the association of the UEs at the FlyBSs. The repositioning of the FlyBSs and the reallocation of their transmission power are outlined in Section IV. Section V focuses on the reuse of the access links through the coalition creation. The simulation scenario and a discussion of the simulation results are delivered in Section VI and Section VII, respectively. Section VIII concludes the article and contemplates possible future research directions.

II. System Model and Problem Formulation

In this section, we outline the system model and formulate the problem.

A. System Model

We consider a multicell scenario with $K+1$ SBSs, where a reference serving cell is surrounded by K adjacent interfering cells (see Fig. 1). Thus, we define the set of SBSs as $\mathcal{K} = \{k_0, k_1, \ldots, k_K\}$, where k_0 is the serving SBS while the rest represent the adjacent interfering SBSs. The serving SBS is further supported by M FlyBSs defined by the set $\mathcal{M} = \{m_1, m_2, \ldots, m_M\}$. The positions of the FlyBSs are denoted as $\boldsymbol{V} = \{\boldsymbol{v_1}, \boldsymbol{v_2}, \ldots, \boldsymbol{v_M}\}$, where $\boldsymbol{v_m} \in \mathbb{R}^3$ represents the position of the mth FlyBS. Then, N UEs in the set $\mathcal{N} = \{n_1, n_2, \ldots, n_N\}$ are associated with either the SBS or one of the FlyBSs.

The SBS splits the whole bandwidth B into N channels so that nth UE is assigned with one channel of a bandwidth B_n. Note that the bandwidth allocation is not in the scope of this article and our proposed solution is suitable for any arbitrary bandwidth allocation. Thus, we do not specify any concrete splitting of B into the channels in the system model.

We focus on the downlink communication, where the communication capacity of the nth UE served directly by the serving SBS is expressed as

$$C^D_{k_0,n} = B_n \log_2\left(1 + \frac{p_{k_0,n} g_{k_0,n}}{B_n \sigma + \sum_{\mathcal{K}\setminus\{k_0\}} p_k g_{k,n}}\right) \tag{1}$$

where $p_{k_0,n}$ is the transmission power of the serving SBS to the nth UE, p_k is the transmission power of the kth neighboring SBS interfering the nth UE, $g_{k_0,n}$ represents the channel gain between the serving SBS and the nth UE, σ corresponds to the noise spectral density, and $g_{k,n}$ is the channel gain between the kth neighboring SBS and the nth UE.

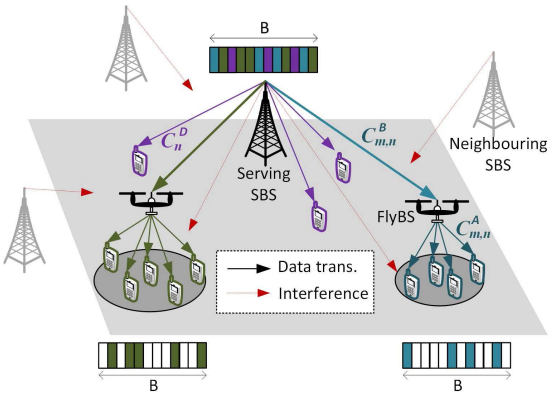

Fig. 1. Illustrative example of the system model.

Due to a scarcity of the available radio spectrum, no channel(s) are dedicated exclusively for either the backhaul link (between the SBS and the FlyBS) or the access link (between the FlyBS and the UEs) as considered, e.g., in [26]. Instead, both the backhaul and access links are facilitated by the channels that are initially assigned to the UEs by the SBS to increase the spectrum reuse. If the nth UE is associated with the mth FlyBS, the mth FlyBS relays data for the nth UE solely over the nth channel (see Fig. 1). Similarly as in many research papers (e.g., [30], [31], [36]), we assume the FlyBSs work in the full duplex mode. However, we also discuss modifications required to be made in our proposal if the half-duplex FlyBSs are adopted. In addition, we analyze the performance of both full and half-duplex FlyBSs via the simulations.

The backhaul channel capacity between the SBS and the mth FlyBS serving the nth UEs via the nth channel is determined as

$$C^B_{m,n} = B_n \log_2\left(1 + \frac{p_{k_0,m} g_{k_0,m}}{B_n \sigma + \sum_{\mathcal{K}\setminus\{k_0\}} p_k g_{k,m}}\right) \tag{2}$$

where $p_{k_0,m}$ is the transmission power of the serving SBS allocated to the mth FlyBS, $g_{k_0,m}$ stands for the channel gain between the serving SBS and the mth FlyBS, and $g_{k,m}$ is the channel gain between the kth neighboring SBS and the mth FlyBS. Similarly, the capacity at the access channel between the mth FlyBS and the nth UE is expressed as

$$C^A_{m,n} = B_n \log_2\left(1 + \frac{p_{m,n} g_{m,n}}{B_n \sigma + \sum_{\mathcal{K}} p_k g_{k,n}}\right) \tag{3}$$

where $p_{m,n}$ is the transmission power allocated by the mth FlyBS for the transmission of data to the nth UE and $g_{m,n}$ represents the channel gain between the mth FlyBS and the nth UE. When compared to the backhaul link, the access link is interfered also by the SBS since the SBS transmits at the same channels as the FlyBS (see Fig. 1).

The relaying gain experienced by the nth UE exploiting the mth FlyBS instead of the SBS is defined as

$$G_{m,n} = \min\left(C^B_{m,n}, C^A_{m,n}\right) - C^D_{k_0,n}. \tag{4}$$

The relaying gain is the function of $\min(C^B_{m,n}, C^A_{m,n})$, since either the backhaul or the access link acts as a bottleneck

whenever $C^B_{m,n} \neq C^A_{m,n}$. To indicate whether the UEs are associated directly with the SBS or with one of the FlyBSs, we introduce a binary association control variable $x_{m,n} \in \{0, 1\}$. If $x_{m,n} = 1$, the nth UE is associated with the mth FlyBS, however, if $x_{m,n} = 0$, the nth UE is not associated with the mth FlyBS.

B. Problem Formulation

The objective of the article is to maximize the sum capacity of the UEs via the transmission power allocation at the FlyBSs $\boldsymbol{P}^*$, the association of the UEs to either the FlyBSs or the SBS $\boldsymbol{X}^*$, and the subsequent repositioning of the FlyBSs $\boldsymbol{V}^*$, while both the backhaul and access links are taken into account. The objective is formulated as

$$\begin{aligned} \boldsymbol{P}^*, \boldsymbol{X}^*, \boldsymbol{V}^* = \underset{\boldsymbol{P},\boldsymbol{X},\boldsymbol{V}}{\operatorname{argmax}} & \sum_n \left(C^D_{k_0,n} + \sum_m x_{m,n} G_{m,n} \right) \\ \text{s.t.} \quad & \text{(5a)} \ \sum_n x_{m,n} p_{m,n} \leq P_{\max} \quad \forall m \\ & \text{(5b)} \ \sum_m x_{m,n} \leq 1 \quad \forall n \\ & \text{(5c)} \ x_{m,n} C^A_{m,n} \leq x_{m,n} C^B_{m,n} \quad \forall m, n \\ & \text{(5d)} \ C_n \geq C^D_{k_0,n} \quad \forall n \end{aligned} \tag{5}$$

where (5a) guarantees that the sum transmission power allocated to all UEs connected to the same FlyBS does not exceed the maximum power budget $P_{\max}$ available at each FlyBS, (5b) ensures that each UE can be associated only with either one of the FlyBSs or the SBS, (5c) assures that the capacity at the access channel does not exceed the backhaul channel capacity, as the FlyBS may not, in principle, send more data over the access channels than the volume of data received over the backhaul channel, and (5d) guarantees that the capacity of the nth UE (C_n) is not lower than the capacity provided initially by the serving SBS (i.e., $C^D_{k_0,n}$). Note that the reuse of the access channels by means of the coalitions is not included in the overall problem formulation. The reason is that the reuse is just a part of the solution that enables a further improvement in the sum capacity via a reduction of the FlyBSs transmission powers to enable a further repositioning of the FlyBSs to increase the sum capacity (see Section V for more details).

The problem defined in (5) is a mixed-integer programming that is hard to be solved jointly. To that end, we divide the problem into several subproblems and solve each sequentially. First, we derive the optimal power allocation at the FlyBSs (Section III-A) and formulate the optimal matching to associate the UEs with the FlyBSs exploiting the derived optimal transmission power allocation (Section III-B). Second, the capacity of the UEs associated with the FlyBS is maximized by the repositioning of the FlyBSs and the optimal reallocation of the transmission power (Section IV). Third, the coalitions among the UEs are created to enable the reuse of the access links and, consequently, to decrease the transmission power of the FlyBSs (Section V). Finally, the FlyBSs may be repositioned again, using the algorithm proposed in Section IV after the coalitions are created, to further boost the capacity of the UEs.

III. Power Allocation and Association of the UEs

This section first defines the subproblem of the FlyBS's power allocation and solves this subproblem optimally. Then, the optimal power allocation is exploited for solving the association problem of the UEs with the FlyBSs.

A. Optimal Power Allocation at the FlyBS

The objective of the power allocation is to maximize the relaying gain $G_{m,n}$ introduced by the mth FlyBS's forwarding data of the nth UE. The problem of the relaying gain maximization is defined as

$$\begin{aligned} \boldsymbol{P}^{**} = \underset{\boldsymbol{P}}{\operatorname{argmax}} \ & x_{m,n} G_{m,n} \\ \text{s.t.} \quad & \text{(6a)} \ x_{m,n} p_{m,n} \leq P_{\max} \quad \forall m, n \\ & \text{(6b)} \ x_{m,n} C^A_{m,n} \leq x_{m,n} C^B_{m,n} \quad \forall m, n. \end{aligned} \tag{6}$$

The relaying gain is limited either by the backhaul or the access link (see term $\min(C^B_{m,n}, C^A_{m,n})$ in (4)). Thus, whenever $C^B_{m,n} \neq C^A_{m,n}$, the resources are not used efficiently as one of the links is underutilized. Since the capacity at the backhaul is given by the transmission power of the SBS and the bandwidth of the corresponding channel to the FlyBS, the FlyBS is not able to affect the backhaul capacity at its current position. However, the transmission power allocation at the FlyBS influences the capacity at the access link. Thus, we define the optimal transmission power allocation of the mth FlyBS in a closed form by Lemma 1 below.

Lemma 1: The optimal transmission power allocated by the mth FlyBS for the communication with the nth UE is

$$p_{m,n} = \begin{cases} \dfrac{\left(2^{\frac{C^B_{m,n}}{B_n}} - 1\right)(B_n \sigma + \sum_{\mathcal{K}} p_k g_{k,n})}{g_{m,n}}, & \text{if (6a) is met} \\ 0 & \text{otherwise.} \end{cases} \tag{7}$$

Proof: To optimize the capacity of the nth UE associated with the mth FlyBS, the transmission power $p_{m,n}$ should be set to such value that the capacity at the access link is the same as the capacity at the backhaul link (i.e., the constraint (6b) is set as $C^A_{m,n} = C^B_{m,n}$). If $p_{m,n}$ would be set to a lower level, the access link is the bottleneck decreasing the achievable association gain. If $p_{m,n}$ would be set to a higher level, the backhaul becomes the bottleneck and the FlyBS wastes its transmission power (and, thus, also increases interference unnecessarily). To obtain the optimal $p_{m,n}$ for which $C^A_{m,n} = C^B_{m,n}$, we substitute $C^A_{m,n}$ by $C^B_{m,n}$ in (3). Thus, (3) is rewritten as

$$C^B_{m,n} = B_n \log_2 \left(1 + \frac{p_{m,n} g_{m,n}}{B_n \sigma + \sum_{\mathcal{K}} p_k g_{k,n}} \right). \tag{8}$$

Then, after several math operations, (8) is rewritten as

$$2^{\frac{C^B_{m,n}}{B_n}} - 1 = \frac{p_{m,n} g_{m,n}}{B_n \sigma + \sum_{\mathcal{K}} p_k g_{k,n}}. \tag{9}$$

After few simple math operations, the transmission power $p_{m,n}$ of the mth FlyBS for the nth UE is expressed from (9) directly in the form as in (7). This concludes the proof. ■

Remark 1: The derivation of the optimal power allocation for the half-duplex FlyBSs is analogous to the full duplex with the following variations: 1) the half-duplex requires to guarantee $TC^B_{m,n} = (1-T)C^A_{m,n}$, where T is the duration of the transmission over the backhaul channel and 2) the UE is not interfered at the access channel from the serving SBS. Then, $p_{m,n}$ for the half duplex is expressed as

$$p_{m,n} = \begin{cases} \dfrac{\left(2^{\frac{TC^B_{m,n}}{(1-T)B_n}}-1\right)\left(B_n\sigma+\sum_{\mathcal{K}\setminus k_0} p_k g_{k,n}\right)}{g_{m,n}}, & \text{if (6a) is met} \\ 0 & \text{otherwise.} \end{cases} \tag{10}$$

B. Association of the UEs

The objective of our article is to maximize the system capacity. Thus, each UE should be associated with the BS (either the SBS or one of the FlyBSs) providing the highest capacity. To decide whether the UEs should be associated with the SBS or with one of the FlyBSs, the relaying gain $G_{m,n}$ calculated in (4) should be adopted. If $G_{m,n} \leq 0$, the nth UE remains associated with the SBS. On the contrary, the nth UE should be associated with the mth FlyBS if $G_{m,n}$ is positive and if associating the nth UE with the mth FlyBS increases the capacity. Nevertheless, considering only $G_{m,n}$ does not necessarily maximize the sum capacity if the backhaul is considered, because the transmission power allocation, as derived in (7), is not taken into account. For example, the UEs with a low channel quality to the SBS should be always associated preferentially to the FlyBSs as these UEs experience a significant relaying gain due to their low $C^D_{k_0,n}$ (see (4)). Nevertheless, if these particular UEs have also the channels to the FlyBSs of a low quality (reflected by a low channel gain $g_{m,n}$), a significant amount of the FlyBSs' transmission power is required to serve these UEs (see (7)). Consequently, only a limited number of the UEs would be served by the FlyBSs and the overall gain introduced by the FlyBSs would be also limited.

Taking both the relaying gain and the required transmission power allocated at the FlyBS into account in the association decision, we define a power-efficiency metric as

$$\eta_{m,n} = \begin{cases} \frac{G_{m,n}}{p_{m,n}}, & \text{if } G_{m,n} > 0 \ \& \ p_{m,n} > 0 \\ 0, & \text{otherwise} \end{cases} \tag{11}$$

where $\eta_{m,n}$ is set to 0 if $G_{m,n} \leq 0$ to ensure that the nth UE always benefits from the association with the mth FlyBS, thus satisfying constraint (5d). Moreover, $\eta_{m,n}$ is also set to 0 if $p_{m,n}$, derived in line with Lemma 1, is 0 (i.e., if the mth FlyBS does not have enough transmission power to serve the nth UE). Note that setting $\eta_{m,n} = 0$ indicates that the nth UE cannot be associated with the mth FlyBS The subproblem of the UEs' association is formulated as

$$\begin{aligned} \boldsymbol{X}^{**} = \underset{X}{\text{argmax}} & \sum_m \sum_n x_{m,n}\eta_{m,n} \\ \text{s.t.} \quad & \text{(12a)} \ \sum_n x_{m,n} p_{m,n} \leq P_{\max} \quad \forall m \\ & \text{(12b)} \ \sum_m x_{m,n} \leq 1 \quad \forall n. \end{aligned} \tag{12}$$

Algorithm 1 Greedy Algorithm for UEs' Association

1: Derive optimal $p_{m,n}$, $\forall m, n$, using Lemma 1
2: Calculate $\eta_{m,n}$, $\forall m, n$, using (11), create matrix $\boldsymbol{\eta}$
3: Set $x_{m,n} = 0, \forall m, n$
4: **while** $\max(\eta_{m,n} \in \boldsymbol{\eta}) > 0$ **do**
5: $\quad \{m, n\} \leftarrow \max(\eta_{m,n} \in \boldsymbol{\eta})$
6: $\quad$ **if** $\sum_n x_{m,n} p_{m,n} + p_{m,n} \leq P_{max}$ **then**
7: $\quad\quad x_{m,n} = 1$ (n-th UE associated with m-th FlyBS)
8: $\quad\quad$ set n-th row in $\boldsymbol{\eta}$ to 0
9: $\quad$ **else**
10: $\quad\quad \eta_{m,n} = 0$
11: $\quad$ **end if**
12: **end while**

The problem defined in (12) represents a many-to-one matching problem, as multiple UEs can be associated with the same FlyBS while each UE can be associated with only one FlyBS (given by (12b)). At the same time, the matching of the UEs with the FlyBSs is constrained by $P_{\max}$ at each FlyBS (defined by (12a)). Thus, (12) is a mixed integer programming problem that is, generally, hard to be solved optimally. One way of finding the optimal association is to employ a high-complexity full search, which tests all possible matching combinations and selects the one yielding the maximum performance. The full search, however, cannot be solved in a polynomial time. To decrease the complexity of the full search, only a subset of all possible combinations can be checked, as each UE can be matched with just one FlyBS. For our specific problem, we can eliminate all combinations, where the UE would be matched with two or more FlyBSs simultaneously. This, then leads to the knapsack problem, as we maximize $\sum_n x_{m,n}\eta_{m,n}$ for each FlyBS separately while guaranteeing (12a). Nevertheless, even the knapsack problem is NP-complete and not solvable in a polynomial time. Thus, we propose a low-complexity greedy algorithm to solve the association problem and we also discuss its optimality.

The UEs' association is described in Algorithm 1. In the beginning, we derive the optimal $p_{m,n}$ for all m and n exploiting Lemma 1 (see line 1 in Algorithm 1). Then, $\eta_{m,n}$ is obtained for all UEs and all FlyBSs and, subsequently, all $\eta_{m,n}$ are inserted into the matrix $\boldsymbol{\eta}$ (line 2). Afterward, $x_{m,n}$ is set to 0 for all m and n to indicate that, initially, no UE is associated with any FlyBS (line 3). Next, the maximum value in $\boldsymbol{\eta}$ is found and this value represents the highest ratio between the relaying gain and the power required to serve the UEs by the given FlyBS (see line 5). The algorithm then checks if the sum transmission power for all served UEs (including the nth UE currently being associated) does not exceed the transmission power budget of the mth FlyBS. If the mth FlyBS has enough transmission power to serve this UE (i.e., if $\sum_n x_{m,n} p_{m,n} + p_{m,n} \leq P_{\max}$) the nth UE is associated with the mth FlyBS and this fact is indicated by setting $x_{m,n} = 1$ (line 7). Then, all $\eta_{m,n}$ in the nth row of $\boldsymbol{\eta}$ are set to 0, as this particular UE cannot be associated with any other FlyBS (line 8). If the mth FlyBS, however, does not have enough transmission power to serve the nth UE, this particular UE is not associated with the FlyBS and only $\eta_{m,n}$ is set to 0.

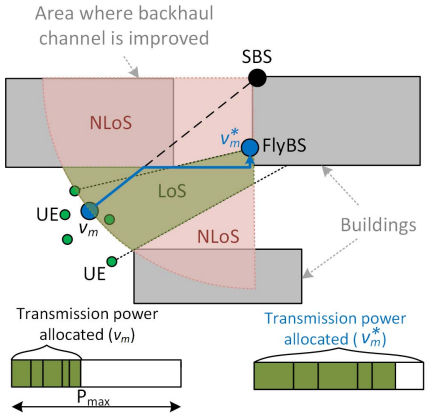

Fig. 2. Illustrative example of the optimal FlyBS's position while keeping the total transmission power at the FlyBS below $P_{\max}$. The red sector of the circle represents the area, where the FlyBS decreases its distance to the SBS with respect to the initial position v_m. The green area further represents the FlyBS's position ensuring LoS for all UEs attached to it. The blue curve is an example of the moving trajectory according to Algorithm 2.

The lines 4–12 in Algorithm 1 are repeated as long as there is at least one positive entry in $\boldsymbol{\eta}$. When $\boldsymbol{\eta}$ contains no positive entry, Algorithm 1 is completed as there is no UE that can be further associated with any FlyBS. Note that the UEs that cannot be served by any FlyBS remain associated with the serving SBS.

The proposed greedy algorithm is optimal as long as the algorithm selects the highest $\eta_{m,n}$ for each UE that benefits from the association with at least one FlyBS (i.e., those UEs having at least one positive entry in the initially created $\boldsymbol{\eta}$). This happens if $\sum_n x_{m,n}p_{m,n} + p_{m,n} \leq P_{\max}$ (i.e., if the condition in line 6 of Algorithm 1 is fulfilled), since (12a) does not impose any constraint on the association problem and the objective function in (12) is maximized. In fact, the greedy algorithm is always optimal for a lower number of UEs as long as the total transmission power allocated at all FlyBSs is well below $P_{\max}$.

Even in the cases when the greedy association would not be optimal, it still gives a close-to-optimal performance for the following reason. The entries (UEs) in $\boldsymbol{\eta}$ with a high value of $\eta_{n,m}$ are selected preferentially by Algorithm 1 and these entries (UEs) require only a very low $p_{m,n}$ allocated at the FlyBSs (see (11)). Thus, these also contribute most significantly into the maximization of the objective function in (12) while keeping a low requirement on the transmission power allocated to the UEs associated with the FlyBSs. Consequently, the entries with the high value in $\boldsymbol{\eta}$ are selected both by the optimal and proposed greedy algorithms. Then, the difference between the optimal and greedy associations can appear only for the UEs having a small $\eta_{n,m}$. However, these UEs contribute only marginally to the overall objective function since $\eta_{n,m} \ll \sum_m \sum_n x_{m,n}\eta_{m,n}$. Thus, the gap between the optimal and greedy associations is very small. Note that we show the optimal association in the simulation results and demonstrate that even for 100 UEs, the greedy algorithm is still optimal.

The complexity of Algorithm 1 is equal to $\mathcal{O}(M\sum_{n=1}^{N} n) = \mathcal{O}(M(N(N-1)/2))$. Since there are usually only few FlyBSs with which the UEs can be associated, the complexity of Algorithm 1 can be considered as $\mathcal{O}(N(N-1) = \mathcal{O}(N^2)$. As assumed in many recent papers (see [27], [38], [39]), Algorithm 1 is executed centrally by the SBS to avoid computation/processing burden of the FlyBSs, which are constrained with a limited energy. Hence, the SBS decides which UEs should stay connected to the SBS and which UEs should be associated with one of the FlyBSs. Note that the FlyBSs are anyway expected to exchange signaling with the SBS to manage radio resources efficiently. Thus, such a centralized approach does not lead to any significant increase in the signaling overhead. Moreover, the algorithm itself can be executed also in a distributed manner provided that all FlyBSs obtain $\boldsymbol{\eta}$, e.g., from the SBS. Then, all FlyBSs can perform the algorithm and choose the UEs simultaneously, since all FlyBSs reach the same association result and the UEs are associated with the FlyBS most profitable for each individual UE.

IV. Repositioning of FlyBSs and Reallocation of Transmission Power

After the optimal power allocation at the FlyBSs and the association of the UEs to them, the capacity can be further increased by the repositioning of the FlyBSs, provided that the transmission power of the FlyBSs is below $P_{\max}$. Note that the capacity of the UEs cannot be increased by a sole increase in the transmission power of the FlyBSs as the backhaul links between the FlyBSs and the SBS would still pose a bottleneck. Hence, the capacity of the UEs can be increased only if the backhaul link quality is improved as well. Since the transmission power of the SBS is assumed to be fixed, the only option to increase the backhaul capacity of the UEs associated to any FlyBS is to move the FlyBS "closer" to the SBS. Of course, if the FlyBS is repositioned, the power allocation for all its associated UEs must be updated since: 1) the backhaul channel capacity changes with the changing position of the FlyBS and 2) the quality of the access links to the UEs changes as well if the FlyBS moves away from its original position. Consequently, we should continuously ensure the optimal power allocation in line with Lemma 1.

The subproblem of the repositioning is formulated as

$$\boldsymbol{V}^{**} = \underset{\boldsymbol{V}}{\operatorname{argmax}} \sum_m \sum_n x_{m,n}G_{m,n}$$
$$\text{s.t.} \quad \text{(13a)} \ \sum_n x_{m,n}p_{m,n} \leq P_{\max} \quad \forall m. \qquad (13)$$

The location of the FlyBS is optimal if the sum capacity of the UEs served by the FlyBS is maximized and, at the same time, if (13a) is not violated. As shown in Fig. 2, the optimal position v_m^* should be always within the area, where the distance to the SBS is shortened compared to its initial v_m position (determined, e.g., by K-means [37]), see the red sector of the circle in Fig. 2. The shortening of the distance to the SBS results in an increase in the backhaul capacity and, subsequently, in an increase in the relaying gain $G_{m,n}$.

The subproblem of finding the optimal position of the FlyBSs defined in (13) cannot be solved analytically, as the derivative of the objective function with respect to V is not

Algorithm 2 FlyBS Repositioning and Power Reallocation

1: Set $i_m = 1$
2: **while** $i_m = 1$ **do**
3: Move to new position
4: Update $\sum_n p_{m,n}$
5: **if** $\sum_n p_{m,n} = P_{max}$ **then**
6: Stop moving and set $i_m = 0$
7: **end if**
8: **if** $\sum_n p_{m,n} > P_{max}$ **then**
9: Go back to previous position
10: **if** Any eligible new moving direction? **then**
11: Adjust moving direction
12: **else** Set $i_m = 0$
13: **end if**
14: **end if**
15: **end while**

known due to the complexity and variation of a general path loss model. Nevertheless, we can adopt a derivative-free numerical optimization approach to solve it. One of the well-known derivative-free optimization numerical approaches is the Nelder–Mead simplex algorithm. However, the algorithm is designed for the unconstrained optimization problems. Thus, we first transform the constrained problem (13) into an unconstraint one and, then, we apply the simplex algorithm. To this end, the problem in (13) is rewritten as

$$\boldsymbol{V}^{**} = \underset{\boldsymbol{V}}{\operatorname{argmax}} \sum_m \sum_n x_{m,n} G_{m,n} - \rho \sum_m \max\left(0, \sum_n x_{m,n} p_{m,n} - P_{\max}\right) \quad (14)$$

where ρ is the penalty for breaking the constraint (13a). If the constraint is satisfied, the second term in (14) is always 0 and no penalty is applied. In the opposite case, a negative penalty is added to the $\sum_m \sum_n x_{m,n} G_{m,n}$ and, thus, the value of the objective function in (14) decreases. Consequently, the simplex algorithm finds the position, where the constraint (13a) is guaranteed (i.e., no penalty is applied) while maximizing the objective function in (14).

The numerical solution based on the Nelder–Mead simplex algorithm is not suitable for real networks due to its high complexity. To that end, we propose the repositioning of the FlyBSs that can be used in practice, depicted in Algorithm 2. The algorithm itself is described for a single FlyBS, as multiple FlyBSs can update their positions simultaneously. In the beginning, the movement indicator i_m is set to 1 indicating that the mth FlyBS can be repositioned (see line 1 in Algorithm 2). As long as $i_m = 1$, the following steps are performed. First, the FlyBS moves continuously to the new position in a straight direction to the SBS (line 4) while the transmission powers allocated to all UEs served by the mth FlyBS are progressively updated (line 5). If the FlyBS is able to serve all these UEs, that is, if $\sum_n p_{m,n} < P_{\max}$, the FlyBS is allowed to keep moving in the same direction toward the SBS. However, if the transmission power of the FlyBS reaches the maximal limit (i.e., $\sum_n p_{m,n} = P_{\max}$), the FlyBS is forced to stop and sets i_m to 0 (line 6).

If the transmission power limit would be exceeded (i.e., if $\sum_n p_{m,n} \geq P_{\max}$), the FlyBS goes back to the last position, where the condition $\sum_n p_{m,n} \leq P_{\max}$ holds (line 9) and decides whether there is another eligible direction for the movement of the FlyBS or not (line 10). The eligible direction is understood as the direction, where the LoS communication between the UEs and the FlyBS is likely and the distance between the FlyBS and the SBS is shortened. Thus, if the FlyBS reaches a building's boundary its movement direction is adjusted so that the FlyBS starts moving along the edge of this building (line 11). If there is no possible way to move the FlyBS closer to the SBS and while keeping LoS communication to all served UEs, i_m is set to 0 and the mth FlyBS is not allowed to move any further (line 12). The example of the moving trajectory of the FlyBS is shown in Fig. 2.

V. Reuse of Access Channels Through Coalitions

So far, we have assumed that the FlyBSs relay data to their UEs on the dedicated orthogonal access channels for each UE. This section elaborates the reuse of the access channels by means of the coalitions. First, we describe the basic principle of the access channel's reuse and define the problem. Then, we solve the problem optimally via the dynamic programming and we also propose a suboptimal, but low-complexity greedy algorithm.

A. Principle and Problem Formulation

If the access channels are not reused, there is no interference to the UEs from the adjacent FlyBSs, but the spectrum efficiency can be degraded (see Fig. 3(a)). To improve the spectrum efficiency, some of the access channels can be, in fact, reused by the multiple UEs. Thus, we propose to reuse the access channels by means of the coalitions in a way that the coalitions significantly increase the channel bandwidth for the individual UEs in the coalitions while *the interference* from other FlyBSs is increased only negligibly. Thus, if the UEs are in the same zth coalition, the respective FlyBSs serve the UEs via the channel $B^z = \sum_{n \in \boldsymbol{u}_z} B_n$ aggregating the access channels of all individual UEs in the zth coalition (see Fig. 3(b)), where $\boldsymbol{u_z}$ is the set of the UEs in the zth coalition. The set of the FlyBSs serving these UEs is denoted as $\boldsymbol{f_z}$.

Whenever the nth UE is in the zth coalition, the nth UE is inevitably interfered, even if only lightly, by the FlyBSs in $\boldsymbol{f_z}$ serving other UEs in the zth coalition. Hence, the optimal transmission power allocation defined by Lemma 1 (see (7)) is modified and the closed-form expression for the transmission power allocated by the FlyBS to any UE in the coalition is defined by the following lemma.

Lemma 2: The optimal transmission power allocated by the mth FlyBS to serve the nth UE within the zth coalition is

$$p^z_{m,n} = \begin{cases} a^z_{m,n}\left(b^z_{m,n} + c^z_{m,n}\right), & \text{if } p^z_{m,n} \leq P_{\max} \\ 0, & \text{otherwise} \end{cases} \quad (15)$$

where

$$a^z_{m,n} = \frac{2^{\frac{C^B_{m,n}}{B^z}} - 1}{g_{m,n}} \quad (16)$$

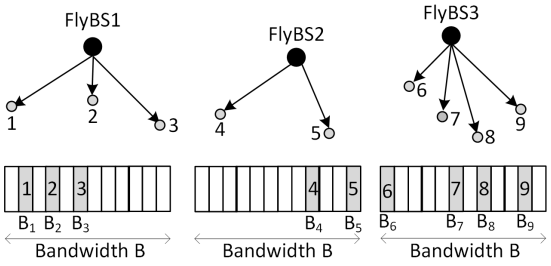

(a)

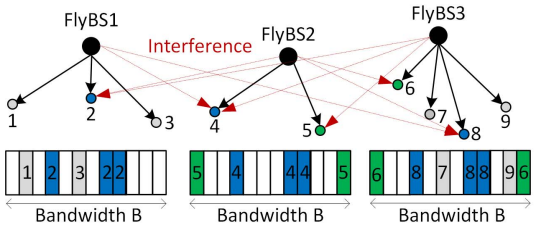

(b)

Fig. 3. Example of the reuse of the access link channels by multiple UEs via created coalitions of the UEs to increase channel bandwidth of individual users while keeping low interference. (a) Allocations of the access channels before the coalition creation. (b) Allocations of the access channels if two coalitions are created: $\boldsymbol{u_1} = \{2, 4, 8\}$ ($\boldsymbol{f_1} = \{1, 2, 3\}$) and $\boldsymbol{u_2} = \{5, 6\}$ ($\boldsymbol{f_2} = \{2, 3\}$) with channel bandwidth $B^1 = B_2 + B_4 + B_8$ and $B^2 = B_5 + B_6$, respectively.

$$b^z_{m,n} = B^z\sigma + \sum_{\mathcal{K}} p^z_k g_{k,n} \tag{17}$$

$$c^z_{m,n} = \sum_{m' \in \boldsymbol{f}_z \setminus m} \sum_{n' \in \boldsymbol{u}_z \setminus n} p^z_{m',n'} g_{m',n} \tag{18}$$

where p^z_k stands for the transmission power of the kth neighboring SBS over the coalition channel bandwidth B^z and $p^z_{m',n'}$ represents the transmission power of the m'th FlyBS allocated to the n'th UE in the zth coalition, and $c^z_{m,n}$ is the interference at the nth UE from the FlyBSs serving the other UEs in the zth coalition.

Proof: Similarly as in the case without the coalitions, the objective is to allocate the transmission power of the mth FlyBS so that $C^B_{m,n} = C^A_{m,n}$. At the access link, the nth UE is interfered by the FlyBSs serving the UEs in the same coalition (i.e., zth coalition); thus, (3) is rewritten as

$$C^A_{m,n} = B^z \log_2\left(1 + \frac{p^z_{m,n} g_{m,n}}{b^z_{m,n} + c^z_{m,n}}\right). \tag{19}$$

Then, considering $C^B_{m,n} = C^A_{m,n}$ and after several math operations similar as in Lemma 1, (19) is rewritten into the form presented in (15). This concludes the proof. ■

Remark 2: If the half-duplex FlyBSs are considered, $a^z_{m,n}$ and $b^z_{m,n}$ are modified as follows:

$$a^z_{m,n} = \frac{2^{\frac{TC^B_{m,n}}{(1-T)B^z}} - 1}{g_{m,n}} \tag{20}$$

$$b^z_{m,n} = B^z\sigma + \sum_{\mathcal{K}\setminus k_0} p^z_k g_{k,n} \tag{21}$$

for the reasons already explained in Remark 1.

As indicated in (15), whenever the transmission power allocation of any FlyBS changes, all UEs within the same coalition are affected and the transmission power allocated to these UEs should be updated by all FlyBSs accordingly. However, this is expected even in the case without the coalitions, as the UEs are interfered from the adjacent cells no matter whether the coalitions are created or not. The reason is that the interference from the adjacent cells can change frequently depending on the allocation of resources in these cells (like channels/resource blocks and power allocation). Still, this is in line with the radio resource management, interference management, or scheduling in 5G and beyond mobile networks, where these procedures are supposed to take place frequently (e.g., each transmission time interval with a duration of 1 ms or even less).

To find the transmission power allocation within the coalition, we form a linear system of equations with multiple variables, where each variable represents the transmission power allocation of individual FlyBSs serving the UEs in the same coalition. Taking the example from Fig. 3(b) with the coalition $\boldsymbol{u_1} = \{2, 4, 8\}$ and applying Lemma 2, the following system of equations is obtained:

$$\begin{aligned} p^z_{1,2} &= a^z_{1,2}b^z_{1,2} + a^z_{1,2}p^z_{2,4}g_{2,2} + a^z_{1,2}p^z_{3,8}g_{3,2} \\ p^z_{2,4} &= a^z_{2,4}b^z_{2,4} + a^z_{2,4}p^z_{1,2}g_{1,4} + a^z_{2,4}p^z_{3,8}g_{3,4} \\ p^z_{3,8} &= a^z_{3,8}b^z_{3,8} + a^z_{3,8}p^z_{1,2}g_{1,8} + a^z_{3,8}p^z_{2,4}g_{2,8}. \end{aligned} \tag{22}$$

Then, (22) is rewritten into a matrix representation as

$$\begin{bmatrix} 1 & -a^z_{1,2}g_{2,2} & -a^z_{1,2}g_{3,2} \\ -a^z_{2,4}g_{1,4} & 1 & -a^z_{2,4}g_{3,4} \\ -a^z_{3,8}g_{1,8} & -a^z_{3,8}g_{2,8} & 1 \end{bmatrix} = \begin{bmatrix} a^z_{1,2}b^z_{1,2} \\ a^z_{2,4}b^z_{2,4} \\ a^z_{3,8}b^z_{3,8} \end{bmatrix}. \tag{23}$$

After that, the transmission power allocation is found by applying Cramer's rule (or any other solver for the system of linear equations). Note that in some cases, the solution to the system of equations would require an allocation of negative transmission powers. This phenomenon occurs if the UEs in the coalition are strongly interfered by the FlyBSs and, thus, this coalition is not profitable. Consequently, the UEs are in the same coalition only if all transmission powers (i.e., $p^z_{1,2}$, $p^z_{2,4}$, and $p^z_{3,8}$) are positive.

To determine which UEs should be in the coalitions, we formulate the coalition creation problem as a constrained coalition structure generation [40]. For any set of players, the coalition structure is understood as a set of coalitions $\boldsymbol{\mathcal{U}} = \{\boldsymbol{u_1}, \boldsymbol{u_2}, \ldots, \boldsymbol{u_Z}\}$ such that each element $\boldsymbol{u_z} \in \boldsymbol{\mathcal{U}}$ is the set of players (i.e., the set of UEs) composing one coalition. Note that each player belongs only to a single coalition. The problem is defined as a constrained one, since the UEs attached to the same FlyBS cannot be in the same coalition. The reason is that we assume simple FlyBSs that are not able to serve multiple UEs at the same resources. Consequently, only the UEs attached to the different FlyBSs can belong to the same coalitions. The objective is, then, to find such a coalition structure ($\boldsymbol{\mathcal{U}}^*$) that minimizes the sum transmission power over all

access channels and over the FlyBSs, i.e.,

$$\begin{aligned} \boldsymbol{\mathcal{U}}^{*} &= \underset{\boldsymbol{\mathcal{U}}}{\operatorname{argmin}} \sum_{m} \sum_{n} x_{m,n} p^{z}_{m,n} \\ \text{s.t.} \quad & \text{(24a)}\ 0 < p^{z}_{m,n} < p_{m,n} \quad \forall m \in \mathcal{M} \quad \forall n \in \mathcal{N} \\ & \text{(24b)}\ m \neq m' \quad \forall m, m' \in \boldsymbol{f}_z \quad \forall z \end{aligned} \tag{24}$$

where the constraint (24a) guarantees that the transmission power allocated by all FlyBSs is not increased by any coalition and the constraint (24b) ensures that the UEs attached to the same FlyBSs cannot be in the same coalition.

The following section first describes the solution for the optimal coalition structure based on the dynamic programming. Then, we outline a low-complexity greedy algorithm.

B. Optimal Coalition Creation

To find the optimal solution for the problem defined in (24) and to determine the optimal structure of the coalitions, the dynamic programming [40] is a suitable option. The problem defined in (24) is, however, different from the conventional coalition structure generation problems due to both constraints. Hence, the dynamic programming is modified as explained below.

The dynamic programming is an iterative two-phase process. In the first phase, a gain function is calculated for all coalitions with a size of 1 (i.e., one UE in each coalition), a size of 2 (two UEs in the coalitions), up to the coalition with a size of N_f, where N_f is the number of UEs connected to the FlyBSs. Note that the UEs attached directly to the SBS cannot be in any coalition as their channel cannot be reused by the FlyBSs. Then, the gain function for each created coalition with the sizes of $1, 2, \ldots, N_f$ is determined as

$$f(\boldsymbol{u}_z) = \begin{cases} \sum_{n \in \boldsymbol{u}_z} \left(p_{m,n} - p^{z}_{m,n}\right), & \text{if (24a), (24b) are met} \\ -\infty, & \text{otherwise.} \end{cases} \tag{25}$$

The definition of $f(\boldsymbol{u}_z)$ reflects the fact that the goal of the coalition creation is to reduce the total transmission power at the FlyBSs. Hence, the coalition is profitable only if all FlyBSs serving the UEs in the same coalition decrease their transmission power. If (24a) or (24b) is not met, $f(\boldsymbol{u}_z)$ is set to $-\infty$ to ensure that this coalition is not selected. Note that we set $f(\boldsymbol{u}_z)$ to $-\infty$ instead of to 0 to distinguish between the coalition that is not allowed and the case when the UE is in the coalition with the size 1, where the gain for such a case is 0 by default, since the FlyBS is not able to decrease its transmission power. Besides the calculation of the gain function for all coalitions with the sizes $1, 2, \ldots, N_f$, the dynamic programming also calculates the gain functions if the coalition of the size 2 or higher are split into smaller coalitions. These gain functions are again enumerated via (25).

Then, in the second phase, the dynamic programming finds the optimal coalition structure recursively. That is, at the beginning, the coalition with the size of N_f is assumed to be the optimal one. Then, the dynamic programming iteratively checks if the gain can be increased by separating the UEs in one larger coalition into two smaller coalitions exploiting the gain functions already calculated in the first phase. If the gain would be increased by the splitting of some UEs, these UEs are not allowed to be in the same coalitions. Otherwise, the UEs are assumed to be in the same coalition.

The dynamic programming-based solution is of a very high complexity equal to $\mathcal{O}(3^{N_f})$. Hence, such a solution is not practical for the real networks and we propose a low-complexity greedy algorithm in the next section to solve the coalitions' creation problem.

C. Low-Complexity Greedy Algorithm for Coalition Creation

As explained in the previous section, the dynamic programming is not suitable for the derivation of the coalitions for a high number of the UEs due to its high complexity. Thus, in this section, we propose the greedy algorithm for the creation of the coalitions.

The proposed greedy algorithm for the coalitions' creation is described in Algorithm 3. In the first step, the gains of any two UEs potentially creating the coalition are calculated according to (25), see line 1 in Algorithm 3. In the next step, the matrix $\boldsymbol{U}$ with a size of NxN is created as (line 2)

$$\boldsymbol{U} = \begin{bmatrix} 0 & U_{1,2} & \ldots & U_{1,N} \\ 0 & 0 & \ldots & U_{2,N} \\ \vdots & \vdots & \ddots & \vdots \\ 0 & 0 & \ldots & U_{N-1,N} \\ 0 & 0 & \ldots & 0 \end{bmatrix}. \tag{26}$$

The diagonal values of $\boldsymbol{U}$ are set to 0, as the UE cannot be in the coalition with itself. The matrix $\boldsymbol{U}$ is symmetric since $U_{n,n'} = U_{n',n}$ and, thus, all values below the diagonal are also zeroed out. In the next step, the maximal value in $\boldsymbol{U}$ is found (line 4) and the corresponding nth and n'th UEs create the coalition (line 5). Then, $U_{n,n'}$ entry in $\boldsymbol{U}$ is set to 0 (line 6). Moreover, all positive entries in the nth row and the n'th column of $\boldsymbol{U}$ are updated (lines 7 and 8). The reasons for this update of the positive values in $\boldsymbol{U}$ are as follows. First, the nth UE can no longer be in the same coalition with any UE attached to the same FlyBS, since the n'th UE and *vice versa*, to guarantee (24b). Thus, all positive entries in the nth row and the n'th column are set to 0. Second, if the nth UE is inserted to the coalition with the n'th UE while at least one of these UEs is already in another coalition with another UE(s), all positive entries in the nth row and the n'th column should be updated, as the gain calculated initially in $\boldsymbol{U}$ is only for two UEs (n and n'). Note that the new gain is calculated according to (25) and the transmission powers of the FlyBSs are derived via (15). This way, we determine whether the coalition composing more than two UEs is of a benefit (indicated by a positive value in the nth row and the n'th column). Otherwise, this entry is set also to 0. After that, the maximum value in $\boldsymbol{U}$ is found again and the whole process (i.e., lines 3–9) is repeated as long as there is at least one positive entry in $\boldsymbol{U}$.

The complexity of the proposed greedy algorithm is $\mathcal{O}(N_f^2 \log N_f)$, as N_f^2 entries are sorted from the highest to the lowest.

D. Repositioning After the Coalitions are Created

Even though the UEs in the same coalition are served over a wider access channel, the backhaul channels are still of the

Algorithm 3 Greedy Algorithm for Coalition Creation

1: Calculate $U_{n,n'}, \forall n, n' \in \mathcal{N}$ acc. to (25)
2: Create matrix $\mathbf{U}$
3: **while** $\max(U_{n,n'}) > 0$ **do**
4: $\{n, n'\} \leftarrow \max(U_{n,n'})$
5: Add n-th and n'-th UEs into the same coalition
6: Set $U_{n,n'}$ to 0
7: Update all positive values in n-th row of $\mathbf{U}$
8: Update all positive values in n'-th column of $\mathbf{U}$
9: **end while**

same bandwidth. Thus, the UEs' benefit from the coalitions cannot be directly translated to their capacity gains, as the capacity of the backhaul links remains unchanged and act as a bottleneck (see (4)). Nevertheless, the created coalitions decrease the transmission power allocated at the FlyBSs while the same capacity at the access links is kept. Hence, the FlyBSs can be further repositioned in the direction to the SBS to increase the capacity at the backhaul links.

The repositioning described in Section IV is applicable also for the case with the coalitions already created. Nevertheless, $p_{m,n}$ for all UEs in the coalitions should always be positive. Note that $p_{m,n}$ for the UEs in the coalitions is derived by solving linear equations, where the found solution may not be feasible, because $p_{m,n}$ can be negative (as described in Section V-A). Thus, (13) should include an additional constraint ensuring that $p_{m,n} \geq 0$ for all m and n. Then, to adopt the Nelder–Mead simplex algorithm, the optimization problem is transformed into the unconstrained one as

$$\begin{aligned} \boldsymbol{V}^{**} = \underset{\boldsymbol{V}}{\operatorname{argmax}} & \sum_m \sum_n x_{m,n} G_{m,n} \\ & - \rho \sum_m \max\left(0, \sum_n x_{m,n} p_{m,n} - P_{\max}\right) \\ & - \rho \sum_m \sum_n \max\left(0, -p_{m,n}\right) \end{aligned} \tag{27}$$

where the penalty ρ is applied if $p_{m,n} < 0$. After that, the Nelder–Mead simplex algorithm is exploited in the same way as described in Section IV. Similarly, Algorithm 2 proposed for the repositioning requires also a minor change. More specifically, the condition in line 8 in Algorithm 2 should include the additional constraint on $p_{m,n}$. Thus, if $p_{m,n} < 0$ for any nth UE in the coalition, the FlyBS should go back to its previous position.

VI. Simulation Scenario, Parameters, and Competitive Schemes

This section describes the simulation scenario and the simulation parameters and outlines the competitive schemes to which our proposal is compared. The performance of the proposed scheme is evaluated in MATLAB. We consider a reference cell with a size of 500×500 m and several buildings to emulate an urban environment (see Fig. 4). The serving SBS is deployed at a fixed position at the left upper corner of the building close to the cell center, as indicated in Fig. 4. The height of each building is generated randomly between

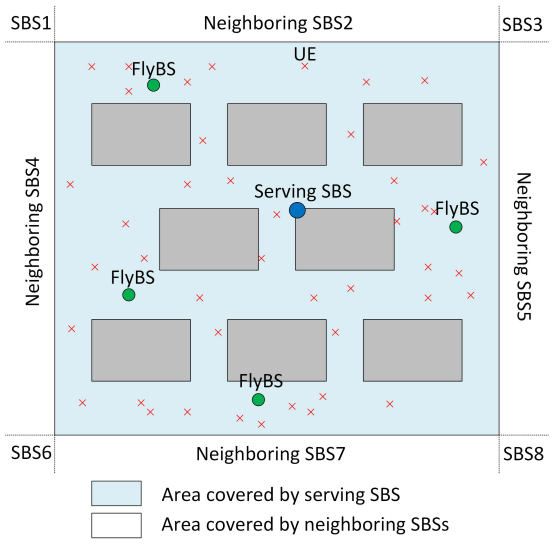

Fig. 4. Illustrative simulation scenario in Urban area with building blocks.

TABLE I
Simulation Parameters

Parameter	Value
Carrier frequency	2 GHz
Simulation area of the reference cell	500x500 m
Number of the adjacent SBSs (K)	8
Number of FlyBSs (M)	4-10
Number of UEs in the reference cell (N)	10-200
Bandwidth available at the SBS in downlink (B)	20 MHz
Channel bandwidth initially allocated to the UE	B/N MHz
Max. trans. power of the SBS and the FlyBSs	20-30 dBm
Noise spectral density (σ_0)	-174 dBm/Hz
Height of the SBS/FlyBSs/UEs antenna	30/30/1 m
Number of the simulation drops	1000

25 and 29 m. Moreover, eight neighboring areas (cells) with the same building's distribution as in the reference cell surround this reference cell. Each neighboring area is under the coverage of one neighboring SBS mounted on top of the building at the same position as the serving SBS in the reference cell. The neighboring SBSs represent the sources of intercell interference to the reference cell.

In the reference cell, N UEs are uniformly deployed in the outdoor areas. We assume, without loss of generality, that the SBS splits the available bandwidth equally among all UEs, i.e., each channel is of a bandwidth $B_n = B/N$ (as in [30]). The UEs are then associated either to the serving SBS or to one of M FlyBS deployed in the area. The initial positions of the FlyBSs are determined with respect to the location of the UEs by K-means, as in [37]. The channel gains between the FlyBSs and the UEs, between the SBS and the UEs, and between the SBS and the FlyBSs are modeled in line with the respective path loss models from [41] considering 2-GHz carrier frequency. While the SBS always communicates with the FlyBSs via LoS (as both the SBS and the FlyBSs are above the buildings), the communication path between the SBS/FlyBSs and the UEs can be obstructed by one or several buildings,

each attenuating the signal by additional 20 dB. The simulation is repeated 1000 times with random positions of the UEs and corresponding FlyBSs positions. The simulation results are then averaged out over all these drops. The simulation parameters are summarized in Table I.

The proposal is confronted with the following schemes.

1) *K-Means:* The association of the UEs and the positions of the FlyBSs is done optimally with respect to the distance between the FlyBSs and the UEs while the reuse of the access channels is not considered [37].
2) *W/O BA:* The positions of the FlyBSs are optimized only with respect to the quality of the access links while neither a backhaul awareness nor the reuse of the access channels is assumed as, e.g., in [5]).
3) *IAB:* The FlyBSs reuse the whole bandwidth at both the backhaul and the access links based on [30]–[33] considering the IAB concept.

We do not compare our proposal with other "backhaul-aware" schemes as these limit the backhaul capacity in a simple way [17], [18], consider out-band frequencies for the backhaul [19]–[22], or address a completely different problem [23]–[28], [34] and, thus, the comparison is not feasible.

We show also a theoretical upper bound of our proposal with the power allocation at the FlyBSs, the association of the UEs, and the coalition creation being optimal while the positions of the FlyBSs are found numerically by the Nelder–Mead simplex algorithm. Note that the performance of the optimal coalitions is shown only for up to 20 UEs, as the results for larger numbers of the UEs cannot be derived due to a very high complexity of dynamic programming.

VII. Simulation Results

This section presents and discusses the simulation results and compares the performance of the proposal with respect to the competitive schemes. We also analyze the contribution of the individual steps of the proposal to the overall performance. Finally, we study the amount of interference generated by the FlyBSs to the underlying devices utilizing the same spectrum in order to demonstrate the benefits resulting from the proposal.

A. Performance Evaluation and Comparison With State-of-the-Art Schemes

Fig. 5 illustrates the performance of the individual schemes for a varying number of the UEs in the simulation area considering the full duplex [Fig. 5(a)] and the half duplex [Fig. 5(b)]. The proposed scheme significantly outperforms all competitive solutions. The sum capacity achieved by the proposal initially decreases with an increasing number of the UEs. This is due to the fact that more deployed UEs share individual FlyBSs and, hence, the FlyBSs have less degree of freedom during the repositioning step. Consequently, the FlyBSs stay further from the SBS resulting in a lower backhaul capacity that also impacts the sum capacity of UEs attached to the FlyBSs. However, the sum capacity saturates and its decrease becomes marginal when more than 140 UEs are deployed. The saturation of

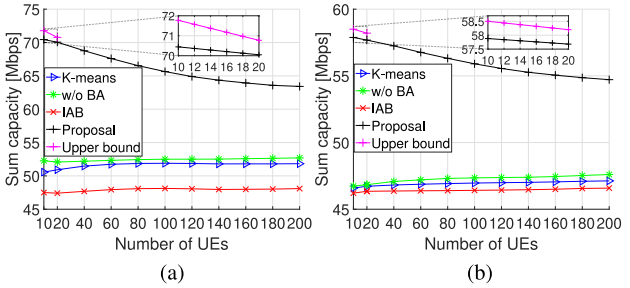

Fig. 5. Sum capacity of the UEs achieved by the proposal and the competitive algorithms over the number of UEs ($P_{\max} = 27$ dBm, $M = 4$); (a) Full duplex. (b) Half duplex.

the sum capacity results from a compensation of the initial decrease in the capacity (due to less degree of freedom of the FlyBSs during repositioning) by the fact that generally more UEs benefit from the FlyBSs deployment.

In case of the full duplex, the proposal increases the sum capacity of the UEs by between 22.4% and 39.3%, between 20.3% and 34.8%, and between 31.9% and 48.3% compared to *K*-means, w/o BA, and IAB schemes, respectively, (see Fig. 5(a)). The reason why *K*-means and w/o BA schemes are significantly outperformed by the proposal is that the FlyBSs are positioned close to the UEs by these schemes and the backhaul links act as a bottleneck. The unsatisfactory performance of the IAB-based scheme is mainly due to a high interference among the FlyBSs that reuse the same bandwidth. Hence, it is more efficient to share only a part of the bandwidth as accomplished by the proposed coalition structure instead of reusing the whole bandwidth by the FlyBSs. The relative improvement in the sum capacity of the proposal with respect to all competitive schemes is slightly decreased for the half duplex when compared to the full duplex, since a lower number of the UEs profit from the relaying in the half duplex. The reason is that the backhaul capacity is decreased, as the FlyBSs receive data in the half duplex from the serving SBS. Nevertheless, even in case of the half duplex, the proposal significantly outperforms *K*-means, w/o BA, and IAB schemes by up to 23.5%, 23.1%, and 24.5%, respectively.

Fig. 5 also demonstrates that the proposed solution is close to the upper bound in terms of the sum capacity. Specifically, the gap between the proposal and the upper bound is only up to 1.9% and up to 1.1% in the case of the full duplex [Fig. 5(a)] and the half duplex [Fig. 5(b)], respectively.

Fig. 6 shows the total transmission power allocated at the FlyBSs depending on the number of UEs. The competitive schemes always allocate and exploit the whole available transmission power $P_{\max}$ disregarding the number of the UEs. Consequently, the total power allocated at the FlyBSs by all competitive schemes is constant and is equal to roughly 2 W (four FlyBSs are considered, each with $P_{\max} = 27$ dBm $\approx$ 0.5 W) in this figure. In case of the proposal, the total transmission power allocated at the FlyBSs slightly increases if the number of the UEs increases up to 20. The reason for this phenomenon is that some FlyBSs may not be exploited at all for some simulation drops with a low number of the UEs and the average total transmission power is decreased. Then,

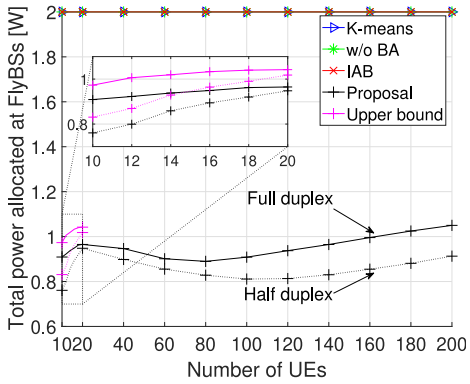

Fig. 6. Total transmission power allocated at all FlyBSs by the proposal and the competitive algorithms ($P_{\max} = 27$ dBm, $M = 4$). Note: the competitive schemes allocate the same total power (roughly 2 W) at the FlyBSs for both the full and half duplex as these optimize only access links.

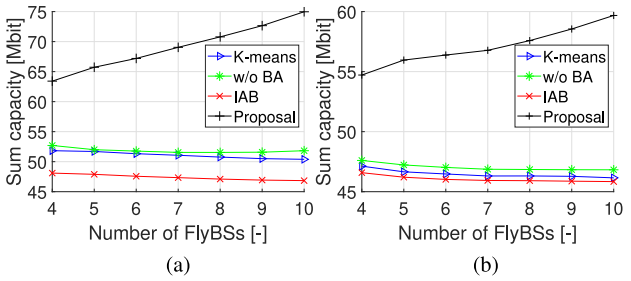

Fig. 7. Sum capacity reached by the proposal and the competitive algorithms over the number of FlyBSs ($P_{\max} = 27$ dBm, $N = 200$); (a) Full duplex. (b) Half duplex.

the total transmission power starts decreasing with more of the UEs in the area (above 20). Still, the total transmission power starts slightly increasing again for more than 80 UEs (and more than 120 UEs in the case of the half duplex). The reasons for this behavior are two opposite trends: 1) the total transmission power *increases* with the number of the UEs, since the FlyBSs serve more UEs in average (i.e., more UEs are associated with each FlyBS) and 2) the total transmission power *decreases* if more UEs are attached to the FlyBSs, since the FlyBSs are not able to move so close to the serving SBS in order to still guarantee high-quality communication access channels for all of, or at least most of, the UEs. While the second trend is more significant for 20–80 UEs in case of the full duplex and for 20–120 UEs in case of the half duplex, the first trend becomes more significant for higher number of the UEs.

Fig. 6 demonstrates the proposal decreases the total transmission power to about one half of the transmission power allocated by the competitive schemes. The main reason for this significant decrease in the transmission power is that if the backahul links are of a lower quality than the access links, the transmission power at the FlyBSs is decreased to keep the same capacity at the access and backhaul links. If the half duplex is applied, up to 14% of the total power is saved at the FlyBSs compared to the full duplex since: 1) the number of the UEs served by the FlyBSs in the half duplex is lower compared to the full duplex and 2) the UEs are not interfered by the serving SBS and, thus, a lower power is allocated to the UEs to ensure $C^A_{m,n} = C^B_{m,n}$ (see Remark 1 in Section III-A).

Fig. 6 also shows the total allocated power in the case of the upper bound is by up to 9% (in the case of the full duplex) and up to 9.2% (for the half duplex) higher than the power allocated by the proposed solution. The reason for this phenomenon is that the numerical positioning of the FlyBSs, which is part of the upper bound and which maximizes the sum capacity, finds the positions for the FlyBSs closer to the SBS than the proposed solution. Consequently, the FlyBSs allocate more transmission power to the UEs, since: 1) slightly more data are transmitted to the UEs (as shown in Fig. 5) and 2) the quality of the access channels is worsen, as the FlyBSs are farther from the UEs and more power should be allocated to them.

The impact of the number of deployed FlyBSs on the sum capacity is depicted in Fig. 7. The sum capacity of K-means and IAB algorithms slightly decreases with more deployed FlyBSs in the area for both the full and half duplex. The reason is that with more FlyBSs in the area, the FlyBSs stay generally "closer" to the UEs, but "farther" from the SBS as the backhaul is ignored. Consequently, the backhaul capacity is degraded and becomes the limiting factor. If the optimization is done solely according to the access links (i.e., w/o BA scheme), the sum capacity starts slightly increasing if seven or more FlyBSs are deployed. In comparison to the competitive schemes, the proposal is able to fully exploit a denser deployment of the FlyBSs and the sum capacity increases almost linearly with the number of FlyBSs. The reason is that with more FlyBSs in the area, a lower number of the UEs is attached to each FlyBS in general. Consequently, the FlyBSs are less restricted in their movement and can be repositioned closer to the SBS by the proposal resulting in a backhaul of a higher quality. Hence, the proposal with the full duplex FlyBSs significantly increases the sum capacity and gains up to 48.8%, 44.7%, and 60.1% when compared to K-means, w/o BA, and the IAB scheme, respectively, if 10 FlyBS are deployed. The sum capacity of all schemes is decreased if the half duplex is considered compared to the full duplex as explained in Fig. 5. Nevertheless, the proposal still outperforms K-means, w/o BA, and IAB schemes significantly up to 29.3%, 27.5%, and 30.2%, respectively.

Fig. 8 shows the impact of the number of deployed FlyBSs on the total transmission power allocated by the FlyBSs. The total transmission power increases linearly with the number of FlyBSs for all competitive schemes as each FlyBS transmits with a fixed transmission power. Also in case of the proposal, the total transmission power is increasing linearly. However, the slope of the increase is much lower compared to the competitive schemes. In fact, the transmission power of a single FlyBS even decreases with the increasing number of the FlyBSs if the proposal is utilized. The main reason is that with more deployed FlyBSs, a lower number of UEs are served by individual FlyBSs and, thus, less power is allocated by these FlyBSs. Consequently, the proposal is able to reduce the transmission power by 64% compared to all competitive schemes and assuming that ten FlyBSs are being deployed. Moreover, Fig. 8 demonstrates that the proposal exploiting only the half

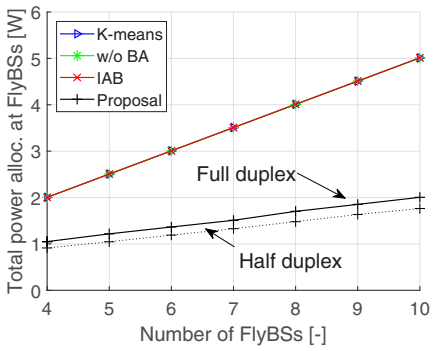

Fig. 8. Total transmission power allocated at all FlyBSs by the proposal and the competitive algorithms ($P_{\max} = 27$ dBm, $N = 200$).

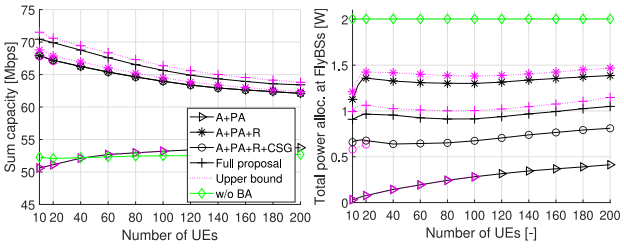

(a) (b)

Fig. 9. Gain of individual steps of the proposal over the number of UEs ($P_{\max} = 27$ dBm, $M = 4$); (a) Sum capacity, (b) Total power allocated at FlyBSs.

duplex reduces the total power allocated at the FlyBSs by up to 14% with respect to the full duplex.

B. Analysis of Gain Introduced by Individual Parts of the Proposal

This section analyzes the gain introduced by the individual steps of the proposal for the full duplex. To that end, we evaluate the sum capacity and the total transmission power allocated at the FlyBSs after the following subsequent steps of the proposal: 1) the joint association of the UEs to the FlyBSs and the power allocation at the FlyBS via the proposed Algorithm 1 (denoted in figures as "A+PA"); 2) the repositioning of the FlyBSs according to the proposed Algorithm 2 (denoted as "A+PA+R"); 3) the creation of the coalitions among the UEs (i.e., the coalition structure generation) by the proposed greedy Algorithm 3 (denoted as "A+PA+R+CSG"); and 4) another repositioning according to Algorithm 2 to further increase the sum capacity (denoted as Full proposal). Note that the Full proposal corresponds to the Proposal scheme in the previous section. Besides the individual steps of the proposal, we also depict the best performing competitive scheme, i.e., w/o BA, as a benchmark.

Fig. 9 illustrates the gain of individual steps of the proposal for a varying number of the UEs. After the association and the initial power allocation, the sum capacity of the proposal is similar to the best performing competitive scheme w/o BA (see line "A+PA" in Fig. 9(a)). Nevertheless, the total transmission power allocated by the proposal at the FlyBSs (Fig. 9(b)) is notably lower as it varies only between 3.8% and 20.7% of the power allocated by the w/o BA.

The subsequent repositioning of the FlyBSs leads to a significant increase in the sum capacity with respect to the sole association [by 15.6% and 31.2% for 200 UEs and 20 UEs, respectively, see line "A+PA+R" in Fig. 9(a)]. The gain is achieved due to the improved backhaul capacity as the FlyBSs get closer to the SBS. Although the repositioning increases also the total power allocated at the FlyBSs to keep the same capacity at the access and the backhaul links (see Lemma 1), the allocated power is still more than 30% lower than the power allocated by the w/o BA scheme disregarding the number of UEs. Note that the trend in the total transmission power is analogous to Fig. 6 for the same reasons. Also, note that the FlyBSs are often not able to move to the positions, where the whole power budget can be utilized due to the buildings obstructing the communication path. In other words, if the FlyBS would move to the position where the UEs become shadowed by the building(s) and the required power to serve the UEs would exceed $P_{\max}$, the FlyBS rather stays at its current position even if the actual allocated power is lower than $P_{\max}$.

The next step, the coalition structure generation, reduces the total transmission power at the FlyBSs significantly (roughly by 50%) with respect to the case without the coalitions. The reason is that the FlyBSs can allocate less power to the UEs in the coalitions and, thus, reduce their total allocated transmission power. As explained in Section V, the formed coalitions by themselves do not improve the sum capacity of the UEs, since the backhaul quality remains the same (see line "A+PA+R+CSG" in Fig. 9(a)). Still, the created coalitions open a space for further "boost" in the sum capacity as the FlyBSs are again repositioned closer to the SBS. This further repositioning boosts the capacity by up to 4.2%. Of course, the repositioning increases again the total transmission power. However, the total transmission power is still significantly lower compared to the competitive schemes (see the Full proposal in Fig. 9(b)). This indicates a possible trade-off as, in some use cases, it can be profitable not to apply the repositioning of the FlyBSs after the coalitions are created and rather keep the transmission power of the FlyBSs low in order to decrease the interference to other underlying devices (we analyze and demonstrate this in Section VII-C).

Fig. 9 also shows the gap between the proposed solution (encompassing proposed Algorithms 1–3) and the upper bound. First, Fig. 9 demonstrates that the proposed Algorithm 1 for the UEs association is optimal for up to 100 UEs (see "A+PA" in Fig. 9). Note that we are not able to show the performance of the full search for more than 100 UEs due to its huge complexity. Second, the gap in the sum capacity between the proposed repositioning (described in Algorithm 2) and the upper bound found by the Nelder–Mead simplex is only negligible as it varies between 1% and 1.5%, as shown in Fig. 9(a). Fig. 9(b) also shows that the upper bound performance of the FlyBSs' repositioning leads to a higher allocated total transmission power at the FlyBSs (between 5% and 12.1%) when compared to "A+PA+R." This is due to the same reasons as described already above in Fig. 6. Finally, Fig. 9(b) shows that the proposed algorithm for the coalition creations (i.e., "A+PA+R+CSG") decreases

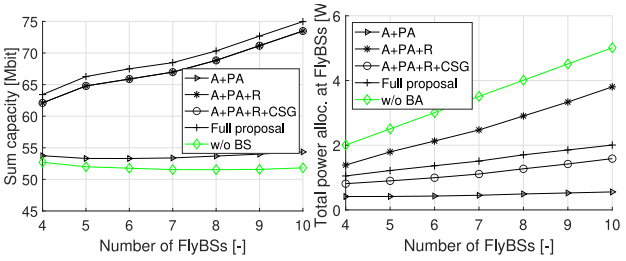

(a) (b)

Fig. 10. Gain of individual steps of the proposal over the number of FlyBSs ($P_{\max} = 27$ dBm, $N = 200$); (a) Sum capacity, (b) Total power allocated at FlyBSs.

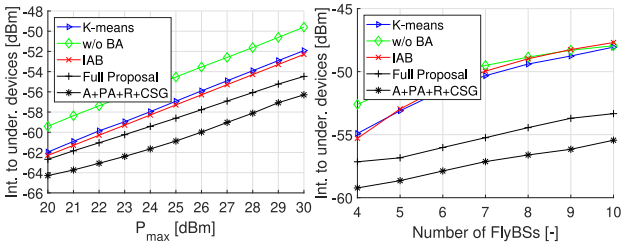

(a) (b)

Fig. 11. Interference generated to underlying devices by the full duplex FlyBSs depending on; (a) Max transmission power P_{max}, (b) Number of FlyBSs.

the total transmission power nearly the same as the high-complexity optimal dynamic programming-based solution, as the gap between the proposal and the optimum varies only from 3.1% to 7%. Note that the sum capacity is not increased when the coalitions are introduced (see Fig. 9(a)) as the coalitions decrease the transmission power only, as explained in Section V.

Fig. 10 depicts the gain of individual proposal steps over the number of the deployed FlyBSs. Similarly as in Fig. 9, a notable gain in the sum capacity is achieved by the repositioning of the FlyBSs in the direction of the SBS with respect to the association and power allocation only (between 15.6% and 35.2%). Then, an additional gain in the sum capacity is observed by the repositioning of the FlyBSs after the coalitions are created (up to 2.6% as shown in Fig. 10(a)). Such relatively small gain is due to the fact that the repositioning of the FlyBSs after the coalitions are created is often restricted by these coalitions. Consequently, the FlyBSs cannot move much closer to the SBS as the FlyBSs serving the UEs in the coalition would interfere to all other UEs. Nevertheless, the formed coalitions significantly decrease the total power allocated at the FlyBSs by up to 58.3% if 10 FlyBSs are deployed (see Fig. 10(b)). Even after the repositioning with the created coalitions that slightly increases the total transmission power, the full proposal decreases the total allocated transmission power roughly 2.5 times compared to the state-of-the-art solutions.

C. Interference to Underlying Devices

One concern regarding the adoption of the FlyBSs into the mobile networks is the increased interference from the deployed FlyBSs to the various underlying devices, such as IoT devices, machines, or sensors, exploiting the same spectrum. Our proposal reduces the transmission power as shown in previous sections and, consequently, mitigates the interference generated by the FlyBSs to these underlying devices. This section shows the average interference generated by the FlyBSs to 100 underlying devices deployed uniformly within the reference cell. In the case of our proposal, we also show the amount of the interference generated if no repositioning after the coalition creation is allowed (i.e., the line "A+PA+R+CSG"). This option is seen as a good tradeoff between the minimization of the interference to the underlying devices and the maximization of the sum capacity of the UEs attached to the FlyBSs.

Fig. 11(a) shows that the interference level at the underlying devices increases if the FlyBSs are allowed to transmit with a higher power. The proposal causes a lower level of the interference to the underlying devices in vicinity when compared to all competitive schemes. More specifically, the full proposal generates up to 2.55, 4.87, and 2.18 dBm less interference with respect to *K*-means, w/o BA, and IAB scheme, respectively. Moreover, if the minimization of the interference to the underlying devices is of a high priority, the interference can be further decreased by the proposal via disabling the second repositioning of the FlyBSs after the coalitions are created (denoted in Fig. 11 as "A+PA+R+CSG"). Note that even without the second repositioning of the FlyBSs, the proposal significantly outperforms all competitive schemes as demonstrated in Fig. 9 and 10. Thus, without the second repositioning, the proposal causes up to 4.37, 6.69, and 4 dBm less interference when compared to *K*-means, w/o BA, and IAB scheme, respectively.

Fig. 11(b) shows that if the number of FlyBSs increases, the interference suppression by the proposal with respect to the competitive schemes is emphasized even more. Hence, the proposal causes up to 5.27, 5.38, and 5.64 dBm less interference than *K*-means, w/o BA, and IAB scheme, respectively, for ten FlyBSs. Again, if the proposal does not adopt the second repositioning of the FlyBSs the interference gap with respect to *K*-means, w/o BA, and IAB scheme increases up to 7.39, 7.49, and 7.75 dBm, respectively. These results demonstrate that the proposal is notably more "friendly" to the underlying devices as it suppresses significantly the interference from the deployed FlyBSs.

VIII. Conclusion

In this article, we have introduced a backhaul-aware framework for the association of the UEs, power allocation of the FlyBSs, their repositioning, and the access links reuse by means of the coalition structure generation. We have demonstrated that the proposed framework significantly outperforms competitive schemes in terms of capacity (up to 60%) and the transmission power reduction (up to 64%) in a wide range of scenarios and for the varying number of UEs and the FlyBSs. In addition, due to the proposed reuse of the access links by means of the coalition creation, the interference to the various underlying devices is significantly decreased (up to 7.7 dB).

The proposed framework can be extended toward joint optimization of the transmission powers of both the FlyBSs and the SBSs. Besides, the mobile users and the related aspects of handover management should further be investigated.

REFERENCES

[1] Y. Zeng, R. Zhang, and T. J. Lim, "Wireless communications with unmanned aerial vehicles: Opportunities and challenges," *IEEE Commun. Mag.*, vol. 54, no. 5, pp. 36–42, May 2016.

[2] M. Mozaffari, W. Saad, M. Bennis, Y.-H. Nam, and M. Debbah, "A tutorial on UAVs for wireless networks: Applications, challenges, and open problems," *IEEE Commun. Surveys Tuts.*, vol. 21, no. 3, pp. 2334–2360, 3rd Quart., 2019.

[3] L. Ruan *et al*, "Energy-efficient multi-UAV coverage deployment in UAV networks: A game-theoretic framework," *China Commun.*, vol. 15, no. 10, p. 194–209, Oct. 2018.

[4] M. Alzenad, A. El-Keyi, and H. Yanikomeroglu, "3-D placement of an unmanned aerial vehicle base station for maximum coverage of users with different QoS requirements," *IEEE Wireless Commun. Lett.*, vol. 7, no. 1, pp. 38–41, Feb. 2018.

[5] X. Zhong, Y. Guo, N. Li, and S. Li, "Deployment optimization of UAV relays for collecting data from sensors: A potential game approach," *IEEE Access*, vol. 7, pp. 182962–182973, 2019.

[6] X. Zhong, Y. Guo, N. Li, and Y. Chen, "Joint optimization of relay deployment, channel allocation, and relay assignment for UAVs-aided D2D networks," *IEEE ACM/IEEE Trans. Netw.*, vol. 28, no. 2, pp. 804–817, Apr. 2020.

[7] Y. Liu, Z. Qin, Y. Cai, Y. Gao, G. Y. Li, and A. Nallanathan, "UAV communications based on non-orthogonal multiple access," *IEEE Wireless Commun.*, vol. 26, no. 1, pp. 52–57, Feb. 2019.

[8] J. Chen and D. Gesbert, "Optimal positioning of flying relays for wireless networks: A LOS map approach," in *Proc. IEEE Int. Conf. Commun. (ICC)*, 2017, pp. 1–6.

[9] J. Plachy, Z. Becvar, P. Mach, R. Marik, and M. Vondra, "Joint positioning of flying base stations and association of users: Evolutionary-based approach," *IEEE Access*, vol. 7, pp. 11454–11463, 2019.

[10] H. El Hammouti, M. Benjillali, B. Shihada, and M.-S. Alouini, "A distributed mechanism for joint 3D placement and user association in UAV-assisted networks," in *Proc. IEEE Wireless Commun. Netw. Conf. (WCNC)*, 2019, pp. 1–6.

[11] H. El Hammouti, M. Benjillali, B. Shihada, and M.-S. Alouini, "Learn-as-you-fly: A distributed algorithm for joint 3D placement and user association in multi-UAVs networks," *IEEE Trans. Wireless Commun.*, vol. 18, no. 12, pp. 5831–5844, Dec. 2019.

[12] X. Xi, X. Xao, P. Yang, J. Chen, T. Quek, and D. Wu, "Joint user association and UAV location optimization for UAV-aided communications," *IEEE Wireless Commun. Lett.*, vol. 8, no. 6, pp. 1688–1691, Dec. 2019.

[13] X. Liu and N. Ansari, "Resource allocation in UAV-assisted M2M communications for disaster rescue," *IEEE Wireless Commun. Lett.*, vol. 8, no. 2, pp. 580–583, Apr. 2019.

[14] S. Yan, M. Peng, and X. Cao, "A game theory approach for joint access selection and resource allocation in UAV assisted IoT communication networks," *IEEE Internet Things J.*, vol. 6, no. 2, pp. 1663–1674, Apr. 2019.

[15] M. Nikooroo and Z. Becvar, "Optimizing transmission and propulsion powers for flying base stations," in *Proc. IEEE Wireless Commun. Netw. Conf. (WCNC)*, Seoul, South Korea, 2020, pp. 1–8.

[16] J. Cui, Y. Liu, and A. Nallanathan, "Multi-agent reinforcement learning-based resource allocation for UAV networks," *IEEE Trans. Wireless Commun.*, vol. 19, no. 2, pp. 729–743, Feb. 2020.

[17] E. Kalantari, M. Z. Shakir, H. Yanikomeroglu, and A. Yongacoglu, "Backhaul-aware robust 3D drone placement in 5G+ wireless networks," in *Proc. IEEE Int. Conf. Commun. Workshops (ICC Workshops)*, 2017, pp. 109–114.

[18] E. Kalantari, I. Bor-Yaliniz, A. Yongacoglu, and H. Yanikomeroglu, "User association and bandwidth allocation for terrestrial and aerial base stations with backhaul considerations," in *Proc. IEEE 28th Annu. Int. Symp. Pers. Indoor Mobile Radio Commun. (PIMRC)*, 2017, pp. 1–6.

[19] M. Gapeyenko, V. Petrov, D. Moltchanov, S. Andreev, N. Himayat, and Y. Koucheryavy, "Flexible and reliable UAV-assisted backhaul operation in 5G mmWave cellular networks," *IEEE J. Sel. Areas Commun.*, vol. 31, no. 11, pp. 2486–2496, Nov. 2018.

[20] Y. Hu, M. Chen, and W. Saad, "Joint access and backhaul resource management in satellite-drone networks: A competitive market approach," 2019. [Online]. Available: arXiv:1908.11038.

[21] G. Castellanos, M. Deruyck, L. Martens, and W. Joseph, "Performance evaluation of direct-link backhaul for UAV-aided emergency networks," *Sensors*, vol. 19, p. 3342, Jul. 2019.

[22] N. Ansari, D. Wu, and X. Sun, "FSO as backhaul and energizer for drone-assisted mobile access networks," *ICT Exp.*, vol. 6, pp. 139–144, Jun. 2020.

[23] M. M. U. Chowdhury, S. J. Maeng, E. Bulut, and I. Güvenç, "3-D trajectory optimization in UAV-assisted cellular networks considering antenna radiation pattern and backhaul constraint," *IEEE Trans. Aerosp. Electron. Syst.*, vol. 56, no. 5, pp. 3735–3750, Oct. 2020.

[24] D. Huang, M. Cui, G. Zhang, X. Chu, and F. Lin, "Trajectory optimization and resource allocation for UAV base stations under in-band backhaul constraint," *EURASIP J. Wireless Commun. Netw.*, vol. 2020, p. 83, Apr. 2020.

[25] G. Feng *et al.*, "UAV-assisted wireless relay networks for mobile offloading and trajectory optimization," *Peer-to-Peer Netw. Appl.*, vol. 12, pp. 1820–1834, Aug. 2019.

[26] C. T. Cicek, H. Gultekin, B. Tavli, and H. Yanikomeroglu, "Backhaul-aware optimization of UAV base station location and bandwidth allocation for profit maximization," 2020. [Online]. Available: arXiv:1810.12395.

[27] E. Kalantari, H. Yanikomeroglu, and A. Yongacoglu, "Wireless networks with cache-enabled and backhaul-limited aerial base stations," *IEEE Trans. Wireless Commun.*, vol. 19, no. 11, pp. 7363–7376, Nov. 2020.

[28] M.-J. Youssef, J. Farah, C. A. Nour, and C. Douillard, "Full-duplex and backhaul-constrained UAV-enabled networks using NOMA," *IEEE Trans. Veh. Technol*, vol. 69, no. 9, pp. 9667–9681, Sep. 2020.

[29] *Technical Specification Group Radio Access Network, Study on Integrated Access and Backhaul*, document 3GPP TR38.874 v16.0.0, 3GPP, Sophia Antipolis, France, Dec. 2018.

[30] M.-J. Youssef, C. A. Nour, J. Farah, and C. Douillard, "Backhaul-constrained resource allocation and 3D placement for UAV-enabled networks," in *Proc. IEEE 90th Veh. Technol. Conf. (VTC-Fall)*, 2019, pp. 1–7.

[31] C. Pan, J. Yi, C. Yin, J. Yu, and X. Li, "Joint 3D UAV placement and resource allocation in software-defined cellular networks with wireless backhaul," *IEEE Access*, vol. 7, pp. 104279–104293, 2019.

[32] A. Fouda, A. S. Ibrahim, I. Guvenc, and M. Ghosh, "UAV-based in-band integrated access and backhaul for 5G communications," in *Proc. IEEE 88th Veh. Technol. Conf. (VTC-Fall)*, 2018, pp. 1–5.

[33] A. Fouda, A. S. Ibrahim, I. Guvenc, and M. Ghosh, "Interference management in UAV-assisted integrated access and backhaul cellular networks," *IEEE Access*, vol. 7, pp. 104553–104566, 2019.

[34] Y. Li, G. Feng, M. Ghasemiahmadi, and L. Cai, "Power allocation and 3-D placement for floating relay supporting indoor communications," *IEEE Trans. Mobile Comput.*, vol. 18, no. 3, pp. 618–631, Mar. 2019.

[35] P. Mach, Z. Becvar, and M. Najla, "Joint association, transmission power allocation and positioning of flying base stations considering limited backhaul," in *Proc. IEEE 92nd Veh. Technol. Conf. (VTC-Fall)*, 2020, pp. 1–7.

[36] H. Wang, J. Wang, G. Ding, J. Chen, Y. Li, and Z. Han, "Spectrum sharing planning for full-duplex UAV relaying systems with underlaid D2D communications," *IEEE J. Sel. Areas Commun.*, vol. 36, no. 9, pp. 1986–1999, Sep. 2018.

[37] B. Galkin, J. Kibilda, and L. A. DaSilva, "Deployment of UAV-mounted access points according to spatial user locations in two-tier cellular networks," in *Proc. Wireless Days (WD)*, 2016, pp. 1–6.

[38] O. Esrafilian and D. Gesbert, "Simultaneous user association and placement in multi-UAV enabled wireless networks," in *Proc. 22nd Int. ITG Workshop Smart Antennas*, Bochum, Germany, 2018, pp. 1–5.

[39] M. Sami and J. N. Daigle, "User association and power control for UAV-enabled cellular networks," *IEEE Wireless Commun. Lett.*, vol. 9, no. 3, pp. 267–270, Mar. 2020.

[40] T. Rahwan, T. P. Michalak, M. Wooldridge, and N. R. Jennings, "A coalition structure generation: A survey," *Artif. Intell.*, vol. 229, pp. 139–174, Dec. 2015.

[41] "Evolved universal terrestrial radio access (E-UTRA); further advancements for E-UTRA physical layer aspects, v 9.2.0," 3GPP, Sophia Antipolis, France, 3GPP Rep. TR 36.913, 2017.

Pavel Mach (Member, IEEE) received the M.Sc. and Ph.D. degrees in telecommunication engineering from Czech Technical University in Prague, Prague, Czech Republic, in 2006 and 2010, respectively.

From 2006 to 2007, he joined the Sitronics Research and Development Center of Prague focusing on emerging mobile technologies and he was involved in research activities of Vodafone Research and Development Center with Czech Technical University in Prague, from 2005 to 2008, where he is currently a Senior Researcher with 5G Mobile Research Lab founded in 2015 at Czech Technical University in Prague focusing on 5G and beyond mobile networks. He has published three book chapters, more than 70 conference or journal papers, and he is a co-inventor of three U.S. patents. He was involved in several European projects, such as FP6 FIREWORKS, FP7 ROCKET, FP7 FREEDOM, and FP7 TROPIC. He was/is a principal investigator in national research projects focused on allocation of radio resources to cognitive small cells and combination of device-to-device communication with visible-light communication. He was on internship in EURECOM, France in 2019. His current research areas include radio resource management for device-to-device communication, specifically focused on relaying techniques and incentive mechanisms given to the relaying users; new techniques for dynamic functional split for C-RAN-based network architectures, positioning of flying mobile base stations, and mobile-edge computing.

Zdenek Becvar (Senior Member, IEEE) received the M.Sc. and Ph.D. degrees in telecommunication engineering from Czech Technical University in Prague, Prague, Czech Republic, in 2005 and 2010, respectively.

He is an Associate Professor with the Department of Telecommunication Engineering, Czech Technical University in Prague. From 2006 to 2007, he joined the Sitronics Research and Development Center of Prague focusing on speech quality in VoIP and he was involved in research activities of Vodafone Research and Development Center with Czech Technical University in Prague in 2009. He was on internships with Budapest Politechnic, Budapest, Hungary, in 2007, CEA-Leti, Grenoble, France, in 2013, and EURECOM, Biot, France, in 2016 and 2019. From 2013 to 2017, he was a representative with Czech Technical University in Prague of ETSI and 3GPP standardization organizations. In 2015, he founded the Laboratory of Mobile Networks–5G Mobile Research Lab, Czech Technical University in Prague, focusing on research toward 5G and beyond mobile networks. He has published four book chapters and more than 90 conference or journal papers and he is a (co-)inventor of four patents. He works on development of solutions for future mobile networks with special focus on optimization of mobility and radio resource management, energy efficiency, device-to-device communication, edge computing, C-RAN, self-optimization, and architecture of radio access network.

Mehyar Najla (Student Member, IEEE) received the Ph.D. degree in telecommunication engineering from Czech Technical University in Prague, Prague, Czech Republic, in 2021.

He is currently a Researcher with Laboratory of Mobile Networks–5G Mobile Research Lab, Czech Technical University in Prague, focusing on research related to future mobile networks. He was/is involved in several national research projects focused on combination of radio-frequency and visible-light communication for device-to-device communication, machine learning for wireless networks, and mobile networks with flying base stations. In 2019, he was on an internship with EURECOM, Biot, France. He has coauthored more than ten conference and journal papers. His research interests include radio resource management in mobile networks, device-to-device communication, hybrid radio-frequency and visible-light communication systems, machine learning for prediction and optimization in mobile networks, game-theoretic techniques for resource allocation in wireless networks, and optimization of mobile networks with flying base stations.

XVI. Appendix CH

This appendix includes conference paper presented at: **P. Mach**, Z. Becvar, and M. Nikooroo, "Multi-hop Relaying with Mixed Half and Full Duplex Relays for Offloading to MEC," in Proc. *IEEE Global Communications Conference (Globecom)*, Kuala Lumpur, Malaysia, Dec. 2023. Available online: https://arxiv.org/abs/2401.06908.

Multi-hop Relaying with Mixed Half and Full Duplex Relays for Offloading to MEC

Pavel Mach[1], Zdenek Becvar[1], Mohammadsaleh Nikooroo[1]
[1]Czech Technical University in Prague, Czech republic, emails: {machp2, zdenek.becvar}@fel.cvut.cz

***Abstract*—In this paper, we focus on offloading a computing task from a user equipment (UE) to a multi-access edge computing (MEC) server via multi-hop relaying. We assume a general relaying case where relays are energy-constrained devices, such as other UEs, internet of things (IoT) devices, or unmanned aerial vehicles. To this end, we formulate the problem as a minimization of the sum energy consumed by the energy-constrained devices under the constraint on the maximum requested time of the task processing. Then, we propose a multi-hop relaying combining half and full duplexes at each individual relay involved in the offloading. We proof that the proposed multi-hop relaying is convex, thus it can be optimized by conventional convex optimization methods. We show our proposal outperforms existing multi-hop relaying schemes in terms of probability that tasks are processed within required time by up to 38% and, at the same time, decreases energy consumption by up to 28%.**

***Index Terms*—offloading, MEC, half/full duplex relaying.**

I. Introduction

The multi-access edge computing (MEC) introduces a concept of offloading computationally demanding tasks from the energy-constrained user equipment (UE) to the MEC server located at the edge of mobile network [1]. Hence, the task processing delay and/or energy consumption of the UE can be reduced [2].

Benefits facilitated by MEC can be further augmented by a relaying of the tasks from the UE to the MEC servers via intermediate relay(s). The exploitation of neighboring UEs as relays and, thus, capitalizing on device-to-device (D2D) relaying concept [3], helps to minimize the task processing delay [4] or increase the number of tasks completed within a required time [5]. Moreover, an adoption of unmanned aerial vehicles (UAVs) acting as the relays can improve quality of experience to the UEs [6] or minimize their energy consumption [7]. Besides, the use of vehicles as the relays is considered in [8] to ensure a reliable offloading from the vehicles in the area without coverage of the MEC servers. Last, also intelligent reflecting surface (IRS) can assist in offloading of tasks to extend coverage [9].

All above-mentioned works assume only two-hop relaying, i.e., only one relay is used in the offloading process. To fully grab the potential of the relays, multi-hop relaying for the offloading purposes has recently drawn an attention from researches. The multi-hop relaying is addressed from a perspective of balancing the load among MEC servers [10], minimizing the processing delay of the tasks offloaded from the vehicles to the MEC servers [11]-[13] or to other computing vehicles [14][15], or to offload the tasks from one UE to other neighboring computing UEs [16].

The primary objective of all existing studies on the offloading with multi-hop relaying is to find a proper route between the offloading UE and the MEC server or other computing UE. All works but [16] assume only less efficient half-duplex (HD) mode adopted at each relay with the task subsequently offloaded over each hop in individual time intervals, thus, increasing communication delay. The paper [16] considers full-duplex (FD) mode, however, the paper fully disregards the problem of self-interference (SI) with which the FD is inevitably plagued [17]. Moreover, none of the existing works optimize multi-hop relaying in terms of radio resource management including *i*) allocation of time slots at each hop, *ii*) allocation of transmission power of the offloading UE as well as relays, and *iii*) allocation of bandwidth at each hop.

Motivated by the above-mentioned gaps, the objective of this paper is to optimize radio resource management aspects of multi-hop relaying for the task offloading. Since the offloading UE and relays are usually energy-constrained, such as smartphones, UAVs, or internet of things (IoT) devices, we formulate the problem as the minimization of the sum energy consumed by the energy-constrained UEs involved in the multi-hop relaying under the constraint on the maximum processing time of the computing tasks. First, we propose several unique relaying cases combining HD and FD at each relay involved in multi-hop relaying. Note that existing works always assume the same relaying mode at all relays. Second, we adapt the general problem for each multi-hop relaying case and we prove its convexity so that we can solve it in an optimal way. Finally, we demonstrate that the proposal increases the probability of the tasks being processed within required time by up to 38% and, at the same time, decreases energy consumption by up to 28% with respect to state-of-the-art works.

II. System Model

This section first describes the network model. Then, communication and computing models are introduced.

A. Network model

We contemplate a scenario with one powerful MEC server located, for example, at the base station (BS). Further, we assume one UE generating highly computationally demanding

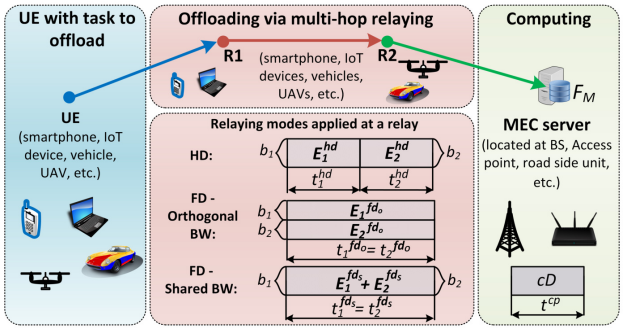

Fig. 1: System model with one UE having a task to offload via multi-hop relaying and computed at MEC server.

tasks offloaded to the MEC servers via multi-hop relaying. We consider the end-to-end relaying link is already established while leaving the joint optimization of relays selection and multiple UEs scenario for future work. In our work, the relays can be any energy-constrained devices, such as smartphones, IoT devices, UAVs, or vehicles. Moreover, we envisage that different types of relays can be exploited at each hop, e.g., the smartphone can be used as the first relay while vehicle or UAV as other relay.

B. Communication and relaying models

We limit our scenario to two relays (labeled as R1 and R2 in Fig. 1), since this number is sufficient to illustrate benefits of the multi-hop relaying in the offloading while fitting page limit and avoiding cluttering of text and derivations. Still, all the math derivations and proposed relaying principles can be extended to more than two relays as well. We assume single antenna devices as this configuration gives enough insight on the benefits of proposed multi-hop offloading.

We consider that each relay can adopt one of the three relaying modes: *i*) *HD*, *ii*) FD with orthogonal bandwidth at each hop (labeled as *FD–Orthogonal*), and *iii*) FD with the same bandwidth utilized at both hops (labeled as *FD–Shared*). All these modes are described in details in the following subsections.

1) HD: In case of HD relaying, the task is first sent over one hop and, then, the same task is relayed over the next hop (see Fig. 1). The capacity at the n-th hop is:

$$C_n^{hd} = b_n log_2\left(1 + \frac{p_n g_n}{b_n\left(\sigma + I_b\right)}\right), \tag{1}$$

where b_n, p_n, g_n are the allocated bandwidth, transmission power, and channel gain at the n-th hop, respectively, σ is the noise spectral density, and I_b is the background interference from other UEs in the neighboring cells, as in real-world scenarios, where such interference is usually present.

The communication delay in the HD is composed of the delays at individual hops (t_1^{hd}, t_2^{hd}), and is expressed as:

$$t^{hd} = t_1^{hd} + t_2^{hd} = \sum\nolimits_n t_n^{hd} = D\sum\nolimits_n \frac{1}{C_n^{hd}}, \tag{2}$$

where D is the size of the task offloaded by the UE. Similarly as in many works (see, e.g., [10]), we neglect the delivery of the computing results back to the UE, as it is insignificant with respect to the whole communication delay.

The sum energy consumed to forward the task in HD is composed of the energies consumed at individual hops (E_n^{hd}):

$$E^{hd} = E_1^{hd} + E_2^{hd} = \sum\nolimits_n E_n^{hd} = \sum\nolimits_n t_n^{hd} p_n. \tag{3}$$

Note that we consider only energy consumption caused by transmission of tasks while a circuit power consumption of the devices is not assumed, as the circuit power consumption is constant and does not change due to offloading.

2) FD–Orthogonal: In this mode, the relay receives and transmits the data simultaneously, but transmission at both hops are orthogonal in frequency domain (see Fig. 1) to avoid SI. Thus, we assume orthogonal bandwidth b_1 and b_2 at the first and second hops, respectively (we derive the optimal bandwidth allocation later in the paper). Then, the capacity $C_n^{fd_o}$ at the n-th hop is expressed as in (1).

Since the propagation delay and time for processing of communication at the relay (both jointly denoted as ϵ) are very short (scale of μs or ms) compared to the offloading time (hundreds of ms or seconds), these can be neglected without breaking a relaying causality and we can assume $t_1^{fd_o} = t_2^{fd_o} + \epsilon \approx t_1^{fd_o}$ for $\epsilon << $ overall offloading time. In practice, the whole offloading task is transmitted in a series of many smaller transport blocks (in scale of ms in 5G) and each block can be forwarded right after its reception and processing by the relay, hence, fulfilling the relaying causality principle for the whole task. Thus, the communication delay is:

$$t^{fd_o} = t_1^{fd_o} = t_2^{fd_o} = \max(D/C_1^{fd_o}, D/C_2^{fd_o}), \tag{4}$$

The energy consumption required to relay the task in FD with orthogonal bandwidth is calculated as:

$$E^{fd_o} = E_1^{fd_o} + E_2^{fd_o} = \sum\nolimits_n E_n^{fd_o} = \sum\nolimits_n t_n^{fd_o} p_n. \tag{5}$$

3) FD–Shared: Similarly as in the previous FD case, the relays can receive and transmit data simultaneously (assuming $\epsilon << $ offloading time as explained for *FD-Orthogonal bandwidth*). The fundamental difference is, however, that the transmissions at both hops share the same bandwidth. Then, the capacities at each hop are:

$$C_1^{fd_s} = b_1 log_2\left(1 + \frac{p_1 g_1}{b_1\left(\sigma + I_b\right) + p_2 g_{1,1}}\right), \tag{6}$$

$$C_2^{fd_s} = b_2 log_2\left(1 + \frac{p_2 g_2}{b_2\left(\sigma + I_b\right) + p_1 g_{1,2}}\right), \tag{7}$$

where $g_{1,1}$ is the channel gain between the transmitter and the receiver of the relay, thus, $p_2 g_{1,1}$ in (6) represents the SI in FD [17]; and $g_{1,2}$ is the channel gain between the transmitter at the first hop and the receiver at the second hop and $p_1 g_{1,2}$ representing interference in (7) from the former to the latter.

The communication delay is analogous to FD with orthog-

onal bandwidth, i.e.,:

$$t^{fd_s} = t_1^{fd_s} = t_2^{fd_s} = \max(D/C_1^{fd_s}, D/C_2^{fd_s}). \quad (8)$$

The energy consumption in this relaying mode is defined as:

$$E^{fd_s} = E_1^{fd_s} + E_2^{fd_s} = \sum\nolimits_n E_n^{fd_s} = \sum\nolimits_n t_n^{fd_s} p_n. \quad (9)$$

C. Computing model

We focus on the offloading of tasks to the MEC server that is able to process F_M central processing unit (CPU) cycles per second. Let c is the average number of CPU cycles to process one bit of the task [2]. Then, we express the computing delay as:

$$t^{cp} = cD/F_M. \quad (10)$$

III. Problem formulation

We formulate a resource allocation problem to minimize the sum energy consumption for the offloading of the task from the UE over N (in this paper $N = 3$) hops as both the UE and relays are assumed to be energy-constrained while the task processing time meets the maximum required processing time T_{max}. This is achieved by optimization of time slots $\boldsymbol{\mathcal{T}}$, transmission power $\boldsymbol{\mathcal{P}}$, and bandwidth allocation $\boldsymbol{\mathcal{B}}$ at individual hops. Hence, the problem is formulated as:

$$\begin{aligned} \boldsymbol{\mathcal{T}}, \boldsymbol{\mathcal{P}}, \boldsymbol{\mathcal{B}} = \quad & \underset{t_n, p_n, b_n}{\operatorname{argmin}} \sum\nolimits_n E_n \\ \text{s.t.} \quad & \text{(a)} \ \sum\nolimits_n t_n \le T_{max} - t^{cp} \\ & \text{(b)} \ t_n > 0, \forall n \\ & \text{(c)} \ p_n \le P_{max}, \forall n \\ & \text{(d)} \ b_n \le B_{max}, \forall n \end{aligned} \quad (11)$$

where (11a) ensures that task is processed within T_{max}, (11b) ensures that each time slot is positive, (11c) limits the transmission power at each hop to P_{max}, and (11d) guarantees bandwidth at any does not exceed B_{max}.

IV. Optimization of multi-hop relaying

In this section, we present the proposed relaying and its optimization. We distinguish three multi-hop relaying cases: *i*) both relays uses HD (labeled as *HD+HD*), *ii*) one relay use *HD* while *FD–Orthogonal* is employed by the other relay (*HD+FD–Orthogonal*), and *iii*) *HD* is exploited by the first relay while *FD–Shared* is used at the second relay (*HD+FD–Shared*). Note that the relaying modes at R1 and R2 can be switched for *ii*) and *iii*) with no impact on derivations presented in the paper. We optimize *i*)-*iii*) in the following subsections.

A. HD+HD relaying case

If both relays employ HD, the task offloading is done during three consecutive time slots (see Fig. 2). The task is sent first by the UE to the R1 within t_1^{hd}, then relayed by the R1 to the R2 during t_2^{hd}, and finally delivered from the R2 to the MEC server in t_3^{hd}. The benefit of this relaying case is no interference to cope with (such as SI) and relays may support only less complex HD relaying.

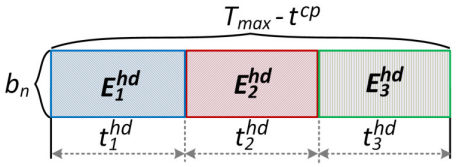

Fig. 2: Optimization of HD+HD by setting of each t_n^{hd}.

To optimize $\boldsymbol{\mathcal{P}}$ in (11), we express p_n from (1) as a function of t_n^{hd} while assuming $C_n^{hd} = D/t_n^{hd}$ (see (2)), i.e.:

$$p_n = \frac{K_n}{g_n}\left(2^{\frac{D}{t_n^{hd} b_n}} - 1\right), \quad (12)$$

where $K_n = b_n(\sigma + I_b)$. Then, the sum energy consumption over all hops is expressed as:

$$\sum_n E_n = \sum_n t_n^{hd} p_n = \sum_n \frac{t_n^{hd} K_n}{g_n}\left(2^{\frac{D}{t_n^{hd} b_n}} - 1\right). \quad (13)$$

To optimize $\boldsymbol{\mathcal{B}}$ in (11), since the first derivative of E_n^{hd} with respect to b_n is decreasing with increasing b_n, E_n^{hd} at any n-th hop is minimized if $b_n = B_{max}$. Thus, we can rewrite (11) for optimizing *HD+HD* case as:

$$\begin{aligned} \boldsymbol{\mathcal{T}} = \quad & \underset{t_n^{HD}}{\operatorname{argmin}} \sum\nolimits_n \frac{K_n t_n^{hd}}{g_n}\left(2^{\frac{D}{t_n^{hd} b_n}} - 1\right) \\ \text{s.t.} \quad & \text{(11a)} - \text{(11c)} \\ & \text{(d)} \ b_n = B_{max}, \forall n \end{aligned} \quad (14)$$

where (14d) ensures that whole bandwidth is used at all hops.

Lemma 1. *The optimization problem in (14) and all its constraints are convex with respect to* $\boldsymbol{\mathcal{T}}$.

Proof. The Hessian matrix H corresponding to the objective function in (14) is:

$$H = \begin{bmatrix} L\frac{2^{\frac{D}{t_1^{hd} B_{max}}}}{t_1^{hd^3} g_1} & 0 & 0 \\ 0 & L\frac{2^{\frac{D}{t_2^{hd} B_{max}}}}{t_2^{hd^3} g_2} & 0 \\ 0 & 0 & L\frac{2^{\frac{D}{t_3^{hd} B_{max}}}}{t_3^{hd^3} g_3} \end{bmatrix} \quad (15)$$

where $L = (\sigma + I_b) D^2 \ln^2 2 / B_{max}$. The entries on the main diagonal of H are positive for $t_1^{hd} > 0$, $t_2^{hd} > 0$, and $t_3^{hd} > 0$. Since the diagonal matrix H is positive definite, the objective function in (14) is convex.

Further, the constraints (11a), (11b), and (14d) are linear, thus, also convex. Last, using (1) while considering $t_n^{hd} = D/C_n^{hd}$ (see (2)), any p_n in (11c) can be rewritten as:

$$t_n^{hd} \ge \frac{D}{B_{max} \log_2(1 + \frac{g_n P_{max}}{K_n})}, \quad (16)$$

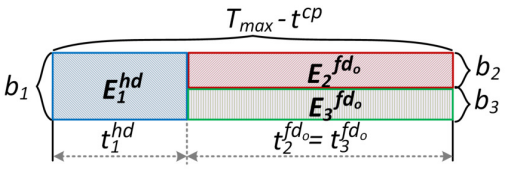

Fig. 3: Optimization of HD+FD - Orthogonal bandwidth by jointly setting t_1^{hd}, $t_2^{fd_o}$, b_2, and b_3.

which is convex (linear) with respect to any $t_n^{hd} > 0$. ■

Since the optimization problem in (14) and all its constraints are convex, any convex optimization method can be used to solve it optimally. We have adopted CVX [18].

B. HD+FD–Orthogonal relaying case

The second case is the combination of *HD* (used by R1) and *FD–Orthogonal* (used by R2), see Fig. 3. Thus, the task is first sent to R1 during t_1^{hd} using b_1. Then, the task is simultaneously sent from R1 to R2 and from R2 to MEC server during $t_2^{fd_o} = t_3^{fd_o}$ (neglecting ϵ as explained in Section II.B) using b_2 and b_3, respectively. Note that relaying modes can be switched at R1 and R2. Similarly as in *HD+HD relaying* case, the advantage of *HD+FD–Orthogonal* case is no SI due to relaying, but devices supporting FD relaying have to be employed.

Like for *HD*, we express p_n as in (12) for all hops as the function of time to solve $\boldsymbol{\mathcal{P}}$ in (11). Then, the sum energy consumption is expressed as:

$$\sum_n E_n = E_1^{hd} + E_2^{fd_o} + E_3^{fd_o} = \frac{t_1^{hd} K_1}{g_1}\left(2^{\frac{D}{t_1^{hd} b_1}} - 1\right) + \\ + \frac{t_2^{fd_o} K_2}{g_2}\left(2^{\frac{D}{t_2^{fd_o} b_2}} - 1\right) + \frac{t_3^{fd_o} K_3}{g_3}\left(2^{\frac{D}{t_3^{fd_o} b_3}} - 1\right). \quad (17)$$

Further, like for *HD*, we can assume $b_1 = B_{max}$, since this minimize E_1^{hd}. Then, we can reformulate (11) as:

$$\begin{aligned} \boldsymbol{\mathcal{T}}, \boldsymbol{\mathcal{B}} = \quad & \underset{t_1^{hd}, t_2^{fd_o}, b_2, b_3}{\text{argmin}} \quad \left(E_1^{hd} + E_2^{fd_o} + E_3^{fd_o}\right) \\ \text{s.t.} \quad & \text{(a) } t_1^{hd} + t_2^{fd_o} \leq T_{max} - t^{cp} \\ & \text{(b) } t_1^{hd} > 0, t_2^{fd_o} > 0 \\ & \text{(c) } b_2 + b_3 \leq B_{max} \\ & \text{(d) } b_2 > 0, b_3 > 0 \\ & \text{(e) } p_n \leq P_{max}, \forall n \end{aligned} \quad (18)$$

where (18a) and (18b) ensure that T_{max} is not violated and the duration of each time slot is positive, respectively, (18c) assures the sum bandwidth at the second and third hops is at most B_{max}, (18d) guarantees bandwidth of b_2 and b_3 is positive, and (18e) is the same as (11c).

Lemma 2. *The optimization problem in (18) and all its constraints are jointly convex with respect to $\boldsymbol{\mathcal{T}}$ and $\boldsymbol{\mathcal{B}}$.*

Proof. Similar as in the proof to Lemma 1, the first term in (17) is convex with respect to t_1^{hd}. To show that the second term in (17) is also convex, we prove that for any non-zero $v_1, v_2 \in R$ we have:

$$\begin{bmatrix} v_1 & v_2 \end{bmatrix} \begin{bmatrix} H_{11} & H_{12} \\ H_{21} & H_{22} \end{bmatrix} \begin{bmatrix} v_1 \\ v_2 \end{bmatrix} > 0, \quad (19)$$

where $\begin{bmatrix} H_{11} & H_{12} \\ H_{21} & H_{22} \end{bmatrix}$ is the Hessian matrix for $E_2^{fd_o}$ in (17) with respect to included variables $t_2^{fd_o}$ and b_2. To this end, the left-hand side in (19) is first expanded and rewritten as:

$$\frac{\sigma + I_b}{g_2}(b_2{}^2 v_1^2 D^2 \ln^2(2)\alpha + t_2^{fd_o}{}^2 v_2^2 D^2 \ln^2(2)\alpha + \\ 2v_1 v_2\big((t_2^{fd_o} b_2)^3(\alpha - 1) - t_2^{fd_o} b_2 \alpha D \ln(2) \times \\ (t_2^{fd_o} b_2 - D\ln(2))\big)) > 0, \quad (20)$$

where $\alpha = 2^{\frac{D}{t_2^{fd_o} b_2}}$. To prove (20) for any non-zero v_1, v_2, according to the Cauchy-Schwarz inequality, it is sufficient to prove that:

$$(t_2^{fd_o} b_2)^3 (2^{\frac{D}{t_2^{fd_o} b_2}} - 1) - t_2^{fd_o} b_2 2^{\frac{D}{t_2^{fd_o} b_2}} \ln(2) \times \\ (t_2^{fd_o} b_2 - \ln(2)) \geq -t_2^{fd_o} b_2 \ln^2(2) 2^{\frac{D}{t_2^{fd_o} b_2}}, \quad (21)$$

or equivalently:

$$2^{\frac{D}{t_2^{fd_o} b_2}} ((t_2^{fd_o} b_2)^2 + 2\ln^2(2) - t_2^{fd_o} b_2 \ln(2)) \geq (t_2^{fd_o} b_2)^2. \quad (22)$$

The inequality in (22) always holds since $2^{\frac{D}{t_2^{fd_o} b_2}} > 1$ and $2\ln^2(2) - t_2^{fd_o} b_2 \ln(2) > 0$. Hence, the Hessian matrix is positive definite. Similarly, the Hessian matrix for $E_3^{fd_o}$ in (17) is positive definite with respect to the variables $t_3^{fd_o}$ and b_3. Last, the constraints (18a)–(18e) are all convex (linear) with respect to the optimization variables. ■

Due to convexity of (18) and all its constraints, we can again use CVX as in Section IV.A.

C. HD+FD–Shared relaying case

The last case is the one combining *HD* and *FD–Shared* (see Fig. 4). The offloading follows the same principle as in *HD+FD–Orthogonal*, but the transmissions at the second and third hops overlap also in frequency resulting in a more efficient utilization of communication resources compared to the previous two relaying cases. Still, the energy consumption at the second hop is affected by SI (see (6)) while the energy consumption at the third hop (at the MEC server) is impacted by interference from R1 (see (7)). Hence, to optimize $\boldsymbol{\mathcal{P}}$ in (11), the transmission power of R1 (i.e., p_2) is expressed from (6) while substituting $\{1, 2\} \Rightarrow \{2, 3\}$ as:

$$p_2 = \frac{K_2 + p_3 g_{2,2}}{g_2}\left(2^{\frac{D}{t_2^{fd_s} b_2}} - 1\right). \quad (23)$$

Similarly, the transmission power of R2 (i.e., p_3) is calculated from (7) assuming $t_2^{fd_s} = t_3^{fd_s}$ and $K_2 = K_3$ (since $b_2 = b_3$,

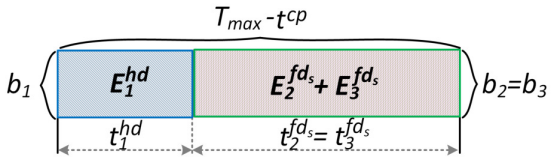

Fig. 4: Optimization of HD+FD - Shared bandwidth by setting t_1^{hd} and $t_2^{fd_s}$.

see Fig. 4), as:

$$p_3 = \frac{K_2 + p_2 g_{2,3}}{g_3}\left(2^{\frac{D}{t_2^{fd_s} b_2}} - 1\right). \tag{24}$$

Next, we solve the system of equations formed by (23) and (24) in order to express p_2 and p_3 independently from each other and only in terms of the other parameters as follows:

$$\begin{aligned} p_2 &= \frac{K_2\Gamma}{g_2(1-\beta\Gamma^2)}\left(1 + \frac{g_{2,2}\Gamma}{g_3}\right), \\ p_3 &= \frac{K_2\Gamma}{g_3(1-\beta\Gamma^2)}\left(1 + \frac{g_{2,3}\Gamma}{g_2}\right), \end{aligned} \tag{25}$$

where $\beta = \frac{g_{2,3}g_{2,2}}{g_2 g_3}$, $\Gamma = 2^{\frac{D}{t_2^{fd_s} b_2}} - 1$.

Then, the energy consumption of this proposed relaying case is expressed as:

$$\begin{aligned} \sum_n E_n = E_1^{hd} + E_2^{fd_s} + E_3^{fd_s} = \frac{t_1^{hd} K_1}{g_1}\left(2^{\frac{D}{t_1^{hd} b_1}} - 1\right) + \\ + \frac{t_2^{fd_s} K_2\Gamma}{g_2(1-\beta\Gamma^2)}\left(1 + \frac{g_{2,2}\Gamma}{g_3}\right) + \frac{t_2^{fd_s} K_2\Gamma}{g_3(1-\beta\Gamma^2)}\left(1 + \frac{g_{2,3}\Gamma}{g_2}\right). \end{aligned} \tag{26}$$

Since the whole B_{max} is used at all hops, as this minimizes the energy consumption (as explained in Section IV.A), the optimization problem in (11) can be formulated as follows:

$$\begin{aligned} \mathcal{T} = \quad & \underset{t_1^{hd}, t_2^{fd_s}}{\text{argmin}} \left(E_1^{hd} + E_2^{fd_s} + E_3^{fd_s}\right) \\ \text{s.t.} \quad & \text{(a) } t_1^{hd} + t_2^{fd_s} \leq T_{max} - t^{cp} \\ & \text{(b) } t_1^{hd} > 0, t_2^{fd_s} > 0 \\ & \text{(11c), (14d)} \end{aligned} \tag{27}$$

where the constraints are analogous to those in (14) and (18).

Lemma 3. *The optimization problem in (27) and all its constraints are convex with respect to* $\mathcal{T}$.

Proof. First, E_1^{hd} in (27) is convex with respect to t_1^{hd}, which is the only variable from $\mathcal{T}$ factoring in E_1^{hd}. This can be proved similarly as shown in the proof to Lemma 1.

Next, we show the convexity of $E_2^{fd_s}$ in (27). Since the Hessian matrix of $E_2^{fd_s}$ is too complex, we first decompose $E_2^{fd_s}$ into simpler factors and use the fact that, the multiplication of any positive, strictly decreasing, and convex functions is also convex. This fact can be verified via the equation $(fg)'' = f''g + fg'' + 2f'g'$ for positive, strictly decreasing, and convex arbitrary functions f and g. Now by considering the factors $t_2^{fd_s} K_2\Gamma$ and $\frac{1}{g_2(1-\beta\Gamma^2)}$ in $E_2^{fd_s}$ taken from (26), both factors are positive, strictly decreasing, and convex with respect to $t_2^{fd_s}$. Hence, their multiplication, which yields the term $\frac{t_2^{fd_s} K_2\Gamma}{g_2(1-\beta\Gamma^2)}$ in (27), is convex. In addition, the multiplication is also positive and strictly decreasing. Next, the term Γ and hence $\left(1 + \frac{g_{2,2}\Gamma}{g_3}\right)$ in (26) is strictly decreasing and convex with respect to $t_2^{fd_s}$. Thus, its multiplication with the term $\frac{t_2^{fd_s} K_2\Gamma}{g_2(1-\beta\Gamma^2)}$, which yields $E_2^{fd_s}$ in (27), is convex.

The third term $E_3^{fd_s}$ in (27) is also convex with respect to $t_2^{fd_s}$, as can be proven analogously to the convexity of $E_2^{fd_s}$.

Last, the constraints in (27) are also convex (linear) with respect to the optimization variables. ■

Since the optimization problem in (27) and all its constraints are convex, we solve it optimally by CVX, analogously as we solve (14) and (18) in Section IV.A and Section IV.B, respectively.

V. Performance Evaluation

In this section, we first describe the simulation models and parameters and then analyze the performance of individual relaying schemes.

A. Simulation models and parameters

For the performance evaluation, we assume the scenario with one UE offloading tasks via two relays to the MEC server (see Fig. 5). To get statistically valid results, we average out the results over 200 000 drops. Within each drop, we randomly generate: *i*) tasks parameters D and c, *ii*) distance between the UE and the MEC server between 25 and 150 m, and *iii*) positions of the relays within the areas shown in Fig. 5. This random generation of the relays' positions substitutes the relay selection process and each drop represents a case

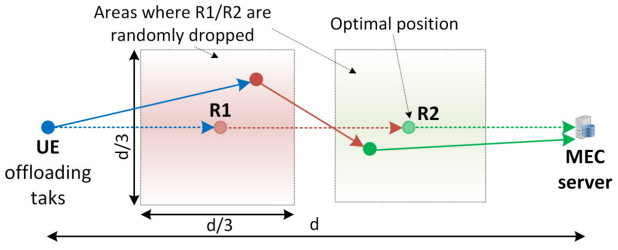

Fig. 5: Simulation scenario.

TABLE I: Parameters and settings for simulations

Parameter	Value	Parameter	Value
distance (d)	25-150 m	I_b	-150 dBm/Hz
Carrier freq.	2 GHz	D	[0.5 2] Mbits [2]
B_{max}	20 MHz	c	[1.5 2]x10^3 cyc./bit [2]
P_{max}	100 mW	F_u	[0.5 2]x10^9 cycles/s [2]
σ	-174 dBm/Hz	F_M	40x10^9 cycles/s [2]

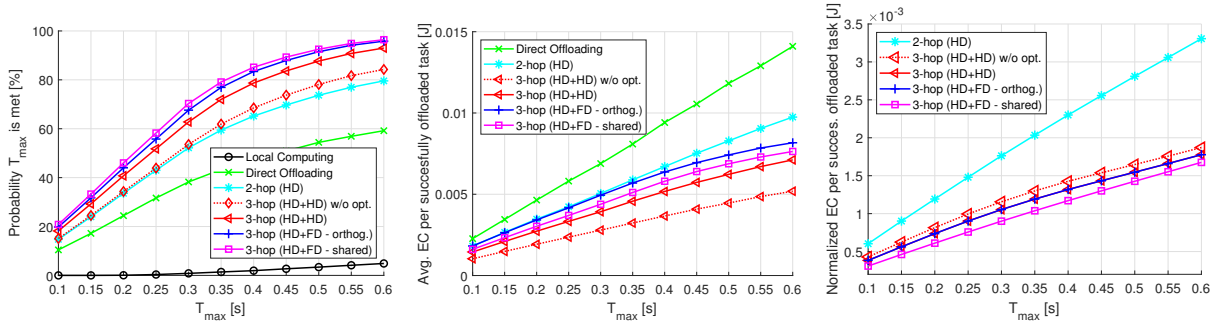

(a) (b) (c)

Fig. 6: Effect of T_{max} on: a) probability that T_{max} is met, b) average energy consumption per successfully offloaded task, c) normalized energy consumption when only tasks successfully offloaded within T_{max} by direct offloading are considered.

with relay at random positions. We adopt general modified COST 231 Hata path loss model at 2 GHz. All important simulation parameters are summarized in Table I.

We compare the results of multi-hop offloading with: *i*) local computing at the UE with computing power (F_u) randomly generated in each drop, *ii*) direct offloading to the MEC server without relays, *iii*) offloading via only relay working in HD usually considered in the related state-of-the-art works (denoted as 2-hop (HD)), *iv*) offloading via multi-hop (i.e., two relays) with HD at both relays while relaying is not optimized, as considered in [10]-[16] (denoted as 3-hop (HD+HD) w/o opt.)

B. Results

In Fig. 6a, we investigate the probability that the tasks are successfully processed within T_{max}. Following the intuition, the probability that the tasks are successfully processed increases with T_{max} for all investigated schemes, as there is more available time to process the tasks. Since we target tasks with relatively high requirements on computation, the local computing is not efficient with only up to 5% probability that tasks are processed within T_{max}. The direct offloading of tasks to MEC server significantly increases the probability that T_{max} is met (up to 60%). The introduction of relaying notably improves the performance of the offloading so that 2-hop relaying and 3-hop relaying without optimization leads to the probability of successful task processing within T_{max} up to 79.5% and 84.2%, respectively, if $T_{max} = 0.6$ s.

Now, let's discuss the probability of successful processing within T_{max} of the proposed optimized multi-hop relaying cases described in Section IV. The superior performance is provided by the multi-hop relaying combining *HD* and *FD–shared*, outperforming the direct offloading, 2-hop relaying, and conventional 3-hop relaying without optimization in terms of probability of T_{max} being met by up to 99.7%, 41.3%, and 38%, respectively. Among the proposed multi-relaying approaches, the worst performance is observed for *HD+HD*, as it is less spectrum efficient. Still even this scheme outperforms direct computing, 2-hop relaying, and conventional 3-hop relaying without optimization in terms of probability T_{max} is met by up to 74.3%, 23.3%, and 20.4%, respectively.

In Fig. 6b, we analyze the average energy consumed per the task successfully processed within T_{max}. We demonstrate that the average energy consumption increases with T_{max} since, generally, offloading can take longer, thus consuming more energy. As expected, the highest energy consumption is spent by the direct offloading. The energy consumption is decreased by more than 30% if 2-hop relaying is introduced. Further significant decrease in the energy consumption (nearly 3 times compared to the direct offloading) is observed for the multi-hop relaying. If the multi-hop relaying is not optimized, it can even consume less energy than the proposed multi-hop relaying cases. This is due to the fact that the optimization of multi-hop relaying allows to accommodate also more demanding tasks within T_{max} that cannot be processed successfully without the proposed optimization. However, these more demanding tasks cost more energy during offloading. As a result, the average energy consumption per successfully offloaded task is increased.

To make the comparison of energy consumed per task fair, in Fig. 6c, we show the normalized energy consumption, i.e., the energy consumption over only those tasks successfully offloaded by all compared schemes. Note that the direct offloading is omitted in Fig. 6c to keep a reasonable scale of the y-axis and also since the energy consumption for the direct offloading is, in fact, the same as in Fig. 6b. Fig. 6c demonstrates that the best performance is yielded by proposed multi-hop relaying combining *HD* with *FD–shared* as it decreases the energy consumption when compared to 2-hop and 3-hop relayings without optimization by up to 51.2% and 28%, respectively.

VI. Conclusions

In this paper, we have focused on offloading of highly computationally demanding tasks to MEC via multi-hop relaying. We have introduced and optimized several relaying cases combining half and full duplex relaying at individual relays. We have demonstrated multi-hop relaying improves the

offloading experience while decreases the energy consumption of energy-constrained devices involved in the relaying. This paper is an initial work and a joint optimization of multi-hop relaying and relay selection should be carried out in the future.

ACKNOWLEDGEMENT

This work was supported by the Czech Science Foundation under the grant no. 23-05646S.

REFERENCES

[1] P. Mach and Z. Becvar, "Mobile Edge Computing: A Survey on Architecture and Computation Offloading," *IEEE Commun. Surveys Tuts.*, vol. 19, no. 3., 3rd Quarter, pp. 1628-1656, 2017.

[2] T. Fang, F. Yuan, L. Ao, and J. Chen, "Joint Task Offloading, D2D Pairing, and Resource Allocation in Device-Enhanced MEC: A Potential Game Approach," *IEEE Internet Things J.*, vol. 9, no. 5, pp. 3226-3237, March 2022.

[3] P. Mach and Z. Becvar, "Device-to-Device Relaying: Optimization, Performance Perspectives, and Open Challenges towards 6G Networks," *IEEE Commun. Surveys Tuts.*, vol. 24, no. 3., 3rd Quarter, 2022.

[4] M. Li, X. Zhou, T. Qiu, Q. Zhao, and K. Li, "Multi-Relay Assisted Computation Offloading for Multi-Access Edge Computing Systems With Energy Harvesting," *IEEE Trans. Vehicular Tech.*, vol. 70, no. 10, Oct. 2021.

[5] J. Peng, H. Qiu, J. Cai, W. Xu, and J. Wang, "D2D-Assisted Multi-User Cooperative Partial Offloading, Transmission Scheduling and Computation Allocating for MEC," *IEEE Trans. Wireless Commun.*, vol. 20, no. 8, Aug. 2021.

[6] S. Zheng, Z. Ren, X. Hou, and H. Zhang, "Optimal Communication-Computing-Caching for Maximizing Revenue in UAV-Aided Mobile Edge Computing," In *Proc. of GLOBECOM*, Taipei, Taiwan, 2020.

[7] X. Diao, W. Yang, L. Yang, and Y. Cai, "UAV-Relaying-Assisted Multi-Access Edge Computing With Multi-Antenna Base Station: Offloading and Scheduling Optimization," *IEEE Trans. Veh. Technol.*, vol. 70, no. 9, pp. 9495-9509, Sept. 2021.

[8] S. Zhang, X. Jiang, J. Liu, L. Qi, and W. Dou, "RAOA: A Relay-assisted Offloading Approach in Edge Computing Environment," in *Proc. of IEEE 24th CSCWD*, Dalian, China, 2021.

[9] G. Chen, Q. Wu, R. Liu, J. Wu, and C. Fang, "IRS Aided MEC Systems With Binary Offloading: A Unified Framework for Dynamic IRS Beamforming," *IEEE J. Sel. Areas Commun.*, vol. 41, no. 2, pp. 349-365, Feb. 2023.

[10] Y. Deng, Z. Chen, X. Chen, and Y. Fang, "Task Offloading in Multi-Hop Relay-Aided Multi-Access Edge Computing," *IEEE Trans. Veh. Technol.*, vol. 72, no. 1, pp. 1372-1376, Jan. 2023.

[11] C.-M. Huanga, S.-Y. Linb, and Z.-Y. Wua, "The k-hop-limited V2V2I VANET data offloading using the Mobile Edge Computing (MEC) mechanism," *Vehicular Communications*, vol. 26, 2020.

[12] Z. Deng, Z. Cai, and M. Liang, "A Multi-Hop VANETs-Assisted Offloading Strategy in Vehicular Mobile Edge Computing," *IEEE Access*, vol. 8, pp. 53062-53071, 2020.

[13] Y. Deng, *et al.*, "Spectrum-aware Multi-hop Task Routing in Vehicle-assisted Collaborative Edge Computing," arxiv, Apr. 2023.

[14] C. Chen, Y. Zeng, H. Li, Y. Liu, and S. Wan, "A Multihop Task Offloading Decision Model in MEC-Enabled Internet of Vehicles," *IEEE Internet Things J.*, vol. 10, no. 4, Feb. 2023.

[15] L. Liu, *at al.*, "Mobility-Aware Multi-Hop Task Offloading for Autonomous Driving in Vehicular Edge Computing and Networks," *IEEE Trans. Intell. Transport. Syst.*, vol. 24, no. 2, Feb. 2023.

[16] J. Xie, Y. Jia, W. Wen, Z. Chen, and L. Liang, "Dynamic D2D Multihop Offloading in Multi-Access Edge Computing From the Perspective of Learning Theory in Games," *IEEE Trans. Netw. Service Manag.*, vol. 20, no. 1, pp. 305-318, March 2023.

[17] H. Wang, J. Wang, G. Ding, J. Chen, Y. Li, and Z. Han, "Spectrum sharing planning for full-duplex UAV relaying systems with underlaid D2D communications," *IEEE J. Sel. Areas Commun.*, vol. 36, no. 9, pp. 1986–1999, Sep. 2018.

[18] M. Grant and S. Boyd. "CVX: MATLAB Software for Disciplined Convex Programming, Version 2.2." Jan. 2020. [Online]. Available: http://cvxr.com/cvx.

XVII. Appendix I

This appendix includes conference paper presented at: E. Gures and **P. Mach**, "Joint Route Selection and Power Allocation in Multi-hop Cache-enabled Networks," in Proc. *IEEE Wireless Communications and Networking Conference (WCNC)*, Dubai, United Arab Emirates, April. 2024. Available online: https://arxiv.org/abs/2401.09060.

Joint Route Selection and Power Allocation in Multi-hop Cache-enabled Networks

Emre Gures, Pavel Mach
Faculty of Electrical Engineering, Czech Technical University in Prague, Prague, Czech Republic
{guresemr, machp2}@fel.cvut.cz

***Abstract*—The caching paradigm has been introduced to alleviate backhaul traffic load and to reduce latencies due to massive never ending increase in data traffic. To fully exploit the benefits offered by caching, unmanned aerial vehicles (UAVs) and device-to-device (D2D) communication can be further utilized. In contrast to prior works, that strictly limits the content delivery routes up to two hops, we explore a multi-hop communications scenario, where the UAVs, the UEs, or both can relay the content to individual users. In this context, we formulate the problem for joint route selection and power allocation to minimize the overall system content delivery duration. First, motivated by the limitations of existing works, we consider the case where the nodes may transmit content simultaneously rather than sequentially and propose simple yet effective approach to allocate the transmission power. Second, we design a low-complexity greedy algorithm jointly handling route selection and power allocation. The simulation results demonstrate that the proposed greedy algorithm outperforms the benchmark algorithm by up to 56.98% in terms of content delivery duration while it achieves close-to-optimal performance.**

***Index Terms*—caching, UAV, D2D relaying, route selection, power allocation, content delivery duration**

I. Introduction

The emerging 6G-based mobile networks will have to cope with unprecedented data transmissions originated form plethora of communicating devices, such as smartphones, sensors, vehicles, or any internet of things (IoT) devices. This will inevitably pose high requirements on provided data rates over backhaul and experienced latencies. To alleviate backhaul load and to enable low latencies, caching of popular content seems to be a very promising approach [1]. Obviously, the popular content should be cached in proximity of a user equipment (UE), such as at a ground base station (GBS).

To improve systems-wide performance, the unmanned aerial vehicles (UAVs) can be exploited as caching servers as well [2]. Such cache-enabled UAVs can store popular contents, thus reducing content delivery duration and backhaul traffic load [3]. The UAV caching can be particularly beneficial during peak hours to offload traffic of the GBSs or to mitigate severe shadowing in urban or mountainous scenarios by leveraging their ability to establish line-of-sight (LoS) connections with ground nodes. The mobile networks can also benefit from the device-to-device (D2D) functionality of UE; to transmit data to other relaying UEs (RUEs) [4]. In such cached-enable, UAV-assisted, and D2D-enabled networks, the main challenges are the selection of proper route over which the content should be traversed in order to reach the UEs, power allocation, content placement, or UAVs' deployment.

This work was supported by Grant No. SGS23/171/OHK3/3T/13.

The problem of route selection and power allocation in cache-enabled UAV-assisted D2D-enabled cellular network is considered in many works targeting various objectives, including optimization of minimum secrecy rate among requesting UEs [5], sum throughput [6], and energy efficiency [7]. Whereas the afore-mentioned studies [5], [6] confine their scope to direct communication, [7] enables two-hop communication using UAV-relaying. Still, as the distance between the source and target nodes increases or the communication environment deteriorates, direct communication or even two-hop communication with single UAV relay is generally insufficient to reduce the content delivery duration [8]. For instance, in a densely populated urban environment, wireless communication links are susceptible to blockage by tall buildings. Consequently, the mitigation of such link blockage problems typically necessitates the employment of multi-hop communication incorporating both UAV relays and the RUEs in order to provide sufficient degrees of freedom.

In addition, some studies propose different methods to minimize content delivery duration. For example, in [9], a deep deterministic policy gradient-based caching placement strategy is proposed. In [10], the UAV deployment and content placement are jointly studied. However, in both [9] and [10], transmission nodes send contents sequentially rather than simultaneously. Nevertheless, this approach does not minimize transmission duration, as the duration is not linearly proportional to the allocated transmission power.

In this article, we aim to cover the gaps of the existing related works. We formulate the problem as joint route selection and power allocation problem minimizing sum content delivery duration. Unlike [5], [6], [7], where up to 2-hop communication is enabled, we target multi-hop scenario (i.e., more than 2 hops). To the best of our knowledge, no multi-hop transmission route selection for delivery of cached content has not been considered so far. The content delivery over multi-hop transmission is expected to decrease latencies in urban scenario with many potential obstacles in the communication path. Note that a deployment of many conventional fixed GBSs can also decrease latencies, but at significant installment cost while these GBS would still not be able to cope with dynamic requirements of users. In addition, compared to [9] and [10], we assume that each transmitting node can send several contents simultaneously to further decrease delivery

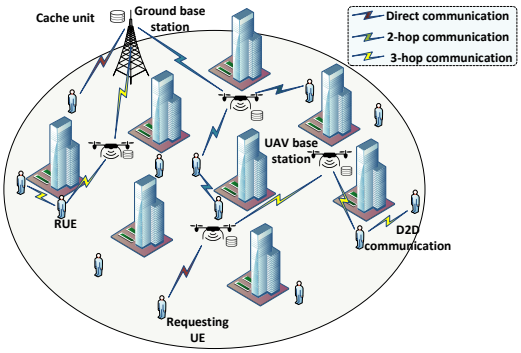

Fig. 1: A multi-hop cache-enabled network in urban area.

of cached content.

The enabling of multi-hop communication, however, makes also the selection of the optimal transmission routes over which content traverse to the requesting UE a very challenging task. The reason is that there are many potential transmission routes for delivering the content to individual UEs. The route selection also affects the power allocation at GBS, UAVs, and/or RUEs that can be potentially involved in delivery of multiple contents, thus impacting the overall content delivery duration. As a result, the route selection and power allocation must be handled jointly. We summarize our main contributions to address above-listed challenges as follows:

- We propose the transmission power allocation managing the splitting of transmission power budget by each transmitting node (i.e., the GBS, the UAV, or RUE) to each content currently being sent. We guarantee the continuous utilization of the entire transmission power by the transmitting nodes, resulting in a reduction in the overall transmission duration.
- We propose a low-complexity greedy algorithm that jointly considers the route selection while exploiting proposed power allocation.
- We show the proposed greedy algorithm decreases overall content delivery duration by up to 56.98% in comparison to the benchmark algorithm. At the same time, we show that greedy algorithm yields close-to-optimal performance.

The rest of the paper is organized as follows. Section II introduces the system model and Section III formulates the problem. In Section IV, we present the proposed greedy based joint route selection and power allocation algorithm. Section V introduces the simulation model and competitive algorithms. In Section VI, simulation findings are examined and discussed. Finally, we briefly summarize the findings in Section VII.

II. System Model

This section describes the network model, cache placement model, and provides details about content delivery duration.

A. Network Model

We consider a cache-enabled, UAV-assisted, and D2D-enabled cellular network, as depicted in Fig. 1. The network is composed from $K+1$ BSs including one GBS and K UAVs acting as flying BSs. Further, we assume there are U UEs in the system from which N are asking for delivery of a content. We consider that the UEs currently not requesting the content can serve as the RUEs, i.e., there are $R = U - N$ RUEs. Note that relaying accomplished by the UEs can be facilitated by D2D relaying concept [4]. The content can be, then, delivered to the UEs: *i*) directly by the GBS, *ii*) directly by the one of the UAVs that can reduce content delivery duration by caching popular content requested by the UEs in cache repositories, or *iii*) by relaying the content either via the UAV and/or RUEs.

Both the UAVs and RUEs operate in half-duplex mode [19]. We limit the number of relaying nodes for delivery of content up to two (i.e., up to 3-hop communication) as more relaying nodes usually yield only minimal gains in delivery duration while the complexity is increased significantly [4]. Considering that the content can be delivered directly by the GBS or UAVs, and through 2-hop or 3-hop routes, there is M possible transmission route options for any requesting UE.

B. Cache Placement Model

We assume the UEs can pick out of F contents, where the size of f-th content is S_f. The users' requests are determined by a content popularity distribution, denoted as $p = \{p_1, p_2, \ldots, p_F\}$. Here, p_f represents the probability of a request for content f whilst $\sum_f p_f = 1$. The popularity of the contents is inherent to them, and it is assumed that the distribution of their popularity follows the Zipf distribution [11], described as $p_f = f^{-\gamma} / \sum_{j=1}^{F} j^{-\gamma}$, where γ is the Zipf exponent indicating the degree of skewness in popularity.

We assume all the contents are stored at GBS while the UAVs store only a subset of the content catalog due to their limited storage capacity. In other words, the UAVs can only cache a part of the files. In accordance with the caching probabilities p_f, each k-th UAV stochastically generates a collection of contents F_k to be cached, as outlined in the probabilistic content caching approach introduced in [12].

C. Content Delivery Duration

The subset of nodes that will deliver content requested by the UE depends on both the cache status of the UAVs and the condition of the wireless channels. We assume that the entire bandwidth B is divided into N orthogonal channels, so that the n-th UE requesting a content is assigned a channel with a bandwidth of B_n. Notice that the bandwidth allocation falls outside the purview of this article, and our proposed method is applicable to any arbitrary allocation of bandwidth. Hence, we assume that B is split equally among N requesting UEs.

The content delivery duration for the f-th content requested by the n-th UE whilst using the m-th transmission route including H_m hops is defined as follows:

$$t_{n,f,m} = \sum_{h_m=1}^{H_m} \frac{S_f}{B_n \log_2(1 + \frac{p_f^{h_m} g^{h_m}}{B_n(\sigma_0 + I_b)})}, \qquad (1)$$

where $p_f^{h_m}$ denotes the transmission power of the node exploited in the h_m-th hop on the m-th transmission route to

deliver the f-th content to the requesting UE, g^{h_m} represents the channel gain at the h_m-th hop of the m-th transmission route, σ_0 is the noise power, and I_b represents the background interference received from neighboring transmitters.

We assume that each transmitter (GBS, UAV, or RUE) can transmit multiple contents simultaneously. Note that this is reasonable assumption as the GBS usually transmits different data to different users albeit at different frequencies. In such case, the delivery duration in (1) is affected by the number of contents sent at the same time since available transmission power budget at the transmitter has to be distributed among all contents. To ensure that maximum transmission power is not violated, we introduce two indicators $y_{k,f,m}$ and $v_{r,f,m}$, to keep track on whether the *k*-th BS and/or the *r*-th RUE are in the *m*-th transmission route selected for the f-th content delivery, respectively. The $y_{k,f,m}$ and $v_{r,f,m}$ are equal to 1 if the *k*-th BS and the *r*-th RUE are on the *m*-th transmission route, respectively, and 0 otherwise.

III. Problem Formulation

The objective of this article is to jointly optimize route selection X^* and power allocation P^*, aiming to minimize the content delivery duration of the requesting UEs. We denote the route selection indicator by $x_{n,f,m} \in \{0,1\}$, where $x_{n,f,m} = 1$ when the *n*-th UE requests the f-th content from the *m*-th route, and $x_{n,f,m} = 0$ otherwise. Then, the targeted optimization problem is formulated as follows:

$$X^*, P^* = \min_{X,P} \sum_n \sum_f \sum_m x_{n,f,m} t_{n,f,m} \tag{2}$$

$$\text{s.t.} \quad \text{(c1)} \quad \sum_n \sum_f P_k y_{k,f,m} \leq P_k^{max}, \forall k \tag{3}$$

$$\text{(c2)} \quad \sum_n \sum_f P_r v_{r,f,m} \leq P_r^{max}, \forall r \tag{4}$$

$$\text{(c3)} \quad \sum_m x_{n,f,m} \leq 1, \forall n, f \tag{5}$$

$$\text{(c4)} \quad H_m \leq H_{max}, \forall m \tag{6}$$

where (c1) and (c2) ensure that the total transmission power allocated by any BS and RUEs sending the content(s) does not exceed P_k^{max} and P_r^{max}, respectively, (c3) ensures each content traverse via one unique route, and (c4) limits the maximum number of hops H^{max} for any *m*-th route.

The optimization problem can be classified as a mixed integer non-linear programming (MINLP) problem due to integer constraint (c3) while the objective function is non-linear with respect to power allocation (see expression of $t_{n,f,m}$ in (1)). These problems are NP-hard, meaning that there is no known polynomial-time algorithm for solving them optimally. The problem is very complicated also since route selection X and transmission power allocation P are coupled problems that should be solved jointly, as the selection of transmission routes depends on the relationship between the requesting user and the nodes, while power allocation affects this relationship.

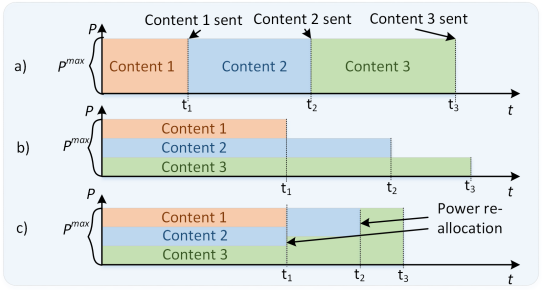

Fig. 2: Principle of power splitting among multiple contents.

One way to find the optimal solution is to use a brute-force search. The brute-force has, however, huge complexity ($O(M^N)$) even for small number of UAVs, the UEs requesting content and the RUEs since all possible route combinations have to be tested. One approach to reduce the complexity of brute-force search is to exclude "bad" combinations that are not able to outperform direct route, e.g., the combinations where the content delivery duration over any hop is actually higher than a direct route. Unfortunately, even this reduction does not make the problem solvable in polynomial time.

IV. Proposed Scheme for Content Delivery

This section explains the power allocation principle that is further exploited in proposed greedy algorithm.

A. Power Allocation

Let's first explain the proposed power allocation principle adopted during the following route selection process. The proposed power allocation deals with the problem when any transmitting node is about to transmit more than one content simultaneously. Of course, each content can be simply sent in a sequential manner, where the transmitting node allocates whole power budget to transmit the first content, then to the second content, and so on (see Fig. 2a), where content 1 is send first and then follow content 2 and content 3) [10]. This option is not minimizing transmission duration since the duration is not linearly proportional to the transmission power allocated for the transmission (see (1)).

To this end, we propose an approach where each transmitting node can, in fact, transmit several contents simultaneously in order to decrease overall transmission duration of the contents while constraints (c1) and (c2) in (2) are not violated. We assume here that the whole transmission power is split equally among individual contents that are being currently transmitted. Note that the optimization of the power splitting itself is left for future research due to limited page number. Since, in general, each content can have different size and can be transmitted over different channels, the transmission of each content can take different transmission duration as well. If the transmission power allocated to each content would remain the same, however, this would inevitably prolong the transmission duration of some contents, as transmission power used to send each content is not always fully used, as illustrated in Fig. 2b.

Hence, we propose that the transmission power allocated to each content is redistributed among the contents after each individual content is fully transmitted to the receiving node. In other words, we ensure that the whole transmission power is used all the time by the transmitting node and, thus, the total transmission duration is reduced by our approach. This is illustrated in Fig. 2c where after content 1 is already transmitted, power is re-allocated to transmit content 2 and 3. Then, when also content 2 is finished, the whole transmission power can be allocated just to transmit the rest of content 3.

In the sequel, we describe in detail the route selection process, where the above-explained power allocation is exploited.

B. Proposed Joint Route Selection and Power Allocation

The main challenge of the problem in (2) is that there are plenty of possible routes over which each content can be sent to the individual requesting UEs. Besides, the selection of route is affected by the number of contents sent by each node and, subsequently, the content delivery duration. The reason is that if any node is sending multiple contents simultaneously, it has inevitably less transmission power that can be allocated to each content, which affects the selection process. Consequently, the route selection and power allocation at individual nodes involved in content delivery must be handled jointly. Thus, we propose a greedy approach solving the problem at reasonable complexity, summarized in Algorithm 1.

At the very beginning, Algorithm 1 selects for each requesting UE the potential source options (L_n) distinguishing which nodes have the requested content (see line 1 in Algorithm 1). Obviously, if no UAV has the requested content, the GBS is always selected as the source option. Otherwise, more than one source options are available. Then, for any *n*-th UE requesting f-th content, Algorithm 1 calculates content delivery durations for all source options, denoted as $t_{n,f,m'}$, where m' indicates only direct routes out of all potential routes (line 2). Next, the direct route selection indicator $x_{n,f,m'}$ is initialized to 0 for all *n* and m', indicating that no UE requesting content f-th has yet selected any direct route (line 3). The direct route for each requesting UE is selected in a sequential manner based on the content delivery duration. In particular, at each iteration, the direct route with the lowest content delivery duration, denoted as $t_{n,f,d}$, is selected for each UE (line 5) and $x_{n,f,m'}$ is set to 1 to indicate that the direct route is selected (line 6). To ensure that the selected route is not selected repeatedly, the content delivery durations of each direct transmission route for the *n*-th requesting UE are set to infinity (line 7). Following the power re-allocation at the BS on the selected direct route according to the route selection (done in line with proposed re-allocation shown in Fig. 2c), content delivery durations are updated for the UEs for which the direct route is not yet selected (line 8). The steps in lines 5-8 are repeated each requesting UE is assigned a direct route.

After the selection of direct route is finished, a decision if a multi-hop route would be more beneficial in terms of delivery content duration follows. Thus, we first calculate a multi-hop gain representing the duration reduction if any *n*-th UE requesting the f-th content would select any m''-th multi-hop route (i.e., $t_{n,f,m''}$) instead of a direct one as (line 10):

$$G_{n,f,m''}, = \begin{cases} t_{n,f,d} - t_{n,f,m''} - t_{m''}, & \text{if } G_{n,f,m''} > 0 \\ 0, & \text{otherwise} \end{cases} \quad (7)$$

where $t_{m''}$ represents an overall prolongation of content delivery duration for other UEs that are already using some nodes at m''-th route to deliver their content. The reason why $t_{m''}$ needs to be considered in (7) is that if some transmitting node(s) at m''-th route are already involved in transmission of other contents for different UEs, the transmitting node(s) must split transmission power as discussed in Section III.A, resulting in prolongation of content delivery duration. On the other hand, if transmitting node in m'' route send no content at the moment $t_{m''}$ is 0. If resulting $G_{n,f,m''}$ in (7) is positive, a multi-hop route is more beneficial to the requesting UE. Otherwise, direct route is kept and $G_{n,f,m''}$ is set to 0, since multi-hop route would increase the overall delivery duration.

In the next step, the multi-hop gains between all requested UEs and transmission routes are inserted into a multi-hop gain matrix $\boldsymbol{G}$, which is of dimension $N \times M - (K+1)$ (excluding direct routes), as showed in line 11. In addition, route selection indicator $x_{n,f,m''}$ is initially set to 0 for all *n* and m'' to indicate that no requesting UE has selected yet any multi-hop transmission route to receive the f-th content (line 12).

Now, the following steps are repeated as long as there is at least one positive entry in $\boldsymbol{G}$. The Algorithm 1 first selects the maximum multi-hop gain in $\boldsymbol{G}$, as this selection decreases the overall content delivery duration by the highest degree (i.e., Algorithm 1 finds max($G_{n,f,m''}$), line 14). Then, $x_{n,f,m''}$ is set to 1 to indicate direct route is changed to multi-hop route (line 15). Then, all entries in *n*-th row of $\boldsymbol{G}$ are set to 0, as this UE cannot select any other transmission route to receive the requested content (line 16).

Next, the Algorithm 1 also has to update all remaining positive entries in $\boldsymbol{G}$ (if any) that include nodes of m''-th multi-hop route according to (7) (line 17). The reason is that the potential gains are decreased as transmission power would need to be divided among more contents. Of course, this also means that the content delivery durations of the UEs

Algorithm 1 Proposed Joint Route Selection and Power Allocation

1: Generate a list of potential source options L_n for each UE *n*
2: Calculate $t_{n,f,m'}$, $\forall n$, $\forall m' \in L_n$
3: Set $x_{n,f,m'} = 0$, $\forall n, m'$
4: **repeat**
5: $\quad t_{n,f,d} \leftarrow \min(t_{n,f,m'})$, $\forall n$
6: $\quad x_{n,f,m'} = 1$
7: $\quad$ Set *n*-th row in $t_{n,f,m'}$ to ∞
8: $\quad$ Update $t_{n,f,m'}$ with power re-allocation
9: **until** all UEs requesting content are assinged to a direct route
10: Calculate $G_{n,f,m''}$, $\forall n, m''$
11: Create matrix $\boldsymbol{G}$
12: Set $x_{n,f,m''} = 0$, $\forall n, m''$
13: **while** $\max(G_{n,f,m''}) > 0$ **do**
14: $\quad \{n, f, m''\} \leftarrow \max(G_{n,f,m''}) \in \boldsymbol{G}$
15: $\quad x_{n,f,m''} = 1$
16: $\quad$ Set *n*-th row in $\boldsymbol{G}$ to 0
17: $\quad$ Update $\boldsymbol{G}$, using (7) with power re-allocation
18: **end while**

that have already selected multi-hop route including these nodes in their transmission routes would be affected. Thus, the increase in overall content delivery duration should be less than the potential reduction achieved by new UEs selecting transmission routes. Therefore, this effect is reflected in the recalculation in $\boldsymbol{G}$ via $t_{m''}$ with the updated power allocations.

Algorithm 1 repeatedly executes lines 14-17 until there are no more positive inputs in the relaying gain matrix $\boldsymbol{G}$. In each iteration, the system updates the power allocation and selects the route with the highest relaying gain accordingly. Note that requesting UEs that do not select a multi-hop transmission route receive their content via the direct route.

Algorithm 1 has, in the worst case, a time complexity of $O([M-(K+1)]\sum_{n=1}^{N} n) = O(N^2[M-(K+1)])$, which means that the time it takes to run the algorithm grows linearly with the number of transmission routes (M) and quadratically with the number of requesting UEs (N).

V. Simulation Setup and Competitive Algorithms

To investigate and validate the proposed model, we performed simulations in MATLAB. We consider a 500×500 m reference cell with multiple buildings to imitate an urban environment (see [19] for more details). The height of each building is randomly generated between 20 and 29 m. The GBS is placed in a fixed position in the upper left corner of the building, near the cell center. Furthermore, 4 UAVs are placed in the simulation area. The positions of the UAVs are determined by K-means clustering, based on the positions of the UEs. Last, we consider 100 UEs from whom up to 30 are requesting the content while other can serve as RUEs. Since the GBS and UAVs are above buildings, they communicate with each other via LoS. On the contrary, the communication path between the GBS/UAVs and the UEs can be obstructed by one or several buildings, each attenuating the signal by additional 20 dB. We run the simulations for 1000 drops. In each such drop, we randomly generate the building heights, the current contents cached at the UAVs, and the UEs locations according to which the UAVs locations are determined. Then, we average the simulation results over all drops. The simulation parameters are summarized in Table I.

The section with results presents the findings of two proposed approaches. The first approach performs joint route selection and power allocation while proposed power allocation is not adopted (labeled as "Proposal: w/o PA"). The second approach is the whole proposal where also proposed power allocation is used (Proposal: with PA). The performance of the proposal is compared with benchmark algorithm (labeled as "Benchmark"), where the transmission route is selected based on caching status and maximum biased received power [13]. Further, we show the performance of brute-force algorithm to show how close to optimal the proposed greedy approach performs. The brute-force algorithm checks all possible transmission routes for each requesting UE and selects the transmission routes that provide the optimal average content delivery time. We illustrate the results for both the case w/o proposed power allocation (Brute-force: w/o PA) and with power allocation enabled (Brute-force: with PA). Note that the brute-force algorithms are only shown for a limited number of requesting UEs because the complexity of testing all transmission route combinations grows exponentially with the number of UEs.

TABLE I: Simulation parameters

Parameter	**Value**
Carrier frequency	2 GHz
Simulation area of the reference cell	500x500 m
No. of UAVs (K), UEs (U), req. UEs (N)	4 [14], 100, 1-30 [13]
Bandwidth (B)	20 MHz [15]
Channel bandwidth allocated to the requesting UEs (Bn)	B/N MHz
Max. trans. power of GBS, UAVs and RUEs	30, 27, 23 dBm
Antenna gain of the GBS, and UAVs	3 dB
Noise spectral density	-174 dBm/Hz
Mean interference from adjacent cells I_b	-130 dBm/Hz [16]
Height of the GBS, UAVs, UEs antenna	35, 100, 1.5 m
Zipf exponent (γ)	0.5 [17]
Content catalog of the GBS, and UAVs	50, 10 files [18]
Content size	10 Mbits [11]
Number of simulation drops	1000

VI. Simulation Results

Fig. 3 illustrates the average content delivery durations achieved by different schemes for different number of requesting UEs. From Fig. 3 can be observed that the content delivery duration of all schemes rises when the number of requesting UEs in the system increases. This is because bandwidth B is divided among a larger number of requesting UEs. Still, the proposed algorithm always outperforms the benchmark algorithm. Take the 30 requesting UEs in Fig. 3 as an example, compared to the benchmark algorithm, the proposed route selection algorithm yields 53.69% gain in terms of reducing the average content delivery duration; this confirms the benefits of the proposed route selection algorithm. This is because the benchmarking algorithm sends the contents sequentially, as shown in Fig. 2a. Furthermore, employing the joint route selection and power allocation algorithm yields a 56.98% gain over the benchmark algorithm.

Fig. 3 also demonstrates that the proposed algorithm provides close performance to the brute-force algorithm in terms of content delivery duration. Specifically, the gap between the

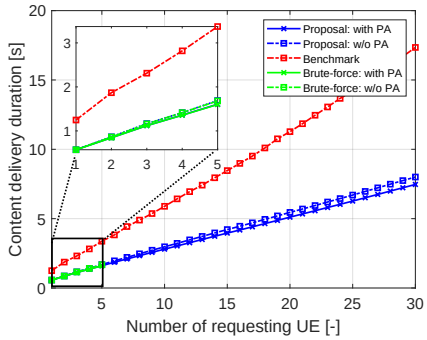

Fig. 3: Average content delivery over no. of req. UEs.

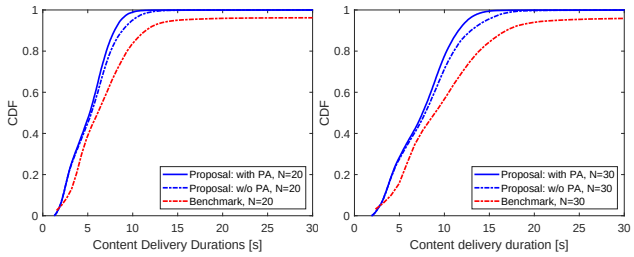

Fig. 4: CDF of content delivery duration for 20 requesting UEs (left figure) and 30 requesting UEs (right figure).

proposed route selection algorithm without power allocation and the brute-force algorithm is only up to 0.52%. Similarly, the gap between the proposed joint route selection and power allocation algorithm and the brute-force algorithm with power allocation is up to 0.30%. The results presented herein provide evidence that the proposed greedy algorithm exhibits a strong correlation in route selection with the brute-force algorithm for content delivery.

While the previous figure showed the average content delivery duration, it does not give any insight on distribution of actual durations. Thus, we also the cumulative distribution function (CDF) of content delivery duration for individual algorithms in Fig. 4. Then, for any given confidence level, the confidence interval for the content delivery duration can be obtained from the CDF curve. Note that since we show results for 20 and 30 requesting UEs in Fig. 4a and Fig. 4b, respectively, we are not able to include brute-force algorithm due to its huge complexity. The benchmark algorithm's CDF curve in Fig. 4 exhibits a prolonged plateau that extends well beyond the content delivery durations of most UEs, so the CDF does not reaching 1 in given interval. This suggests that a small fraction of UEs experience significantly longer delivery durations compared to the majority, highlighting the benchmark algorithm's inefficiency in handling outlier cases. Fig. 4 further shows that the proposed route selection algorithm achieves lower content delivery duration than the benchmark algorithm. In particular, for a high number of requesting UEs, the proposed greedy algorithm produces more consistent results than the benchmark algorithm. For instance, when N = 20 (Fig. 4a), roughly 99% and 85% of requested UEs, respectively, receive their content within 10 s using the proposed joint route selection and power allocation algorithm and the benchmark algorithm. When N = 30 (Fig. 4b), roughly 77% and 55% of requested UEs, respectively, receive their content within 10 s using the proposed joint route selection and power allocation algorithm and the benchmark algorithm.

The result confirms that proposed scheme is an effective solution to defined problem. Besides, the more users are requesting the content, the more significant gap between proposed algorithm and benchmark. These are encouraging results considering the fact that, in general, number of UEs in the future 6G networks is assumed to grow exponentially.

VII. Conclusion

In this article, we have shed light on the problem of joint route selection and power allocation in multi-hop- and cache-enabled networks. Since the defined problem is a mixed-integer non-linear programming problem, thus NP-hard, we have also designed a greedy-based algorithm efficiently managing jointly route selection and power allocation. We have demonstrated that the proposed greedy algorithm reduces overall content delivery duration by up to 56.98% compared to the close related benchmark algorithm while it yields close-to-optimal performance. In the future, the proposed model can be extended by the optimization of power splitting among individual contents, incentivization of relaying users, or smart positioning of the unmanned aerial vehicles.

References

[1] I. Zyrianoff, A. Trotta, L. Sciullo, F. Montori, and M. Di Felice, "IoT edge caching: taxonomy, use cases and perspectives," *IEEE Internet of Things Magazine*, vol. 5, no. 3, pp. 12-18, 2022.

[2] T. Q. Duong, K. J. Kim, Z. Kaleem, M.-P. Bui, and N.-S. Vo, "UAV caching in 6G networks: A survey on models, techniques, and applications," *Physical Communication*, vol. 51, p. 101532, 2022.

[3] N. Zhao *et al.*, "Caching unmanned aerial vehicle-enabled small-cell networks: Employing energy-efficient methods that store and retrieve popular content," *IEEE Veh. Technol. Mag.*, vol. 14, no. 1, 71-79, 2019.

[4] P. Mach, and Z. Becvar, "Device-to-device relaying: Optimization, performance perspectives, and open challenges towards 6G networks," *IEEE Commun. Surv. Tutor.*, vol. 24, no. 3, pp. 1336-1393, 2022.

[5] J. Ji *et al.*, "Joint trajectory design and resource allocation for secure transmission in cache-enabled UAV-relaying networks with D2D communications," *IEEE Internet Things J.*, vol. 8, no. 3, pp. 1557-1571, 2020.

[6] M. S. Al-Abiad *et al.*, "Throughput Maximization of Network-Coded and Multi-Level Cache-Enabled Heterogeneous Network," *IEEE Trans. Veh. Technol.*, vol. 70, no. 10, pp. 11039-11043, 2021.

[7] X. Qi, M. Yuan, Q. Zhang, and Z. Yang, "Joint power-trajectory-scheduling optimization in a mobile UAV-enabled network via alternating iteration," *China Communications*, vol. 19, no. 1, pp. 136-152, 2022.

[8] G. Zhang, H. Yan, Y. Zeng, M. Cui, and Y. Lui, "Trajectory optimization and power allocation for multi-hop UAV relaying communications," *IEEE Access*, vol. 6, pp. 48566-48576, 2018.

[9] D. Wang *et al.*, "Deep Reinforcement Learning for Caching in D2D-Enabled UAV-Relaying Networks," *IEEE ICCC*, 2021, pp. 635-640.

[10] L. Luo, R. Sun, R. Chai, and Q. Chen, "Cost-Efficient UAV Deployment and Content Placement for Cellular Systems With D2D Communications," *IEEE Systems Journal*, 2023.

[11] T. Zhang, C. Chen, D. Yang, "Joint user association and caching placement for cache-enabling UAV networks," *China Communications*, vol. 20, no. 6, pp. 291-309, 2023.

[12] B. Blaszczyszyn, and A. Giovanidis, "Optimal geographic caching in cellular networks," *IEEE ICC*, 2015, pp. 3358-3363.

[13] Z. Gu *et al.*, "Association and caching in relay-assisted mmWave networks: A stochastic geometry perspective," *IEEE Trans. Wirel. Commun.*, vol. 20, no. 12, pp. 8316-8332, 2021.

[14] J. Wang *et al.*, "Learning-based dynamic connectivity maintenance for UAV-assisted D2D multicast communication," *China Communications*, 2023.

[15] 3GPP, "Study on channel model for frequencies from 0.5 to 100 GHz," 2018

[16] Z. Becvar, M. Nikooroo, P. Mach, "On energy consumption of airship-based flying base stations serving mobile users," *IEEE Trans. Commun.*, vol. 70, no. 10, pp. 7006-7022, 2022.

[17] Y.-J. Chen *et al.*, "Multi-agent reinforcement learning based 3D trajectory design in aerial-terrestrial wireless caching networks," *IEEE Trans. Veh. Technol.*, vol. 70, no. 8, pp. 8201-8215, 2021.

[18] X. Gao, Z. Qian, X. Wang, "Delay-Oriented Probabilistic Edge Caching Strategy in a Device-to-Device Enabled IoT System," *IEEE Sens. J.*, 2023.

[19] P. Mach, Z. Becvar, and M. Najla, "Power allocation, channel reuse, and positioning of flying base stations with realistic backhaul," *IEEE Internet Things J.*, vol. 9, no. 3, pp. 1790-1805, 2021.